

**Ultrasound as a non-invasive diagnostic
tool in paediatric neurosurgery:
Relationship between the optic nerve
sheath diameter (ONSD) and intracranial
pressure (ICP)**

Thesis presented for the Degree of
DOCTOR OF PHILOSOPHY
(Neurosurgery)
UNIVERSITY OF CAPE TOWN
August 2015

Candidate: Doctor Llewellyn Padayachy
Supervisor: Professor Anthony Graham Fieggen
Co-supervisor: Doctor Tormod Selbekk

The copyright of this thesis vests in the author. No quotation from it or information derived from it is to be published without full acknowledgement of the source. The thesis is to be used for private study or non-commercial research purposes only.

Published by the University of Cape Town (UCT) in terms of the non-exclusive license granted to UCT by the author.

Abstract

Background: Assessment of intracranial pressure (ICP) is an essential aspect in the management of most neurosurgical conditions in children. While invasive ICP monitoring is considered the criterion standard, the need for a reliable, non-invasive, easy-to-use and accurate method to detect and monitor raised ICP has inspired the development of many useful techniques. The present study examined the relationship between transorbital ultrasound measurement of the optic nerve sheath diameter (ONSD) and invasively measured ICP in children, as well as the influence of relevant physiological and demographic variables on this relationship.

Methodology: ONSD measurement was performed using a high frequency, small footprint linear array probe, prior to invasive ICP measurement. All patients were under general anaesthesia and being mechanically ventilated. Physiological variables including systolic blood pressure (SBP), diastolic blood pressure (DBP), mean arterial pressure (MAP), pulse rate, temperature, respiratory rate and end tidal carbon dioxide (ETCO₂) level were recorded at the time of ONSD measurement. The ONSD measurements were analysed for repeatability, intra- and inter-observer variability as well for correlation between images acquired in different planes and those obtained from either eye. The diagnostic accuracy of ONSD measurement for detecting ICP at different thresholds of 20, 15, 10 and 5 mmHg was analysed. This analysis included evaluation of age-related thresholds for defining different ONSD cut-off values in children. Dynamic image acquisition was performed and analysed to evaluate the relevant pulsatile motion of the ONS as a marker of the sheath stiffness.

Results: One hundred and seventy four children undergoing diagnostic or therapeutic surgical procedures were included in this study. ONSD measurement demonstrated good correlation with ICP across the entire patient cohort ($r = 0.66$, $p < 0.001$), but was better in children > 1 year or with a closed anterior fontanelle (AF) ($r = 0.7$, $p < 0.001$). Age above and below 1 year was found to be an appropriate age threshold for defining two different sets of ONSD cut-off values. The study however, supported using patency of the AF as a stronger clinical marker for describing different ONSD cut-off values in children. The second part of this work described a dynamic technique for analysing the pulsatile

motion of the ONS. Analysis of the deformability index (DI) as an indirect marker of ONS stiffness, revealed a statistically significant relationship with ICP (sensitivity of 90%, specificity of 87% for detecting $ICP \geq 20$ mmHg).

Conclusion: Measurement of the ONSD is a sensitive surrogate marker of raised ICP, but demonstrated poorer specificity. This relationship was more reliable in older children, particularly when the AF was closed. Analysis of the dynamic characteristics of the ONS appeared to provide useful additional information as an independent marker, and may contribute to our overall understanding of ONSD measurement in raised ICP.

Acknowledgements

This work was inspired by the children we work with and the environment we work in, and has only been possible because of them. There is no scarier prospect than handing over the care of your child to someone else. I am eternally grateful for the privilege of being involved in the care of these children, and hope that this work will one day grow to make a small difference in the quality of care we offer. As is the nature of such work, it was a product of interactions between many individuals, disciplines and departments. I would like to acknowledge the important role each has played.

- My supervisor Professor Graham Fieggen who agreed to oversee this project from the very conception stages. For providing a calibre of guidance, support and insight that has become synonymous with great leadership.
- My co-supervisor Tormod Selbekk, who through countless Facetime chats listened to my ideas and helped to fashion them into a useful technique. Reidar Brekken who has spent hours analysing and re-analysing data to find ways of measuring parameters that were not previously thought of. I will always be thankful for your belief in a concept that was often difficult to quantify.
- My colleagues and mentors at the Red Cross War Memorial Children's Hospital (RCWMCH):
 - Professor Jonathan Peter for providing me with sage advice and warm wisdom. Professor Anthony Figaji for spreading what can only be called a contagious passion for research.
 - I would also like to thank Drs Nico Enslin, Mohammed Ben-Hussein, Ncedile Mankhala, Emma Wegoye, Tiago Morgado, Nqobile Thango, Daniel Ochieng and Ursula Rohlwink for each in their own way contributing a vital piece in this puzzle.
 - The radiology department at RCWMCH, Drs Tracy Kilborn, Nicole Wiesenthaler and Ebrahim Banderker for their compliance and flexibility in allowing me the use of 'our shared' ultrasound machine. I would specifically like to thank sonographers Helmien Grovè and Jane Dembe for fine tuning my technique in transorbital sonography, assisting me with ongoing technical expertise and necessary verification of the image quality.
 - Dr Gaelle Ramon and the team at the research office for their vital support and guidance during this often daunting process.
 - Dr. Felicia Padayachy, Dr. Vaishali Padayachy and Barbara Harris for tireless proofreading and editorial assistance

- Ushma Galal and Henri Carrara for their incredible support with the statistical analysis of the data.
- The anaesthetic team, especially Dr. Rebecca Gray for valuable advice and insight.
- Dr Travis Pollock for providing insight into the ocular findings related to raised ICP.
- The team of students both local and international whose curiosity and willingness to help have made a significant difference in getting this project done.
- The Harry Crossley Research Fellowship for the opportunity to travel abroad and expand my insight into a technique that, for neurosurgery is still quite new.

Dedication

This work is dedicated entirely to my most precious girls, who have provided me with inspiration, love, support, energy and comfort to embark on this journey, knowing full well that it would take time from them, a thesis is a selfish undertaking, but fortunately one that can be requited. For Vidya, Shreya, Vaishali and Inez, I am eternally indebted to you and will always be thankful....

*“Nothing that is worth doing can be achieved in our lifetime;
therefore we must be saved by hope.*

*Nothing which is true or beautiful or good makes complete sense in any immediate context of history;
therefore we must be saved by faith.*

*Nothing we do, however virtuous, can be accomplished alone;
therefore we must be saved by love.*

*No virtuous act is quite as virtuous from the standpoint of our friend or foe
as it is from our standpoint.*

Therefore we must be saved by the final form of love which is forgiveness.”

....Reinhold Neibuhr

TABLE OF CONTENTS

		Page
Abstract		III
Acknowledgements		V
Dedication		VII
Table of Contents		VIII
Abbreviations used		XII
List of tables		XVI
List of figures		XX
Chapter 1	Introduction	1
 SECTION A 		
Chapter 2	The eye as a window to the brain	5
2.1.	The optic nerve sheath: Anatomical concepts	7
2.2.	Transorbital ultrasound	16
Chapter 3	Methods of assessing intracranial pressure (ICP)	25
3.1.	Introduction	25
3.2.	Monitoring of ICP	26
3.3.	Invasive ICP monitoring	27

3.4.	Limitations of invasive ICP monitoring	31
3.5.	Non-invasive assessment of ICP	32
3.6.	Discussion	50
Chapter 4	Measurement of ONSD as a non-invasive marker of ICP	51
4.1.	Studies in children	53
4.2.	Adult studies	68
SECTION B		
Chapter 5	The relationship between ONSD measurement and invasively measured ICP in children: <i>Methodology</i>	98
5.1.	Introduction	98
5.2.	Aims of the study	99
5.3.	Methods	100
Chapter 6	The relationship between ONSD measurement and invasively measured ICP in children: <i>Results, discussion and conclusion</i>	107
6.1.	General and demographic data, repeatability, observer variability and correlation testing	108
6.2.	Relationship between ONSD measurement and ICP over the entire patient cohort	122

6.3.	Relationship between ONSD measurement and ICP: using described age-related thresholds for defining ONSD cut-off values in children	130
6.3.1.	Children under 1 year old	131
6.3.2.	Children over 1 year old	136
6.3.3.	Subcategory analysis of children over 1 year old	144
6.4.	The relationship between ONSD measurement and ICP using patency of the anterior fontanelle to describe cut-off values in children	148
6.4.1.	Patients with an open anterior fontanelle	149
6.4.2.	Patients with a closed anterior fontanelle	154
6.5.	Discussion	161
6.6.	Conclusion	171
SECTION C		
Chapter 7	Dynamic assessment of the optic nerve sheath	172
7.1.	Theoretical background	172
7.2.	Relationship between pulsatile dynamics of the optic nerve sheath and ICP: an exploratory in-vivo investigation	177

7.2.1.	Introduction	177
7.2.2.	Methodology	178
7.2.3.	Results	184
7.2.4.	Discussion	190
7.2.5.	Conclusion	194

SECTION D

Chapter 8	Perspective and future direction	195
Appendices		198
Reference list		216

Abbreviations used

ARDS	adult respiratory distress syndrome
ACA	anterior cerebral artery
AF	anterior fontanelle
ALARA	as low as reasonably achievable
AMS	acute mountain sickness
ANOVA	analysis of variance
AUC	area under the curve
AUROC	area under the receiver operating characteristic curve
AVEAx	average of measurements in the axial plane
AVESag	average of measurements in the sagittal plane
BMI	body-mass-index
CA	Cronbach's alpha statistic
CBF	cerebral blood flow
CBV	cerebral blood volume
CCT	cranial CT
CDI	colour Doppler imaging
CNS	central nervous system
CPC	cerebral performance category
CRA	central retinal artery
CRV	central retinal vein
CSF	cerebrospinal fluid
CT	computerised tomography
DBP	diastolic blood pressure
DI	deformability index
DM	diabetes mellitus
DPOAEs	distortion product otoacoustic emissions
ED	emergency department
EFSUMB	European Federation of Societies for Ultrasound in Medicine and Biology
EICP	elevated ICP
EP	emergency physician

ETD	eyeball transverse diameter
ETCO ₂	end tidal carbon dioxide
ETT	endotracheal tube
ETV	endoscopic third ventriculostomy
EVD	external ventricular drain
FDA/CDRH	Food and Drug Administration Center for Devices and Radiological Health
GCS	Glasgow Coma Scale
GOS	Glasgow Outcome Score
GWR	grey matter-to-white matter ratio
ICA	internal carotid artery
ICH	intracerebral haemorrhage
ICP	intracranial pressure
ICU	intensive care unit
IIH	idiopathic intracranial hypertension
IOP	intraocular pressure
IPI	intracranial pressure index
IQR	interquartile ranges
IV	Intravenous
LEAx	left eye axial plane
LESag	left eye sagittal plane
LLS	Lake Louise Score
LP	lumbar puncture
MABP	mean arterial blood pressure
MAP	mean arterial pressure
MRI	magnetic resonance imaging
MS	multiple sclerosis
NF	Neurofibromatosis
NIRS	near infrared spectroscopy
NPV	negative predictive value
OA	ophthalmic artery
OAE	otoacoustic emission
OCT	optical coherence tomography

ON	optic nerve
OND	optic nerve diameter
ONS	optic nerve sheath
ONSD	optic nerve sheath diameter
ONUS	optic nerve ultrasound
OR	odds ratio
OSASW	orbital subarachnoid space width
oVEMP	ocular vestibular evoked myogenic potential
PCC	Pearson's correlation coefficient
PD	Parkinson's disease
PI	pulsatility index
PPV	positive predictive value
REAx	right eye axial plane
RESag	right eye sagittal plane
RI	resistance index
ROC	receiver operating characteristic
RTT	Rotterdam teletransducer
rSO ₂	regional cerebral blood oxygen saturation
SAH	Subarchnoid haemorrhage
SAS	subarachnoid space
SBP	systolic blood pressure
SD	standard deviations
SLT	scanning laser tomography
SPU	septum pellucidum undulation
STROBE	strengthening the reporting of observational studies in epidemiology
SVP	spontaneous venous pulsations
TBI	traumatic brain injury
TCD	transcranial Doppler
TMD	tympanic membrane displacement
TS	tuberous sclerosis
VPS	ventriculo-peritoneal shunt
VEP	visual evoked potentials

vODM	venous ophthalmodynamometry
VOP	venous outflow pressure
VPS	ventriculo-peritoneal shunt
yo	year old

List of tables	Page
Chapter 2	
Table 2.1. Anatomical regions and indications for ocular ultrasound	20
Chapter 3	
Table 3.1. Invasive ICP monitoring techniques	30
Table 3.2. Non-invasive ICP monitoring techniques: Transorbital methods	38
Table 3.3. Non-invasive ICP monitoring techniques: Methods utilising the auditory canal	40
Table 3.4. Non-invasive ICP monitoring techniques: Methods based on fluid dynamic properties	44
Table 3.5. Non-invasive ICP monitoring techniques: Electrophysiological techniques	46
Table 3.6. Non-invasive ICP monitoring techniques: Imaging techniques	49
Chapter 4	
Table 4.1. Ultrasound-based paediatric studies supporting the use of ONSD measurement	57,58
Table 4.2. MRI-based paediatric studies supporting the use of ONSD measurement	62
Table 4.3. Paediatric studies not supporting the use of ONSD measurement	65
Table 4.4. Adult studies supporting the use of ONSD measurement (non-invasive ICP measurement)	72,73
Table 4.5. Adult studies supporting the use of ultrasound measurement of the ONSD (invasive ICP measurement)	79-81
Table 4.6. MRI-based adult studies supporting the use of ONSD measurement	86
Table 4.7. CT-based adult studies supporting the use of ONSD measurement	91

Chapter 6

Table 6.1. Demographic details	109
Table 6.2. Haemodynamic and physiological parameters	110
Table 6.3. LESag values	111
Table 6.4. RESag values	113
Table 6.5. LEAx values	114
Table 6.6. REAx values	115
Table 6.7. Inter-observer variability	117
Table 6.8. AVESsag vs AVEAx ONSD measurements	119
Table 6.9. Right vs Left eye ONSD measurements	121
Table 6.10. Unadjusted and adjusted models for the relationship between ONSD and ICP	124
Table 6.11. Age, ICP and ONSD for specific aetiological groups	125
Table 6.12. Diagnostic accuracy of ONSD for predicting ICP ≥ 20 mmHg in different aetiological groups	125
Table 6.13. Age, ICP and ONSD for ICP dichotomized at 15 mmHg	126
Table 6.14. Age, ICP and ONSD for ICP dichotomised at 10 mmHg	127
Table 6.15. Age, ICP and ONSD for ICP dichotomized at 5 mmHg	128
Table 6.16. Summary of ONSD cut-off values at different ICP thresholds for all patients	129
Table 6.17. Age, ICP and ONSD for ICP dichotomised at 20 mmHg in children ≤ 1 year old	131
Table 6.18. Age, ICP and ONSD for ICP dichotomised at 15 mmHg in children ≤ 1 year old	133
Table 6.19. Age, ICP and ONSD values for ICP dichotomised at 10 mmHg in children ≤ 1 year old	134
Table 6.20. ONSD cut-off values for predicting ICP readings of 20, 15, 10 and 5 mmHg in children ≤ 1 year old	135

Table 6.21. Age, ICP and ONSD values for ICP dichotomised at 20 mmHg in children > 1 year old	137
Table 6.22. Age, ICP and ONSD values for ICP dichotomised at 15 mmHg in children > 1 year old	139
Table 6.23. Age, ICP and ONSD values for ICP dichotomised at 10 mmHg in children > 1 year old	140
Table 6.24. Age, ICP and ONSD values for ICP dichotomised at 5 mmHg in children > 1 year old	141
Table 6.25. ONSD cut-off values for detecting ICP at thresholds of 20, 15, 10 and 5 mmHg	142
Table 6.26. ONSD cut-off values for detecting ICP \geq 20 mmHg in children \leq 1 year and > 1 year old	142
Table 6.27. ONSD cut-off values for detecting ICP at various thresholds using age at 1 year as a dichotomy point	143
Table 6.28. Summary of patient data at different ICP thresholds	144
Table 6.29. Diagnostic accuracy of ONSD in age category > 1 and \leq 4 years old	145
Table 6.30. Summary of patient data at different ICP thresholds	146
Table 6.31. ONSD cut-off values for various ICP thresholds in patients aged > 4 years	146
Table 6.32. ONSD cut-off values for different ICP thresholds within the various age categories	147
Table 6.33. Age, ICP and ONSD for ICP dichotomised at 20 mmHg in children with an open AF	150
Table 6.34. Age, ICP and ONSD values for ICP dichotomised at 15 mmHg in children with an open AF	152
Table 6.35. Age, ICP and ONSD values for ICP dichotomized at 10 mmHg in children with an open AF	152
Table 6.36. Diagnostic accuracy of ONSD cut-off values for ICP at thresholds of 20, 15, 10 and 5mmHg in children with an open AF	153
Table 6.37. Age, ICP and ONSD values for ICP dichotomsied at 20 mmHg in children with an closed AF	155
Table 6.38. Age, ICP and ONSD values for ICP dichotomisd at 15 mmHg in children with a closed AF	157

Table 6.39. Age, ICP and ONSD values for ICP dichotomized at 10 mmHg in children with a closed AF	158
Table 6.40. Age, ICP and ONSD for ICP dichotomised at 5 mmHg in children a closed AF	159
Table 6.41. Diagnostic accuracy of ONSD measurement for detecting ICP at various thresholds in children with a closed AF	160
Table 6.42. ONSD cut-off values for different ICP thresholds in patients with an open and closed AF	160
Table 6.43. ONSD cut-off values in children > 1 year old and children with a closed AF	169

Chapter 7

Table 7.1. Patient data	184
Table 7.2. Results from analysis of all included datasets	186
Table 7.3. Results from analysis where datasets with out-of-plane motion (grade 2) were excluded	188

List of Figures

Chapter 2

Figure 2.1. Axial ultrasound image of the eye.	17
Figure 2.2. Ultrasound image showing the ONS.	18
Figure 2.3. Generously applied coupling gel over transparent protective dressing	22
Figure 2.4. Axial imaging	23
Figure 2.5. Sagittal imaging	23

Chapter 4

Figure 4.1. Axial ultrasound image of ONS	56
Figure 4.2. Ultrasound image with ONSD measurement	56
Figure 4.3. Axial T2-weighted MRI showing ONSD measurement	61
Figure 4.4. Axial CT scan demonstrating the ONS	90

Chapter 6

Figure 6.1. Box-whisker plot of the mean values of each LESag reading	112
Figure 6.2. Box-whisker plot of the mean values of each RESag reading	113
Figure 6.3. Box-whisker plot of the mean values of each LEax reading	114
Figure 6.4. Box-whisker plot of the mean values of each REax reading	115
Figure 6.5. Scatterplot for intra-observer reliability	116
Figure 6.6. Box-whisker plot: measurement 1 (R1) and measurement 2 (R2) (measurement 1 vs measurement 2)	116
Figure 6.7. Box-whisker: observer 1 and observer 2	117
Figure 6.8. Bland-Altman plots. Outer solid lines represent limits of agreement (mean \pm 1.96 times standard deviation, central line depicts the mean of differences).	118

Figure 6.9. Scatter plot: Observer 1 vs Observer 2	118
Figure 6.10. Box-whisker plot AVESag and AVEAx	119
Figure 6.11. Scatter plot of AVESag vs AVEAx	119
Figure 6.12. Scatterplot mean sagittal ONSD vs ICP	120
Figure 6.13. Scatterplot mean axial ONSD vs ICP	120
Figure 6.14. Scatter plot of right eye vs left eye	121
Figure 6.15. Scatterplot of mean ONSD against ICP for entire patient cohort	122
Figure 6.16. Box-whisker graph of ONSD for ICP < 20 mmHg (0), and \geq 20 mmHg (1)	123
Figure 6.17. AUROC for ONSD of 0.55 cm to predict ICP \geq 20 mmHg	123
Figure 6.18. Scatterplot of ONSD vs ICP for children \leq 1 year old	132
Figure 6.19. Box and whisker plot of ONSD for ICP < 20 mmHg (0) and ICP \geq 20 mmHg (1) in children \leq year old	132
Figure 6.20. AUROC for ONSD to detect ICP \geq 20 mmHg in children \leq 1 year old	133
Figure 6.21. Scatterplot of ONSD vs ICP in children > 1 year	136
Figure 6.22. Box and whisker plot of ONSD for ICP < 20 mmHg (0) and ICP \geq 20 mmHg (1) in children > 1 year old	138
Figure 6.23. AUROC for ONSD to detect ICP \geq 20 mmHg in children > 1 year old	138
Figure 6.24. Scatterplot for ONSD vs ICP in patients with an open AF	149
Figure 6.25. Box-whisker plot of ONSD for ICP < 20 (0), and \geq 20 mmHg (1)	150
Figure 6.26. AUROC of ONSD for detecting ICP \geq 20 mmHg	151
Figure 6.27. Scatterplot for ONSD vs ICP in patients with a closed AF	154

Figure 6.28. Box-whisker plot of ONSD for ICP < 20 (0), and ≥ 20 mmHg (1) 155

Figure 6.29. AUROC of ONSD for detecting ICP ≥ 20 mmHg 156

Chapter 7

Figure 7.1. Formula for defining the deformability index (Δ) 178

Figure 7.2. Axial ultrasound image with different magnification. Gray-scale pattern, tracked from time frame to time frame. 180

Figure 7.3. Transorbital ultrasound images magnified, demonstrating d_{Left} and d_{Right} 181

Figure 7.4. Illustration of the image processing in patient with ICP < 20 mmHg and ICP ≥ 20 mmHg 182

Figure 7.5. Curves superimposed 182

Figure 7.6. Box and whisker plot: DI in ICP < 20 mmHg (high ICP) and ≥ 20 mmHg (normal ICP) 189

Figure 7.7. Receiver operator curve for a cut-off value of $\Delta = 0.121$ 189

Figure 7.8. Illustrating the effect of out-of-plane motion 193

Chapter1.

Introduction

Diagnosing neurological disease in children is a formidable challenge for modern medical practitioners, given the spectrum of conditions and the wide array of clinical presentation. The presenting features of most paediatric neurosurgical conditions are often due to an increase in ICP, a condition where early diagnosis is critically important.

The current standard of care for diagnosing raised ICP involves intracranial placement of an invasive monitoring device. This technique has the distinct benefit of providing continuous, real-time monitoring, but is generally limited to patients in a neurocritical care or high care unit.^{1,2} Disadvantages of invasive ICP monitoring include the risk of haemorrhage, infection and catheter misplacement.^{3,4} The ideal ICP monitor would therefore be non-invasive, portable, easy to use, cost effective and allow for continuous monitoring.

There has been a longstanding quest for a reliable, non-invasive technique to assess ICP. In children specifically, decreasing the radiation exposure from repeat computerised tomography (CT) scans, the potential to avoid unnecessary invasive diagnostic surgical procedures and the possibility of improving early detection have been the key elements supporting this avenue of research. The opportunity to make the diagnosis of raised ICP earlier using an appropriate non-invasive technique, makes the applicability of such a method broader than just neurocritical care patients. Despite several promising advances, no single non-invasive method of assessing ICP has been accurate enough as a quantitative measure of ICP to replace invasive monitoring.⁴

The use of ultrasound as a diagnostic and navigation modality in neurosurgery has historically been limited by poor image quality and bulky probes.⁵ Despite the fact that one of the earliest descriptions of ultrasound as a diagnostic tool in medicine involved the attempted diagnosis of a brain tumor,^{6,7} this modality has enjoyed limited use in neurosurgery. However, recent advances in image quality and development of novel techniques have stimulated a resurgence in the use of this modality within neurosurgery,

both as a diagnostic and intra-operative navigation tool.^{7,8,9} The obvious benefit of being radiation-free, portable, widely available and relatively cost effective, makes this modality very appealing,^{10,11} especially in a resource-limited environment.

The diagnostic application of ultrasound in neurosurgery has also been limited by the poor acoustic properties of the bony skull.⁷ In children, use of the AF as a sonographic window has been widely described.^{12,13} The accessible, natural bony windows in the human skull, i.e. orbit, auditory canal and AF (neonates), can potentially allow access to important information about the brain and ICP. In particular, the eye has served as a natural window to the brain, allowing insight into a variety of neurological and other systemic conditions.^{14,15} Transorbital ultrasound measurement of the ONSD as a surrogate marker of raised ICP has enjoyed increasing interest recently.¹⁶⁻²⁷ The direct cerebrospinal fluid (CSF) connection between the peri-optic and intracranial subarachnoid spaces, make this technique a particularly appealing option for assessing ICP.²⁸ This appeal is further enhanced by the favourable acoustic properties and superficial anatomical location of the eye, making it very suitable for transorbital sonographic assessment of the ONS.

1.1) Scope of the thesis

This study investigates the relationship between measurement of the ONSD using a high frequency, small footprint, transorbital ultrasound probe and invasively measured ICP, in a paediatric patient cohort. The goal of validating and defining optimal ONSD cut-off values for detecting raised ICP in children is best approached by comparing this technique to the current ‘gold standard’, which is invasive ICP measurement. In children, this requires evaluating age-related recommendations for defining ONSD cut-off values. The described age thresholds range between 1 year and 4 years old (28-34). This study has therefore used the following age categories for this evaluation, i) ≤ 1 year old, ii) ≥ 1 year old, iii) subcategory analysis of ages 1 to ≤ 4 years and > 4 years old, to for comparison with current literature.²⁸⁻³⁴ The diagnostic accuracy of ONSD measurement was investigated within these age categories, to describe the nature of the ONS response at ICP thresholds of 20 mmHg, 15 mmHg, 10 mmHg and 5 mmHg. An alternative

physiological and anatomical marker, viz patency of the AF, was also assessed as a potential clinical marker for defining different ONSD cut-off values in children. Physiological and demographic factors which may influence this relationship have been analysed for significance.

The elastic nature of the ONS has been described as a significant factor in the ability of the ONS to distend when subjected to increasing ICP. Using a dynamic imaging technique, the final part of this work describes an analysis of the pulsatile motion of the ONS as a potential marker of its stiffness.

1.2) Outline of the thesis

SECTION A

This section provided an overview of the relevant anatomical and sonographic features of the eye that allow transorbital sonographic ONSD measurement. The current measurement techniques for ICP, their underlying principles, benefits and shortcomings and a specific review of the literature describing ONSD measurement in children and adults, are included here.

SECTION B

This section described the working hypothesis, aims and methodology. The results are presented in age-related categories and also use of the AF as a clinical marker for describing different ONSD cut-off values at various ICP thresholds, followed by a discussion of the results.

SECTION C

This section discussed the available literature using ‘dynamic’ assessment of the ONSD, and its association with ICP. Novel data is presented using a technique that analyses the dynamic pulsatile motion of the ONS to describe an index termed the deformability index (DI). These data were analysed in two groups of patients with ICP above and below 20 mmHg.

SECTION D

This section provided an overview of the study findings, placing them in perspective of current literature and described future directions for the development of this work.

SECTION A

Chapter 2.

The eye as a window to the brain

The eye as a window to the soul is an ancient philosophical concept that can be dated all the way back to the biblical era. In particular the size of the pupil has been linked to levels of excitement and arousal.^{35,36} This realization was perhaps best illustrated by Italian women in medieval times who used drops from the dangerous night shade plant (later called ‘belladonna’) to artificially dilate their pupils in an effort to make themselves appear more attractive. This proved to be quite a dangerous practice, and was later abandoned, but certainly highlighted their recognition of the eye not only as an organ facilitating vision, but also as a window into our hidden thoughts and emotions.

These underlying principles were advanced upon in 1964 by the famous psychologist Eckhardt Hess. In his seminal work, Hess provided evidence that the eye is a valuable tool in evaluating mental processes.³⁷ This work was built on by others who demonstrated convincingly that the pupillary response of the eye is linked to cognitive function, a field of study eventually called ‘cognitive pupillometry’.³⁸⁻⁴³

The abstract value of the eye as a window into the soul and mind is of great interest, but as physicians our focus tends to be more on the physical benefit of this natural window to the brain. The ocular manifestation of systemic diseases including diabetes mellitus (DM), hypertension, cardiac disease and neurofibromatosis (NF) have been well described.^{14,44} Examination of the eye specifically as a non-invasive method for detecting underlying disease of the central nervous system (CNS) remains a very attractive option for neurodegenerative diseases like multiple sclerosis (MS), Parkinson disease (PD) and stroke.¹⁵

The description of oedema of the optic disc as a consequence of increased ICP was first made by von Graefe in 1860.^{45,46} By inflating balloons placed in the subdural space of

rhesus monkeys to increase ICP, Hayreh described an increase of CSF in the ONS as being 'essential for the development of oedema of the optic disc'.⁴⁶ Subsequent work has indicated that enlargement of the ONS in conditions of raised ICP may actually precede oedema of the optic disc.²⁹⁶ Several authors have since described a strong association between enlargement of the ONS and an increase in ICP.^{17,28,47-51}

This work describes the relationship between transorbital sonographic measurement of the ONSD and invasively measured ICP. A discussion of the relevant anatomic details is necessary as the structure of the ONS is fundamental to its ability to distend as ICP increases and its relation to the bony optic canal is very important in determining the CSF flow within the ONS.^{46,52,53} The relevant vascular anatomy described has significant impact in SECTION C of this work which involves analysis of the dynamic pulsatile motion of the ONS, a direct consequence of the anatomical relationship between the ONS and the arteries in proximity to it. The sonographic features of the ONS, the measurement technique and safety standards are also discussed below.

2.1. The optic nerve sheath (ONS): Anatomical concepts

The ONS complex is composed of:

- 2.1.1 the optic nerve (ON)
- 2.1.2 the subarachnoid space between the optic nerve and sheath
- 2.1.3 the optic nerve sheath (ONS)
- 2.1.4 blood vessels within the optic nerve sheath complex.

2.1.1. The optic nerve (ON)

The optic nerve has a length of about 40 – 50 mm, and an average diameter of about 4 mm. This nerve is a white matter tract of the central nervous system that originates from within the diencephalon. It grows anteriorly and laterally extending through the optic canal and into the orbit. The optic nerve itself is surrounded by CSF within the subarachnoid space and enveloped by the ONS, which is a continuation of the intracranial dura mater. Anatomically the ON can be divided into 4 parts: an intra-ocular segment, an intraorbital segment, an intracanalicular segment and an intracranial segment.

2.1.1.1 *The intraocular segment* (optic nerve head) of the optic nerve measures about 1 mm in length and is 1.5 – 1.8 mm in diameter. It is composed of the lamina cribrosa, prelaminar region and surface nerve layer, and is the shortest segment of the ON. The mode of insertion of the ON into the eyeball and the shape of the sclera canal determine the shape of the optic disc.⁵⁴ This shape is important for interpreting ophthalmoscopic findings.

2.1.1.2. *The intraorbital segment* extends from the eyeball to the optic canal. It is surrounded by the meningeal sheath consisting of dura, arachnoid and pia mater, and CSF within the subarachnoid space. It is 20 – 30 mm in length and has about 6 mm of slack to accommodate orbital movements.⁴⁶ The central retinal artery perforates the optic nerve

with its accompanying vein and runs within the optic nerve to the retina. This part of the optic nerve has longitudinal and transverse connective tissue septae, which contain blood vessels. The pia mater has a dense vascular plexus on the surface of the orbital optic nerve. The ophthalmic artery lies in close proximity to the optic nerve, initially inferolateral, then usually crosses over the nerve to lie supero-medial to the ON. As the nerve enters the optic canal, the surrounding dural sheath becomes continuous with the dural lining of the orbit and optic canal. The orbital segment of the optic nerve is subdivided into a bulbar segment that is adjacent to the globe and a mid-orbital segment, connecting the bulbar to the intracanalicular component.⁵⁴

2.1.1.3. *The intracanalicular segment* lies in the bony optic canal, surrounded by the meningeal sheath. The ophthalmic artery lies below and lateral to the ON.

2.1.1.4. *The intracranial segment* is about 10 mm in length and culminates in the optic chiasm. The ON lies above the diaphragma sellae initially, then above the cavernous sinus, and is in close relation to the ophthalmic artery inferolaterally, ICA laterally and ACA superiorly.

2.1.2. The subarachnoid space between the optic nerve (ON) and optic nerve sheath (ONS)

The ONS itself has a thickness of 0.4 mm, with the subarachnoid compartment estimated at 0.1 – 0.2 mm in width.⁴⁹ The subarachnoid space surrounding the optic nerve is a heterogeneous, blind-ending (cul de sac) space, which holds about 0.1 ml of CSF.^{52,53}

In the bulbar segment, the enlarged subarachnoid space contains a trabeculated network anchored between the pial and arachnoid layers. These trabeculae are composed of leptomeningeal cells and delicate collagenous fibrils; occasionally they contain one or two blood vessels. In the mid-orbital segment the subarachnoid space is distinctly smaller, containing numerous broad septae and pillars connected through large perforations. These septae and pillars contain leptomeningeal cells and numerous collagen fibrils.

In the intracanalicular segment the subarachnoid space is largely continuous, with one or two larger pillars.^{49,53} The hydrodynamics of CSF within the subarachnoid space surrounding the optic nerve is therefore quite complex. The series of compartments and septae, as well as the ‘cul de sac’ anatomy of the ONS impact not only on the dynamics of the flow but also on the direction of CSF flow which may not follow the same principles as fluid travelling within an ideal tube.⁵³

Direct communication between the perioptic subarachnoid space and the chiasmatal cistern has been demonstrated.^{46,55} CSF pressure could build up in this perioptic subarachnoid space if CSF were forced unidirectionally into this compartment via the chiasmatal cistern due to an increase in ICP.

These findings are especially relevant in this study as they explain to some degree the microstructure determining the expansile nature of the ONS. The description of a subarachnoid space that is widest at the bulbar segment and narrows progressively in the mid-orbital and intracanalicular segment of the ON, provides useful information on where it would be best to measure the diameter of the ONS.^{50,53}

2.1.3. The optic nerve sheath (ONS)

The sheath surrounding the optic nerve is made up of three layers, which are in continuity with the leptomeninges of the brain. In the optic canal the ON is attached to the surrounding dura by thick fibrous bands. At the apex of the orbit the ONS is attached to the annular tendon, to which the various recti muscles are attached. The two layers of the dura are attached within the optic canal, but split at the orbital end of the canal, with the outer layer forming the orbital periosteum and the inner layer forming the dural ONS.

The anatomy of the ONS in the optic canal is especially important as it functions effectively as the ‘access portal’ for CSF entering the ONS from the intracranial subarachnoid space SAS. The thick fibrous bands connecting the dura and pia in the optic canal hold the ON firmly in position, but also maintain the dura and optic nerve in close

proximity. The subarachnoid space is consequently reduced in size to virtually the size of a capillary.⁵⁴

According to Hayreh, the assumption that the bulbous appearance of the ONS was due to distension caused by an increase in ICP, was a contentious one. He initially suggested that the firm, non-elastic collagen fibers of the dural ONS were less capable of being stretched by an increase in CSF volume. This observation was based on experimental evidence from monkeys showing that the ONS was normally a distended space filled with CSF.⁴⁶

The anatomy of the sheath in the region of the optic canal plays a crucial role in the dynamics of CSF between the orbital ONS and the intracranial space. Communication between these two spaces is almost always present,^{54,56} but the percolation of CSF through this space determines the temporal response of ONS distension to an increase in ICP.

The dural sheath accompanies the ON from the optic canal to the sclera. The collagen fiber architecture of the ONS provides distinctive mechanical properties, as a 1 mm diameter collagen fiber is estimated to have a resistance of 10 kg.⁵⁷ The ONS can be divided into the intracranial, intracanalicular and intraorbital segments.

2.1.3.1. Intracranial segment

This is a very short segment formed by invagination of the cranial dura mater at the sphenoid planum at the level of the optic canal. This dural invagination forms the falciform ligament which is a few millimetres in length and does not adhere completely to the bone.

2.1.3.2. Intracanalicular segment

The relationship between the ONS and the bony and meningeal structures in the optic canal is important in understanding the movement of CSF between the intracranial and intra-orbital compartments.

Bony structures The optic canal guides the course of the ONS ventrally and laterally. The anterior clinoid process forms the lateral border of the optic canal, and is attached to the body of the sphenoid by two bony bridges, which form the roof and the floor of the optic canal.⁵⁸

Meningeal structures The dura mater covering the ventral surface of the clinoid process forms a ‘carotid-oculomotor membrane’ which is in contact with the ONS as the ophthalmic artery arises from the ICA.

2.1.3.3. Intraorbital segment

The important relations with this segment of the ONS are vascular and nervous elements. At the exit of the optic canal the ONS is a dense structure, giving rise to the annular tendon. The ONS runs within the orbital cone, together with the abducens nerve, nasociliary nerve, superior and inferior branch of the oculomotor nerve and the ophthalmic artery. The tissue surrounding the ONS is essentially adipose tissue. Five important structures cross the intraorbital segment of the optic nerve dorsally; these are the trochlear nerve, the frontal nerve, nasociliary nerve, the ophthalmic artery and the superior ophthalmic vein.

2.1.4. Blood vessels within the optic nerve sheath(ONS) complex

The arterial network within the ONS is quite intricate, but a working understanding of the anatomical relationship between the ON, the arterial network and the ONS is fundamental to interpreting the pulsatile dynamic response of the ONS described in SECTION C of this work. The following anatomical description is not intended to be exhaustive, but includes the relevant arterial anatomy within the ONS.

2.1.4.1. Arteries within the ONS

The ophthalmic artery (OA) is the first major branch of the intracranial segment of the ICA. It provides the principal arterial supply to the contents of the orbit. The OA arises from the medial border of the ICA, usually between the distal and proximal carotid ring. The origin of the OA determines whether it enters the orbit through the superior orbital fissure or the optic canal. The OA accompanies the optic nerve inferomedially in its sheath.^{58,59} Beyond the optic canal, it travels obliquely through the ONS to join the orbital apex, lateral to the ON. It gives off a recurrent branch in the optic canal which contributes to the vascular supply of the ON in the canal. The OA crosses the ONS dorsally, to lie between the medial rectus and superior oblique muscles before giving rise to the anterior and posterior ethmoidal arteries. It also gives rise to the lacrimal, ciliary, supraorbital, medial palpebral, infratrochlear and dorsal nasal arteries.

Perhaps the most significant branch of the OA, even though it is the smallest, is the central retinal artery, which enters the inferior surface of the ON at the junction between the anterior third and median third, about 20 mm from the optic canal following a short, serpiginous trajectory. It passes to the center of the optic nerve travelling up to the globe to supply the retina.

The intraorbital segment of the optic nerve derives its blood supply from the rich anastomotic network within the pia mater, supplied by the ciliary artery. The optic head is supplied by branches of the ophthalmic artery; multiple anastomoses between the 11 branches of the ophthalmic artery and the external carotid artery allow sufficient blood flow to the choroidal and central retinal arteries.

Within the orbit the OA supplies five major branches and the pial network:

- **The central retinal artery**

The first branch of the ophthalmic artery enters the optic nerve 8 -15 mm behind the globe and arborises in the retina. This end artery supplies the inner two-thirds of the retina and surface nerve layer of the optic nerve (these branches are seen on fundoscopy). It provides little to no vascular supply to the prelaminar, laminar and retrolaminar layers. The central retinal artery may rarely originate from the middle meningeal artery.⁶⁰

- **The posterior ciliary arteries**

The short ciliary branches arise from the ophthalmic artery as it crosses over the optic nerve. The OA divides into 10 – 20 branches as it moves around the optic nerve anteriorly, intertwining with branches of the short ciliary nerves. There are 6 – 8 short branches and 2 longer ones which extend anteriorly to the ciliary bodies and supply the choroid.

- **The lacrimal artery**

This branch extends laterally and anteriorly along the superior surface of the lateral rectus muscle and supplies the lacrimal glands, globe and muscle.

- **Terminal branches**

The terminal branches of the ophthalmic artery are the supratrochlear and supraorbital arteries, which lie superior and medial to the globe.

- **The circle of Zinn-Haller**

This is a rich vascular network, receiving branches from the short posterior ciliary arteries, including the recurrent pial branches and recurrent choroidal arteries.

- **The pial network**

This network is made up of small meningeal branches that come off the central retinal artery as it pierces the pia mater to form an extensive network of vessels.

2.1.4.2. Arterial supply of the optic disc

- **Lamina cribrosa**

Blood supply to this area is mainly from fine centripetal branches originating from the posterior ciliary arteries. Interestingly, the central retinal artery does not supply this region. The vessels lie in the fibrous septae of the lamina cribrosa and form a dense capillary network.^{54,61}

- **Prelaminar region**

This area is supplied mostly by centripetal branches from the peripapillary choroidal vessels, which are mostly end vessels and have little communication with other vessels. This region may also receive some supply from the vessels in the lamina cribrosa region. The central retinal artery does not usually contribute blood supply to this region.⁶¹

- **Surface of the optic disc**

This surface contains the main retinal vessels and a large number of capillaries, which are derived from branches of the retinal arterioles. In this part of the optic disc it is common to find vessels of choroidal origin derived from the prelaminar part of the optic disc which lies adjacent to it. These may enlarge to form the cilioretinal artery. The capillaries on the disc are all interconnected, mostly venous, draining into the central retinal vein or its tributaries. The arterial supply to all the retinal capillaries, except for the cilioretinal artery, comes from the central retinal artery. The blood supply pattern to the optic head is highly variable.⁶¹

2.1.4.3. Veins

Venous drainage of the optic nerve head is simpler than its arterial supply. The main venous drainage of the optic disc is carried out by the central retinal vein. The superior ophthalmic vein exits the orbit via the superior orbital fissure and drains into the cavernous sinus. The inferior ophthalmic vein drains into the pterygoid venous plexus via the inferior orbital fissure. There are numerous connections between these veins, which usually

accompany the arteries. The central retinal vein is susceptible to increased ICP transmitted through the CSF as it passes through the subarachnoid space.

There are no described lymphatic vessels or lymphoid tissue within the ONS.⁶¹

2.2. Transorbital ultrasound

2.2.1. Background

The first reported use of A-scan ultrasonography to examine the eye was performed by Mundt and Hughes in 1956.⁶³ The lack of anatomical detail and considerable operator experience required for A-mode ultrasound use limited the widespread use of the technique. The use of B-mode ultrasonography in ophthalmology was first described by Baum and Greenwood in 1958, using a water bath immersion technique.⁶⁴ This technique was later improved on by Bronson in 1972, who developed a contact method for using ultrasound which made the examination easier to perform on patients, and later became commercially available.⁶⁵ With further advances in the imaging quality of ultrasound technology, the indications for imaging the eye, orbit, optic nerve and its sheath began expanding.

Ossoinig initiated the 'standardised echography' concept, using A-mode scans, in clinical settings.⁶⁶ This early work describing imaging of the ONS was later followed by several important contributions supporting the technique of ONSD measurement using ultrasound.^{49,67,68} The early description of distension of the ONS as a consequence of an increase in CSF volume in the perioptic subarachnoid space due to raised ICP was made by Hayreh,^{46,69} stimulating later work on this topic.^{28,30,68}

Transorbital ultrasonography remains the quickest and simplest method of imaging the eye and the ONS. The additional benefits of real-time imaging and high spatial resolution make ultrasound the preferred imaging modality. The unique anatomy of the eye makes it ideal for ultrasound imaging for the following reasons⁷⁰ :

- It is a fluid-filled, superficial and easily accessible organ.
- The acoustically empty anterior chamber (defined by the structures anterior to the lens, extends from the cornea to the iris and contains the aqueous humour) and vitreous cavity make the outline of the normal structures of the eye clearly visible.
- Moving the transducer over the eye allows the ultrasound beam to reach all parts of the eye with the required close-to-perpendicular inclination.

- There is limited demand for depth penetration, requiring only 30 mm depth for the eye itself and 60 -70 mm for the orbital apex; this allows higher frequency probes than is feasible in other anatomical settings.
- The associated shorter wavelength allows better resolution, with the possibility of finer anatomical detail and tissue differentiation.



Figure 2.1. Axial ultrasound image of the eye.

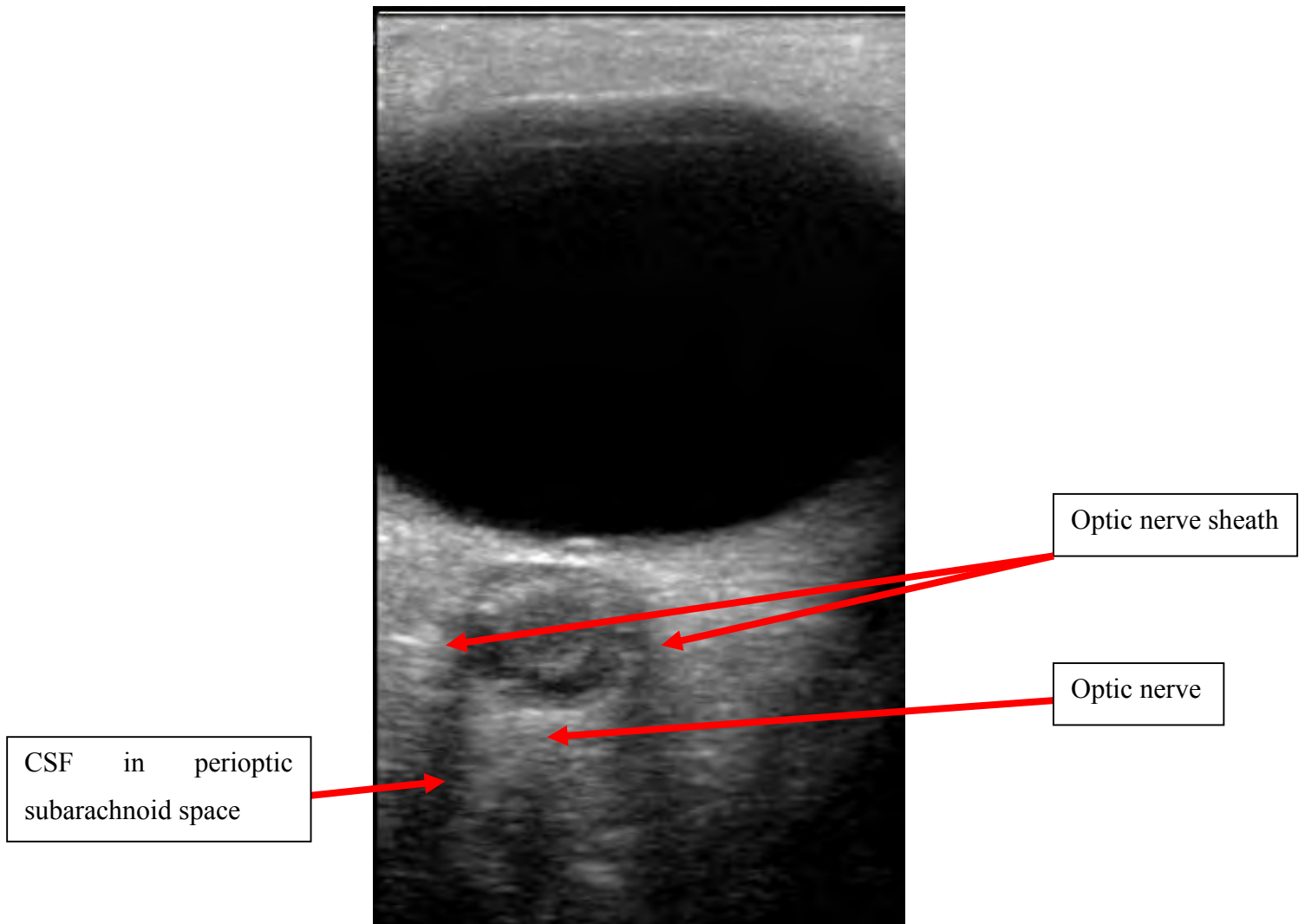


Figure 2.2. Ultrasound image showing the ONS.

2.2.2. Sonographic anatomy of the eye (Figures 2.1 and 2.2) :

- The cornea appears as an isoechoic layer, just below the soft tissue of the eyelids
- The anterior chamber is anechoic
- The posterior chamber (extends posteriorly from the iris to the posterior surface of the lens, also contains aqueous humour) is also anechoic
- The posterior chamber includes the ciliary body, which in cross section is seen as isoechoic triangles lateral to the lens
- The iris appears as linear echogenicities anterior and lateral to the lens
- The lens is mostly anechoic, except for a thin echogenic anterior and posterior rim
- The vitreous chamber which is the largest of the three chambers, contains vitreous humour and extends from the posterior surface of the lens to the ocular wall
- The retina, choroid and sclera (which form the walls of the vitreous chamber) are depicted as a single isoechoic layer
- The optic disk appears as a slight discoid protrusion in the vitreous
- The optic nerve is depicted as a hypoechoic band, posterior to the optic disk, surrounded by the echogenic retrobulbar fat
- Generally the anterior two thirds of the course of the ON can be seen sonographically
- The ONS surrounding the nerve is more echogenic

2.2.3. Indications for transorbital sonography

According to Brunell⁷¹ there are two clinical categories for the use of ophthalmic ultrasound, i) clinical diagnosis by ophthalmologists, and ii) in emergency departments for diagnosing ocular trauma and raised ICP. The use of ocular sonography has also been described by intensive care physicians as well as neurosurgeons for the non-invasive and early detection of raised ICP.^{16-18,30,72,73} The broader indications for ocular sonography are listed in Table 2.1. The specification of the ultrasound probes required for purely ophthalmological use are different to those used for measuring the ONSD.⁷¹

Anatomical region	Indication
Front of the eye	Foreign bodies
	Lens dislocation or subluxation
	Afferent pupillary defects
	Changes in the size of the anterior chamber
	Neoplastic lesions
Optic nerve	Increased ICP (measurement of the ONSD)
	Neoplastic lesions of the optic nerve and sheath
Vitreous	Retinal haemorrhage
	Retinal detachment
	Vitreous haemorrhage
	Vitreous detachment
	Lens dislocation
	Endophthalmitis
	Extraocular
Globe disruption	
Foreign bodies	
Artery/vascular	Central retinal artery occlusion
	Central retinal vein occlusion

Table 2.1. Anatomical regions and indications for transorbital ultrasound

2.2.4. Sonographic technique for imaging of the optic nerve sheath

2.2.4.1. Equipment

The ideal transducer is a linear array, high frequency (> 10 Mhz) probe, with a small footprint to allow adequate imaging of the orbit and its contents, especially in children. The size and shape of the orbit in smaller children is often a limiting factor to optimal image quality.⁷⁴ Although higher frequency transducers are available, in the range of 20 Mhz, their field of view is too limited to evaluate the entire globe. For the purpose of imaging the ONS, a small footprint, high frequency (> 10 Mhz) probe is recommended.

2.2.4.2. Patient positioning

Patients are usually positioned supine, with the head slightly elevated at about 30 degrees. This may vary however, depending on clinical history and age. It is preferable to place the ultrasound machine on the patient's right side and orient the probe so that the indicator is pointing towards the patient's head or toward the patient's right side.

2.2.4.3. Technique

A generous amount of coupling gel is applied over the closed upper eyelid (Figure 2.3). The transducer then can float over the layer of gel and won't come into direct contact with the patient's eyelid. The coupling gel optimises image quality and precludes any pressure being applied to the globe.⁷⁵ A protective transparent dressing can be placed over the closed eyelid in sedated or ventilated patients as an additional measure to prevent any irritation of the conjunctiva. The probe should be held with a pincer grasp between the thumb and index finger, using the remaining fingers for stability by resting them on the maxilla, supraorbital ridge or other bony structures (Figure 2.4). This technique is especially important to prevent any pressure being applied on the globe. The probe is usually placed over the temporal area of the upper eyelid for optimal visualisation of the ONS.⁷⁶

The depth should be adjusted to optimise the visualisation of the intended structures, i.e. the optic nerve, the surrounding CSF space and the ONS.

The gain should be adjusted to create a hypoechoic posterior chamber. If the gain is too high, echoic artefacts could lead to image distortion, and if the gain is too low, image quality can be inadequate. Most modern ultrasound machines have default settings to improve image quality in specific organs.

The eye should be examined in at least two planes: the axial or transverse plane, with the probe oriented in the horizontal, left to right direction; and the sagittal plane, which is imaged by rotating the probe and positioning it in a cranial to caudal orientation (Figures 2.3 and 2.4). The imaging should be performed in both eyes.^{77,78}

The mechanical index should always be adjusted lower than the recommended values for the eye, in order to limit the amount of energy absorbed by the eye (safety guidelines will be discussed below).

At energy levels used for diagnostic purposes, no known adverse effects have been described.^{76,77,78}



Figure 2.3. Generously applied coupling gel over transparent protective dressing



Figure 2.4. Axial imaging

Figure 2.5. Sagittal imaging

2.2.5. Safety of transorbital ultrasonography

The acoustic energy used for diagnostic purposes has no described adverse effects.^{77, 79} Despite stringent output standards for ocular exposure to diagnostic ultrasound, there is limited literature on the subject. The recent bioeffects and safety report by the American Institute of Ultrasound in Medicine (AIUM) makes no specific mention of the eye.⁸⁰ A recent review article provides a very helpful summary of the safety recommendations for transorbital sonography.¹⁵⁸ The United States Food and Drug Administration Center for Devices and Radiological Health (US FDA/CDRH) describes an output intensity limit for all eye exposure of 50 mW/cm^2 , recommending the use of a mechanical index (MI) < 0.23 , and a thermal index (TI) < 1 .⁸¹

The European Federation of Societies for Ultrasound in Medicine and Biology (EFSUMB)⁸² recommend that particular care should be taken to reduce the risk of thermal and non-thermal effects during investigations of the eye.⁸³ To eliminate potential injury to the eye it is recommended that ultrasound output power be kept as low as reasonably achievable (ALARA principle)^{79,84} without impeding the diagnostic quality of the examination, and that examination times be kept as short as possible.^{85,86,158} An equally important prerequisite is that transorbital sonographic ONS examination only be performed by operators adequately trained and experienced in performing the technique. The definition of an experienced operator differs, but this study defined an experienced operator as having performed more than 25 prior transorbital ultrasound examinations.²³

2.2.6. Shortcomings of transorbital ultrasonography

Ocular trauma or disease of the optic nerve complex precludes sonographic examination of the ONS. The technique requires a certain amount of training or experience, as novice users may be prone to erroneous measurement.²³ The artefactual shadow which is thought to be due to the poor insonation angle, has been described by some authors and often makes accurate and repeatable measurement of the echoic borders of the ONS unclear. The lack of consensus regarding the optimal ONSD cut-off value to detect raised ICP, has limited universal acceptance of the technique, despite a growing number of studies demonstrating a good relationship between ONSD and ICP. While the technique causes very minimal discomfort and is well tolerated by most patients, examination in small children can often be quite challenging.

Transorbital sonography of the ONS is a safe and effective technique for visualising the lamina cribrosa, optic nerve and its sheath. In our experience and that of numerous other authors, the technique is promising as a surrogate marker of raised ICP. There are no described adverse effects when the technique is performed by experienced operators, utilising correct equipment and according to safety recommendations.⁷⁸⁻⁸²

This study focussed on the use of transorbital sonography of the ONS to detect raised ICP, using thresholds of 20, 15, 10 and 5 mmHg in neurosurgical patients.

Chapter 3.

Methods of assessing intracranial pressure

3.1. Introduction

The early work by Guillaume and Janny in 1951,⁸⁷ followed by Lundberg's magnum opus in 1960⁸⁸ laid the foundation for monitoring of ICP. Several investigators have since made significant contributions in this field.^{60,89-98,122} The association between raised ICP and poor neurological outcome has been widely reported and has distinct clinical and therapeutic implications.^{90,100-102} Although some reports have questioned the merits of monitoring ICP,^{103,104} the role of invasive monitoring techniques in a neurocritical care environment as a diagnostic and therapeutic tool, especially in TBI are widely supported.^{92,99,105-108} Invasive ICP monitoring has the distinct benefit of allowing continuous, real-time analysis of the ICP waveform.⁸⁸

The benefits of reliably and non-invasively assessing ICP have also been described, and while invasive ICP monitoring remains the gold standard, development of accurate, non-invasive alternatives are ongoing.^{2,109} Perhaps the most significant benefit of a reliable non-invasive technique, lies in the promise of earlier detection of conditions where the clinical presentation of raised ICP may be subtle, a scenario perhaps most applicable to children.

In children determining the threshold for raised ICP is complex because of the variation in physiological norms associated with different ages. Lower ICP treatment thresholds for younger children are often considered appropriate, but there is still a lack of data to support this. The current recommendation in the guidelines for acute medical care of severe traumatic brain injury in neonates, children and adolescents is a treatment threshold of 20 mmHg for children recommendations.^{110,111} These guidelines don't make any age-specific recommendations. As children are a heterogeneous group with significant age-related physiological and anatomical variation, there are likely to be differences in ICP treatment thresholds within children. Chambers et al. described age-related ICP thresholds of 2 to 6

years – 6 mmHg, 7 to 10 years – 9 mmHg and 11 to 15 years – 13 mmHg.⁹⁵ An ICP threshold of 20 mmHg demonstrated a significant correlation with outcome in children with traumatic brain injury⁹⁴. It is possible that cerebral herniation occurs at intracranial pressures < 20 – 25 mmHg, depending on the type and location of the intracranial space occupying lesion. It therefore remains specifically relevant to interpret any recommended ICP threshold in the context of clinical presentation, monitoring of physiological variables (where appropriate) and imaging findings in an individual patient. Recommendations that account for age-related ICP thresholds would be ideal.

3.2. Monitoring of ICP

There is still no ideal method for evaluating ICP. While the benefit of continuous, real-time monitoring provided by invasive ICP monitoring is clear, it comes with distinct limitations, and the appeal of non-invasive ICP monitoring lies in obviating the need for placement of an intracranial device, and avoidance of the risks associated with these procedures. However, current non-invasive ICP monitoring techniques have the limitation of inadequate accuracy^{4,109} for detecting elevated ICP. Most non-invasive techniques are able to provide qualitative estimates of ICP, but lack quantitative value. The benefits and limitations of invasive and non-invasive ICP monitoring are discussed below.

3.3. Invasive ICP monitoring

Invasive ICP monitoring devices are either fluid-coupled or non-fluid-coupled and can be further classified according to the anatomical compartment into which they are placed.

These include:

- 3.3.1 Intraventricular monitoring
- 3.3.2 Intraparenchymal monitoring
- 3.3.3 Subdural monitoring
- 3.3.4 Extradural monitoring
- 3.3.5 Telemetric ICP monitoring
- 3.3.6 Spinal monitoring

3.3.1. Intraventricular monitoring

Insertion of an external ventricular drain (EVD) and measurement of the cerebrospinal fluid CSF pressure is still considered the ‘gold standard’ technique for monitoring ICP.^{88,92} This is a fluid-coupled system, consisting of a catheter placed into the lateral ventricle and connected to a fluid-filled column, which transmits the ventricular pressure to an external strain gauge.¹¹² The opportunity to transduce the pressure readings for continuous monitoring as well as the added benefit of being able to release CSF when ICP is elevated, make this method very appealing as a diagnostic and therapeutic option. Calibration of the system is very simple once it is properly zeroed at the level of the external auditory meatus.

A limitation to placement of a ventricular catheter in raised ICP, is ventricular compression or anatomical distortion, which can make accurate insertion into the ventricle quite challenging. As a fluid filled system, blood or debris in the ventricle can cause obstruction. The main risks associated with EVD placement are infection and haemorrhage. The risk of infection starts to increase after day 5 post-insertion, and is reported as between 1 and 11%.¹¹³⁻¹¹⁵ The risk of haemorrhage from EVD placement is quite low, described as 1.1%, with a 0.5% incidence of clinically significant haematoma.¹¹⁶

3.3.2. Intraparenchymal monitoring

The use of intraparenchymal, fibre-optic, microtransducer probes to monitor ICP has increased significantly.^{2,92,112,117-119} These transducers are usually placed and secured using a twist drill and skull bolt, but can also be placed freehand via a burr hole. The transducers must be calibrated according to the manufacturer specifications, i.e. either in air or water, prior to insertion. These devices have a lower rate of infection and haemorrhage than EVD placement.^{3,114,120-121}

A limitation with microtransducer monitoring is the drift of the readings over time, described as being about 2.1 mmHg over five days.^{123,124} Generally these microtransducers cannot be re-zeroed; however, pneumatic transducers such as the Spiegelberg transducer may be zeroed in-vivo at set time intervals.⁹⁵ Variation in the correlation between fibre-optic microtransducer readings and transduced EVD readings has been reported.^{125,126} The use of invasive, intraparenchymal ICP monitoring is generally limited to neurocritical care or high care units.

3.3.3. Subdural monitoring

The placement of microtransducer probes in the subdural space requires burr hole and freehand placement, as bolt insertion precludes placement into this space. The indications are similar to intraparenchymal placement, but potentially carry a lower risk of intraparenchymal haemorrhage.

3.3.4. Extradural monitoring

The main concern with placement of probes in the extradural space remains poor reliability. This is thought to have somewhat improved, but the level of accuracy remains unclear.⁹²

3.3.5. Telemetric (Implantable) ICP monitoring

Implantable ICP monitors with a catheter-tip transducer connected to a telemetry unit implanted in a skin pouch outside the cranium have been used for long-term ICP monitoring. This technique has the particular advantage of providing continuous data on ICP patterns and has gained increasing interest,¹²⁷ particularly in patients with complicated CSF dynamic disturbances, where repeat invasive pressure monitoring may be required.¹²⁸

3.3.6. Lumbar spinal monitoring

In the neurocritical care setting lumbar CSF pressure is rarely measured. The use of this technique is largely limited to certain forms of hydrocephalus and benign intracranial hypertension. The opening pressure is usually measured with a CSF manometer; depending on the indication a spinal drain could be inserted. Lumbar puncture (LP) opening pressures in children may also overestimate ICP, with a recent study recommending verification of LP opening pressures by formal ICP monitoring.¹²⁹ Neuroimaging to rule out a space occupying lesion or radiological contraindication is mandatory prior to performing the LP.

Type of placement	Advantages	Disadvantages
Intraventricular catheter	Provides a global measure of ICP Can be used to release CSF for control of ICP Can be calibrated in-vivo	Significant risk of infection, haemorrhage, disconnection Difficult insertion in small ventricles
Intraparenchymal	Low complication rate Insertion is simple	Drift of reading over time In-vivo calibration not possible Provides a focal representation of ICP
Subdural	Low complication rate Insertion is simple	Drift of reading over time In-vivo calibration not possible Provides a focal representation of ICP
Extradural	Simple insertion Minimal risk of infection	Accuracy unreliable
Telemetric	Continuous data	Indwelling device
Lumbar spine	Extracranial procedure Can be performed in ambulatory patients	May not reliably reflect ICP Dangerous if ICP is very high or SOL is present

Table 3.1. Invasive ICP monitoring techniques

3.4. Limitations of invasive ICP monitoring

The use of invasive ICP monitoring, despite distinct benefits, is suboptimal in clinical practice. Insertion of intracranial monitoring devices is performed by neurosurgeons, however, a significant number of patients with raised ICP are initially seen by non-neurosurgeons, who do not have access to invasive monitoring. Patients being ventilated in a neurocritical care environment are good candidates for invasive monitoring, but ambulant patients are less suitable, and as a result ICP monitoring may not be performed in many patients in whom it is indicated. Conversely, a suitable non-invasive technique that could reliably screen patients with raised ICP could identify appropriate candidates for invasive monitoring.

The risks associated with the procedure, mainly haemorrhage, infection, misplacement and inaccurate readings, must be weighed against the potential benefits. Sophisticated MR and CT imaging techniques provide invaluable information regarding space occupying lesions, oedema, haemorrhage and hydrocephalus. These images are necessary despite ICP monitoring to describe the actual underlying pathology. ICP monitoring as a standalone modality may provide imprecise impressions of what is actually occurring, depending on the experience of the treating clinician, and subsequently may elicit inappropriate therapeutic interventions. The benefit of multimodal monitoring versus ICP monitoring alone is a contentious issue.

Invasive ICP monitoring remains the standard against which all non-invasive methods of assessing ICP are compared.^{92,116} The gold standard for invasive ICP monitoring remains measurement via a transduced intraventricular catheter. The risks and limitations associated with invasive ICP monitoring have inspired considerable efforts towards the development of non-invasive techniques that are reliable, easy to use, cost-effective and reproducible.^{2,3,4,109} A variety of non-invasive techniques have been described for assessing ICP; their widespread use, however, remains quite limited. The shortcomings of these non-invasive techniques include the range of cut-off values for detecting raised ICP, inter-rater variability and qualitative rather than quantitative measurement of ICP.^{2,3,109}

For a non-invasive technique to be considered reliable, it would have to correlate well with invasively measured ICP, predict ICP within 2 mmHg in the 0 – 20 mmHg range, with a maximum error of 10% for ICP > 20 mmHg, which are the specifications supported by the Brain Trauma Foundation.¹³⁰

3.5. Non-invasive assessment of ICP

A method for reliably assessing ICP that does not require surgery and poses no risk of infection or haemorrhage, is certainly appealing. The ideal technique should be relatively inexpensive, repeatable, portable, radiation-free, user-friendly and allow continuous monitoring. The uses of a non-invasive technique could include screening and triage at point of contact, long-term monitoring (invasive monitoring has a limited duration due to risk of infection and drift), monitoring of ICP for routine assessment in patients with other conditions that may present with raised ICP, e.g. chronic hydrocephalus or stroke survivors.

Methods of non-invasive ICP monitoring usually involve assessing physiological or anatomical characteristics influenced by an increase in ICP. There are a variety of techniques, both clinical and technological, qualitative and quantitative for non-invasively assessing ICP. The accuracy of these techniques varies considerably,^{2,3,109} and for ease of reference, can be divided into the following groups:

- 3.5.1 Clinical assessment
- 3.5.2 Techniques utilizing the natural bony windows in the skull
- 3.5.3 Techniques assessing fluid dynamics
- 3.5.4 Electrophysiological techniques
- 3.5.5 Imaging techniques

3.5.1 Clinical assessment

Clinical neurological assessment remains the most important initial diagnostic and monitoring tool. Despite notable advances in non-invasive monitoring in the modern era, ongoing clinical assessment should remain a fundamental pillar of monitoring.

3.5.1.1. History

Careful history taking can be an invaluable tool in making the diagnosis of raised ICP. The symptoms suggestive of raised ICP are:

- Headache
- Impaired level of consciousness
- Visual disturbance
- Nausea and vomiting
- Developmental delay (in younger children)
- Failure to thrive (in younger children)

In children with an open anterior fontanelle (AF), increasing head circumference and a bulging fontanelle are symptoms that parents will often notice themselves.

These symptoms should always raise the suspicion of raised ICP; however they lack specificity and when interpreted alone can often be misleading to the treating clinician. It is therefore important to interpret these findings in the appropriate clinical context.

3.5.1.2. Clinical examination

The benefit of the clinical evaluation differs in the paediatric and adult population. In children with an open AF, where the skull sutures have not yet fused, an abnormal increase in the head circumference and bulging of the fontanelle are good indicators of raised ICP.^{131,132} In severely raised ICP the sutures may often be separated and palpable. Distended scalp veins may be visible when the head circumference is increased in longstanding raised ICP.

After the sutures have fused, assessment of ICP becomes more difficult. Finding papilledema on fundoscopy is a reliable indicator of raised ICP,¹³³ however this finding is not consistent, especially where there is atrophy of the optic nerve.¹³⁴ Fundoscopic examination can provide significant additional evidence of underlying raised ICP, which includes papilledema, haemorrhage, loss of spontaneous venous pulsation and optic atrophy. Papilledema is usually bilateral and generally develops within 5 days of an increase in ICP.^{135,136}

Cranial nerve palsies, usually the third and sixth cranial nerves and abnormalities of gaze (mostly upward gaze palsy) are usually ominous signs that raised ICP may be present. Bradycardia and hypertension with abnormal respiration (Cushing's response) may accompany cerebral herniation syndromes and are late features, usually signalling critically raised ICP, requiring emergent treatment. The benefit of a thorough history and clinical examination can therefore, not be emphasized enough.

3.5.2 Techniques utilising the natural bony windows of the skull

The most accessible anatomical windows in the bony skull which can be used to assess ICP are, transorbital, the auditory canal and the anterior fontanelle (AF) in infants.

3.5.2.1. Transorbital methods

This thesis focused on the use of ONSD measurement, and it is discussed first in this subsection, but other useful transorbital techniques are also discussed here.

i. Optic nerve sheath diameter (ONSD)

The optic nerve originates ontogenetically from the central nervous system. It is encased by a dural sheath, with a perineural, subarachnoid space between the nerve and the dural sheath. This perineural space is filled with CSF and is in direct communication with the

intracranial subarachnoid space. An increase in ICP results in displacement of CSF along its various pathways. The increase in CSF within the space surrounding the optic nerve results in expansion of the ONS. The region of the ONS located 3mm posterior to the lamina cribrosa of the retina is considered the most distensible and recommended as the most consistent region to acquire the ONSD measurement.⁵⁰ Changes in the ONSD can be visualized using images from ultrasound, MRI and CT scans.^{17,30,151-153} Several studies have demonstrated a strong association between distension of the ONSD and an increase in ICP.^{18,19,73,151,154,155} The suggested cut-off values in these studies range between 4.1 - 5.9 mm and the definition of increased ICP also varies considerably, between 14.7 and 30 mmHg.^{4,18,73,151,154} The main limitations of ultrasound-based ONSD measurements are hyperechoic artefacts, inter-examination variability, small size of the structures and measurements, variation in optic nerve sheath cut-off values and heterogeneity of the patient population.^{15,18,157,158} These shortcomings are accentuated in children because of the age-related variations.²⁸⁻³⁴ Despite these limitations, ONSD measurement has been described as a useful screening method to detect clinically suspected raised ICP, especially where invasive monitoring is not readily available.^{22,23,25,30}

ii. Intraocular pressure (IOP)

The appeal of this technique lies in the anatomical proximity and direct communication between the eye and the intracranial space.¹³⁷ The indirect transmission of ICP to the orbit via intervening venous anatomy has long been recognized.¹³⁸ The use of handheld tonometers by clinicians without any specialised training, has increased the interest in IOP as a rapid screening tool for raised ICP.^{137,139-143} Lehmann et al. demonstrated in their study on rhesus monkeys that a relationship between IOP and ICP did exist, albeit at rather high mean values of ICP (46.8mmHg).¹⁴⁴ Later studies evaluating the relationship between IOP and ICP provide mixed results.^{138,139} A meta-analysis by Yavin et al. concluded that the pooled diagnostic accuracy suggested IOP may be a useful clinical adjunct in the detection of raised ICP, but felt the benefit of the technique would be best assessed in future studies where clinical equipoise exists regarding the use of invasive ICP monitoring.¹⁴⁵ While there appears to be a relationship between an increase in IOP and

raised ICP, IOP does not appear sufficiently accurate for predicting individual patient ICP measurement.¹⁴⁶

iii. Pupillometry

Infrared pupillometry has been used to quantitatively measure subtle changes in pupil size in response to light stimulus. Pupillometers have been found to be more sensitive than manual scoring for noting small changes in pupil size.^{147,148} In normal individuals the pupil decreases by 34-36% in size, in response to a standard light stimulus. This response is reduced to 20% in head-injured patients, with a reduction of less than 10% associated with an ICP > 20 mmHg.^{149,150} While promising, the clinical applicability of this technique requires further investigation.

iv. Optical coherence tomography (OCT)

OCT is a technique using broad-band near-infrared light. This technology can be used to quantitatively measure and monitor the thickness of the retinal nerve fibre layer (RNFL) and the optic nerve head morphology,¹⁵⁹ making it a useful, objective method for distinguishing nerves with papilledema from normal nerves, and optic atrophy. This application has been found useful in adults and children with raised ICP and papilledema.^{160,161}

v. Scanning Laser Tomography (SLT)

SLT uses a laser to produce a 3D scan of the retinal surface. It can be used as an alternative to OCT when measuring the RNFL. The technique has been described as being highly reproducible.^{162,163} Though SLT measurement of the optic nerve volume and height have been found reliable in quantifying papilledema,¹⁶⁴ and have been correlated with CSF pressure measured via LP,¹⁶⁵ its value in reliably estimating ICP has yet to be established.

vi. Spontaneous venous pulsation (SVP)

SVP occurs due to the variation in the pressure gradient between the intraocular and CSF pulse pressure when the retinal vein crosses the lamina cribrosa.¹⁶⁶ SVP is considered to be present when ICP is normal,¹⁶⁷ however SVP may be absent in normal individuals as well. The presence of SVP is therefore a very sensitive marker for normal ICP, but should be interpreted in the context of the patient's clinical presentation.¹⁶⁸

vii. Venous Ophthalmodynamometry (vODM)

This method was originally described by Baurmann in 1925, and involves measurement of the retinal venous outflow pressure (VOP) while observing the retinal vessels with an ophthalmoscope.¹⁶⁹ The technique usually involves applying a suction cup to the globe in order to increase the IOP until the central retinal vein (CRV) collapses, and begins to pulsate, which usually happens at the point when the applied external pressure nears the VOP, which is an approximate of ICP. The venous outflow pressure which has a close linear relationship with ICP¹⁷⁰ is calculated by adding the pressure from the ophthalmodynamometer to the IOP. The technique requires the pupils to be dilated and should be performed by an experienced ophthalmologist. The application of external ocular pressure could also trigger the oculo-cardiac reflex, leading to hypotension, which is undesirable, especially if ICP is increased.

Technique	Level of operator skill required	Quantitative or qualitative assessment of ICP	Continuous monitoring	Main advantage	Main disadvantage
ONSD	Medium	Qualitative	No	Requires minimal	Poor specificity Wide range of described cut-off

				additional training Relatively inexpensive	values to detect raised ICP
IOP	Medium	Qualitative	No	Relatively inexpensive Minimal discomfort to patients Can be performed in awake patients	Appears to only be useful where ICP is very high
Pupillometry	Medium	Qualitative	No	Requires minimal additional training	Limited data available
OCT	High	Qualitative	No	Very sensitive for measuring retinal fibre thickness New techniques described for improving accuracy	Currently limited to use by ophthalmologists
SLT	High	Qualitative	No	Diagnostic for a wide spectrum of ocular disease	Limited data available
SVP	Medium	Qualitative	No	Requires minimal additional training Relatively inexpensive	Subjective interpretation of results Poor specificity for raised ICP
Venous Ophthalmodynamometry	High	Qualitative	No	Can be combined with other techniques to improve accuracy	Cumbersome technique Potential to induce oculo-cardiac reflex

Table 3.2. Non-invasive ICP monitoring techniques: Transorbital methods

3.5.2.2. Methods utilising the auditory canal

The cochlea of the ear is in direct communication with the intracranial subarachnoid space via the cochlear aqueduct. Methods investigating displacement of the tympanic membrane and measurement of sound generated by movement of the ossicles have been described as markers of ICP.

i. Tympanic Membrane Displacement (TMD)

Tympanic membrane vibration is usually transmitted through the ossicles in the middle ear to the cochlea. Contraction of the stapedius and tensor tympani muscles is accompanied by a small, measurable displacement of the tympanic membrane from its resting position. As the perilymph and CSF communicate through the cochlear aqueduct, an increase in ICP is directly transmitted to the footplate of the stapes leading to a change in the direction and magnitude of the TMD.

Movement of the tympanic membrane caused by stimulation of the stapedial reflex can be quantitatively assessed. This movement is altered by increased ICP, but limited accuracy of the technique means it is merely suited to providing qualitative information about ICP.^{171,172} In the study by Shimble et al, no valid measurement of TMD could be made in about 60% of patients, casting doubt on the clinical value of the technique.¹⁷³ Patency of the cochlear aqueduct, integrity of the tympanic membrane and strength of the acoustic reflex influence the TMD, which is further limited by poor inter-subject reproducibility.¹⁷⁴

ii. Otoacoustic emissions (OAEs)

OAEs are sounds originating from movement of the sensory hair cells within the cochlea in response to auditory stimulation. These sounds can be recorded by a probe placed in the ear canal. OAE is often used in clinical practice to test for hearing deficits in young children where cooperation is poor.

Auditory measurements of OAEs that depend on middle-ear function are theoretically influenced by changes in ICP.¹⁷⁵ This method has been used as an alternative to TMD,

specifically a technique called distortion product otoacoustic emissions (DPOAEs) has been shown to change with ICP.^{175,176} It has the advantage over TMD of not requiring the middle-ear reflex arc, which involves brainstem pathways. Poor inter-subject variability limits its use in measuring ICP, but it could be useful for monitoring patients once baseline ICP has already been measured.^{4,177}

Technique	Level of operator skill required	Quantitative or qualitative assessment of ICP	Continuous monitoring	Main advantage	Main disadvantage
TMD	Medium	Qualitative	Potentially	Simple, cost-effective	Limited by anatomical variation
OAEs	Medium	Qualitative	Potentially	Excludes the brainstem pathway	Difficult in older patients

Table 3.3. Non-invasive ICP monitoring techniques: Methods utilising the auditory canal

3.5.2.3. Assessment of the anterior fontanelle (AF)

The term fontanelle refers to a fibrous, membrane-covered space or ‘soft spot’ occurring between two juxtaposed cranial bones. There are usually two prominent fontanelles in the midline, the AF and posterior fontanelle (PF). The AF is roughly diamond shaped and located at the junction between the sagittal and coronal sutures, between the frontal and parietal bones. It usually closes between the ages of 6 – 18 months (median age of 13.8 months).¹⁷⁸ The PF usually closes by age 8 weeks and is of less clinical significance.

Palpation of the AF, measurement of the head circumference, assessing shape of the head and palpation of suture ridges during clinical examination are basic, but extremely valuable assessments which can be performed by health care workers at all levels. Evaluation of the AF provides a window for determining whether raised ICP is present in infants. The size and shape of the AF vary significantly according to age, position and

pathology and delayed closure of the AF is associated with a number of conditions. The most common causes, which usually have other associated features as well, include achondroplasia, congenital hypothyroidism, Down syndrome, rickets and raised ICP. Raised ICP in infants usually causes a bulging or tense AF, and this should serve as a warning prompting further investigation.

Described techniques for assessing ICP via the AF include measuring pulsation of the AF,^{179,180} use of an aplanation transducer and modified Shiotz tonometer¹³² and the Rotterdam Teletransducer (RTT).¹⁸¹ None of these have been widely used in routine practice and are largely of historical significance. Where the AF is closed or not reliably patent, other non-invasive techniques may be required to assess ICP.

3.5.3. Methods based on fluid dynamic properties

Studying the dynamic changes in ICP, cerebral blood flow (CBF) and cerebral compliance can be quite challenging. Non-invasive techniques for assessing these parameters are therefore rather limited. Ultrasound, MRI and infrared spectroscopy have been used to examine some of these dynamic changes and will be discussed below.

3.5.3.1. Transcranial Doppler sonography (TCD)

TCD measures the velocity of blood flow through major intracranial vessels by emitting a high frequency (> 2 MHz) wave, and detecting the frequency shift between the incident and reflected wave. This difference directly correlates with the speed of blood flow (the Doppler effect).¹⁸²

TCD as a technique for evaluating cerebral haemodynamics was first described by Aaslid in 1982.¹⁸³ It has since been used to measure the cerebral blood flow (CBF) velocity in the circle of Willis and the vertebrobasilar system, both diagnostically and to adjust treatment strategies in a variety of neurovascular disorders.¹⁸⁴⁻¹⁸⁷ Insonation of one of the arteries, usually the middle cerebral artery, produces an arterial waveform. Using this arterial waveform, the most commonly assessed parameters are the peak systolic and diastolic velocity, mean velocity, resistance index (RI) and pulsatility index (PI). The criteria for adequate vessel insonation are: the cranial window used, transducer position, angle of insonation, depth of sample volume, direction of blood flow, relative flow velocity and experience of the investigator.^{182,188}

The measurement is taken over regions of the skull with the thinnest bony windows (temporal region, through the eye or at the back of the head). TCD is most suited to providing a qualitative estimate (low, normal or high) of ICP.^{189,184}

In an adult study, the PI (difference between systolic and diastolic flow velocity divided by the mean flow velocity) correlated well with ICP (correlation coefficient of 0.938, $p < 0.001$).¹⁸⁴ A study in children with severe traumatic brain injury (TBI) found the PI to be a less reliable indicator of absolute ICP values,¹⁹⁰ while a subsequent study also in children found TCD to be an excellent first-line examination for identifying patients likely to need invasive ICP monitoring.¹⁹¹

TCD remains an attractive alternative to invasive ICP because of its ability to detect cerebral ischemia, its relative cost effectiveness and widespread availability. The main disadvantages are that it requires a trained and skilled operator to perform and interpret the measurements and the limited accuracy for estimating absolute ICP.¹⁹⁰

Two-depth TCD assessment involves pressure application to the orbit in order to equalize blood flow in the intra- and extracranial segments of the ophthalmic artery. This technique was shown to correlate well with absolute ICP measurements,^{192,193} but also appears currently limited by operator dependence and inadequacy of the current indices to accurately reflect true ICP.

3.5.3.2. Magnetic resonance imaging (MRI)-based elastance index

MRI-based cine phase-contrast pulse sequences are used to determine the blood and CSF volumetric flow rates within the brain. A method described by Alperin uses the arterial inflow, venous outflow and CSF flow between the cranium and spinal compartment to calculate changes in intracranial volume; these measurements can then be used to derive ICP using an elastance index.^{194,230} Prediction of ICP using this dynamic MRI technique has been strongly correlated with invasive ICP measurement. In children with hydrocephalus, dynamic MRI was shown to correlate well with the shunt valve opening pressure.¹⁹⁵ A significant association with symptom resolution in hydrocephalic patients has also been demonstrated.¹⁹⁶ This promising technique still requires investigation in a larger cohort of patients. It is also quite expensive and impractical for continuous monitoring.

3.5.3.3. Near infrared spectroscopy (NIRS)

Transcranial NIRS is a method for assessing regional changes in cerebral blood oxygen saturation (rSO₂) and cerebral blood volume (CBV) and CBF.¹⁹⁷ NIRS works in the infrared spectrum (700-1000 nm) of light, where low absorption allows it to easily pass through skin and bone resulting in deep-tissue penetration. This light is both scattered and absorbed as it passes through brain tissue. Variations in the absorption of infrared light by different substances allow the detection of changes in deoxyhaemoglobin and oxyhaemoglobin concentration. A significant difference in rSO₂ values was demonstrated in a study of severe TBI patients with normal and raised ICP.¹⁹⁸ Changes in cerebral oxygenation were also shown to correlate with vasogenic ICP slow waves in CSF infusion studies and patients with TBI.¹⁹⁹ NIRS allows for the calculation of certain indices which have been correlated with cerebrovascular pressure reactivity in patients with TBI.²⁰⁰ At present NIRS does not provide an estimation of absolute ICP values nor does it facilitate

the detection of changes in ICP.¹⁰⁹ The technique is also limited by the requirement for specialised equipment and the extended period required to obtain the required indices.²⁰⁰

Technique	Level of operator skill required	Quantitative or qualitative assessment of ICP	Continuous monitoring	Main advantage	Main disadvantage
TCD	High	Qualitative	No	Versatile technique with a wide array of indications	Technical expertise limit its widespread use
MRI-based elastance index	Medium	Qualitative	No	Exquisite detail, with potential for describing new indices	High cost with extensive infrastructure required
NIRS	Medium	Qualitative	Yes	Allows long-term monitoring	Readings are influenced a number of variables

Table 3.4. Non-invasive ICP monitoring techniques: Methods based on fluid dynamic properties

3.5.4 Electrophysiological techniques

3.5.4.1. Electroencephalography (EEG)

EEG represents spontaneous electrical activity of the cerebral cortex recorded through electrodes placed on the scalp. These electrical signals are then amplified, filtered and displayed according to the number of channels required (generally 8 or 16 channels).

The use of a novel technique called EEG power spectrum analysis has recently been reported on by Chen et al.²⁰¹ Power spectral analysis allows a graphical representation of the EEG readings over time. An index called the intracranial pressure index (IPI) was derived using the EEG power spectrum analysis, and this was then correlated with ICP

measurements obtained via lumbar puncture. The authors concluded that there was a correlation between the IPI and ICP. Its clinical utility will depend on validation in further studies. EEG can be continuously recorded for 8 -12 hours, before the conductive gel dries out, requiring the leads to be replaced. Recent development of both wireless, portable and field deployable EEG systems have improved the application of this technique.²⁰¹

3.5.4.2. Visual evoked potentials (VEP)

VEPs are recorded from electrodes positioned in the occipital scalp and accurately reflect disturbances of the visual pathways.^{202,203} Rosenfeld described a method using flashing light into the eye and estimating ICP through recordings obtained from a few occipital EEG electrodes, using the latency of the second negative-going wave (N2).²⁰³ A linear relationship between ICP and the latency of the third positive-going wave (P3) has also been reported using high-density electrode arrays and independent component analysis extraction.²⁰⁴ The N2 wave appears to be stable and easily identifiable using flash evoked VEPs in healthy control patients. Earlier studies by York et al. demonstrated a strong correlation between the N2 latency of the VEP and ICP in children with hydrocephalus and young adults with head trauma.^{205,206} The relationship between a prolonged N2 latency period and raised ICP has subsequently also been reported in children.^{207,208} A recent study has, however, demonstrated a high intersubject variability, suggesting a limited ability to predict ICP.²⁰⁹

3.5.4.3. Ocular vestibular evoked myogenic potentials (oVEMPs)

This technique employs vestibular stimulation of the extraocular muscles to generate electromyographic activity. These evoked potentials can be recorded from the

contralateral eye using surface electrodes. A recent study has suggested this technique may have a role in non-invasive ICP assessment.¹⁷²

Technique	Level of operator skill required	Quantitative or qualitative assessment of ICP	Continuous monitoring	Main advantage	Main disadvantage
EEG	High	Qualitative	Yes	Allows high quality data that can provide information about other conditions as well, i.e. seizures, ischemia	Requires trained personnel to setup and interpret
VEP	High	Qualitative	Potentially	Ability to provide data that on a spectrum of visual abnormalities	Lack of clear evidence to support correlation with ICP
oVEMP	Medium	Qualitative	No	Still unclear	Paucity of data

Table 3.5. Non-invasive ICP monitoring techniques: Electrophysiological techniques

3.5.5. Imaging techniques

Radiological imaging has historically been a fundamental tool in making the diagnosis of raised ICP. Skull x-rays were used to assess whether chronically raised ICP was present by detecting separation of the skull sutures, ‘copper beaten’ appearance of the skull and erosion of the clinoid.^{210,211,212} This technique has been found less useful in the modern era.²¹³ Imaging features on CT and MRI consistent with clinical findings of raised ICP have been well described.^{210,214-218} These features are discussed below.

3.5.5.1. CT scan

CT scan still remains the most commonly used diagnostic imaging modality when assessing patients with acutely raised ICP. A variety of findings on CT have been associated with raised ICP, depending on the underlying aetiology. These findings include:

- Absence/compression of the basal cisterns and/or ventricles
- Midline shift
- Enlarged ventricles (hydrocephalus)
- Transependymal fluid shift
- Presence of haematoma/space occupying lesion
- Blood in the subarachnoid space
- Size of sulci
- Gray/white differentiation

The benefit of the initial CT scan has been investigated widely in the context of traumatic brain injury.^{210,215,218,220} CT scan still forms the cornerstone of acute imaging in hydrocephalus, where imaging features depend on the aetiology and relate to the level of obstruction, presence of transependymal fluid shift, volume of CSF in the subarachnoid space and shape of the the third ventricle.^{267,268} Planning of specific surgical interventions for hydrocephalus, eg. endoscopic third ventriculostomy (ETV), usually requires an MRI scan.

The discussion regarding which of these CT findings and correlate best with raised ICP is still ongoing.^{4,109,218-220} While CT scans remain a valuable diagnostic adjunct in the acute

diagnosis of raised ICP, it must be remembered that a ‘normal’ CT scan does not rule out raised ICP. In children the additional radiation exposure to the susceptible, developing brain and the possible sequelae over the lifetime of the child must always be considered.²²¹⁻²²⁵ To this effect the ‘image gently’ recommendations for children should always be kept in mind (www.imagegently.org).

3.5.5.2. MRI scan

MRI provides superb quality images of the brain, but can be time consuming and costly as a first line diagnostic modality in the acute care setting. MRI techniques for evaluating ICP are based on the relationship between intracranial compliance and pressure.^{194,226} Using a motion-sensitive technique to measure the arterial, venous and CSF flow into and out of the cranial cavity during the cardiac cycle, Alperin et al. demonstrated a strong correlation between the MRI-derived elastance index and invasively measured ICP.¹⁹⁴ These results, however, were found to have poor repeatability in a subsequent study, due to technical errors in measurement and intra-individual variation, with the authors suggesting caution when interpreting individual measurements.²²⁷ Despite these shortcomings, specific MRI sequences appear promising, both for screening in acutely raised ICP and for assessment of ICP in other conditions, like hydrocephalus.²²⁹ MRI has also been used to evaluate the optic nerve sheath diameter as a marker for raised ICP,²²⁸ and appears to be more accurate than ultrasound in assessing the CSF filled subarachnoid space surrounding the optic nerve.²³¹ The current role of MRI as a diagnostic and monitoring tool in neurosurgery, far outweighs its function as a purely non-invasive technique for assessing ICP.

Technique	Level of operator skill required	Qualitative or quantitative assessment of ICP	Continuous Monitoring	Main advantage	Main disadvantage

CT scan	Medium	Qualitative	No	Available at most facilities	Radiation exposure to the developing brain
MRI scan	High	Qualitative	No	Exquisite soft tissue detail	Not yet widely available

Table 3.6. Non-invasive ICP monitoring techniques: Imaging techniques

3.6. Discussion

Despite a relatively long history of innovative thinking involving the pursuit of suitable techniques for non-invasively assessing ICP, the process is still in a relatively exploratory phase. The main limitations remain inadequate diagnostic accuracy for consistently detecting raised ICP, poor quantitative estimation of ICP and lack of continuous monitoring capability. Most methods appear suitable to identify subjects with low to normal ICP or very high ICP, but are poor at detecting moderately raised ICP, which arguably, is the most important group. The idea of combining selected non-invasive techniques to improve accuracy, in a ‘non-invasive multi-modality model’ is certainly appealing in principle.

Non-invasive ICP assessment is still most suitable as a screening tool for patients with suspected raised ICP. Patients in a neurocritical care unit often require continuous ICP monitoring, usually as part of a multimodal monitoring approach. These objectives are currently only achievable using invasive monitoring techniques.

Future development of non-invasive techniques will likely depend on substantial improvements in the accuracy, ease of use and potential for continuous monitoring. This need is perhaps most distinct in the children, where early detection of increasing ICP may facilitate the diagnosis of a number of underlying neurological conditions. The potential to spare the developing nervous system unnecessary exposure to radiation from repeated CT scans or limit the need for invasive monitoring in certain cases makes this quest worthwhile.

This study has identified measurement of the ONSD using transorbital ultrasound as a promising technique in children, and the next section of this work discusses the role of ONSD measurement as a non-invasive marker of raised ICP.

Chapter 4.

Measurement of the optic nerve sheath diameter (ONSD) as a non-invasive marker of intracranial pressure (ICP)

The optic nerve originates from the diencephalon and is an extension of the white matter tract of the central nervous system (CNS). As the optic nerve extends into the orbital cavity it is enveloped by a dural sleeve which is continuous with the intracranial dura mater. CSF within the intracranial subarachnoid space is in continuity with the perineural subarachnoid space surrounding the optic nerve. This perineural space, surrounded by a dural sheath, is known as the ONS.^{53,56}

An increase in ICP above a certain threshold can result in displacement of CSF from the intracranial cavity. Depending on the underlying aetiology, this CSF displacement can often be seen on imaging as a decrease in the volume of CSF surrounding the cerebral cortex.^{33,232} The direct continuity between the intracranial and perineural subarachnoid space allows the displacement of intracranial CSF causing an increase in the CSF volume within the optic nerve sheath.^{28,50} This increase in CSF volume within the ONS results in distension of the ONS and widening of its diameter. The space between the optic nerve and dural sheath is not a homogeneous space, but rather a trabeculated, septated system that likely plays a role in the CSF dynamics between the perineural space surrounding the optic nerve and the subarachnoid space of the intracranial cavity.⁵³

The relationship between an increase in ICP, increase in CSF within the ONS and oedema of the optic disc was described by Hayreh in 1964.⁴⁶ The initial ultrasound-based observation of the thickness of the optic nerve, the amount of perineural fluid and the thickness of the surrounding dural sheath were described by Ossoinig in his seminal work entitled “Standardised Echography” in 1979.⁶⁶ This was later followed by the description of an increase in subarachnoid fluid surrounding the optic nerve and the link to increased ICP.⁴⁷ This observation was validated by Galetta who demonstrated a reduction in the optic nerve diameter after lumbar puncture in a patient with pseudotumor cerebri.⁴⁸ Liu

demonstrated a linear relationship between subarachnoid pressure of the optic nerve and ICP in a cadaver model.⁴⁹

Hansen and Helmke performed a study using specially prepared optic nerve specimens. The technique involved forcefully injecting gelatin into the perineural space surrounding the optic nerve, demonstrating that dilatation of the ONS was maximal in the anterior 3 mm segment. The observation that the change in ONSD may be influenced by dural elasticity and the trabecular network density as well as different pressure loads, remains an important consideration when interpreting the ONS response to an increase in ICP. This study marked one of the earliest validations of ultrasonic measurement of pressure-induced distension of the ONS.²⁸ The distensibility of the ONS, its elastic properties, individual baseline variability and the bony anatomy of the optic canal were further explored in experimental studies by the same group, highlighting the complexity of the relationship between ONS distension and ICP-related changes.^{50,154}

Following on this early work, numerous investigators have explored the relationship between distension of the ONS and ICP.¹⁶⁻³³ The most relevant literature on this topic will be discussed in this section, reviewing material on paediatric and adult studies involving ONSD separately. The different modalities for measuring ONSD, i.e ultrasound, MRI and CT will also be subcategorised under these headings.

4.1. Studies in children

Literature evaluating the role of ONSD measurement as a non-invasive marker of ICP in children is quite sparse. The discussion of paediatric studies has been divided into two parts. The first part evaluates studies supporting the use of ONSD measurement and the second part evaluates studies against its use.

4.1.1 Support for the use of ONSD measurement

4.1.1.1. Ultrasound-based measurement

Some of the earliest work on this concept was done by Helmke and Hansen²⁸ who performed a prospective study on 39 children admitted to the intensive care unit (ICU), and compared them to 51 control patients. The study aimed to investigate whether the ‘phenomenon’ of ONS distension happened under conditions of acute intracranial hypertension. 15 patients did not have elevated ICP, while 24 had elevated ICP (7 with invasive ICP monitoring to verify elevation above 20 mmHg). In control subjects the range of ONSD measurements differed in the first 4 years of life when compared to ONSD measurements in older children. The difference between mean ONSD in the ICU groups with and without raised ICP was 2.3 mm ($p = 0.007$). This study remains fundamental as it marks one of the earliest efforts to demonstrate dilatation of the ONS in acutely raised ICP. Taking into consideration the error under repeated measurements of 0.3 mm, the authors recommended that in children older than 4 years, an ONSD of 4.5 mm may be considered ‘borderline’, while an ONSD exceeding 5.0 mm is definitely enlarged, whereas in children under 4 years old, an ONSD of > 4.0 mm can be considered ‘definitely’ enlarged.²⁸

Aiming to establish normal age-related values for ONSD in infants and older children (up to the age of 15 years old), Ballantyne and colleagues conducted a prospective study in

102 children without any neurological or ophthalmological disease. This study demonstrated a clear increase in ONSD during the first year of life, approaching maximum (adult) values by the age of 2 years. Results from this study suggest that an ONSD value greater than 4 mm in children under 1 yo, and greater than 4.5 mm in older children should be considered abnormal.²⁹

Children with 'shunted hydrocephalus' were evaluated in a later study by Newman et al,³⁰ comparing 23 children with shunted hydrocephalus with 102 control patients. The shunted hydrocephalus group was further subdivided into i) normotensive (n=6), ii) symptomatic but not requiring intervention (n=5) and iii) symptomatic requiring intervention (n=12). The mean ONSD values were 3.1 ± 0.36 mm in the control group, 2.9 ± 0.5 mm in group i), 3.1 ± 0.4 mm in group ii) and 5.9 ± 0.6 mm in group iii). The authors demonstrated a correlation between increasing age and increasing optic nerve sheath diameter ($r^2 = 0.48$), with the greatest increase occurring in the first year of life. The most significant recommendation from this study was an age related cut-off point for normal ONSD values of 4.0 mm in children under the age of 1 year, and 4.5 mm in children over the age of 1 year. This finding was consistent with the recommendation by Ballantyne et al,²⁹ but at odds with the findings from the Helmke study.²⁸

The majority of studies evaluating the role of ONSD measurement, are based on using a combination of clinical assessment and imaging findings as the reference standard for diagnosing raised ICP. Malayeri and co-workers conducted a case-controlled, prospective study on 156 children, 78 control patients and 78 patients symptomatic of raised ICP. The investigators found a mean ONSD value of 5.6 ± 0.6 mm in the symptomatic group and 3.3 ± 0.6 mm in the control group ($p < 0.01$). They also found no significant age-related difference in the ONSD measurement in the symptomatic group, but a significant age-related difference in the control group, citing a probable difference in the expansile structure and anatomic characteristics of the optic nerve sheath as a possible explanation for the disparity. The study made no recommendation regarding the optimal ONSD cut-off value in children.³²

A Malawian study conducted by Beare and colleagues prospectively investigated the benefit of ONSD measurement in 51 children, 21 with neurological disease and 30 control

patients. 14 patients had clinically suspected raised ICP, with a mean ONSD of 5.4 mm. The mean ONSD was 3.6 mm in the group without clinically raised ICP and 3.5 mm in the control group. The investigators suggest a cut-off point of 4.2 mm with a sensitivity of 100% and specificity of 86%, as the upper limit of normal, with measurements ≥ 4.5 mm indicative of raised ICP. A limitation of the study was that the control group included patients with gastroenteritis and sepsis, both of which are particularly susceptible to dehydration, making the ONSD values quite difficult to interpret, as they were potentially lower than would be expected for 'normal children'. No age-related threshold was investigated in this study.³³

The first study to suggest that ONSD values in children may be higher than previously described was performed by McAuley and colleagues. In a review of ONS ultrasound examinations in children with a clinical suspicion of hydrocephalus, the study presented data on 331 examinations performed in 160 children. The authors did not recommend specific cut-off values in this paper but concluded that the baseline ONSD value in asymptomatic patients was higher than previously reported by Newman et al.³⁰ The change in mean ONSD values in symptomatic patients from their own recorded asymptomatic baseline was significant. Another relevant finding was that in 24/29 (82.8%) patients the ONSD correlated with shunt block, and in 19/24 (79.2%) of these patients, no change in ventricular configuration was demonstrated on imaging findings. The authors concluded that ONSD measurement was increased in symptomatic patients from their own baseline, and that multiple examinations might be useful in evaluating the ONSD pattern in individual patients, possibly playing a better predictive role in the assessment of ventriculoperitoneal shunt (VPS) malfunction.²³⁴ Even though no specific cut-off values were provided, this study was significant in that it highlighted the role of repeat measurement of the ONSD in assessing patients with shunted hydrocephalus.

Tsung et al. reported on 3 paediatric cases of TBI in the emergency department (ED), concluding that bedside ocular ultrasonography may be useful in the ED for screening patients with potentially raised ICP prior to performing either lumbar punctures or CT scans.²³⁵

The only study in children that specifically compared ONSD measurement to invasive ICP assessment was performed by Agrawal and co-workers. This study was conducted on patients admitted to a paediatric neurosurgical ICU, and included only 11 children. The authors did however manage to demonstrate a difference in the ONSD measurements in patients with raised ICP compared to those with normal ICP. Using 15 mmHg as the ICP threshold, the median ONSD was 5.15 mm where ICP was considered raised, compared to 3.95 mm in the normal ICP group, suggesting that ONSD measurement might be helpful in selecting TBI patients requiring invasive ICP monitoring, and possibly avoid the risk of unnecessary procedures. No ONSD cut-off value for predicting raised ICP was suggested in this study.²³⁶



Bulge of
the optic
disc

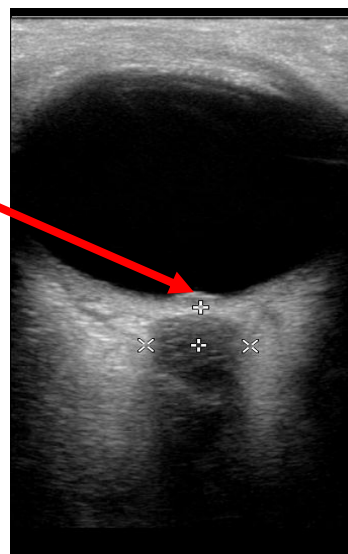


Figure 4.1. Axial ultrasound image of ONS

Figure 4.2. Ultrasound image with ONSD measurement

Author	Type of study	Reference standard	Aetiology of raised ICP	Study size	Year	Type of probe used	Described ONSD values	Diagnostic accuracy	Recommendation
Helmke	Prospective	Clinical symptoms, radiological findings and invasive ICP measurement	TBI, metabolic disorder	39 (51 control patients)	1996	7.5 MHz linear array probe)	< 4 years old – 4 mm, > 4 years old - 4.5 mm (borderline), 5 mm (definitely abnormal)	Not done	ONSD is useful in acutely raised ICP, and the upper limit differs in children above and below 4 years old
Ballantyne	Prospective	Neurologically normal children	Normal (without neurological or ophthalmological disease)	102	1999	7 Mhz sector probe	4.0 mm < 1 year old, 4.5 mm > 1 year old is considered abnormal	Not done	Maximal increase in ONSD occurs in the first year of life, with a diminished growth rate over the next 14 years
Newman	Prospective	Clinical symptoms and signs of raised V/P shunt dysfunction	Shunted hydrocephalus vs control group	125 (102 controls vs 23 with shunted hydrocephalus)	2002	7 Mhz phased array probe	4.0mm < 1 year old 4.5mm > 1 year old	Not performed	ONSD measurement is a reliable technique for rapid diagnosis and monitoring of raised ICP
Malayeri	Case-controlled, prospective	Clinical and radiological (CT scan) assessment	Mixed	156 (78 symptomatic, 78 case-controlled)	2005	7.5 Mhz linear probe	Mean 5.6 ± 0.6 mm in symptomatic group, and 3.3 ± 0.6 mm in control group. Children with elevated ICP have an ONSD > 4.55 mm, irrespective of their age.	Not specified	Transorbital sonography could be a first-line diagnostic modality in patients with suspected raised ICP.

Author	Type of study	Reference standard	Aetiology of raised ICP	Study size	Year	Type of probe used	Described ONSD values	Diagnostic accuracy	Recommendation
Beare	Prospective	Clinical signs and symptoms of raised ICP. CT scan diagnosis of raised ICP in 8 patients	Mixed	51 (21 with neurological disease and 30 control patients)	2008	7 Mhz curved array	4.2 mm	Sensitivity-100% Specificity-86%	Sonographic ONSD assessment is a useful method in resource limited settings. Control patients had pneumonia, gastro-enteritis, sepsis – the effect of these on the hydration status of the patients and also on ONSD are difficult to predict
McAuley	Retrospective	Clinical assessment of raised ICP	Shunted hydrocephalus	160	2009	8 – 13 Mhz linear array probe	The mean change from baseline ONSD in symptomatic patients requiring intervention was 1.29 mm, vs 0.68 mm in asymptomatic patients	Not performed	Symptomatic patients demonstrate an increase in ONSD from their asymptomatic baseline.
Agrawal	Prospective	Invasive ICP measurement	TBI	11	2012	10 Mhz probe	Used historical cut-off value of > 4.5 mm to predict ICP > 15 mmHg	Not specified	Only study comparing ONSD to invasive ICP measurement, but in a small number of patients

Table 4.1. Ultrasound-based paediatric studies supporting the use of ONSD measurement

4.1.1.2. MRI – based measurement

MRI provides superb detail when dedicated sequences are performed through the orbit. The measurement of the ONSD is likely to be less variable between observers than on ultrasound imaging. The reported measurements in children also appear to be larger on MRI than on ultrasound,^{237,238,239} justifying a separate discussion.

The ideal region for measurement of the ONSD was addressed by Shofty and colleagues in a study reviewing the MRI scans of 115 patients, 86 healthy control patients and 29 patients with idiopathic intracranial hypertension (IIH). A positive correlation between age and ONSD was demonstrated in the control group ($r = 0.414$). A potential limitation to interpreting the results of this study is the location used for the MRI measurement, i.e. 10 mm anterior to the optic foramen, which doesn't conform to the historically recommended location 3 mm posterior to the globe.^{30,50} The authors validated using the more posterior location because of the possible confounding effect of globe position on the measurement. The two groups, were each subdivided into 4 age categories. The authors demonstrated significant differences in ONSD measurement between the two groups in each of the age categories, concluding that ONSD enlargement on MRI in the paediatric population, once population-based norms had been established, was an important non-invasive diagnostic tool for detecting increased ICP.²⁴⁰

Change in ONSD measurement after successful treatment of hydrocephalus was described by Singhal and co-authors in a retrospective analysis of 16 patients with successfully treated hydrocephalus via endoscopic third ventriculostomy (ETV) and/or posterior fossa tumor resection. The study compared ONSD on axial T2-MRI scans pre- and post-surgery. The mean ONSD pre-surgery was 6.21 mm compared to 5.71 mm ($p = 0.0017$) post-surgery. The authors also evaluated other optic nerve parameters, namely optic disc bulge and optic nerve tortuosity, concluding that serial ONSD measurement and optic disc bulge might be useful in assessing the outcome of hydrocephalus treatment.²³⁸

Change in ONSD as a marker of outcome after a specific treatment intervention, was investigated in a recent retrospective study by Padayachy et al, using pre- and post-

operative MRI scans of patients who had undergone an ETV as treatment for their hydrocephalus. The study included 24 children (≤ 14 yo) where, among other parameters, the ONSD was measured pre- and post-operatively. The mean change in ONSD in the successfully treated group was 0.73 mm (SD 0.26), vs 0.18 mm (SD 0.34) in group where the ETV had failed ($p < 0.0007$). Change in ONSD demonstrated a sensitivity of 92.9%, specificity of 85.7% and a diagnostic odds ratio of 78 for predicting outcome from the procedure, suggesting that change in ONSD correlated well with outcome from ETV in hydrocephalus.²³⁹

The described normal values for ONSD measurement were challenged in a study by Steinborn et al, which aimed to validate the accuracy of ONSD measurement by comparing transbulbar sonography to MRI measurement. The measurements were performed in a group of 65 patients for a wide range of indications, who had adequate MRI scans of the brain, which included sequences through the orbit. The mean ONSD values were 5.86 ± 0.66 mm on MRI and 5.86 ± 0.71 mm for transbulbar sonography, with an assumed mean normal value in the range of 5 mm for children, depending on age. The study also demonstrated good correlation between between the two modalities (CCC = 0.68), dependent on image quality.²³⁷

In a later study on 99 normal children, the same author described an overall mean ONSD of 5.75 ± 0.52 mm on ultrasound and 5.69 ± 0.31 mm on MRI. The most significant finding of this study is the ONSD value of around 5.7 mm which is substantially larger than previously reported values in children.³⁴

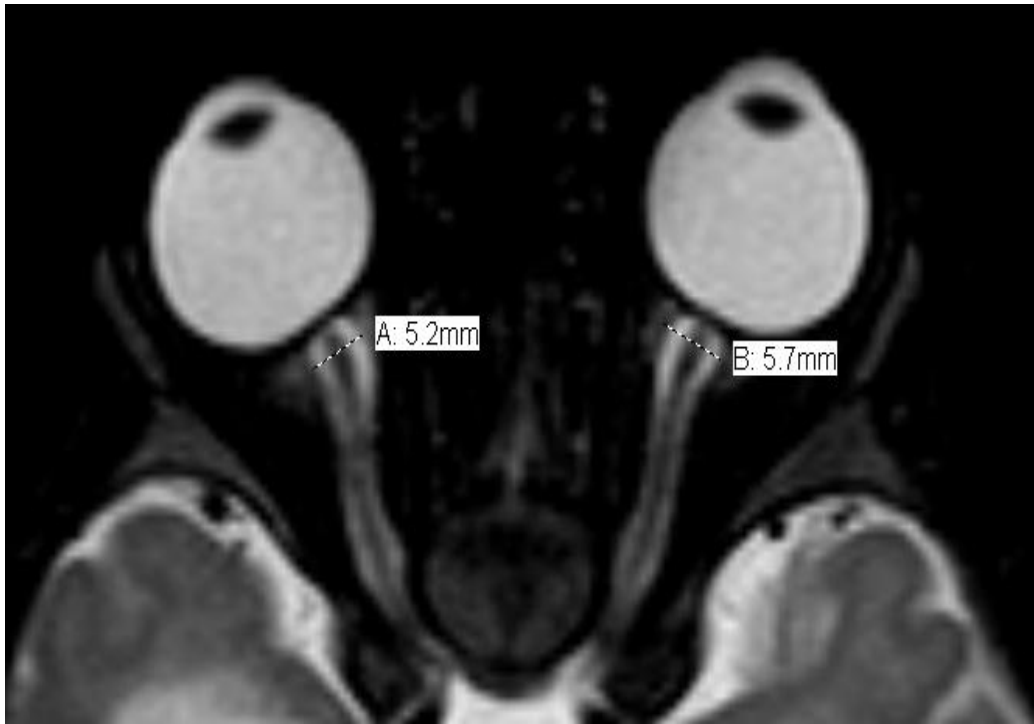


Figure 4.3. Axial T2-weighted MRI showing ONSD measurement

Author	Type of study	Reference standard	Aetiology of raised ICP	Study size	Year	Image sequence	Described ONSD values	Diagnostic accuracy	Recommendation
Shofty	Prospective	Clinical findings	Children with IHH and a control group of healthy children	115 (86 in control group and 29 with IHH)	2012	T2-weighted turbo spin echo sequence and ultrasound	A significant difference was demonstrated between the two groups in each of the four age categories	Not done	Optic nerve enlargement may be used as an important diagnostic tool in IHH.
Singhal	Retrospective	Clinical response to treatment	Successfully treated children with hydrocephalus	16	2012	T2-weighted axial	Mean ONSD of 6.21 mm pre-operatively and 5.71 mm post-operatively	Not done	Serial ONSD and optic disk bulge measurements may be useful in assessing treatment outcomes in hydrocephalus
Padayachy	Retrospective	Clinical and radiological markers of raised ICP	Children with hydrocephalus treated with an ETV	24	2015	T2-weighted axial	The mean change in ONSD was 0.73 mm vs 0.18 mm in the 2 groups	Change in ONSD of 7.5% sensitivity of 92.9%, specificity of 85.7%	Change in ONSD is a useful radiological parameter for assessing ETV outcome
Steinborn	Retrospective	Children having MRI brain	Diverse indications for brain MRI	65	2011	T2-weighted Axial and ultrasound	5.86 mm on MRI and 5.86 mm on ultrasound	Not done	ONSD values on transbulbar sonography correlate well with MRI values

Table 4.2. MRI-based paediatric studies supporting the use of ONSD measurement

4.1.2. Studies not supporting the use of ONSD measurement in children

Several studies examining the value of ONSD measurement in children have found the technique to be of limited benefit. All of these studies were performed using transorbital ultrasound.^{72,241,242}

The use of sonographic ONSD measurement was directly compared to fundoscopy in a study using ONSD measurement performed ‘during the daytime’ in 128 children with syndromic craniosynostosis. The authors found ONSD measurement less sensitive than fundoscopy when screening for raised ICP, and contrary to previous studies,^{30,46} found that a widened ONSD did not precede papilledema. This study also demonstrated no relationship between increase in ONSD and age. While invasive ICP monitoring was performed in some patients, no comparison was made between ONSD and direct ICP measurement. The authors did, however, raise an interesting question regarding the change in ONSD in chronic or repetitive ICP elevation rather than acutely raised ICP. The study ultimately found that ONSD measurement was not accurate enough to replace fundoscopy as a screening tool for increased ICP.²⁴¹

Perhaps the most convincing work demonstrating a limited value of ONSD measurement was performed by Le and co-workers, who prospectively investigated 64 children presenting to the emergency department with suspected raised ICP. 24 (37%) had a confirmed diagnosis of raised ICP (CT scan criteria/invasive ICP monitoring/LP). The ONSD cut-off values for normality used in this study were based on recommendations from earlier studies.^{23,30,243} The authors tested the sensitivity and specificity of ONSD values of > 4.5 mm, as well > 5 mm for predicting raised ICP. Using 4.5 mm as a cut-off point provided a sensitivity of 83%, and specificity of 38%, whereas 5.0 mm as a cut-off point decreased the sensitivity to 78% and increased the specificity to 68%. The authors concluded that the use of a mean ONSD measurement was not adequate to guide clinical decision making in children with suspected raised intracranial pressure.²⁴²

In a more recent study aimed at evaluating the role of ONSD measurement as a screening tool for VPS failure, Hall and co-workers prospectively evaluated 39 children presenting to the emergency department with a VPS in situ for hydrocephalus. The mean ONSD was

4.5 ± 0.9 mm in patients with clinical shunt failure and 5.0 ± 0.6 mm in patients without clinical shunt failure ($p < 0.03$). Using historical cut-off figures of > 4.0 mm in children under 1 year and > 4.5 mm in children over 1 year (30), a low sensitivity and specificity for predicting VPS dysfunction was demonstrated (61.1% and 22.2% respectively). The decision regarding VPS failure was based entirely on the neurosurgical decision to operate. The authors acknowledge that lack of invasive ICP measurement limited the ability to interpret the accuracy of ONSD measurement.⁷²

Author	Type of study	Criterion standard	Aetiology of raised ICP	Study size	Year	Modality	Described ONSD values	Diagnostic accuracy	Recommendation
Driessen	Prospective	Clinical signs of raised ICP	Syndromic craniosynostosis	128	2011	Ultrasound vs fundoscopy	Not specified	Sensitivity-11%; Specificity-97%	ONSD is less sensitive than fundoscopy for screening in raised ICP
Le	Prospective	Clinical findings and imaging (CT scans) findings suggestive of raised ICP	Mixed	64	2009	Ultrasound	Used mean ONSD of 4.5 and 5.0 mm as cut-off points	Using 4.5 mm sensitivity of 83%, and specificity of 38%. Using 5.0 mm sensitivity decrease to 78% and specificity increased to 68%	Sensitivity of 83% (95% CI: 0.6 – 0.94) and specificity of 38% (95% CI: 0.23 – 0.54)
Hall	Prospective	Clinical presentation in patients with a V/P shunt	Shunted hydrocephalus	39	2013	Ultrasound	Mean ONSD value of 4.5 ± 0.9 in patients with shunt failure, and 5.0 ± 0.6 in patients without shunt failure	Sensitivity 61.1% and specificity of 22.2%	Beside ocular ultrasound measurement is insensitive and nonspecific for identifying potential VPS dysfunction in children presenting to the ED. Multiple operators performed the imaging resulting in a wide range of measurements which may have affected the accuracy of the technique

Table 4.3. Paediatric studies not supporting the use of ONSD measurement

4.1.3. Discussion

The diagnostic accuracy of ONSD measurement for detecting raised ICP varies considerably.^{31,157,261} In children this issue is further complicated by the description of age categories defined at 1 and 4 years old to describe different upper ONSD limits.²⁸⁻³¹ The variation in the recommended age categories makes interpretation of the ONSD measurement in children particularly challenging.

The recommendation of age above and below 1 year as a threshold for defining different ONSD values for children was supported in the study by Newman,³⁰ however other authors only describe a significant difference between mean ONSD measurements in the asymptomatic group.³² The use of ONSD cut-off values of 4.2 mm and 4.5 mm to predict raised ICP, has also yielded inconsistent findings.^{32,72,241,242}

A review paper described the recommended ONSD upper limit of normal in children as³¹ :

- 4 mm for patients \leq 1 year,
- 4.5 mm for patients aged between 1 and 4 years,
- 5 mm for patients $>$ 4 years old

Recent work using a high resolution ultrasound probe describes an ONSD upper limit of around 5.7 mm in children, substantially greater than previously reported, but doesn't mention any specific age-related variation.³⁴

Issues like observer-variability, different imaging modalities to visualise the ONS and limited data using invasively measured ICP for comparison, have hampered the widespread use of this technique as a non-invasive surrogate marker of ICP in children. The only study in children comparing ONSD to invasively measured ICP did not recommend any cut-off value for ONSD.²³⁶

The positive relationship between ONSD enlargement and increasing ICP in children has been demonstrated in a number of studies,^{23,28-30,32,33,50,234,238-240} however the diagnostic accuracy varies.

These studies demonstrate that the relationship between ONSD and ICP in children certainly warrants further investigation. The current literature also highlights a distinct paucity of data evaluating this non-invasive technique in children and the need for a prospective study comparing ONSD measurement to the gold standard of directly measured ICP.

In an effort to address some of these shortcomings, the working hypothesis of this thesis was that ONSD measurement had a positive relationship with invasively measured ICP and the study therefore aimed to address some of the disparity surrounding inter-observer variability, age-related thresholds in children and limited understanding of the elastic nature of the ONS.

The following section discusses the available literature evaluating ONSD measurement in adults.

4.2. Adult studies

The volume of adult literature evaluating ONSD measurement as a non-invasive marker of ICP is significantly larger than in children. The majority of available literature compares ONSD to clinical or image-based assessment of ICP^{21-26,244} however, there are a number of papers comparing ONSD to directly measured ICP.^{16-20,73,154,155,245-247} Some of these studies support the use of ONSD while others have found it of little value. This section will analyse these studies according to the reference standard and modality used. These studies will then be discussed together at the end of the chapter.

4.2.1. Support for the use of ONSD as a marker of raised ICP

Several studies evaluating ONSD measurement have demonstrated a significant relationship between ONSD and ICP. Most of these studies were performed using ultrasound, but some have used MRI and more recently also CT scans.

4.2.1.1. Ultrasound-based studies

i. Non-invasive ICP assessment (clinical and imaging-based assessment)

The majority of studies evaluating the role of sonographic ONSD measurement were performed in an emergency department (ED) setting. The reference standard in most of these studies is clinical assessment or CT-evidence of raised ICP, given the lack of access to invasive ICP measurement in this environment.

Aiming to evaluate the convenience and utility of optic nerve ultrasound (ONUS) in the ED, Girisgin and co-workers reported their findings in 28 patients admitted to the emergency department with evidence of elevated ICP (EICP) on cranial CT scan (CCT). The findings were compared to 26 healthy volunteers. The mean ONSD measurement in

patients with EICP findings on CCT was 6.4 mm (SD 0.7), compared to a mean of 4.6 mm (SD 0.3) in the control group ($p < 0.001$). The authors did not suggest a cut-off value, but recommended ONUS as a useful and practical method for evaluation and follow-up of ICP.²²

Several subsequent used an ONSD cut-off of > 5 mm to evaluate the accuracy for detecting suspected raised ICP.

One of the earliest studies evaluating the use of ONSD in a clinical setting in was performed on 35 adults with suspected raised ICP. The mean ONSD in patients with evidence of raised ICP on CT scan was 6.27 mm, compared with a mean of 4.42 mm in patients without evidence of raised ICP. The difference between ONSD measurements in the two groups was described as 1.85 mm ($p = 0.001$). Using a previously recommended ONSD cut-off value > 5.0 mm (248,249,154), the authors demonstrated a sensitivity of 100% and specificity of 95%.²⁴³

Using the described ONSD cut-off of 5 mm, Tayal et al. (the same team as the earlier Blaivas study), performed a prospective blinded observational study in the emergency department on 59 adult patients with a mean age of 38 years, suspected of having raised ICP. The mean ONSD in patients with CT evidence of raised ICP was 6.37 mm, and in the group without evidence of raised ICP, the mean ONSD was 4.94 mm. Using 5 mm as a cut-off point, the study described a sensitivity of 100%, and specificity of 63% for predicting raised ICP.²³

A comparison of clinical findings, ONUS and CT evidence of raised ICP in 100 adults with head injury, interestingly demonstrated a poor correlation between clinical features of raised ICP and CT findings suggestive of raised ICP ($p = 0.9267$). The mean ONSD in the group with CT evidence of raised ICP was 5.8 ± 0.57 mm, vs 3.5 ± 0.75 mm ($p < 0.0001$) in the group without evidence of raised ICP on CT. Using a cut-off value for ONSD of > 5 mm for predicting raised ICP on CT, the study demonstrated good diagnostic accuracy (sensitivity of 98.6%, specificity of 92.6%).²⁴

Again using CT evidence of raised ICP as the reference standard, Major and co-workers evaluated 26 adult patients presenting to the ED to determine if ONSD could accurately

predict the presence of raised ICP. Using an ONSD value > 0.5 cm, the described sensitivity was 86% with specificity of 100%.²⁵

The use of ONSD measurement specifically in the hyperacute phase (within 6 hours) to detect intracranial haemorrhage (ICH), was investigated by Skoloudik and colleagues. This study included 31 patients with ICH, comparing them to 31 control patients. Sonographic ONSD measurements were performed at 3 and 12 mm behind the globe. Relative ONSD enlargement of > 0.66 mm ($> 21\%$) demonstrated an accuracy of 90.3% for predicting an ICH volume $> 2.5\text{cm}^3$. The authors then used an ONSD value of > 5 mm, demonstrating a sensitivity of 0.708 (95% CI 0.620 – 0.708), specificity of 1.000 (0.697 – 1.000), positive predictive value of 1.000 (95% CI 0.875 – 1.000) and a negative predictive value of 0.500 (0.348 – 0.652), concluding that enlargement of the ONSD may be detectable in the hyperacute stage of increased ICP.⁽²⁶⁾ The use of ONSD to evaluate the clinical evolution of ICH beyond the acute stage was also later confirmed.²⁵⁰

Qayyum et al. investigated the value of an ONSD > 5 mm for predicting features of raised ICP on CT scan in 24 adult patients, demonstrating a sensitivity of 100% and specificity of 75% for predicting elevated ICP on CCT scan. An interesting observation was the good quality of images, despite the limited intrinsic ability of the ultrasound machine, suggesting that a high specification machine / probe was not necessary to perform ONSD measurement.²⁵¹

In an ICU-based study on 101 adults (60 with suspected raised ICP and 41 control patients), a lower optimal ONSD-cut-off value of 4.716 mm was demonstrated. Shirodkar et al. The mean ONSD in the control group was 4.6 ± 0.09 mm for females and 4.8 ± 0.10 mm for males, vs 5.1 ± 0.62 mm for females and 5.08 ± 0.58 mm for males in the study group. 35 patients displayed radiological findings consistent with raised ICP, in this subgroup the mean ONSD was 5.4 mm for females and 5.44 mm for males. Diagnostic accuracy analysis demonstrated a sensitivity of 77.8% and specificity of 100% for predicting raised ICP on imaging.²⁴⁴

Bauerle and co-investigators conducted a prospective study in 40 adult volunteers to establish normal values and to assess the intra- and inter-observer reliability of ONSD

measurement. The mean ONSD was 5.4 ± 0.6 mm, with a wide range of normality between 4.3 – 7.6 mm and no significant difference between the right and left eyes. The investigators also demonstrated no correlation between ONSD and age, gender or body-mass-index (BMI), but found that transorbital B-mode ultrasound was a reliable method for assessing ONSD, highlighting the need for additional studies investigating this technique.²⁷

Author	Type of study	Comparison standard	Aetiology of raised ICP	Study size	Year	Frequency and type of probe	Described ONSD value	Diagnostic accuracy	Recommendation
Blaivas	Prospective	CT scan	Mixed	35	2002	10 MHz linear array probe	5.0 mm	Sensitivity of 100% and specificity of 95%	There is a close correlation between ONSD on ocular ultrasound and evidence of raised ICP on CT scan
Girisgin	Prospective	CT scan	Heterogeneous population with findings of EICP on cranial CT scan	28 patients with EICP, and 26 control patients	2007	7.5 MHz linear probe	6.4 (0.7) mm in patients with EICP, and 4.6 (0.3) mm in control patients	Not performed	ONSD measurement can be used to identify patients at risk for raised ICP, potentially prior to lumbar puncture and CT scan
Tayal	Prospective blinded observational	CT scan	Mixed	59	2007	7.5 MHz, linear array probe	5.0 mm	Sensitivity 100%, specificity 63%	Bedside ONSD measurement using ultrasound is beneficial for detecting raised ICP in the ED
Goel	Prospective blinded observational	Clinical findings and CT scan	Head injury	100	2008	7.5 MHz linear array probe	5.0 mm	Sensitivity 98.6%, specificity 92.8%, positive predictive value 97.26%, negative predictive value 96.3%	ONUS is potentially useful in head injury patients by avoiding unnecessary CT scans and serial monitoring to detect enlarging hematomas
Major	Prospective observational	CT scan	Trauma and non-trauma patients	26	2010	7.5 MHz probe	> 5 mm	Sensitivity of 86% and specificity of 100% for raised ICP. Sensitivity of 60% and specificity of 100% for detecting any acute intracranial abnormality	ONSD measurement with minimal training is a useful marker of raised ICP on CT scan

Author	Type of study	Comparison standard	Aetiology of raised ICP	Study size	Year	Frequency and type of probe	Described ONSD value	Diagnostic accuracy	Recommendation
Skoloudik	Prospective (bi-centre)	CT scan	Patients with ICH	31 ICH patients, 31 control patients	2011	10 and 12 MHz linear array probes	Enlargement of the ONSD > 0.66 mm (>21%) demonstrated a 90.3% accuracy for predicting ICH volume > 2.5cm ³	Using an ONSD cut-off of > 5mm demonstrated sensitivity of 0.708 and specificity of 1.0 for predicting ICH > 2.5cm ³	Sonography of the ONSD may be useful in detecting raised ICP in the hyperacute phase after ICH
Qayyum	Prospective diagnostic	CT scan	Mixed	24	2013	7.5 MHz linear array probe	> 5.0 mm	Sensitivity of 100% and specificity of 75%	Ultrasound measurement of the ONSD is accurate for detecting intracranial hypertension
Shirodkar	Prospective observational	CT/MRI scan	Not specified (patients presenting with clinical symptom of raised ICP)	101 (41 control, 60 study patients)	2014	10 MHz linear array probe	4.716 mm	Sensitivity of 84.6% in females and 75% in males, specificity of 100% in both genders	Bedside ONSD measurement is a useful test for identifying raised ICP
Bauerle	Prospective study	Clinical presentation	Healthy subjects	40	2012	9-3 MHz linear array probe	5.4 ± 0.6 mm as the mean in normal subjects	Nil	Transorbital B-mode sonography is a reliable method to assess the ONSD.

Table 4.4. Adult studies supporting the use of ONSD measurement (non-invasive ICP measurement)

Summary – Ultrasound-based ONSD measurement (non-invasive ICP measurement)

Most studies comparing ONSD measurement to clinical assessment or CT-based evidence of raised ICP have used 5.0 mm as a default cut-off value for predicting raised ICP. None of these studies evaluated an optimal cut-off value within their own environment, but rather validated pre-existing described values with variable diagnostic accuracy.^{22-26,243,251} This limitation is described and acknowledged in most of these studies, and is entirely due to the lack of access to invasive ICP measurement in the ED setting. These studies, however, are important as they reflect the reality faced in most acute care units. The need for invasive ICP monitoring, as the ‘gold standard’ against which ONSD measurement should be validated has been highlighted repeatedly. The literature describing invasive ICP measurement as the reference standard will be discussed in the following section.

ii. Invasive ICP assessment

Early work by Hansen and Helmke⁵⁰ involved a prospective, in vivo study in twelve adult patients with clinical suspicion of raised ICP. Patients underwent a lumbar spinal infusion test, where Ringer's lactate was delivered into the thecal sac via lumbar. CSF pressure was transduced via a second spinal needle. Ultrasound evaluation of the ONS was performed in B-mode at regular intervals of 2 – 4 minutes during these infusion tests. Changes in the ONSD were clearly demonstrated, with maximum dilation of 0.7 – 3.1 mm (15 – 89%) from the baseline diameter. ONSD of > 5 mm consistently coincided with CSF pressures of ≥ 30 mmHg. Testing the correlation between ONSD and CSF pressure yielded a high correlation coefficient ($r > 0.83$). The authors made the observation that changes in ICP would remain undetected by ONSD measurement if the ICP was too low (average ICP 22 mmHg), attributing this observation to the elastic structure, i.e. specialized collagen fibril texture, which determines the sheath's pressure response. Two very important statements from this seminal paper are that “that elastic structures determine the sheath's pressure response” and “At higher CSF pressure levels, the ONS may lose its ability for further dilation, which corresponds to a depleted capacity for further expansion.” These observations likely form the fundamental principles of the ONS response to change in ICP. The pressure threshold for sheath dilation was found to be above the range of normal ICP (18 – 30 mmHg). The authors conclude that serial ONS assessment provides a fast, non-invasive estimate of the level of CSF pressure, but cannot accurately estimate absolute ICP.¹⁵⁴

Despite a number of studies using clinical assessment and imaging features as a surrogate marker of raised ICP against which ONSD measurement was compared,^{21,23,29,243} it was almost a decade later that Geeraerts and colleagues¹⁶ performed a prospective blinded observational study comparing ONSD measurements to invasively measured ICP. This study included 31 adult patients with severe TBI and compared them to 31 control patients, examining the relationship between ONSD measured on admission to ICU and raised ICP (> 20 mmHg for 30 minutes) within the first 48 hours after trauma. The mean ONSD in TBI patients with raised ICP was 6.25 ± 0.5 mm, in TBI patients with normal ICP was 5.05 ± 0.7 mm, and in control patients was 4.85 ± 0.4 mm ($p < 0.0001$ vs control and normal ICP groups). The authors suggest an optimal ONSD cut-off value of 5.9 mm, with a sensitivity of 87% and a specificity of 94% for predicting raised ICP in the first 48

hours.^{16,17} The same team later published results from a prospective study in 37 adult TBI patients evaluating the relationship between ultrasound measurement of ONSD and invasively measured ICP, again demonstrating a strong relationship between mean ONSD and ICP ($r = 0.71$) and described a cut-off ONSD value of 5.86 mm (sensitivity of 95%, specificity of 79%) for predicting raised ICP, concluding that ONSD was a promising method for estimating ICP and also that changes in ONSD were strongly related to changes in ICP.¹⁷

The concept of combining two non-invasive techniques to assess ICP and potentially improve their accuracy, was described by Soldatos and co-workers.¹⁹ This study investigated the relationship between ONSD measurement, TCD and invasively measured ICP in 76 critical care patients. The investigators reported a good correlation between ONSD measurement, non-invasive (TCD) ($r = 0.8$, 95% CI: 0.62 – 0.9, $p < 0.0001$) and invasive ICP ($r = 0.68$, 95% CI: 0.43 – 0.83, $p = 0.0002$) measurement of ICP in severe TBI, but poor correlation in moderate TBI ($r = 0.32$, $p = 0.11$) and in healthy control individuals ($r = 0.29$, $p = 0.15$). The best ONSD cut-off value to predict an elevated ICP (> 20 mmHg) was 5.7 mm, with a sensitivity of 74.1% and specificity of 100%.¹⁹

Also using an ICP threshold of 20 mmHg, Moretti and Pizzi demonstrated that ONSD measurement may be useful as a screening tool to assess the need for invasive ICP monitoring, but could not be used for absolute ICP measurement. In this prospective study including 53 patients with intracerebral haemorrhage ($n = 23$) and subarachnoid haemorrhage ($n = 30$), as well as 53 control patients, the group with ICP > 20 mmHg demonstrated a mean ONSD of 6.2 ± 0.6 mm compared with 5.0 ± 0.5 mm in the low ICP group ($p < 0.01$). The mean ONSD in the control group was 4.9 ± 0.4 mm. Correlation between ONSD and ICP at admission was significant ($r = 0.69$, $p < 0.01$). The optimal ONSD cut-off point for detecting an ICP > 20 mmHg, was 5.2 mm with a sensitivity of 94% (95% CI: 88 – 100), specificity of 76% (95% CI: 65 – 87).²⁰

Rajajee et al. performed a prospective blinded observational study on 65 patients in the ICU. All patients in the study had either had an EVD or intraparenchymal ICP monitor in situ. The authors used individual as well as mean ONSD values to account for possible fluctuation in the ICP during ONSD measurement. For the individual ONSD

measurements the median was 0.53 cm for ICP > 20 mmHg, and 0.4 cm for ICP < 20 mmHg ($p < 0.0001$). An ONSD of 0.48 cm demonstrated a sensitivity of 96% and specificity of 94% for predicting ICP > 20 mmHg. The authors suggested that the optimal criteria for ONSD measurement should be validated internally.¹⁸ The same author later published a retrospective review of this data, aiming to assess the accuracy of ONSD measurement in patients with acutely fluctuating ICP. 73 patients were included in the review. ‘Acutely fluctuating ICP’ was defined as measurements above and below 20 mmHg during the same ONSD measurement cluster or a change in ICP of > 10 mmHg, demonstrating that the specificity and positive predictive value of ONSD measurement declined when ICP fluctuated acutely, suggesting this may be due to a delay in reversal of the nerve sheath distension.⁵¹

In another study also based in the neurocritical care unit, Frumin and co-workers investigated 27 patients with invasively measured ICP. The optimal ONSD for predicting raised ICP (> 20 mmHg) in this study was 5.2 mm, with a sensitivity of 83.3% (95% CI = 35.9 – 99.6%), specificity of 100% (95% CI = 83.9 – 100%), positive predictive value (PPV) of 100% (95% CI = 48 – 100%) and negative predictive value (NPV) of 95.5% (95% CI = 77.2 – 99.9%).²⁴⁶

Despite not providing diagnostic accuracy analysis, the study by Cammarata and colleagues which compared ONSD measurement in 11 TBI patients in the ICU with 10 non-trauma ICU patients, demonstrating a significant difference between the two. The ONSD in control patients was 5.51 ± 0.32 mm, 5.52 ± 0.36 mm in head trauma patients with normal ICP (< 20 mmHg) and 7.0 ± 0.58 mm in head trauma patients with raised ICP (> 20 mmHg).²⁴⁵

Using an ICP threshold of 20 cmH₂O, Kimberly and co-workers conducted a prospectively studied 15 adult patients. The authors performed 38 ocular ultrasound examinations, demonstrating a mean ONSD of 5.4 ± 0.49 mm in the group with ICP >20 cmH₂O, and 4.4 ± 0.49 mm in the group with ICP < 20 cm H₂O, with a mean difference between the two groups of 1.2 mm. The study also supported an optimal cut-off value for ONSD > 5.0 mm, which yielded a sensitivity of 88% and a specificity of 93% for detecting raised ICP.⁷³

Also using an ICP threshold of 20 cm H₂O measured during LP, Amini and colleagues reported an ONSD > 5 mm demonstrating a sensitivity and specificity of 100% for predicting ICP ≥ 20 cm H₂O. In this study of 50 non-traumatised patients, 36 patients had a normal ICP and 14 had increased ICP.²⁴⁷

A blinded cross-sectional study conducted only in Chinese patients also used a lumbar CSF opening pressure of 20 cm H₂O. The study conducted by Wang et al included 279 subjects and sought to identify potential factors influencing the relationship between ONSD and ICP. A much lower ONSD cut-off point of 4.1 mm, with a sensitivity of 95% and a specificity of 92% was reported in this study. The authors described a number of possibilities for the discrepancy between their findings and previous reports, acknowledging that little was known about the factors influencing the relationship between ICP and ONSD, ascribing the inconsistency of their lower ONSD values to differences in ethnicity and severity of illness.¹⁵⁵

Author	Type of study	Aetiology of raised ICP	Study size	Year	Frequency and type of probe	ICP threshold	Described ONSD value	Diagnostic accuracy	Recommendation
Hansen	Prospective	Patients undergoing neurological testing	12	1997	7.5 Mhz probe		Nil	Nil	ONS distension occurs within a limited CSF pressure interval. A threshold of 22mmHg needs to be exceeded for an increase in ONSD to be detected. The lumbar infusion test performed would not be reproducible in most other centres
Geeraerts (2007)	Prospective blinded observational	TBI	31 TBI patients, 31 control patients	2007	7.5MHz linear probe	20 mmHg	5.9 mm	Sensitivity of 87%, and specificity of 94%	ONSD measurement in the early posttraumatic period predicts raised ICP in the 48 hours following TBI
Geeraerts (2008)	Prospective	TBI	37	2008	7.5 MHz linear array	20 mmHg	5.86 mm	Sensitivity of 95%, specificity of 79% for predicting ICP > 20 mmHg	ONSD measurement in sedated neurocritical care patients is a promising method for predicting raised ICP
Soldatos	Prospective	TBI	76 (50 TBI and 20 control patients)	2008	9 MHz linear array	20 mmHg	5.7 mm	Sensitivity 74.1%, specificity 100%	ONSD measurement correlates well with non-invasive (TCD) and invasive ICP measurement in TBI
Moretti	Prospective blinded observational	Spontaneous ICH	53 patients with intracranial pathology, 53 control patients	2009	7.5MHz linear array probe	20 mmHg	5.2 mm predictive of ICP > 20 mmHg	Sensitivity of 94%, specificity of 76%	Ultrasound measurement of the ONSD is a useful in the early diagnostic evaluation of patients with ICH

Author	Type of study	Aetiology of raised ICP	Study size	Year	Frequency and type of probe	ICP threshold	Described ONSD value	Diagnostic accuracy	Recommendation
Rajajee	Prospective blinded observational	Mixed	65	2011	13-6 MHz, linear array probe	20 mmHg	4.8 mm	Sensitivity of 96%, specificity of 94%	ONSD measurement is an accurate, non-invasive technique for detecting raised ICP in a neurocritical care setting, performed by an experienced operator
Cammarata	Unclear	TBI	11 head injured patients (10 control patients)	2011	10 MHz linear array probe	20 mmHg	With ICP > 20mmHg, ONSD \pm 7mm, with ICP < 20 mmHg, ONSD \pm 5.5 mm	Not done	Ocular ultrasound is a good alternative for rapid indirect evaluation of ICP in head trauma patients
Frumin	Prospective blinded observational	Mixed	27	2014	5 -10 MHz linear array probe	20 mmHg	5.2 mm	Sensitivity of 83.3%, specificity of 100%, positive predictive value of 100%, negative predictive value of 95.5%	Bedside ultrasound is useful for early diagnosis of raised ICP in the emergency department
Kimberly	Prospective blinded observational	TBI and ICH	15	2008	10MHz linear probe	20 cm H ₂ O	ONSD > 5.0 mm	Sensitivity of 88%, specificity of 93%	Bedside measurement of ONSD correlates well with invasively measured ICP. Small patient sample. Using a ICP cut-off of 20cm H ₂ O, makes comparison slightly difficult

Author	Type of study	Aetiology of raised ICP	Study size	Year	Frequency and type of probe	ICP threshold	Described ONSD value	Diagnostic accuracy	Recommendation
Amini	Descriptive prospective	Non-trauma neurologic patients	50	2013	7.5 MHz linear array probe	20 H ₂ O	ONSD > 5.5 mm	Sensitivity and specificity of 100%	ONSD is a strong predictor of increased ICP
Wang	Blinded cross-sectional	101 with raised ICP, 178 control patients	279	2015	9 MHz linear array probe	20 cmH ₂ O	4.1 mm for predicting raised ICP (> 20 cmH ₂ O)	Sensitivity of 95%, specificity of 92%, AUROC 0.965.	ONSD cut-off value in Chinese population may be smaller than historical values reported in the Caucasian population. ICP threshold of 20cmH ₂ O is not the ideal value for comparison, and ICP measured via lumbar puncture makes the readings less robust

Table 4.5. Adult studies supporting the use of ultrasound measurement of the ONSD (invasive ICP measurement)

Summary – Ultrasound based measurement of the ONSD (invasive ICP measurement)

These studies all support a significant relationship between ONSD and increasing ICP. The reported ONSD cut-off values however, range from 4.1-5.9 mm.^{16-20,73,154,155,245-247} The variable diagnostic accuracy reflects the discrepancy regarding optimal ONSD cut-off values to detect raised ICP. Studies using an ICP threshold of 20 mmHg, describe ONSD cut-off values between 4.8 and 5.9 mm and three studies using 20 cmH₂O as the ICP threshold, describe ONSD cut-off values between 4.1 and 5.5 mm. These findings underscore the fact that using different ICP thresholds in these studies may influence the variability of described ONSD cut-off values, but it certainly isn't the only factor. The variation in individual baseline measurements and the difficulty in estimating the distensibility of the ONS are perhaps the two most significant factors responsible for the poor specificity of this technique.²⁵² The effect of treatment modalities, sedation, physiological parameters that influence ICP and site of measurement (some studies use LP opening pressures) likely also have some effect on the relationship between ONSD and ICP. The imaging modality used for ONSD measurement has been described as a significant factor. MRI and CT-based studies will therefore be discussed separately in the following sections.

4.2.1.2. MRI-based studies

MRI provides exquisite detail and multiplanar imaging of the ONS, but unfortunately limits simultaneous measurement of ICP. Relatively limited access to MRI and the necessity for patient transfer to specialised MRI suites are the major limitations with this modality.

Using MRI measurements acquired before and after drainage of subdural collections, Watanabe et al studied 12 adult patients who underwent bur-hole drainage of subdural collections. A high ICP in this group was defined as $> 20 \text{ cmH}_2\text{O}$. Coronal fat saturated T2-weighted, fast spin echo sequences of the orbit were performed, demonstrating a mean ONSD before surgery of $6.1 \pm 0.7 \text{ mm}$, and after surgery of $4.8 \pm 0.9 \text{ mm}$ ($p = 0.003$). An acknowledged limitation of the study was the use of subdural pressure measurement, which may not be representative of ventricular pressure, due to resistance from membranes within the subdural space. The authors proposed an ONSD measurement of 5.8 mm taken just behind the globe as the upper limit of normal, suggesting that a value of 6.0 mm would be indicative of raised ICP in this population.²⁵³

The study by Geeraerts et al. described ONSD measurements which were strikingly similar to previous reports from the same group, using ultrasound to measure the ONSD. This retrospective analysis on 38 adult patients with severe TBI, reviewed T2-weighted turbo spin-echo, fat-suppressed images acquired on a 3 Tesla MRI scanner, and compared the results with 36 healthy volunteers. Both the ONSD and optic nerve diameter (OND) were measured and correlated with ICP, using a threshold of 20 mmHg for raised ICP. The mean ONSD in TBI patients with raised ICP was $6.31 \pm 0.5 \text{ mm}$, in TBI patients with $\text{ICP} < 20 \text{ mmHg}$ was $5.29 \pm 0.48 \text{ mm}$, and in healthy volunteers ONSD was $5.08 \pm 0.52 \text{ mm}$. The inter-observer variability was 0.11 mm, which is lower than reported in ultrasound-based studies. The authors suggested an optimal ONSD cut-off of 5.82 mm, with a sensitivity of 90% and specificity of 92% for predicting raised ICP.¹⁵¹

In a unique study, Xie et al. attempted to predict lumbar CSF pressure using a formula which includes orbital subarachnoid space width (OSASW), BMI and mean arterial blood

pressure (MABP). This was a prospective observational, comparative study on 72 patients with neurological disease requiring a lumbar puncture, aiming to evaluate the OSASW as a surrogate marker for ICP and develop an MRI-based method for assessing CSF-pressure. The MRI sequences in this study were performed on a 3-Tesla machine in an oblique coronal plane, perpendicular to the optic nerve, with measurements performed at distances of 3, 9 and 15 mm posterior to the globe. MR imaging was performed 24 – 48 hours prior to the lumbar puncture being performed. The authors also performed a bi-spectral OCT analysis of retinal nerve fibre thickness and measured intraocular pressure (IOP) as other non-invasive markers of ICP. The ICP measurements in this cohort ranged from 3.7 mmHg to 26.5 mmHg (increased ICP defined as > 20 mmHg). The authors performed a four-step analysis of the data to identify and control for potential confounding factors, i.e. body-mass-index (BMI) and mean arterial blood pressure (MABP), to best describe the relationship between the OSASW and ICP. Applying the described analytic models to the data, the authors derived formulas for assessing ICP, based on OSASW, BMI and MABP. These formulas were applied to a subset of 30 test group patients and found to be ‘relatively precise’ in assessing ICP, concluding that MRI-assisted OSASW measurement could be a helpful non-invasive tool in ICP measurement.²⁵⁴

In a study examining astronauts after exposure to microgravity during a space mission, Kramer and colleagues retrospectively analysed images from 8 astronauts, acquired using a 3-Tesla MRI scanner. Aiming to demonstrate the spectrum of intraorbital and intracranial findings following such a mission, the authors analysed a number of parameters, similar to those observed in idiopathic intracranial hypertension (IIH) including: OND, posterior flattening of the globe, optic nerve protrusion, kinking of the optic nerve sheath, central T2 hyperintensity of the optic nerve and concavity of the pituitary dome. The mean ONSD measured at 4 mm behind the sclera was $6.2 \text{ mm} \pm 1.1$ (range 4.7 – 10.8), and the mean OND was $3.0 \text{ mm} \pm 0.5$ (range 2.4 – 4.5) The measured ONSD values in this study were considerably larger than other reported MRI measurements.¹⁵¹ The retrolaminar OND and ONSD appeared larger in cases where there was associated optic nerve kinking and central T2 hyperintensity of the optic nerve. The abnormal findings of the OND and ONSD in this group certainly highlight their value as radiological markers of raised ICP.²⁵⁵

Author	Type of study	Comparison standard	Aetiology of raised ICP	Study size	Year	Modality	Described ONSD value	Diagnostic accuracy	Recommendation
Watanabe	Not clearly stated	Invasively measured subdural pressure	CSDH and hygroma	12	2008	Fat saturated T2-weighted fast spin echo MRI	Suggested value of 6.0 mm to predict raised ICP	Not done	Measurement of ONSD on T2-weighted MRI can potentially identify abnormally high ICP in patients with subdural collections. Also the demonstrated decrease in ONSD following decompression suggests that a change in ONSD may be helpful in monitoring ICP.
Geeraerts	Retrospective	Invasive ICP measurement	TBI	38 patients, 36 healthy control	2008	3T-MRI	5.82	Sensitivity of 90%, specificity of 92%	ONSD measurement on routine MRI for TBI patients correlates with invasive ICP
Xie	Prospective observational, comparative	Lumbar CSF pressure measurement	Patients with neurological disease	72	2013	3T-MRI	Measurements were taken at 3, 9 and 15 mm behind the globe, the authors proposed algorithms for the association between CSF pressure and OSASW at each of these locations	Correlation was demonstrated between CSF-P and OSASW, within a CSF-P range of 3.7 – 26.5 mmHg.	Measurement of the ONSD at various distances from the globe using MRI scans, could provide a means for invasively assessing ICP.
Kramer	Retrospective	Clinical presentation and radiological evidence of raised ICP	Exposure to microgravity	27	2012	3T-MRI	The ONSD ranged between 4.7 – 10.8 mm, but no cut-off values were recommended	Nil	Exposure to microgravity induces changes in the morphology of the optic nerve and its sheath. The conclusions are difficult to generalise to a clinical setting

Table 4.6. MRI-based adult studies supporting the use of ONSD measurement

Summary - MRI-based studies

The number of MRI studies are quite limited and the described ONSD cut-off value in these studies are 5.8 and 5.82 mm, to detect ICP above 20 cmH₂O and 20 mmHg, respectively. Kramer,²⁵⁵ however described a range of values between 4.7 and 10.8 mm, which are substantially larger than any other reported ONSD values. The values described in the other three studies, however, fall within the range described in previous ultrasound-based reports of 4.1 – 5.9 mm.^{16-20,73,154,155,245-247} Three of the four studies were performed using a 3 Tesla Machine, which raises the question of whether images on 1.5 Tesla machine are sufficient, however reports in children²³⁸⁻²⁴⁰ and the study by Watanabe,²⁵³ suggests that these images are adequate. The general agreement is that MRI-derived measurement has lower inter-observer variability and provides better detail of the structures within the ONS complex.

4.2.1.3. CT-based studies

More recently there has been an interest in CT-based measurement of the ONSD. This is especially interesting, as CT scans are widely used as an early imaging modality in the acute care setting, to detect features of raised ICP.

The first study to investigate ONSD measurement on the initial CT scan and outcome from severe TBI was prospective study involving 77 TBI patients admitted to the neurosurgical ICU. ONSD measured on initial CT scan correlated well with survival and Glasgow outcome score (GOS) at 6 months ($p = 0.03$). The mean ONSD in the non-survivor group was 7.8 ± 0.1 mm versus 6.8 ± 0.1 mm in the survivor group. The optimal ONSD cut-off value was > 7.3 mm, with a sensitivity of 86.4% and a specificity of 74.6% for predicting mortality.²⁵⁶

In large, prospective cohort study involving 400 adults with healthy eyes and optic nerves, Vaiman and colleagues investigated the correlation between ONSD, the eyeball and the optic canal. The study demonstrated that the ONSD varied between 3.65 mm and 5.17 mm at different locations within the orbit (3 mm and 10 mm behind the globe respectively), and suggested that measurement at a distance of 10mm, rather than 3mm posterior to the globe was more suitable, largely due to changes in the ONSD caused by eyeball movements.⁵⁰ Use of the ONSD/ETD (Eyeball Transverse Diameter) index, with a normal described value of 0.19, is suggested as a means of improving the precision of this technique.²⁵⁷

Aiming to determine whether ONSD measured on initial CT scan could predict neurological outcome, Kim et al performed a retrospective analysis of 98 comatose cardiac arrest patients. The study used the cerebral performance category [CPC] scale to measure neurological outcome in post-cardiac arrest patients. The additional predictive feature assessed on brain CT scan was the grey matter-to-white matter ratio (GWR). The intra- and inter-rater correlation for ONSD measured on CT scan was 0.888 and 0.833 respectively. The mean ONSD was 5.57 ± 0.30 mm in the good CPC group and 6.29 ± 0.46 mm in the poor CPC group ($p < 0.001$). A cut-off value of 5.87 mm for ONSD, 1.21

for GWR and 3 for Glasgow Coma Scale (GCS) most accurately predicted poor neurological outcome. The authors then adjusted these to gain a specificity of 100%, resulting in ONSD of 6.21 mm (sensitivity of 55.9%, 95% CI: 43.3 – 67.9%) and GWR of 1.23 mm (sensitivity of 83.8%, 95% CI: 72.9 – 91.6%). The authors concluded that ONSD measured on initial brain CT scan acquired within 24 hours of return of spontaneous circulation following a cardiac arrest, was associated with neurologic outcome, and combining ONSD and GWR potentially improved prognostic performance, compared to either variable used alone.²⁵⁸

Use of a portable bedside CT scan was investigated by Sekhon et al. in a retrospective study of 57 adult patients aimed at assessing the relationship between ONSD measurement and ICP. All patients in the study had invasive ICP monitoring. The mean ONSD measurement was 6.7 mm (SD 0.75) and the mean ICP during CT was 21.3 mmHg (SD 8.4). The correlation between ONSD and ICP was significant ($r = 0.74$ $p < 0.001$). Using an ONSD cut-off value of 6.0 mm for predicting ICP > 20 mmHg demonstrated a sensitivity of 97%, specificity of 42%, positive predictive value of 67% and a negative predictive value of 92%. The authors performed a simple (model A) and multivariable linear regression models (models B and C). Model A demonstrated an R^2 value of 0.56, model B (comparing CT predictors of raised ICP to invasive ICP readings) demonstrated an R^2 of 0.21, while model C (addition of ONSD to CT predictors of ICP) improved the R^2 value to 0.60. The ONSD measurements also demonstrated excellent agreement between raters of 0.89 (95% CI: 0.83 – 0.93) and between the right and left sides of 0.96 (95% CI: 0.93 – 0.98). The authors concluded that ONSD measured on non-contrast, portable CT scan demonstrated a strong association with invasively measured ICP, was highly discriminatory of ICP > 20 mmHg, and demonstrated superior predictive value for increased ICP when compared to classical CT findings associated with raised ICP.¹⁵³ The same author later published a separate retrospective study on 220 patients, involving 2 centres, aimed at evaluating the relationship between ONSD measured on CT scan and mortality in patients with severe TBI. In a univariate analysis, a 1mm increase in ONSD demonstrated a twofold increase in odds of hospital mortality (OR 2.1, 95% CI: 1.4 – 3.2, $p < 0.001$). With multivariable adjustment, the relationship persisted (OR 2.0, 95% CI: 1.2 – 3.2, $p = 0.007$). Linear regression indicated that ONSD was associated with increased

ICP (> 20 mmHg) in the first 48 hours, with and without multivariable adjustment. The authors determined that estimation of increased ONSD on initial CT scan in patients with severe TBI was associated with mortality, and also demonstrated a linear relationship with invasively measured ICP.²⁵⁹

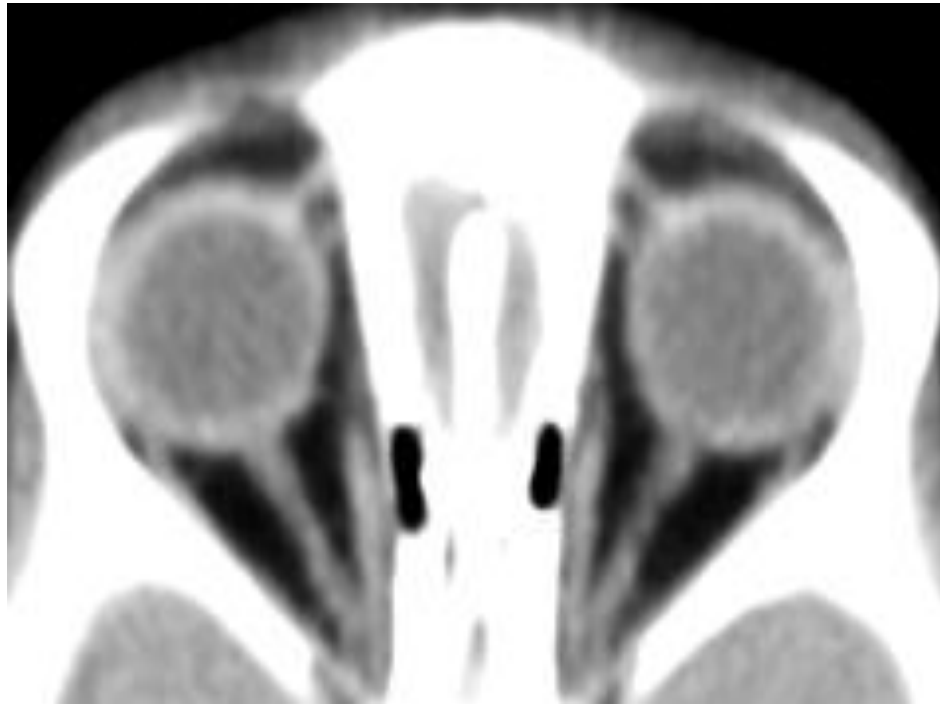


Figure 4.4. Axial CT scan demonstrating the ONS

Author	Type of study	Comparison Standard	Aetiology of raised ICP	Study size	Year	Modality	Described ONSD value	Diagnostic accuracy	Recommendation
Legrand	Prospective observational	Clinical outcome (ICU mortality)	TBI	77	2013	CT scan (initial)	> 7.3 mm	Sensitivity 86.4% and specificity 74.6% for predicting ICU mortality	ONSD measurement on initial CT scan correlates well with mortality in ICU after severe TBI
Vaiman	Prospective cohort	Nil (normative data)	Normal subjects	400	2014	CT scan	ONSD varies between 3.65 and 5.17mm at different locations in the orbit (3 and 10 mm behind the globe)	Not done	Calculating the ONSD/ETD index is more precise the ONSD measurement alone and measurement at 10 mm behind the globe is most stable
Kim	Retrospective	Clinical outcome (Post-cardiac arrest neurologic outcome)	Comatose patients who had a cardiac arrest	98	2014	CT scan (initial)	ONSD 5.87 mm accurately predicted poor neurological outcome. The prognostic performance was increased when combined with GWR (1.23)	Not done	Combining ONSD and GWR measured on initial CT scan could provide prognostic information in cardiac arrest patients
Sekhon, Griesdale	Retrospective	Invasive ICP monitoring	TBI with raised ICP	57	2014	CT scan (portable)	ONSD > 6 mm was tested to predict ICP > 20 mmHg	Sensitivity of 97%, specificity of 42%, PPV of 67%, NPV of 92%, AUROC of 0.83	ONSD measured on non-contrast portable CT scan was highly predictive of ICP > 20 mmHg, superior to classical CT findings
Sekhon, McBeth	Retrospective	Invasive ICP monitoring, clinical outcome	TBI	220	2014	CT scan (portable)	Nil	Nil	A 1mm increase in ONSD demonstrates twofold increase in odds of hospital mortality.

Table 4.7. CT-based adult studies supporting the use of ONSD measurement

Summary – CT based studies

Measurement of the ONSD on CT scan seems like a sensible approach, given the widespread use of CT as an early diagnostic modality in patients with raised ICP. The values described in the studies above range from 5.87 – 7.3 mm, when used to predict mortality from TBI and ICP above 20 mmHg. The study by Sekhon and colleague²⁴² demonstrated that measurement of ONSD on bedside portable CT scan is a better predictor of raised ICP than classical CT findings associated with raised ICP. Definition of the ONS on CT scan is dependent on the imaging window used and not always as clear as the appearance on MRI, this may influence the inter-observer variability

4.2.2. Studies not supporting the use of ONSD measurement

Blehar and co-investigators set out to compare visual with coronal axis measurements in 27 healthy volunteers. The mean ONSD in the coronal view was 3.4 mm, which did not correlate ($R: 0.51 - 0.69$) with axial view measurements taken at various distances posterior to the globe (2, 3, 6, 9, 12 and 15 mm). The persistently larger axial view measurement was thought to be due to artefactual shadowing, which in the opinion of the authors was a likely explanation for the discrepancy in ONSD values described in the literature.²⁶⁰

Assessing both unilateral and bilateral injuries, Strumwasser and co-workers investigated the accuracy of ONSD for detecting elevated ICP. This was prospective blinded study on 10 trauma patients requiring ICP monitoring. Using data obtained from performing 114 ONSD measurements, the authors demonstrated poor correlation of ONSD measurement with unilateral ($R^2 = 0.45$, $p < 0.01$) and bilateral head injury ($R^2 = 0.21$, $p = 0.01$). No significant difference in ONSD measurement was found pre- and post-ICP monitor insertion ($p = 0.3$). Despite a very small number of patients in the study, the authors concluded quite firmly that measurement of ONSD was not reliable enough as a basis for clinical decision-making regarding ICP assessment, and suggested the technique be used with caution.²⁶¹

Keyes and colleagues conducted a study on 57 adult volunteers to evaluate the relationship between increased ONSD and acute mountain sickness (AMS) related to rapid ascent. The authors found an increased ONSD at high altitude in subjects with AMS, but demonstrated no clear correlation between the variables they examined, i.e AMS symptoms, oxygen saturation, clinical response to oxygen and dexamethasone Lake Louise Score (LLS). The mean ONSD values of 0.4 cm in all subjects at baseline and 0.43cm in subjects with AMS symptoms 18 hours after ascent to 4300 m, while significantly different, are both relatively small measurements when compared to ONSD measurements described in other studies.^{17,18,19,20,24,253} The authors acknowledged this discrepancy and attributed this to differences in ascent profile and the scanning technique used in their study. They

concluded that raised ICP might not play a role in mild to moderate AMS, and that optic nerve sheath measurement with ultrasound might not be an adequate tool to investigate this issue.²⁶²

Caffery and colleagues performed a prospective observational trial involving 51 adult patients presenting to the emergency department, who underwent an LP. In all cases the underlying aetiology was non-traumatic. Raised ICP was defined as an opening pressure on LP of ≥ 20 cmH₂O, and an ONSD cut-off value of ≥ 5 mm was defined as abnormal. 24 (47%) of patients had opening pressures greater than 20 cmH₂O. There was a correlation between mean ONSD and opening CSF pressure ($r = 0.53$). The cut-off value of ≥ 5 mm yielded a sensitivity of 0.75 (0.53 – 0.9) and a specificity of 0.44 (0.25 – 0.65). The best cut-off value found by the authors was 5.5 mm, with a sensitivity of 0.58 (0.37 – 0.78) and specificity of 0.74 (0.54 – 0.89). The authors found that the cut-off value of ≥ 5 mm resulted in misidentification of 25% of patients with elevated ICP, and therefore questioned the utility of ONSD measurement in non-traumatic patients with suspected raised ICP.²⁶³

Summary - adult studies not supporting the use of ONSD measurement

The use of ONSD measurement as a non-invasive technique to predict raised ICP has also demonstrated limited diagnostic accuracy, using values > 5 mm to detect raised ICP resulted in misidentification of 25% of patients.⁽²⁶³⁾ The issues involving measurement in a single plane, user variability and diagnostic modality all contribute to the inconsistency in reported diagnostic accuracy.^{72,193,241,242,260,261,263} The poor specificity of ONSD measurement may also make it less accurate than other non-invasive techniques.¹⁹³

4.2.3. Discussion

The majority of available literature evaluating the use of ONSD measurement in adults are from studies performed in the ED or ICU, using transorbital ultrasound. As a result, the reference standard against which ONSD was measured in these studies was often clinical or radiological evidence of raised ICP. The most commonly used ONSD cut-off value was $> 5\text{mm}$.^{21-26,251,244} Not surprisingly this value is different in studies comparing ONSD to invasive measurement of CSF pressure, with a range of 4.1 -5.9 mm.^{17,18,19,20,73,155,246,247} The difficulty in describing a universally acceptable reference range is largely due to variation in the definition of raised ICP, inter-observer variability, patient heterogeneity and a limited understanding of the elastic characteristics of the ONS. The use of MRI and CT imaging of the ONSD also further dilutes the value of this technique. Despite clear description of a strong relationship between ONSD and increasing ICP, the optimism surrounding this technique is blurred by the lack of consensus regarding optimal cut-off values. A pooled diagnostic odds ratio (OR) of 51 (95% CI: 22-121) for detecting raised ICP was described in a meta analyses, favouring the diagnostic accuracy of ONSD measurement.¹⁵⁷ The best ONSD cut-off values for predicting raised ICP ranged between 5 - 5.9 mm with a diagnostic OR of 25.68 (95% CI: 14.405 – 45.571) in a review by Moretti and Pizzi,³¹ which also described the upper ONSD limit in children as: 4 mm for patients aged < 1 year, 4.5 mm for patients aged between 1 and 4 years old and 5 mm for patients aged $>$ years. A research group was recently formed to establish an individual patient-level database and possibly define standardised ONSD cut-off values. This study group however excludes patients under the age of 18 years, but the results of this effort will be eagerly awaited.²⁶⁴ The specific limitations of ONSD measurement have been highlighted in a number of studies which have found the technique inadequate for detecting raised ICP.^{263, 260, 261,193,242,72,241} There are however no descriptions of any complications related directly to the use of transorbital sonographic measurement of the ONSD.³¹

The lack of adequate specificity implies that a widened ONS may be present despite the absence of raised ICP, which is perhaps best explained in the work by Hansen and Helmke,^{154,252} describing the importance of the elastic characteristics or stiffness of the ONS as a factor determining the distensibility of the ONS. Improved understanding of

the elastic character of the ONS would certainly help with our interpretation of ONSD measurement and could help to differentiate a widened ONS due to individual baseline variation from one caused by raised ICP. The description of ‘hysteresis’ of the ONS by the same authors,²⁵² further complicates our understanding of the ONS response, but raises very important issues fundamental to improving our understanding of this technique. An analysis of the dynamic response of the ONS would be helpful in deciphering the elastic nature of the ONS.

The current literature highlights the need for a prospective study comparing ONSD to invasively measured ICP, defined according to an accepted treatment threshold. The ONSD study group is a promising initiative aiming to answer some of these questions in adults.²⁶⁴ Unfortunately patients under the age of 18 years are excluded from this study.

SECTION B

Chapter 5.

The relationship between optic nerve sheath diameter (ONSD) measurement and invasively measured intracranial pressure (ICP) in children: *Methodology*

5.1. Introduction

As discussed in the preceding chapter, the need for a reliable, non-invasive technique to assess ICP in children is fundamental.

The working hypothesis for this study was that ONSD measurement was a good surrogate marker of increasing ICP. ONSD was compared to the criterion standard of invasive ICP measurement in a large cohort of paediatric patients undergoing a neurosurgical procedure. Relevant physiological and demographic variables were analysed to best describe the the relationship between ONSD and ICP. Recommended age-related ONSD cut-off values that best predicted raised ICP^{28,29,30,32} were examined by selecting a range of ICP thresholds and analysing the relationship between ICP and ONSD at these thresholds.

5.2. Aims of the study

Primary aim:

- To describe the relationship between ONSD and directly measured ICP in children

Secondary aims:

- To identify and analyse confounding variables which may influence this relationship;
- To examine the correlation between individual repeat measurements acquired in the same plane of the same eye as an assessment of repeatability of the technique;
- To examine the correlation between mean ONSD measurements by the same observer at different timepoints as a marker of intra-observer variability;
- To examine the inter-observer variability;
- To examine correlation between the mean values in the sagittal and axial plane;
- To examine correlation between the mean values acquired in each eye;
- To determine the diagnostic accuracy of ONSD for detecting ICP above and below 20 mmHg (using 20 mmHg as a recommended treatment threshold), across the entire cohort of patients;
- To examine the relationship between ONSD and ICP across the entire cohort of patients, at various ICP thresholds:
 - 20 mmHg;
 - 15 mmHg;
 - 10 mmHg;
 - 5 mmHg
- To examine described age-related cut-off values for ONSD^{28-30,32} :
 - ≤ 1 year old;
 - > 1 year old;
 - Children between 1 and 4 years old and those above 4 years old
- To examine the use of patency of the AF as a reliable clinical marker for defining different ONSD cut-off values in children.

5.3. Methods

Study design: This study was a prospective, observational analysis of a paediatric cohort of patients who had direct measurement of ICP and concurrent ultrasound measurement of the ONSD.

Reporting of data in this study was in accordance with the ‘strengthening the reporting of observational studies in epidemiology’ (STROBE) guidelines.^{265,266} (included as appendix I)

Patients: Paediatric patients under the age of 14 years old treated at the Red Cross War Memorial Children’s Hospital, Cape Town, were eligible for enrolment into the study, if they were undergoing a surgical procedure for diagnostic or therapeutic purposes, and appropriate informed consent was obtained from the parents/caregivers to be enrolled into the study. The study was conducted between March 2013 and August 2014.

Inclusion criteria were:

- Patients requiring invasive ICP monitoring, based on clinical/radiological findings;
- Patients undergoing surgical procedures to treat suspected raised ICP, e.g. VPS insertion, evacuation of space occupying lesions and decompressive procedures;
- Patients undergoing a neurosurgical procedure during which measurement of ICP could be performed safely, without negatively impacting the patients well-being.

Exclusion criteria were:

- Patients who had ocular pathology, e.g. orbital trauma or cataract, which would preclude sonographic measurement of the ONSD;
- Patients with signs of critically raised ICP, needing urgent surgery;
- Patients who were haemodynamically unstable between ONSD acquisition and ICP measurement;

- Patients receiving medication that would decrease ICP between ONSD imaging and ICP measurement, i.e. mannitol, hypertonic saline or steroids;
- Time between ONSD imaging and ICP measurement exceeded 1 hour.

Acquisition of the ONSD images did not influence the management of patients during the study, as this was purely an observational study.

5.3.1. Acquisition of ONS images

All ultrasound image-acquisition was performed by a single investigator, experienced in the use of ultrasound in neurosurgical patients. The investigator was blinded to the actual invasive ICP measurement at the time of image acquisition, as the ONSD measurements were always performed just prior to ICP measurement. While the investigator was blinded to actual ICP measurement, some bias may still have existed as the reason for patients requiring surgery was often known to the investigator. Repeat measurements of the ONSD were performed by two investigators, experienced in the use of transorbital ultrasound in 30 cases. Data from the examinations were used to test repeatability, intra- and inter-observer variability.

In all cases, patients had undergone anaesthetic induction and were being mechanically ventilated. ONSD measurement was performed when haemodynamic parameters were most stable, just prior to insertion of the ICP monitor. All ONSD measurements were performed with patients in the supine position, with the head central and elevated to approximately 30 degrees. A clear film protective dressing was placed over both eyes to protect the globe from any potential injury. A layer of coupling gel was applied over the closed upper eyelid. To identify and image the ONS the ultrasound probe with the smallest available footprint – a 7-15 Mhz linear array probe with a ‘hockey stick’ configuration (See Figure 2.3) (Philips, Bothell, USA) was used in all cases. Positioning of the probe over the eye was always carefully performed. This process included use of the middle finger and left hand to palpate the bony surface of the superior orbital rim, glabella and inferior orbital rim, to ensure that the application of the probe over the surface of the eyelid never exerted any pressure on the globe itself.

Recommended techniques for imaging of the ONS are discussed under ocular sonography (Chapter 3, Section B).

The depth was set to 4 cm as a default setting and the magnification was then adjusted to provide the best quality of imaging for individual patients. The setting with the lowest MI and TI (as discussed below were always chosen). ONSD measurement was performed at an angle perpendicular to the optic nerve, at a depth of 3 mm posterior to the lamina cribrosa of the sclera surface.

Three measurements were acquired in the sagittal plane, followed by clockwise rotation of the probe and acquisition of three measurements in the axial plane for each eye to ensure that the measurements could be appropriately analysed for correlation and accuracy. The mean binocular ONSD measurement for each patient was then obtained. This mean value was used for comparison with the invasively recorded ICP reading. The digital calliper measuring tool on the ultrasound machine was used to measure the ONSD. All images were saved in both JPEG and DICOM format on a secure external hard drive. The time of image acquisition, the length of the imaging and the time from ONSD measurement to ICP measurement were recorded.

5.3.2. Measures to ensure safety of the technique

The FDA/CDRH recommend using an $MI < 0.23$, and a $TI < 1$.⁸¹ The 2006 revised statement by the EFSUMB (described in chapter 3) were used to guide our clinical safety practice when performing ocular ultrasonography.^{82,82} We adjusted the output settings on our machine to comply with these recommendations. In keeping with the ALARA (As Low As Reasonably Achievable) principle suggested in both the safety guidelines, we kept the image acquisition time to a minimum.

5.3.3. Haemodynamic and intracranial parameters

Measurement of the ONSD was performed when the haemodynamic parameters were stable. The AF was palpated and described as open or closed. In cases where the AF was almost closed and barely palpable it was classified as closed. The systolic blood pressure (SBP), diastolic blood pressure (DBP), mean arterial pressure (MAP), pulse rate, respiratory rate, temperature, weight and end tidal carbon dioxide (ETCO₂) were all recorded at the time of ONSD measurement. Any medication given after ONSD measurement was documented. If any of these agents given between ONSD measurement and ICP measurement were thought to affect the ICP, data from these patients were excluded from the analysis.

5.3.4. Measurement of ICP

All ICP measurements were recorded at the time of surgery. Intraparenchymal microsensor probes were generally inserted for ICP monitoring in TBI and craniosynostosis patients, using the initial and most stable reading from the monitor. A ventricular catheter was inserted if CSF drainage was required. For the remainder of patients requiring ventricular catheter insertion, CSF pressure was measured by connecting a CSF manometer to the ventricular catheter immediately after cannulating the ventricle. Particular care was taken not to lose any CSF between ventricular cannulation and connection of the manometer. The external auditory meatus was used as a reference point for 'zeroing' the CSF manometer readings. In cases where measurement was not possible or where the reading was not considered accurate, the data were excluded.

Patients in whom intraparenchymal microsensors were placed had ICP recorded directly in mmHg, and patients with ventricular catheter placement had ICP measured at insertion of the catheter with a CSF manometer in cm H₂O. All ICP recordings were then converted to mmHg (1 mmHg = 1.36 cmH₂O) for uniformity and to allow comparison of data with similar published studies.

5.3.5. Anaesthetic protocol

The goal during each anaesthetic was to maintain normotension, normothermia, normonatremia, normocapnia and normovolemia. The agents used for induction, maintenance and analgesia differed depending on the procedure and anaesthetist. The effect of the anaesthetic on the ICP is always a challenging factor to quantify; especially volatile anaesthetics are known to cause cerebral vasodilation and a presumed increase in CBF. The effect of reduced smooth muscle tension in the vessel wall and subsequent vasodilation predominates when anaesthesia is maintained above 1.0 MAC.^{269,270} ONSD image acquisition and ICP measurement were always performed during the same anaesthesia/procedure. Minimum alveolar concentration (MAC) of the volatile agent used was maintained as constant as possible between ONSD image acquisition and invasive ICP measurement. MAC values ranged between 0.5 – 1.2 MAC. Use of positive end expiratory pressure (PEEP) was in accordance with the study by Pulitano et al,²⁷¹ and age appropriate tidal volumes were used to maintain normocarbia. Selected physiological parameters recorded at the time of ONSD acquisition were included in a multivariate regression model to test for effect on the relationship between ONSD and ICP.

Briefly, the anaesthetic for specific procedures involved:

Hydrocephalus (VPS/EVD/ETV)

- Induction was with sevoflurane, oxygen and air or nitrous oxide if no intravenous (IV) access was available. IV access was secured after induction. If IV access was present on arrival intravenous induction with propofol and remifentanil was performed
- Maintenance was with isoflurane, oxygen and air. Analgesia consisted of an opiate based regime utilising a remifentanil infusion, fentanyl boluses and/or morphine with intravenous paracetamol

Craniofacial/TBI

- Induction was with sevoflurane, oxygen and air or nitrous oxide. IV access was secured after induction
- Maintenance was with isoflurane, oxygen and air. Analgesia was administered as a sufentanil infusion with IV paracetamol

Intracranial tumour resection

- Intravenous induction was followed by a target controlled infusion of propofol for maintenance using the Paedfusor regime. Analgesia was achieved with a sufentanil infusion and IV paracetamol

5.3.6. Sample size calculation

Based on results from a local pilot study, the sample size estimate for comparison of means was calculated at 58 patients, to achieve 80% power, with an alpha of 5 ($p < 0.05$). Based on the available literature the results were expected to differ according to age category, with described age-related variation at 1 year, between 1 and 4 years and old above 4 years old. Due to the variation and inconsistency in the ages of patients at presentation, and aiming to recruit around 58 patients into each of the 3 age categories, the total sample size for the study was set at 174 patients across all ages (≤ 14 years old). With an estimated 10% loss due to exclusion criteria and data loss, the study aimed to recruit 192 patients.

5.3.7. Statistical analysis

Data were tested for normality of distribution using the Shapiro-Wilks test. Parametric data were reported as means and standard deviations (SD) and non-parametric data reported as medians and interquartile ranges (IQR). All analyses were done using Stata IC version 12.0 (Stata Corporation LP, College Station, Texas, USA) statistical software. The general association between means of numeric variables was tested by applying either Pearson's (PCC) or Spearman's correlation coefficient (SCC), depending on normality of data distribution. Analysis of variance (ANOVA) testing was used to determine within and between group variances for the individual ONSD readings acquired per eye.

Cronbach's alpha statistic (α), which is a model of internal consistency, was used to test correlation and covariance for within observer testing, i.e. repeatability and intra-

observer testing. Bland-Altman analysis was used to test inter-observer agreement, using limits of agreement and mean differences. Statistical significance was set at $p < 0.05$ and all significance testing was two sided. The independent Student t-test was used for comparing mean values, and the Wilcoxon sum rank test/Mann-Whitney test was used to compare median values. The diagnostic accuracy of ONSD measurements to detect ICP at various thresholds was described using sensitivity, specificity, positive predictive values (PPV), negative predictive values (NPV), area under the receiver operating characteristic (AUROC) curves and odds ratios (OR), as well as their 95% confidence intervals.

The association between ONSD, ICP and various physiological parameters was tested in a univariate model. A multivariate regression model was then used to test the effect of the significant covariables on the relationship between ONSD and ICP.

5.3.8. Study approval

Approval for the study was granted by the Human Research Ethics Committee of the University of Cape Town (HREC REF: 674/2013). Approval for this study was also granted by the Research Committee of the Red Cross War Memorial Children's Hospital. Written consent was obtained from parents/care-givers for all children included in the study.

Chapter 6.

The relationship between optic nerve sheath diameter (ONSD) measurement and invasively measured intracranial pressure (ICP) in children: *Results, discussion and conclusion*

The results in this section are presented in four parts:

- 6.1 General and demographic data, repeatability, observer variability and correlation testing;
- 6.2 Relationship between ONSD and ICP over entire patient cohort;
- 6.3 Relationship between ONSD and ICP according to historically described age-related thresholds;
- 6.4 Using the anterior fontanelle (AF) as a clinical marker for defining OSND cut-off values in children

The results are followed by the:

- 6.5 Discussion;
- 6.6 Conclusion

6.1. General and demographic data, repeatability, observer variability and correlation testing

6.1.1. Demographic data

In total, ONSD measurements were performed on 195 patients. Data from 21 patients were excluded for the following reasons:

- i. Haemodynamic instability or time between ONSD imaging and ICP measurement exceeded 1 hour: $n = 5$
- ii. Physiological manipulation required to optimise ICP: $n = 2$
 - Hyperventilation to decrease PaCO₂
 - Change in head position
- iii. ICP lowering agents administered between ONSD imaging and ICP measurement: $n = 3$
 - Steroid administration
 - Mannitol
 - Hypertonic saline
 -
- iv. Incomplete datasets: $n = 3$
- v. Equipment failure: $n = 1$
- vi. Initial ICP measurement inaccurate: $n = 7$
 - Inaccurate catheter placement
 - Loss of CSF prior to measurement

Data for the remaining 174 patients were available for the final analysis. In total 2,062 out of a total of 2,088 (98.8%) ONSD measurements (acquiring 3 images in the axial plane and 3 images in the sagittal plane from each eye) were suitable for the analysis, with no measurement performed on 26 images because the image quality was considered suboptimal.

Most excluded patient data ($n = 7$) resulted from inaccurate measurement of ICP, mostly due to loss of CSF at the time of measurement during ventricular catheter

insertion. This exclusion was necessary to ensure the quality of the invasive ICP measurement.

There were 52 (30.9%) females and 122 (69.1%) males, with a female to male ratio of 0.43:1. The median age was 36 months (IQR 8-82). 56 (32.2%) children were ≤ 1 year old and 118 (67.8%) > 1 year old. The aetiology reflected the typical spectrum of neurological disease encountered in routine practice and included: hydrocephalus (52.9%), traumatic brain injury (17.2%), tumour (with or without hydrocephalus) (9.2%), craniosynostosis (9.2%), cystic malformation (6.9%), other (4.6%) [Chiari I malformation, spinal dysraphism, effusion and macrocephaly]. Demographic details are summarised in the table below.

Parameter		Total	ICP < 20 mmHg	ICP \geq 20 mmHg
Number (%)		174	100 (57.5%)	74 (42.5%)
Age (median age in months)		36 (8 – 82)	16.5 (IQR 4 – 72.5)	59.5 (IQR 21 -91)
Aetiology				
	Hydrocephalus	92 (52.9%)	54	37
	Traumatic brain injury	30 (17.2%)	20	10
	Tumour	16 (9.2%)	0	16
	Craniosynostosis	16 (9.2%)	9	7
	Cystic malformation	12 (6.9%)	11	1
	Other (Chiari I malformation, spinal dysraphism, subdural effusion, macrocephaly)	8 (4.6%)	6	3
Gender				
	Female	52	29	23
	Male	122	71	51

Table 6.1. Demographic details

6.1.2. Intra-operative haemodynamic parameters

Physiological parameters were recorded at the time of ONSD image acquisition, these parameters included: SBP, DBP, MAP, pulse rate, respiratory rate, end tidal CO₂, weight and temperature. These physiological parameters were analysed in two groups according to ICP, < 20 mmHg and ≥ 20 mmHg (Table 6.2). The relationship between individual potential confounding variables, both physiological and demographic, and ONSD were tested in a univariate model. Statistically significant variables were then entered into a multivariate logistic regression model.

Physiological Parameter	ICP < 20mmHg	ICP ≥ 20 mmHg	p – value
Systolic Blood pressure (mean and SD in mmHg)	81.77 (21.5)	88.94 (13.3)	p = 0.02*
Diastolic blood pressure (mean and SD in mmHg)	49.48 (16.1)	51.65 (12.4)	p = 0.39
Mean arterial blood pressure (mean and SD in mmHg)	62.87 (17.4)	67.05 (10.6)	p = 0.1
Pulse rate (mean and SD in beats per minute)	121.75 (27.3)	114.91 (26.6)	p = 0.14
Respiratory rate (median and IQR in breaths per minute)	21.00 (17 – 26)	19.00 (15.5 – 23)	p = 0.89
Temperature (median and IQR in degrees Celsius)	36.40 (36.05 – 36.6)	36.20 (35.7 – 36.5)	p = 0.06
Weight (median and IQR in kilogr ANOVA)	12.00 (IQR 5.27 – 20)	16.50 (IQR 9.2 – 21.95)	p = 0.15
End tidal CO ₂ (median and IQR in mmHg)	4.10 (3.6 – 4.8)	4.40 (4 – 4.6)	p = 0.26
ICP (mean and SD in mmHg)	11.68 (4.5)	23.87 (4.3)	p < 0.001*
ONSD (mean and SD in mm)	5.08 (0.76)	6.28 (0.64)	p < 0.001*

Table 6.2. Haemodynamic and physiological parameters

6.1.3. Length of time for ultrasound image acquisition and time between image acquisition and ICP measurement

The median length of time required to acquire ONS images in two planes from both eyes in this study was 116 seconds (IQR 95 - 129). The recorded median time from acquisition of ONSD images to ICP measurement was 23 minutes (IQR 15 - 32 minutes).

6.1.4. Testing for repeatability of individual measurements

To evaluate the repeatability of ONSD measurement with transorbital ultrasound, the three individual measurements in the same plane of each eye (sagittal plane of the left and right eye and axial plane of the left and right eye) were compared using ANOVA testing, and Cronbach's alpha statistic (CA).

6.1.4.1. Sagittal plane of the left eye (LESag)

A total of five hundred and nineteen ONSD measurements were acquired in the LESag, with a mean ONSD of 5.61 mm (SD 1) (Table 6.3). The measurements were repeated three times (LESag1, LESag2, LESag3), and the mean value was used for comparison with ICP.

Reading	Number of observations	Mean (mm)	SD	Min (mm)	Max (mm)
LESag 1	174	5.60	1	3.3	8.2
LESag 2	174	5.57	1	3.2	8.0
LESag 3	171	5.66	1	3.3	8.5
Total	519	5.61	1	3.2	8.5

Table 6.3. LESag values

Comparison of the individual measurements demonstrated excellent correlation ($\alpha = 0.97$, CA). No statistically significant difference was demonstrated between the readings ($F = 0.33$, 2 degrees of freedom, $p = 0.72$) using ANOVA testing. (Figure 6.1)

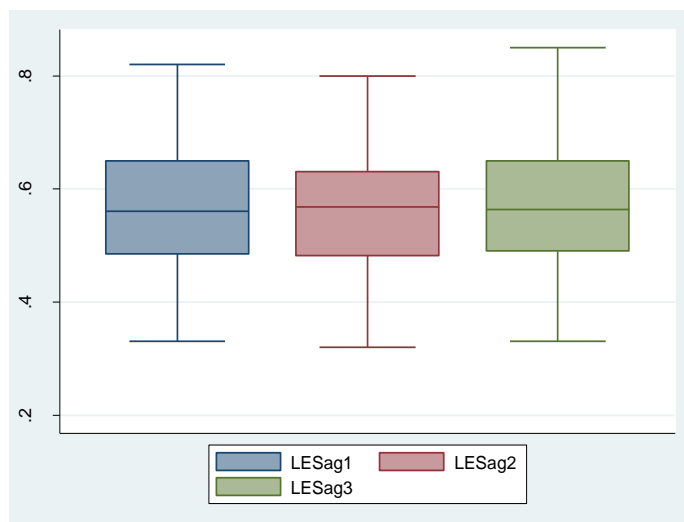


Figure 6.1. Box-whisker plot of the mean values of each LESag reading

6.1.4.2. Sagittal plane of the right eye (RESag)

A total of five hundred and fifteen ONSD measurements were performed in the RESag, with a mean ONSD of 5.63 mm (SD 0.99) (Table 6.4).

These results demonstrated excellent correlation between the measurements ($\alpha = 0.97$, CA). There was no statistically significant difference between these readings according to analysis of variance testing ($F = 0.17$, 2 degrees of freedom, $p = 0.84$). (Figure 6.2).

Reading	Number of observations	Mean (mm)	SD	Min (mm)	Max (mm)
RESag 1	172	5.60	1.00	3.00	8.12
RESag 2	173	5.64	0.98	3.00	8.00
RESag 3	170	5.66	1.00	3.39	8.64
Total	515	5.63	0.99	3.00	8.64

Table 6.4. RESag values

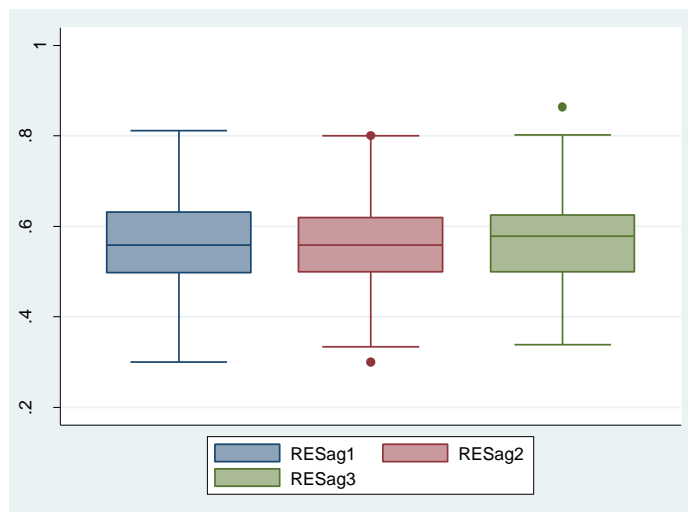


Figure 6.2. Box-whisker plot of the mean values of each RESag reading

6.1.4.3 Axial plane of the left eye (LEAx)

A total of five hundred and eighteen ONSD measurements were acquired in the LEAx, with a mean ONSD of 5.51 mm (SD 0.98) (Table 6.5).

Reading	Number of observations	Mean (mm)	SD	Min (mm)	Max (mm)
LEAx 1	174	5.49	0.97	3.0	7.58
LEAx 2	173	5.50	0.96	3.4	8.0
LEAx 3	171	5.55	1.00	3.0	7.87
Total	518	5.51	0.98	3.0	8.0

Table 6.5. LEAx values

These measurements also demonstrated excellent correlation ($\alpha = 0.98$, CA). Using ANOVA testing demonstrated no statistically significant variation between these readings ($F = 0.21$, 2 degrees of freedom, $p = 0.81$). (Figure 6.3)

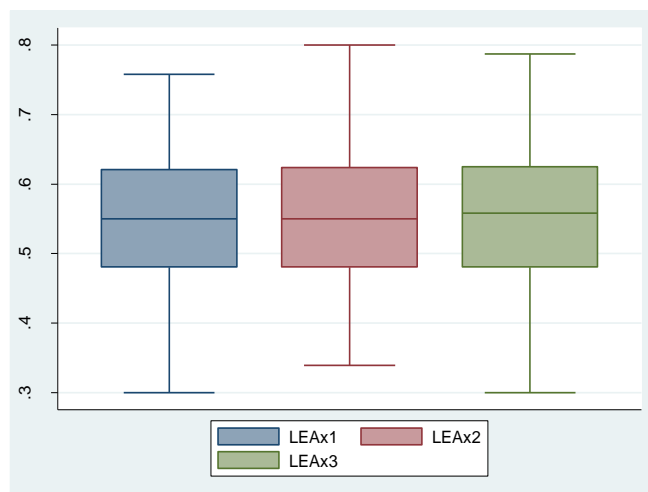


Figure 6.3. Box-whisker plot of the mean values of each LEAx reading

6.1.4.4. Axial plane of the right eye (REAx)

In this plane, there were five hundred and ten ONSD measurements, with a mean ONSD of 5.59 mm (SD 0.96). (Table 6.6) There was excellent correlation between the individual measurements ($\alpha = 0.98$, CA). There was no statistically significant difference between the individual readings in this plane according to ANOVA testing ($F = 0.10$, 2 degrees of freedom, $p = 0.91$). (Figure 6.4)

Reading	Number of observations	Mean (mm)	SD	Min (cm)	Max (cm)
REAx 1	173	5.62	0.97	3.0	8.0
REAx 2	172	5.59	0.96	3.3	7.8
REAx 3	165	5.58	0.96	3.5	7.5
Total	510	5.59	0.96	3.0	8.0

Table 6.6. REAx values

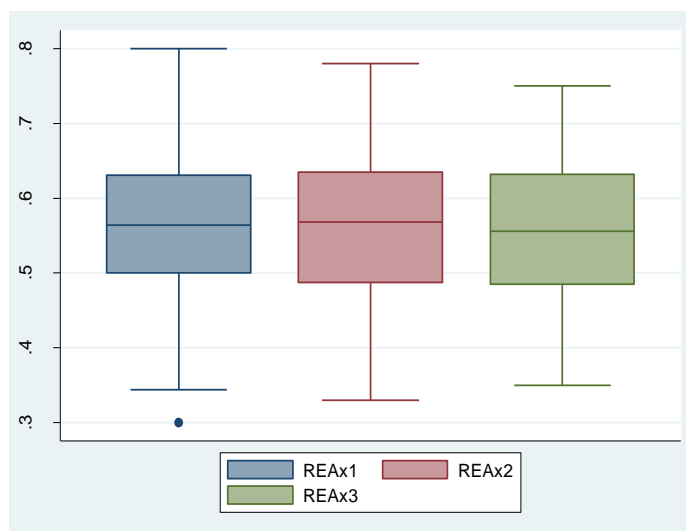


Figure 6.4. Box-whisker plot of the mean values of each REAx reading

6.1.5. Testing for intra-observer variability

To assess the intra-observer variability, repeat measurements of the ONSD were performed on 41 randomly selected patients at a later time, by the same observer, blinded to the original measurements. The mean ONSD at the first reading was 5.58 mm (SD 0.85) and at the second reading was 5.56 mm (SD 0.84) ($p = 0.92$). The intra-observer variability testing demonstrating excellent correlation ($\alpha = 0.99$, CA) (Figures 6.5 and 6.6).

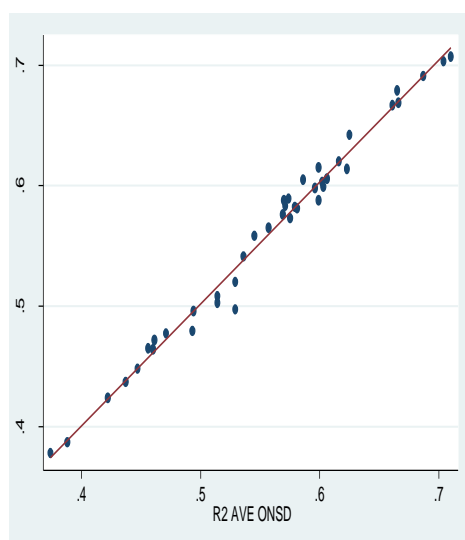


Figure 6.5. Scatterplot for intra-observer reliability

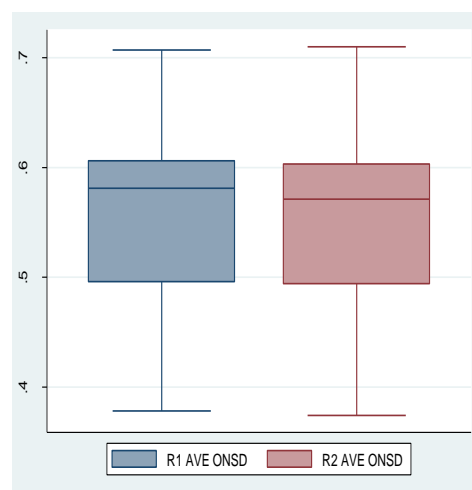


Figure 6.6. Box-whisker plot: measurement 1 (R1 AVE ONSD) and measurement 2 (R2 AVE ONSD)

6.1.6. Testing for inter-observer variability

The test for inter-observer variability was performed by comparing the ONSD measurements performed independently by two observers experienced in the use of transorbital ultrasonography. Inter-observer variability was tested by comparing the mean ONSD measurements performed in 30 patients. The data were correlated using Pearson's correlation coefficient (PCC) and Bland-Altman analysis to test for agreement between the observers. The mean ONSD measurement by observer 1 was 5.63 mm (SD 0.071) and by observer 2 was 5.36 mm (SD 0.064). (Table 6.7 and Figure 6.7)

Observer	Number of observations	Mean ONSD (in mm)	SD	Minimum (in mm)	Maximum (in mm)
Observer 1	30	5.63	0.71	3.87	6.89
Observer 2	30	5.36	0.64	3.47	6.31

Table 6.7. Inter-observer variability

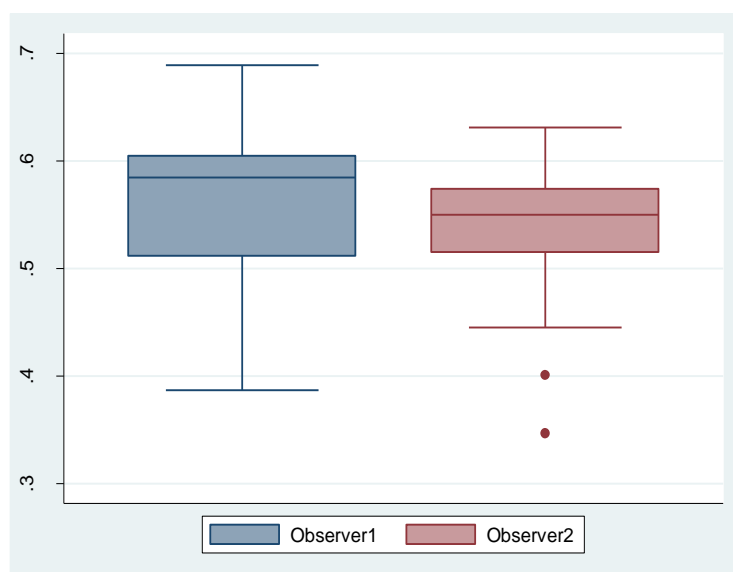


Figure 6.7. Box-whisker plot. Observer 1 and Observer 2

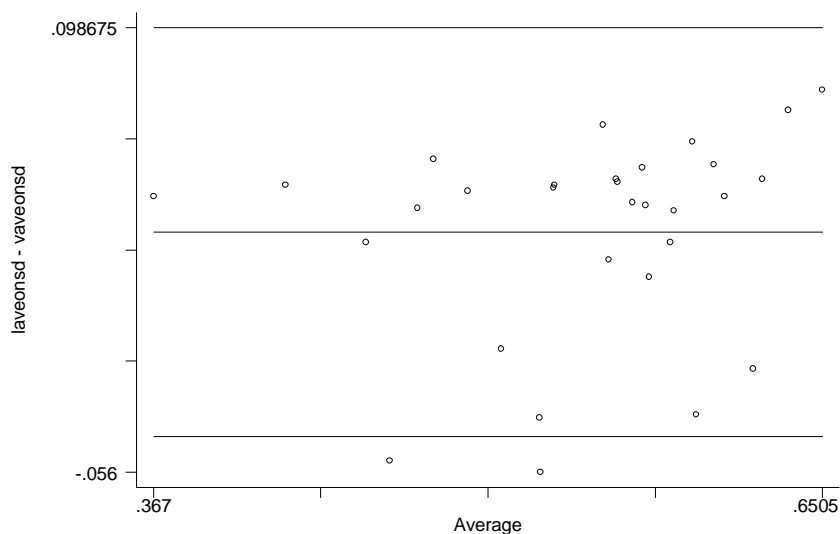


Figure 6.8. Bland-Altman plots. Outer solid lines represent limits of agreement (mean \pm 1.96 times standard deviation, central line depicts the mean of differences).

Bland-Altman analysis revealed a mean difference between the two observers of 0.28 mm (95% CI: 0.014 – 0.041), with limits of agreement between -0.44 – 0.99. (Figure 6.8). Correlation between the 2 observers was very good ($r = 0.87$, $p < 0.001$, PCC).(Figure 6.9)

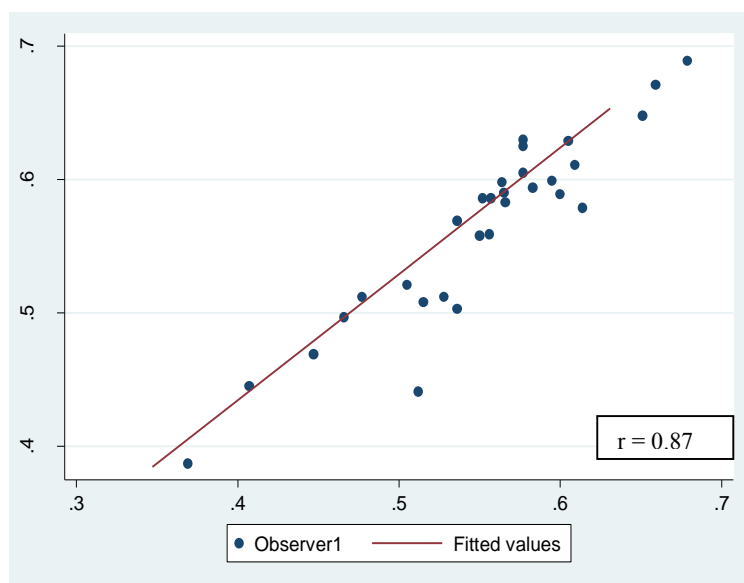


Figure 6.9. Scatter plot: Observer 1 vs Observer 2

6.1.7. Correlation between sagittal and axial imaging

The relationship between ONSD measurements performed in the sagittal and axial plane were examined, as well as their respective relationship with ICP.

The average value of the three ONSD measurements performed in the sagittal (AVESag) and axial (AVEAx) plane of both eyes were calculated and the mean values in each plane were compared. (Table 6.8)

The mean AVESag value was 5.62 mm (SD 0.96) and the mean AVEAx value was 5.56 mm (SD 0.92) ($p = 0.55$, Student's t-test).(Figure 6.10) The correlation between AVESag and AVEAx was excellent ($r = 0.93$, $p < 0.001$, PCC). (Figure 6.11)

Plane	Number of observations	Mean (mm)	SD	Min (mm)	Max (mm)
AVESag	174	5.62	0.96	3.39	8.00
AVEAx	174	5.56	0.92	3.38	7.54

Table 6.8. AVESag vs AVEAx ONSD measurements

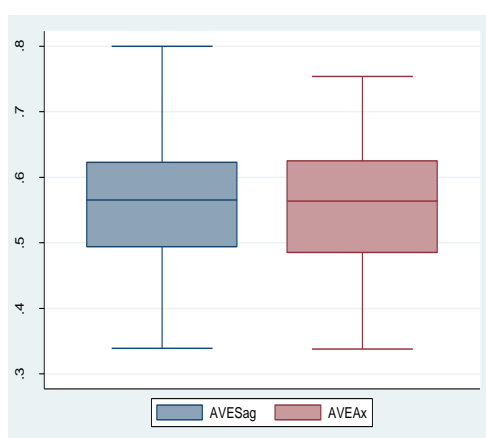


Figure 6.10. Box-whisker plot AVESag and AVEAx

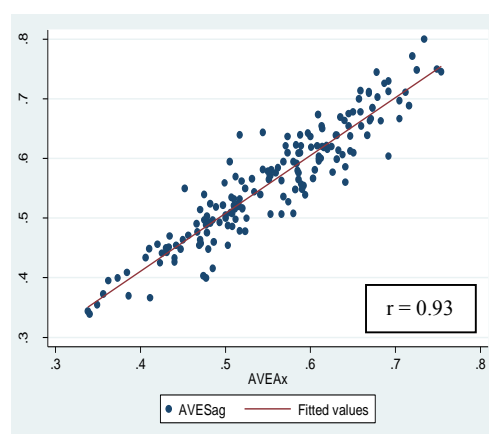


Figure 6.11. Scatter plot of AVESag vs AVEAx

6.1.8. Relationship between sagittal and axial plane measurements with ICP

The image acquisition plane, which provides the optimal ONSD measurement for comparison with ICP is still quite unclear. The mean ONSD in each plane was therefore tested independently to describe their respective relationships with ICP.

When correlated with ICP, AVESag demonstrated a slightly better relationship ($r = 0.66$, $p < 0.001$, PCC) than AVEAx ($r = 0.64$, $p < 0.001$, PCC) (Figures 6.12 and 6.13).

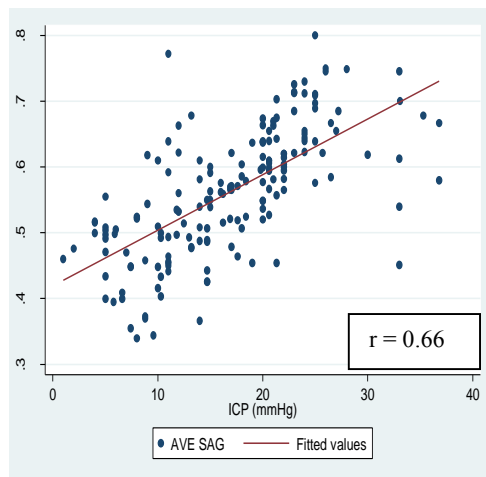


Figure 6.12. Scatterplot mean sagittal ONSD vs ICP

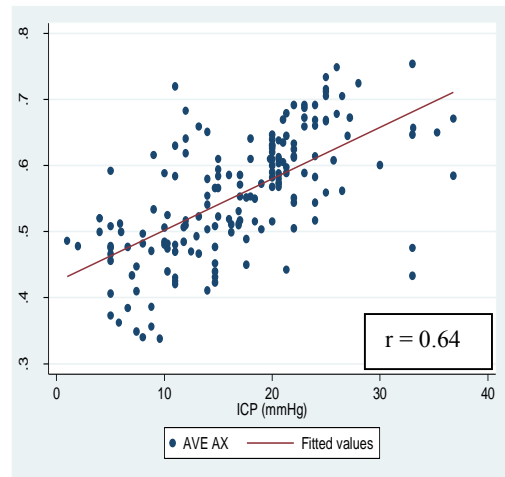


Figure 6.13. Scatterplot mean axial ONSD vs ICP

6.1.9. Correlation between right and left eye measurements

The correlation between ONSD measured in the right and left eye was tested using the mean values of three hundred and forty eight (sagittal and axial) measurements from the right left eye. The mean ONSD in the right eye was 5.61 mm (SD 0.95) and in the left eye was 5.55 mm (SD 0.97) (Table 6.9)

Eye	Number of observations	Mean (mm)	SD	Min (mm)	Max (mm)
Right	348	5.61	0.95	3.30	7.9
Left	348	5.56	0.97	3.17	8.2

Table 6.9. Right vs Left eye ONSD measurements

Correlation of the ONSD measurements between the two eyes was excellent ($r = 0.9$, $p < 0.001$, PCC).(Figure 6.14)

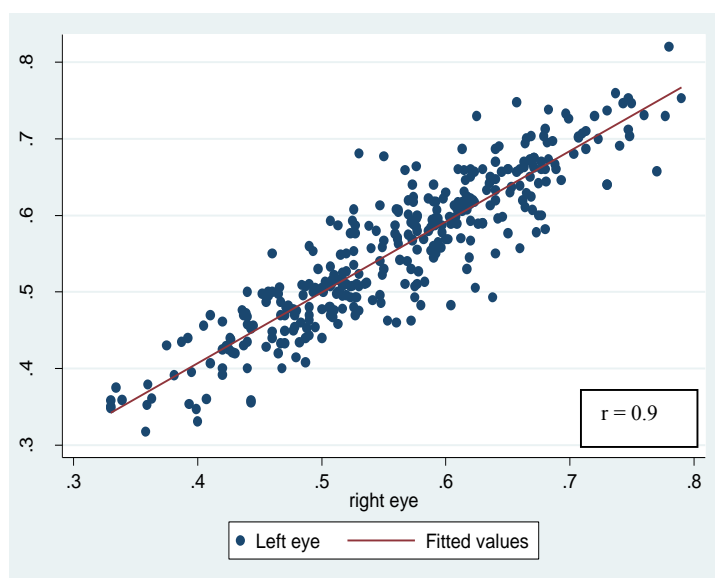


Figure 6.14. Scatter plot of right eye vs left eye

6.2. Relationship between ONSD measurement and ICP over the entire cohort of patients

The treatment threshold of 20 mmHg was used to evaluate the relationship between ONSD and ICP over the entire cohort of patients in this study. This relationship was further assessed at ICP thresholds of 15, 10 and 5 mmHg to evaluate relevant ONSD cut-off values for these ICP readings.

6.2.1. ICP dichotomised at 20 mmHg for all patients

There were one hundred and seventy four patients included in this study. The median age was 36 (IQR 8 – 82) months. 100 patients had an ICP < 20 mmHg, with a mean ICP reading of 11.68 mmHg (SD 4.5) and 74 patients had an ICP \geq 20 mmHg, with a mean ICP reading of 23.87 mmHg (SD 4.33). The correlation between mean ONSD and ICP over the entire cohort was good ($r = 0.66$, $p < 0.001$, PCC).(Figure 6.15)

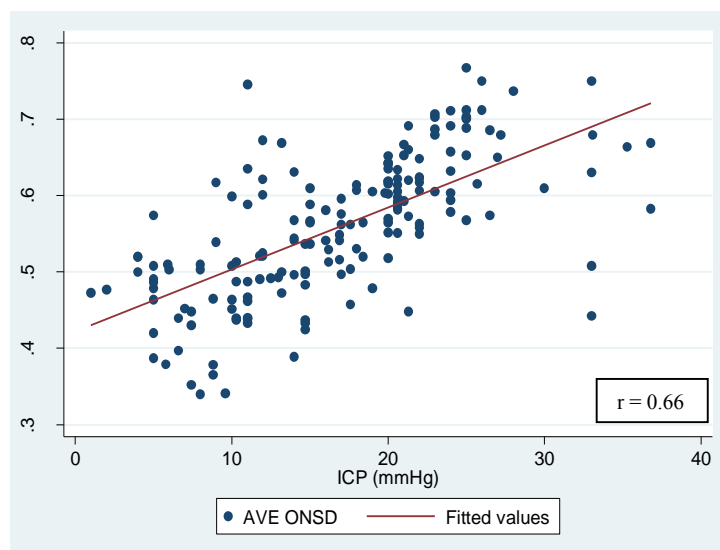


Figure 6.15. Scatterplot of mean ONSD against ICP for entire patient cohort

The mean ONSD in the group with ICP < 20 mmHg was 5.08 mm (SD 0.76), and in the group with ICP \geq 20 mmHg was 6.28 mm (SD 0.64) ($p < 0.001$). (Figure 6.16)

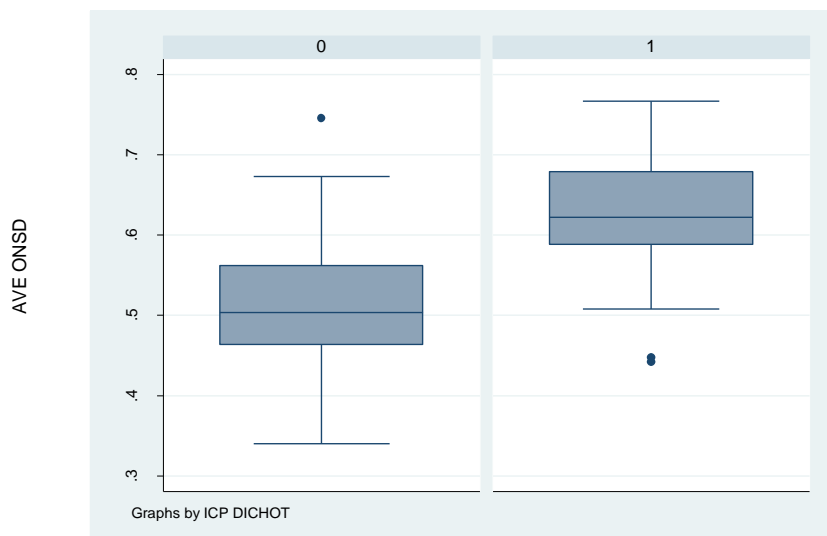


Figure 6.16. Box-whisker graph of ONSD for ICP < 20 mmHg (0), and \geq 20 mmHg (1)

The optimal ONSD cut-off point for detecting an ICP \geq 20 mmHg was 5.5 mm with a sensitivity of 93.2%, a specificity of 74% , PPV of 72.6%, NPV of 93.7%, AUROC of 0.84 (Figure 6.17), and an odds ratio (OR) of 39.3. (Table 6.16)

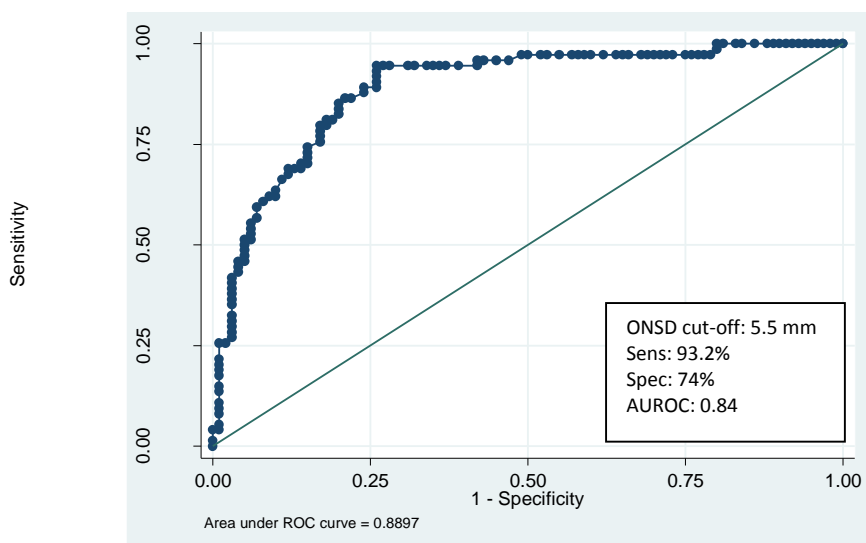


Figure 6.17. AUROC for ONSD of 5.5 mm to detect ICP \geq 20 mmHg

Applying a linear regression model to the data and controlling for age, revealed that with a baseline value of 4.03 mm, for every 10 mmHg increase in ICP the ONSD increased by 0.75 mm (95% CI: 0.62 – 0.88, $R^2 = 0.52$, $p < 0.001$). In the group with $ICP \geq 20$ mmHg, with a baseline value of 5.69 mm this change in ONSD was 0.24 mm (95% CI: 0.09 – 0.5, $R^2 = 0.03$, $p = 0.16$) for every 10 mmHg increase in ICP.

The effects of certain physiological and demographic variables were tested in a univariate analysis. Variables found to have a significant effect on the relationship between ONSD and ICP were entered into a multivariate logistic regression model to adjust for this effect. In the unadjusted model, the OR was 39.28, for an ONSD value of 5.5 mm to detect an $ICP \geq 20$ mmHg. In the adjusted model (adjusted for confounding variables, SBP, temperature, $ETCO_2$, age, pulse and aetiology) the OR was reduced to 26.88. Even though the OR decreased in the adjusted model, the relationship between ONSD and ICP remained statistically significant in both the unadjusted and adjusted models (Table 6.10).

	Variable	Odds ratio (OR)	95% Confidence interval	p – value
	Unadjusted model for ONSD of 5.5 mm to predict $ICP \geq 20$ mmHg	39.28	14.28 – 108.03	$p < 0.001$
	Adjusted model for ONSD of 5.5 mm to predict $ICP \geq 20$ mmHg	26.88	8.54 – 84.62	$p < 0.001$
	SBP	1.00	0.97 – 1.03	$p = 0.9$
	Temperature	0.48	0.24 – 0.98	$p = 0.06$
	$ETCO_2$	1.03	0.62 – 1.71	$p = 0.92$
	Age (months)	1.01	0.99 – 1.01	$p = 0.85$
	Pulse	1.00	0.98 – 1.02	$p = 0.87$
	Aetiology	0.92	0.71 – 1.21	$p = 0.57$

Table 6.10. Unadjusted and adjusted models for the relationship between ONSD and ICP

Various aetiologies for raised ICP in children have been described in studies evaluating the usefulness of ONSD measurement.^{28,29,30-34,161} Aetiology was therefore analysed

to assess its effect on the ONSD measurement in this study. Results were reported in each aetiological group, and are summarised in Table 6.11.

Aetiology	Number (%)	Age in months median (IQR)	ICP in mmHg mean (SD)	ONSD in mm mean (SD)
Hydrocephalus	92 (52.9)	22.50 (5 -74)	16.9 (7.9)	5.4 (0.9)
TBI	30 (17.2)	80.50 (55 -94)	16.4 (6.9)	5.8 (0.9)
Tumour	16 (9.2)	66.50 (29 – 105.5)	23.4 (2.6)	6.4 (0.7)
Craniosynostosis	16 (9.2)	15.50 (12 – 26)	17.5 (3.1)	6.1 (0.4)
Intracranial cyst	12 (6.9)	0.55 (0.185 – 25)	13.0 (7.9)	4.8 (0.9)
Other	8 (4.6)	60.00 (30 – 75.5)	9.7 (7.3)	5.4 (0.8)

Table 6.11. Age, ICP and ONSD for specific aetiological groups

The diagnostic accuracy of ONSD measurement for detecting ICP \geq 20 mmHg in each aetiological group are summarised in Table 6.12. No diagnostic accuracy analysis was performed in the tumour group as all patients in this group had an ICP \geq 20 mmHg.

Aetiology	ONSD cut-off value (mm)	Sensitivity % (95% CI)	Specificity % (95% CI)	PPV% (95% CI)	NPV% (95% CI)	AUROC (95% CI)	OR (95% CI)
Hydrocephalus	5.50	91.9 (78.1-98.3)	83.6 (71.2-92.2)	79.1 (64-90)	93.9 (83.1-98.7)	0.88 (0.81-0.94)	57.90 (15.2-216)
TBI	5.79	80.0 (44.4-97.5)	65 (40.8-84.6)	53.3 (26.6-78.7)	86.7 (59.5-98.3)	0.73 (0.56-0.89)	7.43 (1.33-39.4)
Craniosynostosis	6.17	85.7 (42.1-99.6)	88.9 (51.8-99.7)	85.7 (42.1-99.6)	88.9 (51.8-99.7)	0.87 (0.7-1)	48.00 (3.09-100)
Intracranial cysts	4.50	50 (1.26-98.7)	20 (6.67-65.2)	12.5 (3.16-52.7)	75 (19.4-99.4)	0.4 (0-0.912)	0.43 (0-100)
Other	5.50	100 (15.8-100)	83.3 (35.9-99.6)	66.7 (9.43-99.2)	100 (47.8-100)	0.92 (0.75-1)	N/A

Table 6.12. Diagnostic accuracy of ONSD for detecting ICP \geq 20 mmHg in different aetiological groups.

6.2.2. ICP dichotomised at 15 mmHg for all patients

Seventy three patients had an ICP < 15 mmHg, with a mean ICP of 9.71 mmHg (SD 3.54) and 101 patients had an ICP \geq 15 mmHg, with a mean ICP of 22.04 mmHg (SD 4.84). The mean ONSD in the group with ICP < 15 mmHg was 4.92 mm (SD 0.8), compared to 6.08 mm (SD 0.7) ($p < 0.001$) in the group with ICP \geq 15 mmHg. The results and comparative p – values for the difference between groups with ICP above and below 15 mmHg are summarised in Table 6.13.

ICP in mmHg	N (%)	Median age in months (IQR)	Mean ICP in mmHg (SD)	Mean ONSD in mm (SD)
Overall	174	36 (8 -82)	16.87 (7.5)	5.59 (0.9)
< 15	73 (42)	17 (3 – 76)	9.71 (3.54)	4.92 (0.8)
\geq 15	101 (58)	40 (14 - 82)	22.04 (4.84)	6.08 (0.7)
p – value		$p = 0.18$	$p < 0.001$	$p < 0.001$

Table 6.13. Age, ICP and ONSD for ICP dichotomised at 15 mmHg

The optimal ONSD cut-off point for detecting ICP \geq 15 mmHg was 5.29 mm, with a sensitivity of 88.1%, a specificity of 78.1% and an OR of 26.4 (Table 6.16).

6.2.3. ICP dichotomised at 10 mmHg for all patients.

Thirty one patients had an ICP < 10 mmHg, with a mean ICP of 6.23 mmHg (SD 2.11) and 143 patients had an ICP \geq 10 mmHg, with a mean ICP of 19.17 mmHg (SD 6.1). The results and comparative p – values (comparing values above and below 10 mmHg) for this group are summarised in the Table 6.14.

ICP in mmHg	N (%)	Median age in months (IQR)	Mean ICP in mmHg (SD)	Mean ONSD in mm (SD)
Overall	174	36 (8 - 82)	16.87 (7.5)	5.59 (0.9)
< 10	31 (17.8)	55 (1.6 – 82)	6.23 (2.11)	4.60 (0.7)
\geq 10	143 (82.2)	34 (8 – 82)	19.17 (6.1)	5.81 (0.8)
p – value		p = 0.58	p < 0.001	p < 0.001

Table 6.14. Age, ICP and ONSD for ICP dichotomised at 10 mmHg

The optimal ONSD cut-off point for detecting an ICP \geq 10 mmHg was 5.04 mm, with a sensitivity of 79%, a specificity of 74.2% and an OR of 10.8 (Table 6.16).

6.2.4. ICP dichotomised at 5 mmHg for all patients

Five patients had an ICP < 5 mmHg, with a mean ICP of 3 mmHg (SD 1.4) and one hundred and sixty nine patients had ICP \geq 5 mmHg, with a mean ICP of 17.28 mmHg (SD 7.2). The mean ONSD in the group with ICP < 5 mmHg was 4.98 mm (SD 0.2), compared to a mean ONSD of 5.61 mm (SD 0.9) ($p = 0.13$) in the group with ICP \geq 5 mmHg. The results and comparative p – values are summarised in Table 6.15.

ICP in mmHg	N (%)	Median age in months (IQR)	Mean ICP in mmHg (SD)	Mean ONSD in mm (SD)
Overall	174	36 (8 -82)	16.87 (7.5)	5.59 (0.9)
< 5	5 (2.9)	76 (75 – 143)	3.00 (1.4)	4.98 (0.2)
\geq 5	169 (97.1)	34 (8 – 81)	17.28 (7.2)	5.61 (0.9)
p – value		$p = 0.01$	$p < 0.001$	$p = 0.13$

Table 6.15. Age, ICP and ONSD for ICP dichotomised at 5 mmHg

The optimal ONSD cut-off point for detecting ICP \geq 5 mmHg was 5 mm, with a sensitivity of 72.8%, a specificity of 60% and an OR 4.01 (Table 6.16).

The diagnostic accuracy of ONSD measurement for detecting ICP at thresholds of 20, 15, 10 and 5 mmHg across the entire patient cohort are summarised in Table 6.16.

ICP (mmHg)	ONSD cut-off (mm)	Sensitivity% (95%CI)	Specificity % (95%CI)	PPV% (95%CI)	NPV % (95%CI)	AUROC (95%CI)	OR (95%CI)
\geq 20	5.50	93.2 (84.9-97.8)	74 (64.3-82.3)	72.6 (62.5- 81.3)	93.7 (85.8- 97.9)	0.84 (0.78-0.89)	39.30 (14.6-105)
\geq 15	5.29	88.1 (80.2-93.7)	78.1 (66.9-86.9)	84.8 (76.4-91)	82.6 (71.6- 90.7)	0.83 (0.77-0.89)	26.40 (11.7-59.6)

≥ 10	5.04	79 (71.4-85.4)	74.2 (55.4-88.1)	93.4 (87.4- 97.1)	43.4 (29.8- 57.7)	0.77 (0.68 - 0.85)	10.80 (4.47- 26.1)
≥ 5	5.00	72.8 (65.4-79.3)	60 (14.7-94.7)	98.4 (94.3- 99.8)	6.12 (1.28- 16.9)	0.66 (0.42-0.91)	4.01 (0.77 - .)

Table 6.16. Summary of ONSD cut-off values at different ICP values for all patients

6.3. Relationship between ONSD measurement and ICP: using described age-related thresholds for defining ONSD cut-off values in children

The use of transorbital ultrasound as a non-invasive imaging tool to measure the ONSD in children is perhaps even more appealing than it is in adults. The limitation in children remains the disparity regarding the optimal cut-off values for different age groups. The available literature uses either 1 year of age^{29,30} or 4 years of age^{28,31,32,33} as suggested age-related thresholds for defining different ONSD cut-off values to detect raised ICP in children.

This section of the study aims to evaluate the current age-related recommendations for ONSD cut-off values in children. The relationship between ONSD and ICP was assessed within the following age categories:

6.3.1. Under 1 year old (≤ 1 year old);

6.3.2. Above 1 year (> 1 year old);

6.3.3. Subcategory analysis of children > 1 year:

i. Ages between 1 year (> 1 year old) and 4 years (≤ 4 years old);

ii. Older than 4 years (> 4 years old)

6.3.1. Children under 1 year old (≤ 1 year old)

The relationship between ONSD and ICP in this age group was analysed to describe the optimal ONSD cut-off value for detecting ICP at thresholds of 20, 15, 10 and 5 mmHg.

6.3.1.1. ICP dichotomised at 20 mmHg

There were fifty six patients aged ≤ 1 year old. The median age in this group was 4.0 (IQR 1 – 8) months. Forty six patients had an ICP < 20 mmHg with a mean ICP reading of 12.23 mmHg (SD 3.77) and 10 patients had an ICP ≥ 20 mmHg, with a mean ICP reading of 22.53 mmHg (SD 4.06). The results and comparative p – values are summarised in Table 6.17. There was good correlation between ONSD and ICP ($r = 0.65$, $p < 0.001$, PCC) in this group.(Figure 6.18)

ICP in mmHg	N (%)	Median age in months (IQR)	Mean ICP in mmHg (SD)	Mean ONSD in mm (SD)
Overall	56	4.0 (1 – 8)	14.07 (5.49)	4.9 (0.8)
< 20	46 (82.1)	3.5 (0.75 – 8)	12.23 (3.77)	4.8 (0.8)
≥ 20	10 (17.9)	7.5 (2 – 8)	22.53 (4.06)	5.6 (0.8)
p – value		p = 0.095	p < 0.001	p = 0.003

Table 6.17. Age, ICP and ONSD for ICP dichotomised at 20 mmHg in children ≤ 1 year old

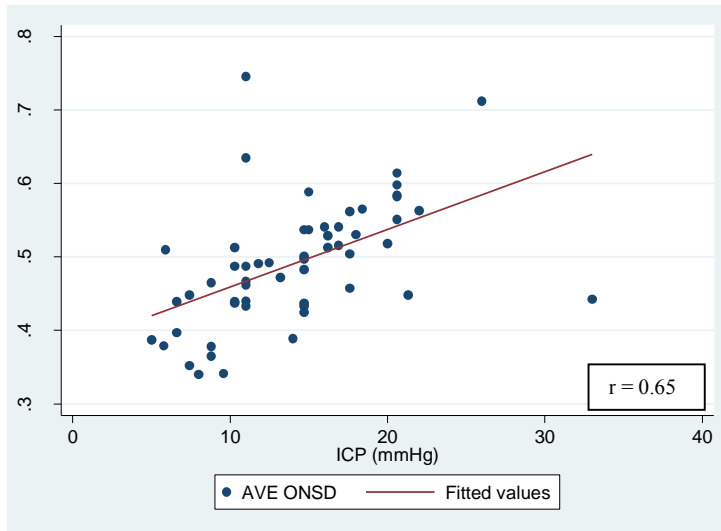


Figure 6.18. Scatterplot of ONSD vs ICP for children ≤ 1 year old

The mean ONSD in the group with ICP < 20 mmHg was 4.8 mm (SD 0.8) compared to 5.6 mm (SD 0.8) ($p = 0.003$) in the group with ICP ≥ 20 mmHg (Figure 6.19).

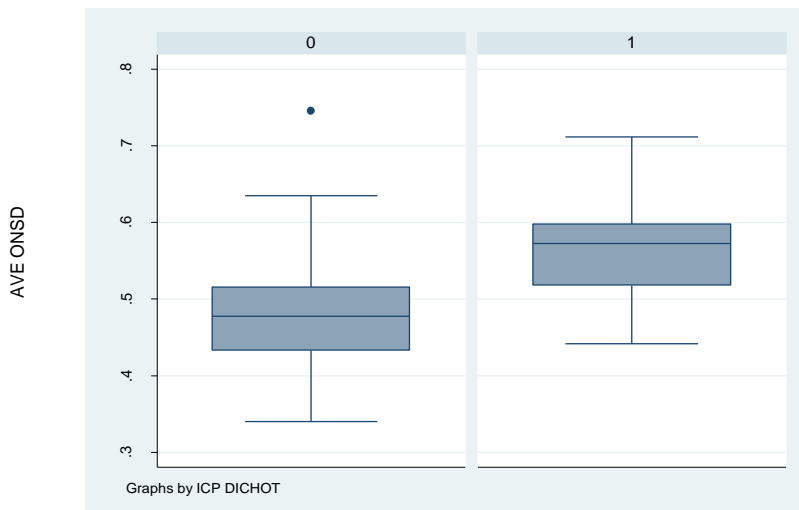


Figure 6.19. Box and whisker plot of ONSD for ICP < 20 mmHg (0) and ICP ≥ 20 mmHg (1) in children ≤ 1 year old

In children under the age of 1 year, the optimal ONSD cut-off point for detecting an ICP ≥ 20 mmHg was 5.16 mm with a sensitivity of 80%, specificity of 76.1% , PPV of 42.1%, NPV of 94.6%, an AUROC of 0.81 (Figure 6.20) and a diagnostic OR of 12.7 (Table 6.20)

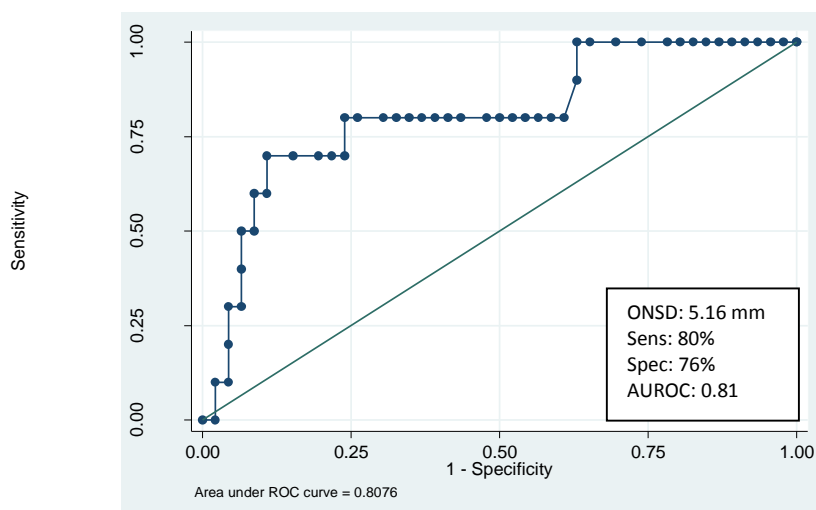


Figure 6.20. AUROC for ONSD to detect ICP ≥ 20 mmHg in children ≤ 1 year old.

6.3.1.2. ICP dichotomised at 15 mmHg

Thirty four children in this group had an ICP < 15 mmHg and 22 children had an ICP ≥ 15 mmHg. The results are summarised in Table 6.18.

ICP in mmHg	N (%)	Median age in months (IQR)	Mean ICP in mmHg (SD)	Mean ONSD in mm (SD)
Overall	56	4.0 (1 – 8)	14.07 (5.49)	4.90 (0.8)
< 15	34 (60.7)	1.8 (0.5)	10.63 (2.96)	4.56 (0.8)
≥ 15	22 (39.3)	7.5 (4 – 8)	19.40 (4.04)	5.50 (0.6)
p – value		$p < 0.001$	$p < 0.001$	$p < 0.001$

Table 6.18. Age, ICP and ONSD for ICP dichotomised at 15 mmHg in children ≤ 1 year old

The optimal ONSD cut-off value to detect an ICP ≥ 15 mmHg in this age group was 4.97 mm, with a sensitivity of 86.4%, specificity of 82.4% and an OR of 29.6 (Table 6.20).

6.3.1.3. ICP dichotomised at 10 mmHg

Twelve children in this age group had an ICP < 10 mmHg and 44 children had an ICP ≥ 10 mmHg, the results and comparative p – values are summarised in Table 6.19.

ICP (in mmHg)	N (%)	Median age in months (IQR)	Mean ICP in mmHg (SD)	Mean ONSD in mm (SD)
Overall	56	4 (1 – 8)	14.07 (5.49)	4.9 (0.8)
< 10 mmHg	12 (21.4)	1 (0.11 – 3)	7.39 (1.44)	4.0 (0.5)
≥ 10 mmHg	44 (78.6)	5 (1.63 – 8)	15.89 (4.71)	5.2 (0.7)
p – value		p = 0.02	p < 0.001	p < 0.001

Table 6.19. Age, ICP and ONSD for ICP dichotomised at 10 mmHg in children ≤ 1 year old

In the group of patients under 1 year of age, the optimal ONSD cut-off value for detecting an ICP ≥ 10 mmHg was 4.3 mm, with a sensitivity of 90.9%, specificity of 66.7% and an OR of 20 (Table 6.20).

6.1.3.4. ICP dichotomised at 5 mmHg

Of the fifty six patients under 1 year old, the minimum ICP was 5 mmHg, so none of the patients in this group had an ICP <5 mmHg.

The diagnostic accuracy of the ONSD cut-off values for predicting ICP readings of 20, 15, 10 and 5 mmHg in children under the age of 1 year are summarised in Table 6.17.

ICP (mmHg)	ONSD cut-off (mm)	Sensitivity% (95%CI)	Specificity % (95%CI)	PPV% (95%CI)	NPV % (95%CI)	AUROC (95%CI)	OR (95%CI)
≥ 20	5.16	80 (44.4-97.5)	76.1 (61.2-87.4)	42.1 (20.3-66.5)	94.6 (81.8-99.3)	0.81 (0.64-0.93)	12.7 (2.58 - .)
≥ 15	4.97	86.4 (65.1-97.1)	82.4 (65.5-93.2)	76 (54.9-90.6)	90.3 (74.2-98)	0.84 (0.75-0.94)	29.6 (6.85-125)
≥ 10	4.30	90.9 (78.3-97.5)	66.7 (34.9-90.1)	90.9 (78.3-97.5)	66.7 (34.9-90.1)	0.79 (0.64-0.93)	20 (4.33-93.2)
≥ 5	Nil	Nil	Nil	Nil	Nil	Nil	Nil

Table 6.20. ONSD cut-off values for predicting ICP readings of 20, 15, 10 and 5 mmHg in children < 1 yo

6.3.2. Children above 1 year old (> 1 year old)

One hundred and eighteen children over the age of 1 year were evaluated as a combined group in this section. The median age was 65.5 months (IQR 35 – 94), with a mean ICP of 18.19 mmHg (SD 7.94), and a mean ONSD measurement of 5.92 mm (0.7). There was good correlation between ONSD and ICP ($r = 0.7$, $p < 0.001$, PCC) in this age group. (Figure 6.21). The diagnostic accuracy of ONSD measurement was analysed at ICP thresholds of 20, 15, 10 and 5 mmHg.

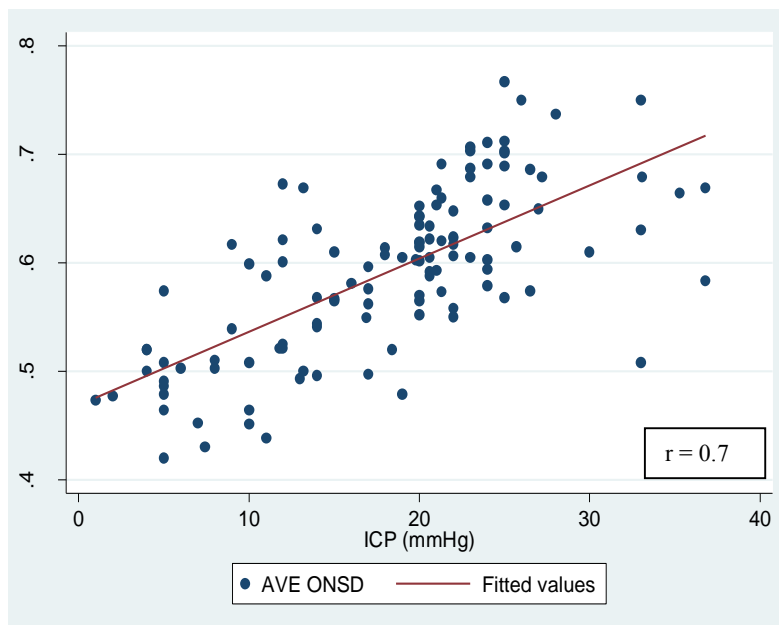


Figure 6.21. Scatterplot of ONSD vs ICP in children > 1 year

6.3.2.1. ICP dichotomised at 20 mmHg

In this age group fifty four patients had an ICP < 20 mmHg, with a median age of 64.5 months (IQR 42 – 94) and a mean ICP reading of 11.22 mmHg (SD 5.02). Sixty four patients had an ICP \geq 20 mmHg with a median age of 66.5 months (IQR 32.5 – 95) and a mean ICP reading of 24.08 mmHg (SD 4.37). The results and comparative p – values are summarised in Table 6.21.

ICP	N (%)	Median age in months (IQR)	Mean ICP in mmHg (SD)	Mean ONSD in mm (SD)
Overall	118	65.5 (35 – 94)	18.19 (7.94)	5.92 (0.8)
< 20 mmHg	54	64.5 (42 – 94)	11.22 (5.02)	5.36 (0.6)
\geq 20 mmHg	64	66.5 (32.5 – 95)	24.08 (4.37)	6.38 (0.5)
p – value		p = 0.96	p < 0.001	p < 0.001

Table 6.21. Age, ICP and ONSD for ICP dichotomised at 20 mmHg in children > 1 year old

The mean ONSD in the group with ICP < 20 mmHg was 5.4 mm (SD 0.6), compared to 0.64 cm (SD 0.05) in the group with ICP \geq 20 mmHg (p < 0.001). (Figure 6.22)

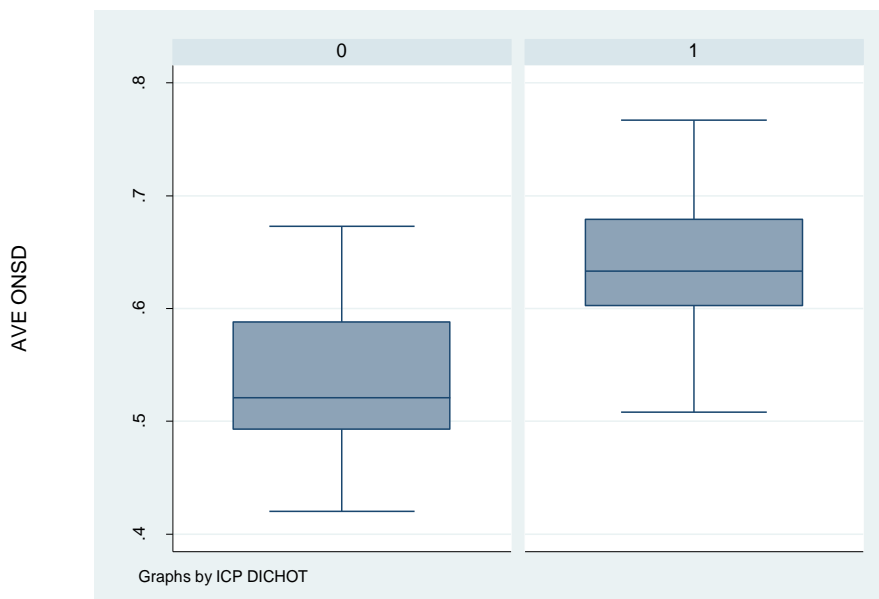


Figure 6.22. Box and whisker plot of ONSD for ICP < 20 mmHg (0) and ICP \geq 20 mmHg (1) in children > 1 year old

The ONSD value with the best diagnostic accuracy for detecting an ICP \geq 20 mmHg was 5.75 mm, with a sensitivity of 85.9%, specificity of 70.4% , PPV of 77.5%, NPV of 80.9% and AUROC of 0.78 (Figure 6.23). The diagnostic OR was 14.5. (Table 6.25)

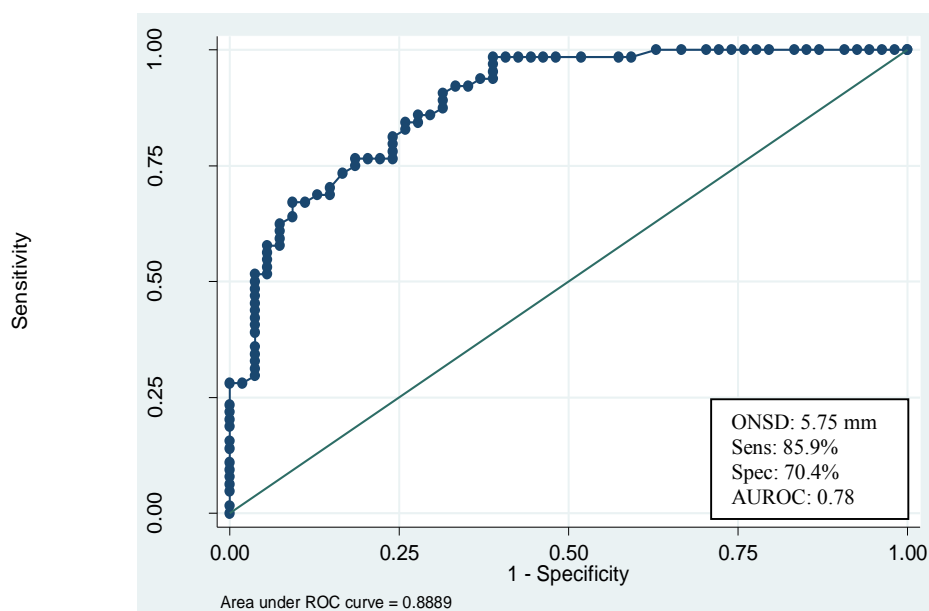


Figure 6.23. AUROC for ONSD to detect ICP \geq 20 mmHg in children > 1 year old

6.3.2.2. ICP dichotomised at 15 mmHg

In this age group, thirty nine children had an ICP < 15 mmHg and seventy nine children had an ICP \geq 15 mmHg. The data and comparative p – values are summarised in Table 6.22.

ICP	N (%)	Median age in months (IQR)	Mean ICP in mmHg (SD)	Mean ONSD in mm (SD)
Overall	118	65.5 (35 – 94)	18.19 (7.94)	5.92 (0.7)
< 15 mmHg	39 (33.1)	75.0 (55 - 98)	8.91 (3.85)	5.20 (0.63)
\geq 15 mmHg	79 (66.9)	61.0 (30 - 92)	22.78 (4.81)	6.30 (0.59)
p – value		p = 0.11	p < 0.001	p < 0.001

Table 6.22. Age, ICP and ONSD for ICP dichotomised ay 15 mmHg in children > 1 year old

The cut-off value for ONSD that best predicted an ICP \geq 15 mmHg was 5.49 mm, with a sensitivity of 93.7%, specificity of 74.4% and an OR of 42.9 (Table 6.25).

6.3.2.3. ICP dichotomised at 10 mmHg

Nineteen children had an ICP < 10 mmHg and ninety nine had an ICP \geq 10 mmHg in this age group. The results are summarised in Table 6.32.

ICP	N (%)	Median age in months (IQR)	Mean ICP in mmHg (SD)	Mean ONSD in mm (SD)
Overall	118	65.5 (35 – 94)	18.19 (7.94)	5.92 (0.7)
< 10 mmHg	19	75.0 (57 – 116)	5.50 (2.2)	4.98 (0.5)
\geq 10 mmHg	99	65.0 (32 - 94)	20.63 (6.1)	6.09 (0.7)
p – value		p = 0.08	p < 0.001	p < 0.001

Table 6.23. Age, ICP and ONSD for ICP dichotomised at 10 mmHg in children > 1 year old

The cut-off value for ONSD that best predicted an ICP \geq 10 mmHg was 5.2 mm, with sensitivity of 88.9%, specificity of 84.2% and an OR of 42.7 (Table 6.34).

6.3.2.4. ICP dichotomised at 5 mmHg

There were five children in this age category with an ICP < 5 mmHg and one hundred and thirteen with an ICP \geq 5 mmHg. Table 6.24 summarises the results and comparative p – values in this group.

ICP	N (%)	Median age in months (IQR)	Mean ICP in mmHg (SD)	Mean ONSD in mm (SD)
Overall	118	65.5 (35 – 94)	18.19 (7.94)	5.92 (0.7)
< 5 mmHg	5	76.0 (75 – 143)	3.00 (1.4)	4.98 (0.2)
\geq 5 mmHg	113	65.0 (34 – 94)	18.87 (7.42)	5.96 (0.8)
p – value		p = 0.12	p < 0.001	p = 0.005

Table 6.24. Age, ICP and ONSD for ICP dichotomised at 5 mmHg in children > 1 year old

The cut-off value for ONSD that best predicted an ICP \geq 5 mmHg was 5.1 mm, with a sensitivity of 81.4%, specificity of 60% and an OR of 6.6. (Table 6.25)

The diagnostic accuracy of ONSD measurement for detecting ICP at thresholds of 20, 15, 10 and 5 mmHg in children > 1 year old, are summarised in Table 6.25.

ICP (mmHg)	ONSD cut-off (mm)	Sensitivity% (95%CI)	Specificity% (95%CI)	PPV% (95%CI)	NPV% (95%CI)	AUROC (95%CI)	OR (95%CI)
≥ 20	5.75	85.9 (75 – 93.4)	70.4 (56.4 – 82)	77.5 (66 – 86.5)	80.9 (66.7 – 90.9)	0.78 (0.71 – 0.86)	14.5 (5.87 – 35.8)
≥ 15	5.49	93.7 (85.8 – 97.9)	74.4 (57.9 – 87)	88.1 (79.2 – 94.1)	85.3 (68.9 – 95)	0.84 (0.77 – 0.92)	42.9 (13.8 – 133)
≥ 10	5.20	88.9 (81-94.3)	84.2 (60.4 – 96.6)	96.7 (90.7 – 99.3)	59.3 (38.8 – 77.6)	0.87 (0.78 – 0.96)	42.7 (11.2 – 159)
≥ 5	5.10	81.4 (73 – 88.1)	60 (14.7 – 94.7)	97.9 (92.5 – 99)	12.5 (2.7 – 32.4)	0.71 (0.46 – 0.95)	6.6 (1.2 – 35)

Table 6.25. ONSD cut-off values for detecting ICP at thresholds of 20, 15, 10 and 5 mmHg

In children above and below the age of 1 year, the diagnostic accuracy of ONSD measurement for detecting ICP \geq 20 mmHg are summarised in Table 6.26.

Age	ONSD cut-off (mm) for ICP \geq 20 mmHg	Sensitivity% (95%CI)	Specificity% (95%CI)	PPV% (95%CI)	NPV% (95%CI)	AUROC (95%CI)	OR (95%CI)
All ages	5.50	93.2 (84.9 – 97.80)	74 (64.3 – 82.3)	72.6 (62.5 – 81.3)	93.7 (85.8 – 97.9)	0.84 (0.78 – 0.89)	39.3 (14.6 – 105)
\leq 1 year	5.16	80 (44.4 – 97.5)	76.1 (61.2 – 87.4)	42.1 (20.3 – 66.5)	94.6 (81.8 – 99.3)	0.81 (0.64 – 0.93)	12.7 (2.58 – 100)
$>$ 1 year	5.75	85.9 (75 – 93.4)	70.4 (56.4 – 82)	77.5 (66 – 86.5)	80.9 (66.7 – 90.9)	0.78 (0.71 – 0.86)	14.5 (5.87 – 35.8)

Table 6.26. ONSD cut-off values for detecting ICP \geq 20 mmHg in children \leq 1 year and $>$ 1 year old.

ONSD cut-off values for ICP thresholds of 20, 15, 10 and 5 mmHg in children above and below the age of 1 year are summarised below in Table 6.36.

ICP (in mmHg)	Age threshold (in years)	ONSD cut-off value (in mm)
≥ 20	Overall	5.50
	≥ 1	5.75
	< 1	5.16
≥ 15	Overall	5.30
	≥ 1	5.49
	< 1	4.97
≥ 10	Overall	5.04
	≥ 1	5.20
	< 1	4.30
≥ 5	Overall	5.00
	≥ 1	5.10
	< 1	N/A

Table 6.27. ONSD cut-off values for detecting ICP at various thresholds using age at 1 year as a dichotomy point

6.3.3. Subcategory analysis of children over the age of 1 year

For comparison with the literature, a subgroup analysis of children over the age of 1 year was performed to determine the validity of age at 4 years as an age-related threshold.^{28,31}

6.3.3.1. Children aged between 1 and 4 years (> 1 and ≤ 4 years old)

Of the one hundred and eighteen children over the age of 1 year, thirty nine were > 1 and ≤ 4 years old. The data for children in this age category are summarised according to ICP thresholds in Table 6.28. (A detailed analysis for this age category is included in the appendix, appendix II)

ICP in mmHg	N (%)	Median age in months (IQR)	Mean ICP in mmHg (SD)	Mean ONSD in mm (SD)
Overall	39	23 (17 – 35)	19.15 (6.04)	5.94 (0.6)
< 20 mmHg	16 (41)	22.5 (16.5 – 34.5)	13.75 (4.3)	5.43 (0.6)
≥ 20 mmHg	23 (59)	23 (18 – 35)	22.91 (3.8)	6.29 (0.4)
< 15 mmHg	8 (20.5)	25.5 (16.5 – 43)	10.78 (4.1)	5.28 (0.6)
≥ 15 mmHg	31 (79.5)	23 (18 – 34)	21.31 (4.3)	6.11 (0.5)
< 10 mmHg	2 (5)	43 (42 – 44)	4.5 (0.7)	4.92 (0.4)
≥ 10 mmHg	37 (95)	23 (17 – 34)	19.94 (5.1)	6.00 (0.6)
< 5 mmHg	1 (2.5)	42	4	5.20
≥ 5 mmHg	38 (97.5)	23 (17 – 34)	19.55 (5.6)	5.96 (0.6)

Table 6.28. Summary of patient data at different ICP thresholds

The diagnostic accuracy of ONSD measurement for detecting ICP at the described thresholds in this age category are reported in Table 6.29.

ICP (mmHg)	ONSD cut-off (mm)	Sensitivity% (95%CI)	Specificity % (95%CI)	PPV % (95%CI)	NPV % (95%CI)	AUROC (95%CI)	OR (95%CI)
≥ 20	5.92	82.6 (61.2-95)	81.3 (54.4-96)	86.4 (65.1-97.1)	76.5 (50.1-93.2)	0.82 (0.69-0.95)	20.6 (4.1-102)
≥ 15	5.50	90.3 (74.2-98)	75 (34.9-96.8)	93.3 (77.9-99.2)	66.7 (29.9-92.5)	0.83 (0.66-0.99)	28 (4.19-185)
≥ 10	5.40	86.5 (71.2-95.5)	100 (15.8-100)	100 (89.1-100)	28.6 (3.7-71)	0.93 (0.88-0.99)	Nil
≥ 5	5.20	86.8 (71.9-95.6)	100 (2.5-100)	100 (89.4-100)	16.7 (0.42 – 64.1)	0.93 (. - 1)	Nil

Table 6.29. Diagnostic accuracy of ONSD in age category > 1 and ≤ 4 years old

6.3.3.2. Children over 4 years of age (> 4 years old)

There were seventy nine children over the age of 4 years in this study. The data for this age group are summarised according to ICP dichotomised at thresholds of 20, 15, 10 and 5 mmHg respectively in Table 6.30.

ICP in mmHg	N (%)	Median age in months (IQR)	Mean ICP in mmHg (SD)	Mean ONSD in mm (SD)
Overall	79	82 (65 – 108)	17.72 (8.7)	5.90 (0.8)
< 20 mmHg	38 (48.1)	81.5 (63 – 107)	10.15 (5)	5.33 (0.6)
≥ 20 mmHg	41 (51.9)	87 (69 – 125)	24.74 (4.6)	6.43 (0.6)
< 15 mmHg	31 (39.2)	86 (63 -114)	8.43 (3.7)	5.22 (0.6)
≥ 15 mmHg	48 (60.8)	82 (68 – 107)	23.72 (4.9)	6.34 (0.6)
< 10 mmHg	17 (21.5)	76 (57 – 116)	5.61 (2.3)	4.99 (0.5)
≥ 10 mmHg	62 (78.5)	89 (69 – 107)	21.04 (6.6)	6.15 (0.7)
< 5 mmHg	4 (5.1)	109.5 (75.5 – 148.5)	2.75 (1.5)	4.93 (0.2)
≥ 5 mmHg	75 (94.9)	82 (65 – 107)	18.52 (8.2)	5.96 (0.8)

Table 6.30. Summary of patient data at different ICP thresholds

The diagnostic accuracy of ONSD measurement for detecting ICP at the described thresholds, in this age category, is summarised in Table 6.31.

ICP (mmHg)	ONSD cut-off (mm)	Sensitivity% (95%CI)	Specificity % (95%CI)	PPV % (95%CI)	NPV % (95%CI)	AUROC (95%CI)	OR (95%CI)
≥ 20	5.70	87.8 (73.8 – 95.9)	68.4 (51.3 – 82.5)	75 (60.4 – 86.4)	83.9 (66.3 – 94.5)	0.78 (0.69 – 0.87)	15.6 (5 – 48.2)
≥ 15	5.49	93.8 (82.8 – 98.7)	74.2 (55.4 – 88.1)	84.9 (72.4 – 93.3)	88.5 (69.8 – 97.6)	0.84 (0.75 – 0.93)	43.1 (10.9 – 167)
≥ 10	5.20	88.7 (78.1 – 95.3)	82.4 (56.6 – 96.2)	94.8 (85.6 – 98.9)	66.7 (43 – 85.4)	0.86 (0.75 – 0.96)	36.7 (8.8 – 150)
≥ 5	5.00	80 (69.2 – 88.4)	75 (19.4 – 99.4)	98.4 (91.2 – 100)	16.7 (3.6 – 41.1)	0.78 (0.53 – 1)	12 (1.6 – .)

Table 6.31. ONSD cut-off values for various ICP thresholds in patients aged > 4 years

The optimal ONSD cut-off values for detecting ICP at thresholds of 20, 15, 10 and 5 mmHg, within the various described age categories are summarised below in Table 6.32.

ICP in mmHg	Age threshold (in years)	ONSD cut-off values (in mm)
≥ 20	Overall	5.50
	≤ 1	5.16
	$> 1 - \leq 4$	5.94
	> 4	5.70
≥ 15	Overall	5.30
	≤ 1	4.97
	$> 1 - \leq 4$	5.50
	> 4	5.49
≥ 10	Overall	5.04
	≤ 1	4.30
	$> 1 - \leq 4$	5.40
	> 4	5.20
≥ 5	Overall	5.00
	≤ 1	Nil
	$> 1 - \leq 4$	5.20
	> 4	5.00

Table 6.32. ONSD cut-off values for different ICP thresholds within the various age categories

6.4. The relationship between ONSD and ICP using patency of the anterior fontanelle (AF) to describe ONSD cut-off values

The concept of using age limits in children to describe different cut-off values for ONSD has been analysed in the preceding section. The inconsistency of current recommendations contributes to the difficulty in describing acceptable ONSD cut-off values in children. Using patency of the AF as a clinical marker for defining different ONSD cut-off values may be a valuable alternative to approaching this challenge, and perhaps standardising these recommendations. Closure of the AF is quite variable, usually between 6 and 18 months, but the AF can usually be classified as either open, if reliably palpable or closed if not palpable. This section examined the validity of using patency of the AF as a physiological and anatomical indicator to define the diagnostic accuracy of ONSD measurement in children and also compared these results to the age-related findings described earlier.

6.4.1. Patients with an open anterior fontanelle (AF)

Of the one hundred and seventy four patients included in this study, sixty two (35.6%) had an open AF, and one hundred and twelve (64.4%) had a closed AF. The diagnostic accuracy of ONSD for detecting ICP at thresholds of 20, 15, 10 and 5 mmHg were analysed within these two groups.

The median age of the sixty two patients in this group was 5 months (IQR 1 – 8). Correlation between ONSD and ICP in the group of patients with an open AF was fair ($r = 0.56$, $p < 0.001$, PCC) in the (Figure 6.30).

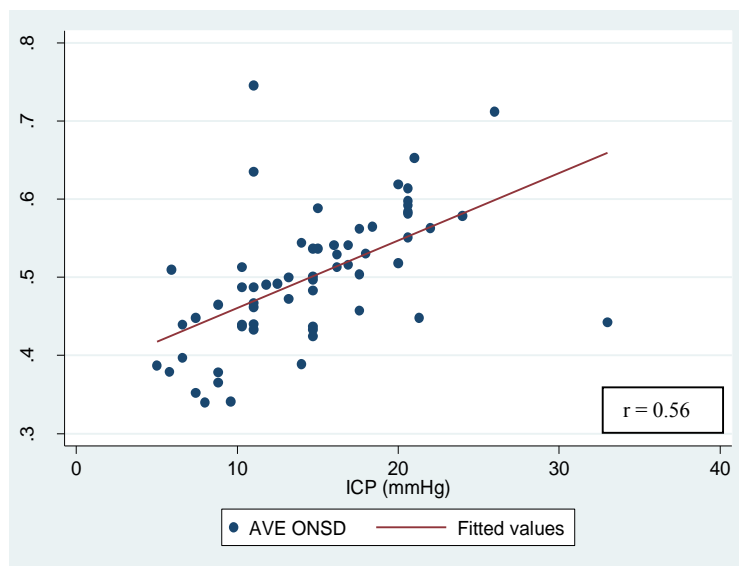


Figure 6.24. Scatterplot for ONSD vs ICP in patients with an open AF

6.4.1.1. ICP dichotomised at 20 mmHg

In the group of patients with an open AF, forty eight had an ICP < 20 mmHg with a mean ICP reading of 12.29 mmHg (SD 3.7) and fourteen patients had an ICP \geq 20 mmHg with a mean ICP reading of 22.21 mmHg (SD 3.53) (Table 6.33).

ICP in mmHg	N (%)	Median age in months (IQR)	Mean ICP in mmHg (SD)	Mean ONSD in mm (SD)
Overall	62	5 (1- 8)	14.52 (5.54)	5.0 (0.9)
< 20	48 (77.4)	4 (0.88 – 8)	12.29 (3.7)	4.8 (0.8)
\geq 20	14 (22.6)	8 (7 – 14)	22.21 (3.53)	5.8 (0.7)
p – value		p = 0.003	p < 0.001	p = 0.001

Table 6.33. Age, ICP and ONSD for ICP dichotomised at 20 mmHg in children with an open AF

In the group with ICP < 20 mmHg, the mean ONSD was 4.8 mm (SD 0.8), and in the group with ICP \geq 20 mmHg the mean ONSD was 5.8 mm (SD 0.7) (Figure 6.25).

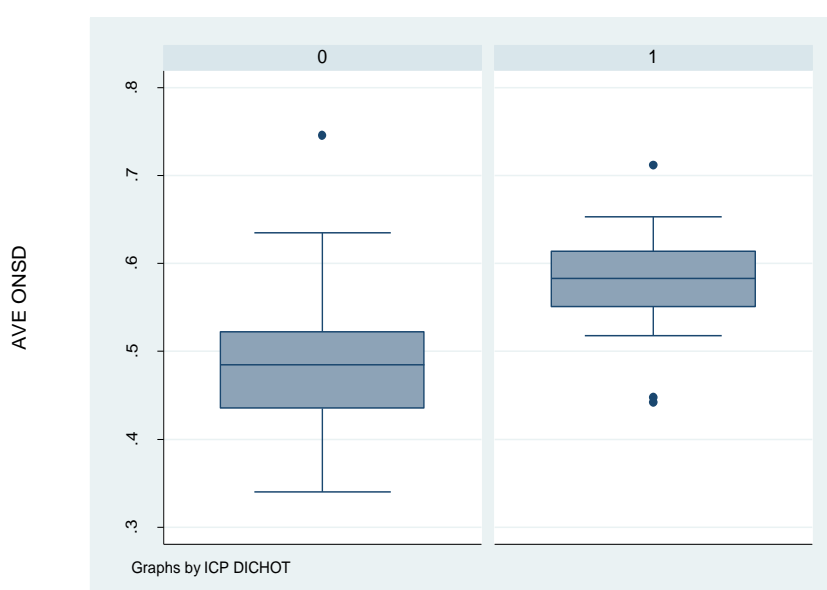


Figure 6.25. Box-whisker plot of ONSD for ICP < 20 (0), and ICP \geq 20 mmHg (1)

In patients with an open AF, the ONSD cut-off value with the best diagnostic accuracy for detecting an ICP ≥ 20 mmHg was 5.16 mm with a sensitivity of 85.7%, specificity of 75%, PPV of 50%, NPV of 94.7%, an AUROC of 0.804 (Figure 6.32) and a diagnostic OR of 18.(Table 6.36)

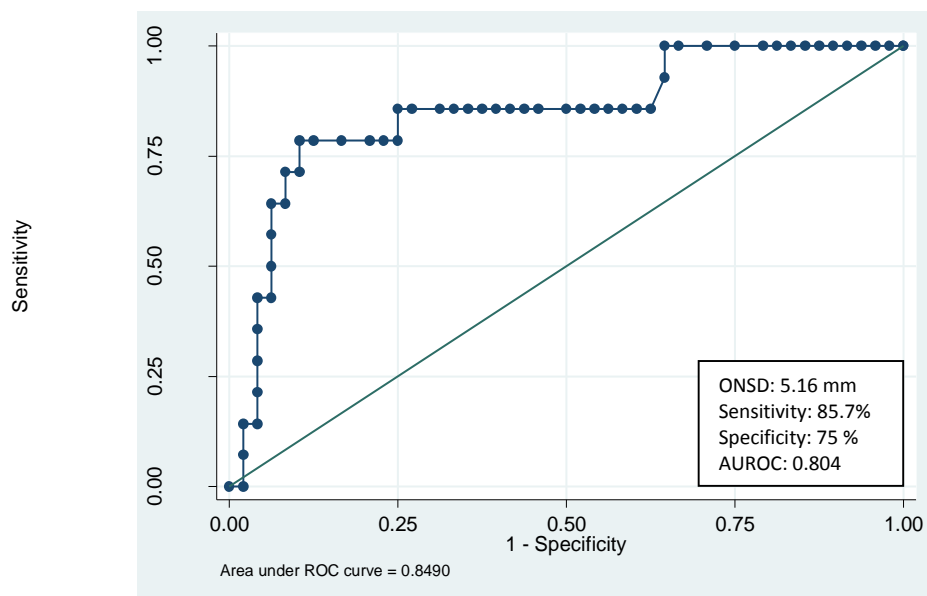


Figure 6.26. AUROC of ONSD for detecting ICP ≥ 20 mmHg

6.4.1.2. ICP dichotomised at 15 mmHg

There were thirty six children in this group with an ICP < 15 mmHg and twenty six with an ICP ≥ 15 mmHg. The results and their comparative p – values are summarised in table 6.34.

ICP in mmHg	N (%)	Median age in months (IQR)	Mean ICP in mmHg (SD)	Mean ONSD in mm (SD)
Overall	62	5 (1 – 8)	14.52 (5.54)	5.0 (0.9)
< 15	36 (58.1)	2.5 (0.5 – 7)	10.79 (2.96)	4.6 (0.8)
≥ 15	26 (41.9)	8 (5 – 10)	19.7 (3.82)	5.6 (0.6)
p – value		p = 0.002	p < 0.001	p < 0.001

Table 6.34. Age, ICP and ONSD values for ICP dichotomised at 15 mmHg in children with an open AF

In the group with an open AF, the optimal ONSD cut-off value for predicting an ICP ≥ 15 mmHg was 5 mm with a sensitivity of 88.5%, specificity of 83.3% and an OR of 38.3 (Table 6.36).

6.4.1.3. ICP dichotomised at 10 mmHg

There were twelve children in this group with an ICP < 10 mmHg and 50 with an ICP ≥ 10 mmHg. Table 6.35 summarises the results and comparative p – values.

ICP	N (%)	Median age in months (IQR)	Mean ICP in mmHg (SD)	Mean ONSD in mm (SD)
Overall	62	5 (1 – 8)	14.5 (5.53)	5.0 (0.9)
< 10 mmHg	12 (19.4)	1 (0.11 – 3)	7.39 (1.44)	4.0 (0.5)
≥ 10 mmHg	50 (80.6)	6.5 (2 – 9)	16.24 (4.72)	5.2 (0.7)
p – value		p = 0.009	p < 0.001	p < 0.001

Table 6.35. Age, ICP and ONSD values for ICP dichotomized at 10 mmHg in children with an open AF

In patients with an open AF, the optimal ONSD cut-off value for predicting an ICP \geq 10 mmHg was 4.4 mm, with a sensitivity of 86%, specificity of 75% and an OR of 18.4.(Table 6.36)

6.1.4.4. ICP dichotomised at 5 mmHg

None of the patients with an open AF in this study had an ICP $<$ 5 mmHg.

The diagnostic accuracy of ONSD measurements for detecting ICP at thresholds of 20, 15, 10 and 5 mmHg in children with an open AF, are summarised below in table 6.36

ICP (mmHg)	ONSD cut-off (mm)	Sensitivity% (95%CI)	Specificity % (95%CI)	PPV% (95%CI)	NPV % (95%CI)	AUROC (95%CI)	OR (95%CI)
≥ 20	5.16	85.7 (57.2 – 98.2)	75 (60.4 – 86.4)	50 (29.1 – 70.9)	94.7 (82.3 – 99.4)	0.804 (0.69 – 0.92)	18 (3.84 - 100)
≥ 15	5.00	88.5 (69.8 – 97.6)	83.3 (67.2 – 93.6)	79.3 (60.3 – 92)	90.0 (75.7 – 98.1)	0.86 (0.77 – 0.95)	38.3 (9.01 – 160)
≥ 10	4.40	86 (73.3 – 94.2)	75 (42.8 – 94.5)	93.5 (82.1 – 98.6)	56.3 (29.9 – 80.2)	0.81 (0.67 – 0.94)	18.4 (4.2 – 79.5)
≥ 5	Nil	Nil	Nil	Nil	Nil	Nil	Nil

Table 6.36. Diagnostic accuracy of ONSD cut-off values for ICP at thresholds of 20, 15, 10 and 5mmHg in children with an open AF

6.4.2. Patients with a closed anterior fontanelle (AF)

Of the one hundred and seventy four patients in this study, one hundred and twelve (64.4%) had a closed AF. The median age in this group was 70 months (IQR 41 – 97.5) with a mean ICP of 18.16 mmHg (SD 8.1) and a mean ONSD 5.9 mm (SD 0.8). The correlation between ONSD and ICP in patients with a closed AF was good ($r = 0.7$, $p < 0.001$, PCC). (Figure 6.33)

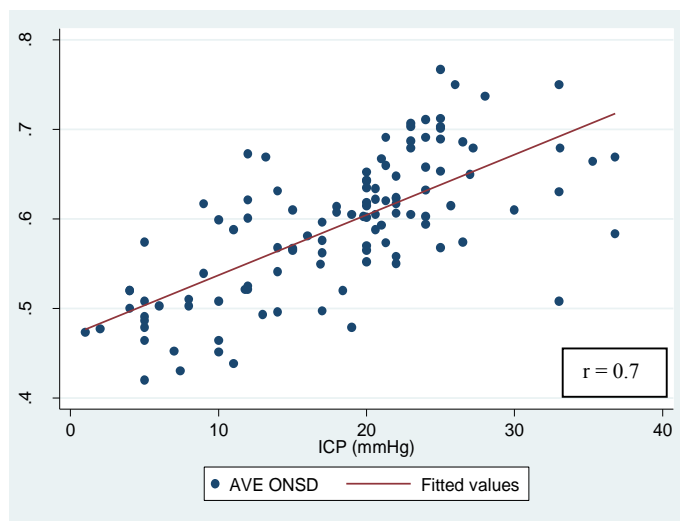


Figure 6.27. Scatterplot for ONSD vs ICP in patients with a closed AF

The diagnostic accuracy of ONSD measurement was analysed in children with a closed AF, for detecting raised ICP at the thresholds described previously in this study.

6.4.2.1. ICP dichotomised at 20 mmHg

Of the one hundred and twelve patients with a closed AF, fifty two had an ICP < 20 mmHg with a mean ICP of 11.13 mmHg (SD 5.09). Sixty patients had an ICP \geq 20 mmHg with a mean ICP of 24.26 mmHg (SD 4.44). Table 6.37 summarises the results and comparative p – values.

ICP	N (%)	Median age in months (IQR)	Mean ICP in mmHg (SD)	Mean ONSD in mm (SD)
Overall	112	70 (41 – 97.5)	18.16 (8.1)	5.90 (0.8)
< 20 mmHg	52 (46.4)	68 (45.5 – 96)	11.13 (5.09)	5.37 (0.6)
\geq 20 mmHg	60 (53.6)	70 (38 – 101)	24.26 (4.44)	6.40 (0.6)
p – value		p = 0.9	p < 0.001	p < 0.001

Table 6.37. Age, ICP and ONSD values for ICP dichotomised at 20 mmHg in children with a closed AF

The mean ONSD was 5.37 mm (SD 0.6) in the group with ICP \geq 20mmHg and 6.4 mm (SD 0.6) in the group with ICP < 20 mmHg.(Figure 6.28)

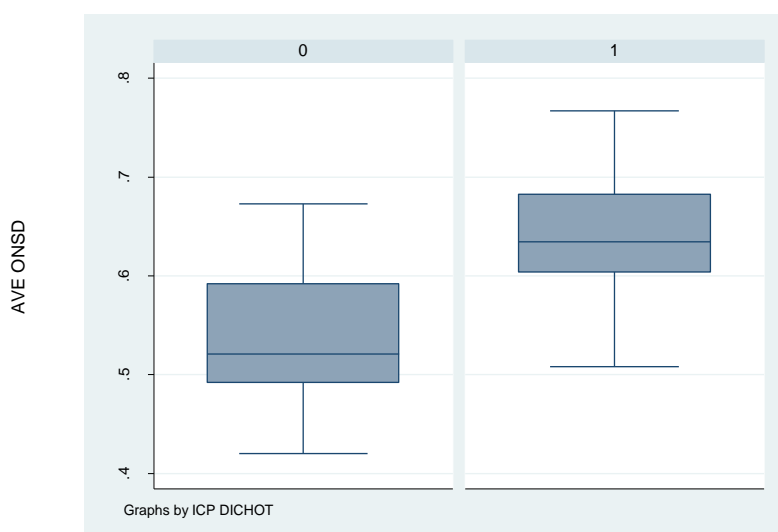


Figure 6.28. Box-whisker plot of ONSD for ICP < 20 (0), and ICP \geq 20 mmHg (1)

In patients with a closed AF, the optimal ONSD cut-off value for detecting an ICP \geq 20 mmHg was 5.81 mm with a sensitivity of 85%, specificity of 73.1%, PPV of 78.5%, NPV of 80.9%, AUROC of 0.79 (Figure 6.29) and an OR of 15.4.(Table 6.41)

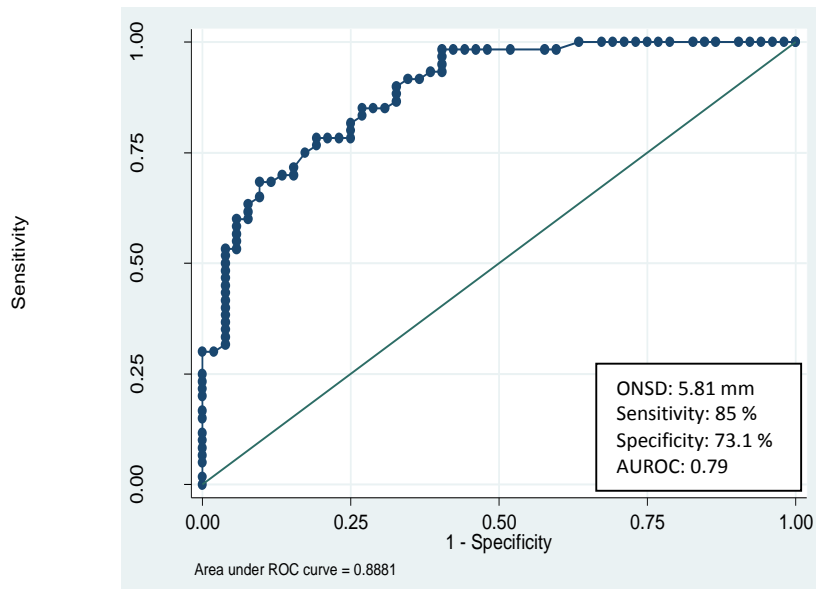


Figure 6.29. AUROC of ONSD for detecting ICP \geq 20 mmHg

6.4.2.2. ICP dichotomised at 15 mmHg

There were thirty seven children in this group with an ICP < 15 mmHg and seventy five with an ICP \geq 15mmHg. Table 6.38 summarises the results and comparative p – values.

ICP	N (%)	Median age in months (IQR)	Mean ICP in mmHg (SD)	Mean ONSD in mm (SD)
Overall	112	70 (41 – 97.5)	18.16 (8.1)	5.92 (0.8)
< 15 mmHg	37 (33)	76 (57 – 98)	8.7 (3.8)	5.20 (0.6)
\geq 15 mmHg	75 (67)	66 (33 – 93)	22.9 (4.9)	6.30 (0.6)
p – value		p = 0.09	p < 0.001	p < 0.001

Table 6.38. Age, ICP and ONSD values for ICP dichotomised at 15 mmHg in children with a closed AF

In patients with a closed AF, the cut-off value for ONSD that best predicted an ICP \geq 15 mmHg was 5.5 mm with a sensitivity of 93.3%, specificity of 73% and an OR of 37.8.(Table 6.41)

6.4.2.3. ICP dichotomised at 10 mmHg

There were nineteen patients in this group with an ICP < 10 mmHg and ninety three patients with an ICP \geq 10 mmHg. The results and comparative p – values are summarised in table 6.39.

ICP	N (%)	Median age in months (IQR)	Mean ICP in mmHg (SD)	Mean ONSD in mm (SD)
Overall	112	70 (41 – 97.5)	18.16 (8.1)	5.92 (0.8)
< 10 mmHg	19 (17)	75 (57 – 116)	5.5 (2.2)	4.98 (0.5)
\geq 10 mmHg	93 (83)	69 (35 – 97)	20.75 (6.2)	6.10 (0.7)
p – value		p = 0.15	p < 0.001	p < 0.001

Table 6.39. Age, ICP and ONSD values for ICP dichotomized at 10 mmHg in children with a closed AF

In patients with a closed AF, the ONSD cut-off value that best predicted an ICP \geq 10 mmHg was 5.2 mm with a sensitivity of 89.2%, specificity of 84.2 and an OR of 44.3 (Table 6.41).

6.4.2.4. ICP dichotomised at 5 mmHg

Five patients in this group had an ICP < 5 mmHg and one hundred and seven patients had an ICP \geq 5 mmHg. Table 6.40 summarises the results and comparative p – values in this group.

ICP	N (%)	Median age in months (IQR)	Mean ICP in mmHg (sd)	Mean ONSD in mm (sd)
Overall	112	70 (41 – 97.5)	18.16 (8.1)	5.92 (0.8)
< 5 mmHg	5 (4.5)	76 (75 – 143)	3 (1.4)	4.98 (0.2)
\geq 5 mmHg	107 (95.5)	67 (39 – 97)	18.9 (7.6)	5.97 (0.8)
p – value		p = 0.15	p < 0.001	p = 0.005

Table 6.40. Age, ICP and ONSD for ICP dichotomised at 5 mmHg in children a closed AF

In patients with a closed AF, the ONSD cut-off value that best predicted an ICP \geq 5 mmHg was 5 mm, with a sensitivity of 86.9%, specificity of 60% and an OR of 10 (Table 6.41).

The diagnostic accuracy of ONSD measurement for detecting ICP at thresholds of 20, 15, 10 and 5 mmHg in children with a closed AF are summarised below in Table 6.4.

ICP (mmHg)	ONSD cut-off (mm)	Sensitivity% (95%CI)	Specificity % (95%CI)	PPV% (95%CI)	NPV % (95%CI)	AUROC (95%CI)	OR (95%CI)
≥ 20	5.80	85 (73.4 – 92.9)	73.1 (59 – 84.4)	78.5 (66.5 – 87.7)	80.9 (66.7 – 90.9)	0.79 (0.71 – 0.87)	15.4 (6.1 – 38.8)
≥ 15	5.50	93.3 (85.1 – 97.8)	73 (55.9 – 86.2)	87.5 (78.2 – 93.8)	84.4 (67.2 – 94.7)	0.83 (0.75 – 0.91)	37.8 (12.1 – 118)
≥ 10	5.20	89.2 (81.1 – 94.7)	84.2 (60.4 – 96.6)	96.5 (90.1 – 99.3)	61.5 (40.6 – 79.8)	0.87 (0.78 – 0.96)	44.3 (11.5 – 167)
≥ 5	5.00	86.9 (79 – 92.7)	60 (14.7 – 94.7)	97.9 (92.6 – 99.7)	17.6 (3.8 – 43.4)	0.74 (0.49 – 0.98)	10 (3.8 – 54.4)

Table 6.41. Diagnostic accuracy of ONSD measurement for detecting ICP at various thresholds in children with a closed AF

A summary of the results from assessing patency of the AF as a clinical marker for describing different ONSD cut-off values in children at ICP thresholds of 20, 15, 10 and 5 mmHg, are provided in table 6.42.

ICP threshold (in mmHg)	Patency of AF	ONSD cut-off value (in mm)
≥ 20	Overall	5.50
	Open AF	5.16
	Closed AF	5.81
≥ 15	Overall	5.30
	Open AF	5.00
	Closed AF	5.50
≥ 10	Overall	5.04
	Open AF	4.40
	Closed AF	5.20
≥ 5	Overall	5.00
	Open AF	Nil
	Closed AF	5.00

Table 6.42. ONSD cut-off values for different ICP thresholds in patients with an open and closed AF

6.5. Discussion

In this study the relationship between ONSD measurement and the criterion standard of invasive ICP measurement was prospectively examined in a paediatric group of patients. The aetiology demonstrated in this study reflects most of the commonly encountered paediatric neurosurgical conditions. Majority of the patients included in the study had hydrocephalus (52.9%), followed by TBI (17.2%), with tumors and craniosynostosis, each forming 9.2%. The benefit of a safe and reliable, non-invasive diagnostic tool for detecting raised ICP would be most beneficial in these clinical conditions. The concepts of repeatability and user variability remain core aspects of a suitable diagnostic modality. Specifically for transorbital ultrasonography, the most appropriate plane of imaging and the requirement for bilateral image acquisition remain relevant questions, especially with the paucity of data on this technique in children.^{34,156,272}

6.5.1. Repeatability, intra-observer variability and inter-observer variability

Early work done by Ballantyne examined the observer variation in normal adult patients, demonstrating a median intra-observer variation of $\pm 0.2 - 0.4$ mm and an inter-observer variation of $\pm 0.6 - 0.7$ mm, reporting that standardisation of the technique reduced observer variability.²⁹ A study analysing the correlation and agreement between two independent investigators, demonstrated good correlation ($r = 0.83$) and robust agreement, with mean differences close to zero between the two observers.²⁷ A later study by the same group comparing the accuracy of ONSD measurement on ultrasound with MRI, demonstrated mean differences of $< 5\%$ ($r \geq 0.82$, $p < 0.001$) between observers using MRI measurements, with increased inter-observer variability when using ultrasound measurements, with a mean difference of 9.4% ($r = 0.62$, $p < 0.001$).²⁷³ In a study evaluating ONSD on MRI, a mean difference between observers of 0.11 mm was described.¹⁵¹ This difference was again shown to be larger when using ultrasound, with a median inter-observer difference of 0.25 mm described in an ultrasound-based study.²⁰ Different ultrasound probes and imaging techniques, i.e. axial vs coronal could impact on

ONSD measurement and inter-observer reliability with a reported adjusted difference of 0.21 mm between observers, using a ‘standard probe’.²⁷⁴ Lagreze also described smaller coefficients of variation using MRI compared to ultrasound.²³¹

The factors described by Bauerle et al^{27,273} were specifically addressed in the current study, by testing the relationship between repeat measurements performed in the same plane of the same eye, as a test for repeatability, and by testing intra-and inter-observer reliability. Three ONSD measurements were performed to allow adequate testing for the repeatability of measurements. The results from this study demonstrated excellent repeatability between each of the three ONSD measurements performed in the same plane of each eye ($\alpha = 0.97 - 0.98$, CA). These findings were consistent in both the axial and sagittal plane.

The intra-observer variability was excellent with mean ONSD values of 5.56 mm (SD 0.85) and 5.58 mm (SD 0.84), from the first and second measurement respectively ($\alpha = 0.99$, CA).

Inter-observer testing revealed a mean difference of 0.28 mm between observers. This is consistent with other described values of 0.2 mm and 0.34 mm.^{17,20,28,34,274} Correlation between the two observers was very good ($r = 0.87$, $p < 0.001$, PCC). These findings confirm that ONSD measurement on ultrasound yields consistent and acceptable intra- and inter-observer variability.

6.5.2. Sagittal versus axial plane and correlation of values between right and left eye

The ideal plane in which to measure the ONSD is still unclear. Axial images were usually obtained because of the ease of acquisition and the size of the ultrasound probes used. Early work by Hansen suggested that the axial plane provided more accurate measurements,¹⁵⁴ but this was based on a relatively small sample size and did not factor in the benefit of the smaller footprint probes available today. As the ONS is not a perfect sphere,^{260,275} there is likely to be some difference in the measurements acquired in different planes, even if only minimal.

When evaluating the optimal plane for measurement, i.e. sagittal vs axial, this study demonstrated a slight advantage in the sagittal plane over the axial plane ($r = 0.66$ vs $r = 0.64$). This difference however, was minimal, suggesting that measurement in either plane was an acceptable option. This study allowed adequate imaging in the sagittal plane largely because of the small footprint, high frequency probe used, a feature that differentiates it from most other studies which used high frequency probes with a larger footprint.^{23,30,33,234,241} Acquiring ONSD images in both planes and using the average of the two measurements, where possible, is likely the safer alternative, given the variety of probes available on the market. The image acquisition is also influenced by the unfavourable intromission angle of 180° to the ON which limits lateral resolution and in children the age of the child and size of the orbit also play an important role.³⁴

Differences between measurements obtained in the left and right eye were analysed and the results demonstrated a good correlation between ONSD values from both eyes ($r = 0.9$, $p < 0.001$, PCC). The benefit of using the mean value of ONSD measurements from both eyes however, remains a logical option based on described individual anatomical variation and the possibility of unilateral pathology.^{46,154} Given the findings from this study and the excellent correlation demonstrated between the three measurements, if the imaging quality is considered adequate, it may be acceptable to perform two measurements in each eye, in either the sagittal or axial plane (depending on the probe shape and size), and use the mean ONSD measurement for estimating ICP.

6.5.3. Analysis over the entire cohort

The linear relationship between ONSD and ICP has been described in a number of publications, recommending the technique as a simple bedside method for non-invasively assessing ICP.^{17,18,20,30,156,157} The diagnostic accuracy for raised ICP and the optimal cut-off values are however, still unclear,^{31,157,261} making the relationship between ONSD and ICP, a promising research avenue with significant clinical implications, particularly in children.

Specific limitations of this technique have hampered its widespread use; these include poor specificity, variation in the recommended ONSD cut-off values for predicting raised ICP, inter-rater variability and a limited understanding of the elastic properties of the ONS. The recommended ONSD cut-off value in adults ranges widely, from 4.1 – 5.9 mm.^{17-20,73,155} In children there are recommended age-related upper limits of ONSD measurement. These age-related thresholds in children however, are inconsistent. Using age at 1 year to define different upper limits of normality for ONSD was supported by Ballantyne and Newman,^{29,30} while other authors recommend 4 years as the appropriate age-related threshold.^{28,32} In a review by Moretti and Pizzi, age categories of < 1 year old, 1- 4 years old and > 4 years old were described with specific ONSD upper limits for each category.³¹

The issue of the optimal cut-off point is further limited by the sub-millimetric measurements involved in this technique, the wide variation in individual baseline values and limited knowledge about the elastic nature of the ONS.

Evaluating the entire patient cohort in this study, demonstrated a mean ONSD in the group with ICP < 20 mmHg of 5.08 mm (SD 0.76), and in the group with ICP \geq 20 mmHg of 6.28 mm (SD 0.64) ($p < 0.001$). The optimal ONSD cut-off point in this study for detecting ICP \geq 20 mmHg across the entire patient cohort, was 5.5 mm with good diagnostic accuracy revealing a sensitivity of 93.2%, a specificity of 74% and an OR of 39.3 (Table 6.16). In a multivariate model adjusting for appropriate confounding variables, the OR was adjusted to 26.9 (Table 6.10), suggesting that the likelihood of detecting an ONSD measurement > 5.5 mm is 26.9 times higher in children with an ICP \geq 20 mmHg than in children with an ICP < 20 mmHg. In a recent systematic review, Dubourg et al describe an even higher pooled diagnostic OR of 51, and recommended that a high sensitivity be favoured over a high specificity when using sonographic ONSD measurement to estimate ICP.¹⁵⁷ It is worth noting that this review only included work done in adults.

The number of patients included in the present study made it possible to perform both linear and logistic regression analyses. The described change in ONSD from a baseline diameter of 4.03 mm, was 0.75 mm (95% CI: 0.62 – 0.88, $R^2 = 0.52$, $p < 0.001$), after controlling for age as a confounding variable, for every 10 mmHg change in ICP. This is

useful in describing the relationship between ONS distension and increase in ICP. This relationship was weaker when ICP was ≥ 20 mmHg, i.e. 0.24 mm (95% CI: 0.09 – 0.5, $R^2 = 0.03$, $p = 0.16$) for every 10 mmHg change in ICP, suggesting a variation in the response of the ONS at different ICP thresholds. This is consistent with experimental data reporting that ONSD distensibility differed at certain ICP thresholds, and likely approached a maximum distensibility at higher ICP values.^{154,252} The described change in ONSD was 0.25 mm for every 10 mmHg increase in ICP in the Hansen study, but no baseline diameter was described.¹⁵⁴ These findings underscore the need to investigate the elasticity of the ONS as a marker of its stiffness or distensibility.

The mean ONSD values, mean ICP values and relevant ONSD cut-off values in different aetiologies have been described in the results section (Table 6.11). Despite the sample size calculation in this study being based on age and not aetiology, the difference in aetiological groups is noteworthy. The higher cut-off values detected for children with craniosynostosis (6.17 mm) and lower cut-off values with intracranial cysts (4.5 mm) suggest that aetiology may have a role to play in determining the baseline ONSD and the response to an increase in ICP. While the mean ICP in these two groups was also significantly different ($p = 0.047$, Student's t-test), this finding does raise the concern that ONSD cut-off recommendations should take aetiology into account.

The diagnostic accuracy of ONSD measurements were also examined at ICP thresholds of 15 mmHg, 10 mmHg and 5 mmHg. The benefit of describing the ONSD at these ICP thresholds relates to the lack of uniformity regarding the optimal treatment threshold for raised ICP in children. Determining ONSD cut-off values at various ICP thresholds may provide additional diagnostic benefit in a clinical environment.

The ONSD cut-off values with the best diagnostic accuracy for ICP ≥ 15 mmHg, ≥ 10 mmHg and ≥ 5 mmHg described in this study were 5.3 mm, 5.04 mm and 5 mm respectively (Table 6.16). The diagnostic accuracy of ONSD was better for detecting an ICP ≥ 20 mmHg than it was for and ICP ≥ 5 mmHg (OR of 39.5 vs. 4.01). These values do support a significant overall relationship between ONSD and increasing ICP in this study. The paediatric literature evaluating ONSD measurement suggests that age is very likely a confounding factor.^{22,23,28,29,30,33} For this reason the historically described age

thresholds of 1 year old^{29,30} and 4 years old^{28,31} were used to subcategorise the data for further analysis and comparison to published data.

6.5.1. Age-related threshold

This study was unique in that it described ONSD cut-off values for various ICP thresholds and analysed the diagnostic accuracy of ONSD measurement for detecting ICP at thresholds ranging from 20 to 5 mmHg. This analysis was performed in the specific age categories, i.e. ≤ 1 year old and > 1 year old, and a subgroup analysis, i.e. ages > 1 to ≤ 4 years and > 4 years old.

≤ 1 year: the highest diagnostic accuracy for predicting ICP ≥ 20 mmHg was achieved with an ONSD cut-off value of 5.16 mm, sensitivity of 80%, specificity of 76.1% and an OR of 12.7 (Table 6.23). At ICP thresholds of 15 and 10 mmHg, the optimal ONSD cut-off values were 4.97 mm and 4.3 mm, respectively (Table 6.18). There were no ICP measurements under 5 mmHg in this age category. In children ≤ 1 year old, the diagnostic accuracy of ONSD measurement for detecting an ICP ≥ 15 mmHg was the strongest, with an OR of 29.6.

> 1 to ≤ 4 years: 39 patients fell into this age category. The optimal ONSD cut-off value for detecting an ICP ≥ 20 mmHg was 5.92 mm, with a sensitivity of 82.6%, specificity of 81.3% and OR of 20.6 (Table 6.23). At ICP thresholds of 15, 10 and 5 mmHg, the optimal ONSD values were 5.5, 5.4 and 5.2 mm respectively. Comparing these values to the next age category, i.e. > 4 years old, demonstrated ONSD values that were at odds with descriptions in the literature,³¹ as the optimal ONSD values described here were higher than those in the > 4 years old category, making this age category less useful as a recommendation.

> 4 years old: there were 79 patients in this age category. The optimal ONSD cut-off value for detecting ICP ≥ 20 mmHg was 5.75 mm, with a sensitivity of 82.9%, specificity of 71.1% and an OR of 11.9 (Table 6.28). The ONSD cut-off values described in this age category were lower than in the previous category and similar to the results from children aged > 1 year (Table 6.29).

Children above the age of 1 year were analysed as a combined group. A total of 118 children were included in this age category, with an optimal ONSD cut-off value of 5.75 mm for predicting an ICP \geq 20 mmHg, sensitivity of 85.9 %, specificity of 70.4% and an OR of 14.5.

The ONSD cut-off values in this study appear larger than the described historic values in children,^{28, 29,30,33} but are similar to values reported more recently.^{34,237} A likely explanation for this finding is the high frequency, small footprint probe used, which provides excellent image quality, allowing clearer identification of the ONS borders.^{34,237} The group of patients analysed in this study were under general anaesthesia, and were already due have a surgical procedure, which potentially biases the results, especially when comparing them to existing literature in children, which are almost entirely based on a clinical and image-based suspicion of raised ICP.^{23,28,29,30,31,32,33} The value of 5.75 mm for predicting an ICP \geq 20 mmHg in older children described in this study was consistent with some of the adult literature.^{17,20,31,151}

The described ONSD cut-off values at 15, 10 and 5 mmHg respectively are interesting findings, as they underscore the relationship between ONSD and increasing ICP, and possibly serve to flag patients at potential risk of developing raised ICP, in the correct clinical context.

The relationship between ONSD and ICP in children below the age of 1 year appeared less robust than this relationship in children older than 1 year ($r = 0.65$ vs. $r = 0.7$). Interestingly though, the ONSD cut-off value of 4.3 mm for predicting an ICP \geq 10 mmHg, was consistent with values described by Newman et al,³⁰ suggesting that some children in this group may become clinically symptomatic at an ICP above 10 mmHg. The best OR in children above and below the age of 1 year was described for detecting and ICP \geq 15 mmHg (OR 42.9 and 29.6, respectively).

The ONSD cut-off values at various ICP thresholds described in this study (Table 6.27) may be quite helpful in decision-making where patients are thought to be at risk of raised ICP. Even though 20 mmHg may represent a preferred treatment threshold, described in

children with TBI^{111,276} in some centres, this threshold may differ in other centres treating children.

v) Anterior Fontanelle (AF)

Current literature in children suggests an age-related upper limit of ONSD to best detect raised ICP.²⁸⁻³⁴ The studies on which these recommendations were based however, largely compare ONSD to clinical and image-based estimates of ICP. The age-related ONSD values recommended for children can be quite useful, but the lack of uniformity makes the question of the appropriate upper limit of ONSD in children more difficult to determine. Data from this study support the use of age at 1 year as an appropriate age at which to describe different ONSD cut-off values for detecting raised ICP in children (Table 6.27). The difficulty however, lies in using very different values for children that may be just above or below the age of 1 year, based on absolute age-related cut-off values. This can be quite problematic, given the physiological heterogeneity encountered in children of similar age.

In an effort to simplify and improve the implementation of ONSD measurement in children, this study evaluated the patency of the AF as a clinical marker for determining the upper threshold of ONSD in children, and compared these findings to using age at 1 year.

The ONSD measurements listed in table 6.42 serve to demonstrate the significant difference between the two groups when using patency of the AF as a physiological threshold. This finding makes clinical and physiological sense as the open AF serves as a reliable clinical window for assessing ICP in neonates, and as such the measurement of ONSD in this group of patients is potentially less of a requirement. The presence of this natural window suggests that compliance of the bony skull is still present, making the displacement of CSF along the subarachnoid space somewhat unreliable, as explained by the Monroe-Kellie doctrine. Therefore using transorbital ultrasound ONSD measurement after the AF has closed is conceivably a physiologically more balanced approach, where the need for a reliable, non-invasive technique to detect raised ICP becomes more prudent.

In patients with an open AF the ONSD measurement that best predicted an ICP of ≥ 20 mmHg was 5.16 mm, compared to 5.81 mm in patients with a closed fontanelle ($p = 0.007$). This difference in ONSD cut-off values between the two groups was consistent at ICP thresholds of 15 and 10 mmHg. None of the patients in this study who had an open AF also had an ICP reading below 5 mmHg, hence no recommendation was made regarding the optimal ONSD cut-off for ICP < 5 mmHg in this group. The correlation between ONSD and ICP was also much better in children with a closed AF than those with an open AF ($r = 0.7$ vs $r = 0.56$, $p < 0.001$, PCC).

In this study, the ONSD measurements in children with a closed AF compare very well with those for children over the age of 1 year old, for all the described ICP thresholds. (Table 6.47).

ICP threshold (in mmHg)	ONSD cut-off in children over 1 year old (in mm)	ONSD cut-off in children with a closed AF (in mm)
≥ 20	5.75	5.81
≥ 15	5.49	5.50
≥ 10	5.20	5.20
≥ 5	5.10	5.00

Table 6.43. ONSD cut-off values in children > 1 year old and children with a closed AF

vi) Limitations

This study was conducted on patients undergoing anaesthesia and a neurosurgical procedure. Despite efforts to control for possible confounding variables, this may bias the results when compared to studies performed on awake patients. Assessment of the presence and patency of the AF remains a subjective clinical marker, albeit a reliable one. Palpation to determine whether the AF is normal, bulging or sunken could potentially vary

depending on patient position and examination technique; however, assessment of the AF is a fundamental clinical tool which all paediatric clinicians should be comfortable with. The use of this clinical assessment as a marker for describing ONSD upper limits may therefore be more helpful than using different values for children that are 1 year old versus those that are only slightly older. The described inter-observer variability in this study, while consistent with descriptions in the literature, needs to be factored into the interpretation of the findings. The ONSD values were compared to the initial and most stable ICP value at surgery, ideally the ICP trend and repeated ONSD measurement should be evaluated to determine the relationship between between these two parameters.

6.6. Conclusion

This study aimed to validate the technique of sonographic ONSD measurement by comparison to directly measured ICP in a large cohort of paediatric patients. A good correlation between ONSD and ICP was demonstrated, with age at 1 year supported as an appropriate age at which to define different ONSD cut-off values for detecting raised ICP in children. Additionally, use of the AF was recommended as a more suitable clinical marker than age for defining these different ONSD cut-off values in children. Results from this study may likely serve as a platform for further work and recommendations using ONSD measurement to estimate ICP in children.

SECTION C

Chapter 7. Dynamic assessment of the ONS

7.1. Theoretical background

The current technique of ONSD measurement involves static ultrasound image acquisition to determine the size of the ONS. The literature generally supports a good level of diagnostic accuracy for this technique.^{31,157,158} The static imaging technique however, provides limited information about the elasticity of the ONS and we therefore have little idea about the degree to which the ONS is distended from its baseline value. Hansen and colleagues describe a variation in the response of the ONS after exposure to different ICP levels and for different lengths of time, reporting that the tensile characteristics of the ONS have an influence on its response to change in ICP.⁵⁰ The challenges when interpreting the ONSD measurement present mostly in cases where the sheath elasticity is low or where the ability to return to its baseline size is impaired.^{154,252} An improved understanding of the elastic nature and subsequent distensibility of the ONS which ultimately determine its response to change in ICP, would add significantly to our current understanding. A dynamic assessment of the ONS response under conditions of normal and raised ICP could provide valuable information regarding the elastic nature and distensibility of the ONS.

Available literature describing a dynamic assessment of the ONS, generally compare the ONSD measured before and after a particular intervention or involve dynamic assessment of ocular blood flow using Doppler flow measurement. There are currently no data specifically evaluating the dynamic response of the ONS as a direct function of pulsation induced motion.

The importance of evaluating the distensibility and elastic characteristics of the ONS were perhaps best emphasised in the study by Hansen.²⁵² This was a post-mortem study performed on 10 optic nerve preparations, demonstrating that the ONS did not completely return to its baseline value after reduction in the SAS pressure, especially when the applied pressure exceeded 45mmHg. The investigators reported that the elastic properties

of the sheath influenced its capability to retract after exposure to high pressures, suggesting that the ONSD be interpreted with caution in certain circumstances due to an observation they call the 'plastical deformation' of the ONS.²⁵²

The 'dynamic change' in ONSD due to hyperventilation induced CO₂ fluctuation, was examined in 14 patients undergoing anterior cervical spine surgery. The study described a rapid response in ONSD caused by change in ETCO₂. The investigators used a flexible clamp to hold the ultrasound probe in position in order to assess the dynamic response. The ONSD was measured at two separate ETCO₂ levels, i.e. 30 mmHg and 40 mmHg and at 1 and 5 minutes after reaching each of these levels, demonstrating a significant change between the ONSD values.²⁷⁷

Drainage of CSF to reduce ICP and the subsequent change in ONSD measurement was reported by Moretti and Pizzi (20). This study was performed on 63 adult patients presenting with SAH (n = 34) or ICH (n = 29). The mean ONSD was 6.16 ± 0.57 mm in patients with an ICP > 20mmHg, and 5.0 ± 0.49 mm in the group with low ICP. The ONSD decreased from 5.89 ± 0.61 mm to 5 ± 0.33 mm in cases where CSF was released to control ICP. The optimal ONSD cut-off for identifying an ICP > 20 mmHg was 5.2 mm (sensitivity of 93.1%, specificity of 73.85%).²⁰

The use of mannitol to control increased ICP and the rate of ONSD variation was described in a study evaluating 13 severe TBI patients. The median ONSD prior to mannitol osmotherapy was 6.3 mm (6.1 - 6.7) versus 5.7 mm (5.5 - 6.3) (p = 0.0007) after mannitol administration, with a change in median ICP from a baseline of 35 mmHg to 25 mmHg. TCD derived pulsatility indices also showed a significant decrease after mannitol administration. The authors conclude that change in ONSD can be useful to monitor interventions such as osmotherapy, but cautioned that there was some heterogeneity in the ONSD response to changes in ICP.²⁷⁸

Using ultrasound analysis of the ONS, Whiteley and colleagues aimed to determine whether ICP increased to > 20 mmHg during robot-assisted laparoscopic radical prostatectomy (RARLP).²⁷⁹ Initial measurement of the ONSD was performed after induction of general anesthesia and then again at the end of the procedure. The mean

preoperative ONSD was 4.5 ± 0.5 mm, and the mean post-operative ONSD was 5.5 ± 0.5 mm. A 10 mmHg rise in MAP resulted in a 0.023 mm increase in postoperative ONSD. Based on the ONSD findings, the authors concluded that ICP rises to > 20 mmHg during RALRP surgery.²⁷⁹ A similar study, also during RALRP surgery demonstrated a 12.5% increase in ONSD after CO₂ pneumoperitoneum and steep Trendelenberg positioning.²⁸⁰

The change in ONSD related to a 'quick' change in ICP was studied in 18 ventilated, TBI patients. ONSD measurements were taken 30-60 seconds prior to suctioning, during suctioning and 30-60 seconds after suctioning of the endotracheal tube (ETT). ICP increased to > 20 mmHg in all patients during ETT suctioning, which was associated with an increase in the ONSD to > 5 mm, with both parameters returning to baseline after suctioning. Correlation between ONSD and ICP was good ($R^2 = 0.8$). An ONSD cut-off value of > 5.0 mm to detect ICP > 20 mmHg, demonstrated a sensitivity of 94%, specificity of 98%, confirming that ultrasonography of the ONSD is accurate to detect not only increased ICP but also immediate changes in ICP.²⁸¹

Aiming to describe the ONSD response to LP and its potential for detecting raised ICP Bauerle et al. studied 10 newly diagnosed patients with IIH, comparing the findings to 25 control patients. The study describes an optimal ONSD cut-off value of 5.8mm and a significant reduction in ONSD after LP.¹⁵⁶

Karakitsos and colleagues reported that patients with an OND measurement of > 5.9 mm (sensitivity of 74% and specificity of 65%) and a 2.5 mm increase in OND between repeated measurements (sensitivity of 81% and specificity of 70%) had a high probability to progress to brain tamponade and death. The mean admission OND measurement of 4.84 ± 1.2 mm in the brain injury patients was significantly higher than that found in the control group at 3.49 ± 1.1 mm ($p < 0.001$).²⁸² A recent case report also describing a decrease in ONSD measurement in a patient with idiopathic intracranial hypertension (IIH), used measurements 30 minutes prior to and 30 minutes after performing the LP. The opening and closing CSF pressures were measured via CSF manometry, demonstrating a 'real-time' reduction in ONSD, within 30 minutes of LP induced pressure changes.²⁸³

The only other description involving dynamic assessment of the ONS, uses Doppler sonography to assess blood flow. A novel and promising dynamic technique described by Querfurth et al²⁸⁴ involved color Doppler imaging to measure arterial pulsatility indices for both the OA and CRA. By combining an adaptation of the Balliart ophthalmodynamometer, the VOP measured by CRV occlusion was combined with the arterial pulsatility indices to create an empiric index using venous and arterial parameters (VOP / Gosling Pulsatility Index [GPI]), which correlated better with absolute ICP ($r = 0.95$, $p < 0.005$, $ICP = 0.29 + 0.74 [VOP/ GPI (OA)]$) than either parameter alone. Studies by the same group described ocular hemodynamics, using colour Doppler sonography to measure blood flow velocity and resistance indices in the OA, CRA and vODM and demonstrated a good relationship with actual ICP at mild to moderately elevated levels.^{285,286}

Using spectral Doppler imaging to determine the blood flow velocity in the CRA and CRV, Miller and co-workers demonstrated a reduction in these parameters in children with elevated ICP.²⁸⁷

Data on this technique in children is quite sparse, as most studies evaluating the dynamic orbital and optic nerve blood flow using colour Doppler have been described in the context of diabetic retinopathy and other vascular eye disease.^{288,289}

A very promising study performed in patients with glaucoma, evaluated the relationship between ONSD and retrobulbar blood flow velocity using colour Doppler imaging (CDI). The authors demonstrated that there was a negative correlation between ONSD and retrobulbar flow velocities in glaucoma patients but not in healthy patients, concluding that the pressures determining the ONSD can have a significant impact on ocular blood flow. This study makes an interesting comment regarding the elasticity of the ONS and its potential effect on the ONSD and ocular blood flow.²⁹²

Summary – available literature describing dynamic assessment of the ONSD

Change in ONSD measurements performed before and after interventions including hyperventilation, drainage of CSF, administration of mannitol , tracheal manipulation and LP appear to correlate well with the induced change in ICP.^{20,156,277,278,281,156} These reported changes in ONSD are useful in understanding the relationship between the ONS and ICP. The variability in the ONS response depending on the degree of ICP elevation, time of exposure and underlying elastic nature of the ONS described by Hansen, however, is still an important factor.^{50,68,154,252} The described techniques assessing dynamic ocular blood flow velocity using Doppler imaging are certainly promising,^{284-287,292} but as the authors acknowledge, still require validation in larger studies.

The use of a dynamic imaging technique to detect pulsatile motion of the ONS and subsequent variation in this motion has not been described before. The possibility that such a technique could allow us some insight into the elastic nature and response of the ONS and evaluate differences in this elasticity at high and low ICP states is a promising one. The final section of this work describes a novel technique for analysing the pulsatile motion of the ONS and its possible relationship with ICP.

7.2. Relationship between pulsatile dynamics of the optic nerve sheath and intracranial pressure: an exploratory in-vivo investigation

7.2.1. Introduction

The relationship between ICP and optic nerve sheath diameter (ONSD) has been described by several authors, but with varying accuracy.^{17,18,20,30,156,157} As discussed in the previous section of this work, the relationship between the ONSD and ICP in children is important, but may involve a number of confounding variables. In children, age above or below 1 year and patency of the AF play an important role in defining ONSD cut-off values. The elastic nature of the ONS however, remains a poorly understood factor in its response to changes in ICP.

The final part of this study describes a novel, dynamic imaging analysis aimed at evaluating the motion of the ONS. An increase in ICP resulting in CSF displacement and subsequent distension of the ONS may lead to increased stiffness of the sheath. Analyzing ONS dynamics may then provide information that is complementary to the static measurements of ONSD. The objective of this part of the study was therefore to develop a method for analyzing in-vivo dynamic properties of the ONS using transorbital ultrasound imaging, and to investigate a possible relationship with ICP. This work was based on the idea that cardiovascular pulsation, (i.e. caused directly by arterial pulsation, or transmission of pulsatility through the CSF) induced motion of the ONS. Hypothesizing that the ONS becomes stiffer with increasing ICP, it was suggested that the transverse motion (i.e. perpendicular to the ONS) was more equal on each side of the sheath with high ICP compared to normal ICP. This was quantified by the absolute difference between the transverse pulsatile displacements on the left (d_{Left}) and right (d_{Right}) side of the ONS, normalized by the sum of displacements. The value of this parameter indicates how much the ONS deforms during cardiovascular pulsation, and was therefore interpreted physically as a measure of deformability, and referred to as the *deformability index*. (Figure 7.1)

$$\Delta = \frac{|d_{Left} - d_{Right}|}{d_{Left} + d_{Right}}$$

Figure 7.1 Formula for defining the Deformability Index Δ

According to the hypothesis, since the ability to deform was inversely related to stiffness,^{297,298} this parameter was expected to be smaller in the group with ICP ≥ 20 mmHg when compared to the group with ICP < 20 mmHg.

7.2.2. Methodology

i. Patients

This was an exploratory research study, retrospectively analyzing data from 16 patients (age ≤ 14 years old) managed at the Red Cross War Memorial Children's Hospital (RCWMCH) (Cape Town, South Africa). This study was nested within the parent study evaluating the relationship between ONSD and invasively measured ICP, and formed part of a collaborative research initiative between the Department of Neurosurgery at the University of Cape Town (UCT) and The Foundation for Scientific and Industrial Research (SINTEF), Trondheim, Norway. Inclusion criteria were the same as described in the previous section of this work.

ii. Image acquisition

A single investigator experienced in the use of transorbital ultrasonography acquired ultrasound images from both eyes, using a 15 MHz linear array probe (L15-7io, Philips, Bothell, USA). All images were acquired after the patients were anaesthetised, intubated and being mechanically ventilated, prior to insertion of the invasive ICP monitor. The image acquisition technique was the same as for measurement of the ONSD described in the earlier section of this work. The acquired dynamic/video images ranged in length from 5 to 10 seconds per eye and were all acquired in the axial plane, for uniformity. The elbow of the investigators dominant arm was stabilised against the bed to further minimise movement during image acquisition. The machine settings were exactly the same as for the static image acquisition. Physiological parameters were recorded at the time of image acquisition as in the ONSD measurement technique. Ultrasound acquisition was performed when the haemodynamic parameters were stable. The image depth varied from 3 to 5 cm, and spatial image resolution from 0.06 to 0.11 mm per pixel. The temporal resolution varied from 40 to 56 frames per second.

iii. Image processing

The anonymised imaging data were then processed by the engineers at SINTEF, and the analysis was performed according to anatomical specification agreed upon by the neurosurgery and engineering team. The acquired images were then magnified to the required size to identify specific regions on either side of the ONS complex before image processing.(Figure 7.2) The objective of the image processing was to utilise the high temporal resolution of the ultrasound images for analyzing motion related to cardiovascular pulsation on each side of the ONS.

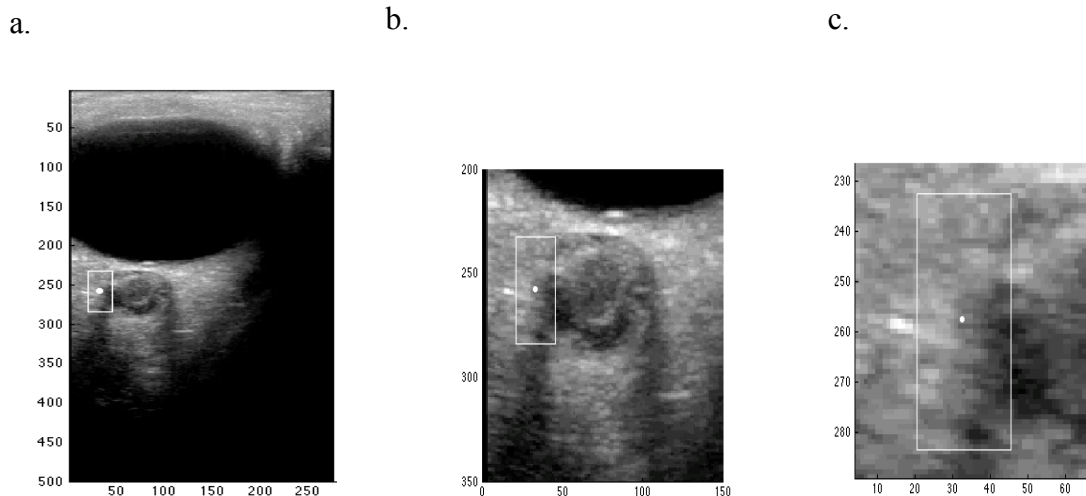


Figure 7.2 (a-c). Axial ultrasound image with different magnification.
 Gray-scale pattern, tracked from time frame to time frame.

1st step: Tracking

Tracking was initialized by manually selecting a point at similar depths on both sides of the ONS in the first frame of each image sequence. Cardiovascular pulsation causes a motion d_{Left} on the left side of the ONS and a motion d_{Right} on the right side of the ONS. Within a region of interest, the motion was automatically tracked over the entire sequence using normalized two-dimensional cross-correlation²⁹³ from frame to frame for a region of interest (25 by 61 pixels) around the selected points (Figure 7.3). The ultrasound data were interpolated, and parabolic approximation²⁹⁴ was applied to the correlation matrix for sub-pixel motion estimation. The motion component transverse to the nerve (i.e. in the horizontal image direction) was extracted for further analysis. Motion in this plane was used as it represented the plane in which the ONS expanded under conditions of raised ICP.

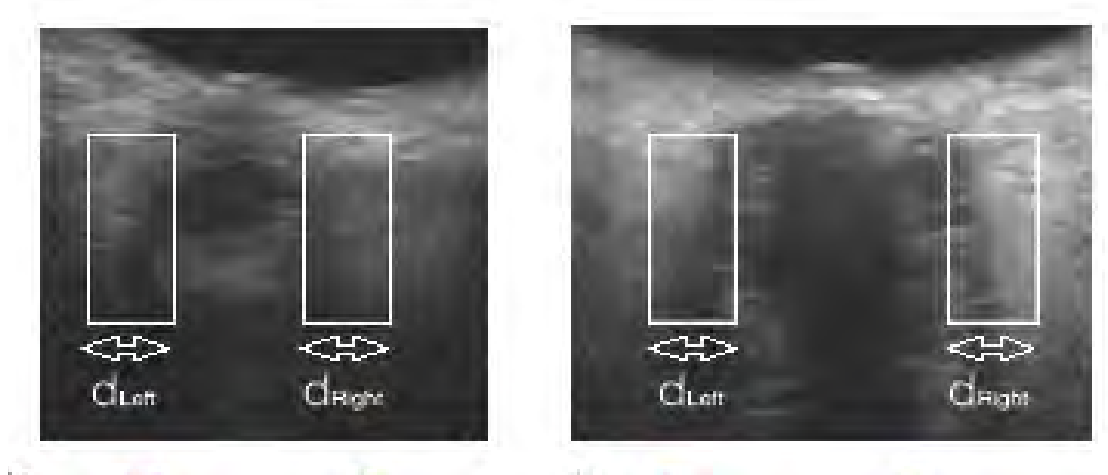


Figure 7.3. Transorbital ultrasound images magnified, demonstrating d_{Left} and d_{Right} .

Cardiovascular pulsation causes a motion d_{Left} on the left side of the ONS and a motion d_{Right} on the right side. The rectangles show the regions used for tracking the motion.

2nd step: Fourier analysis

To extract the motion that was related to the cardiovascular pulsation, Fourier analysis^{295,296} was applied to obtain the frequency components of the transverse motion. The amplitude of the (fundamental) frequency component corresponding to the pulse rate of each patient was extracted for the left and right side of the ONS in each dataset, yielding the transverse pulsatile displacements d_{Left} and d_{Right} , respectively (Figure 7.4 and Figure 7.5).

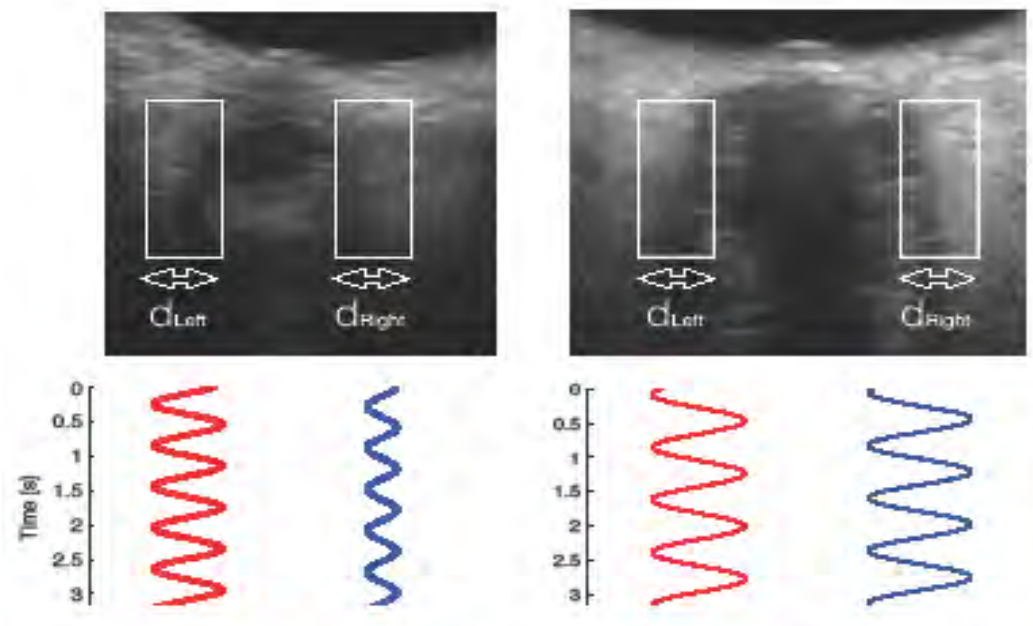


Figure 7.4. Illustration of the image processing, with a normal ($< 20 \text{ mmHg}$) (left) and a high ICP ($\geq 20 \text{ mmHg}$) patient (right). Transverse pulsatile displacements as a function of time (vertical axis) after extraction of the motion component corresponding to the fundamental heart rate frequency. Note that the curves are strongly zoomed in compared to the images in the upper row (the squares are 25 pixels wide, pulsation is approx. 0.1 pixel)

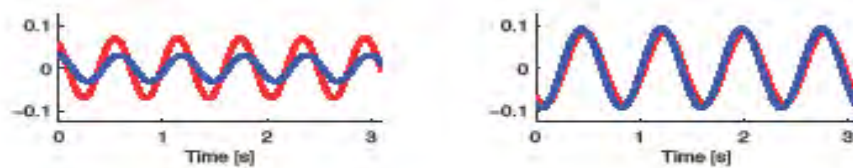


Figure 7.5. The same curves superimposed, with transverse pulsatile displacement along the vertical axis and time along the horizontal axis, ($ICP < 20 \text{ mmHg}$ on the left, and $ICP \geq 20 \text{ mmHg}$ on the right).

iv. Data analysis and statistics

Since the data were retrospectively analyzed, we expected some out-of-plane motion., Despite stabilising the arm during image acquisition, there was likely still some movement which caused this out-of-plane motion. This out-of plane motion is known to deteriorate correlation-based tracking.^{293,294} To address and compensate for this issue, each dataset was graded with regard to acquisition-based artefactual movement, by one blinded operator. The grading was performed on a scale from 0-2 as described below:

- Grade 0: steady acquisition, barely perceivable probe movement
- Grade 1: perceivable probe motion, no loss of ONS appearance
- Grade 2: distinct probe movement, with some loss of ONS appearance

The motion analysis was run five times for the left and five times for right side of the ONS, in both eyes for each dataset (appendix III). This was to account for variability due to the manual initialization of the tracking region. The mean of the five displacement values was used as the motion estimate, and the variation was quantified using pooled standard deviation.

Δ was calculated using equation (1), and one-sided Mann-Whitney U-test was used to statistically compare the two groups. Diagnostic accuracy was investigated using receiver operating characteristic (ROC) curves. The algorithm was then implemented in Matlab for analysis. (MathWorks, Natick, MA, USA).

7.2.3. Results

Sixteen patients were included in this analysis. The median age in the group with ICP < 20 mmHg was 45 months (IQR 9.5 – 83), and the median age in the group with ICP \geq 20 mmHg was 80 months (IQR 35.5 – 122) ($p = 0.3$). Demographic and physiological data are summarised in table 7.1.

Patient	Age (months)	Gender	Heart rate (bpm)	Diagnosis	ICP (mmHg)
A	120	M	78	Posterior fossa tumour (hydrocephalus)	28
B	116	F	103	Hydrocephalus	33
C	132	M	168	Trauma	32
D	33	M	117	Posterior fossa tumour (hydrocephalus)	37
E	24	F	92	Hemispherical tumour	20
F	124	F	112	Hydrocephalus	30
G	38	F	69	Hydrocephalus	26
H	44	M	134	Hydrocephalus	36
I	36	M	100	Tethered cord	10
J	9	M	150	Hydrocephalus	8
K	72	F	92	Chiari I malformation	5
L	54	M	102	Spinal dysraphism	10
M	144	M	80	Hydrocephalus	10
N	10	M	120	Hydrocephalus	11
O	8	M	130	Hydrocephalus	10
P	94	M	103	Trauma	10

Table 7.1. Patient data

A total of thirty two datasets were analysed from all sixteen patients initially, including those with out-of plane motion artefact.(Table 7.2) The transverse pulsatile displacement on each side of the ONS was assessed five times for each dataset (individual measurements included in appendix III). The mean value of transverse pulsatile displacement d_{Left} and d_{Right} of the ONS for both eyes yielded a value of 8.3 (SD 0.54), measured in percentage of a pixel.

Seven datasets were scored as grade 2 by the blinded operator and were subsequently excluded, leaving twenty five datasets for further analysis. The twenty five datasets were analysed according to ICP and divided into a group with $\text{ICP} \geq 20$ mmHg, and a group with $\text{ICP} < 20$ mmHg, comprising ten and fifteen datasets, respectively.(Table 7.3)

	Patient	Left eye			Right eye		
		d _{Left}	d _{Right}	Δ	d _{Left}	d _{Right}	Δ
Group with ICP \geq 20mmHg	A	8.12	8.99	0.05	7.34	1.55	0.65*
	B	7.76	8.75	0.06	9.88	9.23	0.03
	C	3.08	6.25	0.34*	2.73	3.42	0.11
	D	5.17	4.17	0.11	9.13	11.42	0.11
	E	15.37	13.58	0.06	13.74	17.44	0.12
	F	20.49	26.12	0.12	12.81	10.87	0.08
	G	4.78	11.23	0.40*	11.22	9.79	0.07
	H	6.76	5.37	0.11	3.51	5.97	0.26*
	I	5.65	3.16	0.28	2.52	3.78	0.20
	J	4.01	1.83	0.37	5.70	3.63	0.22
Group with ICP < 20 mmHg	K	13.68	8.38	0.24	7.22	3.04	0.41
	K	7.98	4.60	0.27	9.12	11.78	0.13
	M	17.47	10.64	0.24	13.84	12.23	0.06*
	N	5.20	3.62	0.18	1.52	5.69	0.58
	O	15.94	16.83	0.03*	8.15	3.96	0.35
	P	4.90	5.61	0.07*	5.52	10.32	0.30

Table 7.2. Results from analysis of all included datasets

Transverse pulsatile displacements d_{Left} and d_{Right} were measured in percentage of a pixel.

* Values that are wrongly classified using a cut-off value of 0.121.

The DI (Figure 7.1) of the ONS was then calculated for each dataset. The median DI was $\Delta = 0.11$ for the group with $ICP \geq 20$ mmHg, compared to $\Delta = 0.24$ for the group with $ICP < 20$ mmHg ($p = 0.002$, Mann-Whitney U-test). Fig 7.6 shows a boxplot illustrating the median and spread for each group.

	Patient	Left eye				Right eye			
		d _{Left}	d _{Right}	Δ	Grade	d _{Left}	d _{Right}	Δ	Grade
Group with ICP ≥ 20 mmHg	A	-	-	-	2	-	-	-	2
	B	7.76	8.75	0.06	1	9.88	9.23	0.03	1
	C	-	-	-	2	2.73	3.42	0.11	1
	D	5.17	4.17	0.11	1	-	-	-	2
	E	15.37	13.58	0.06	0	13.74	17.44	0.12	1
	F	20.49	26.12	0.12	1	-	-	-	2
	G	-	-	-	2	11.22	9.79	0.07	1
	H	6.76	5.37	0.11	1	3.51	5.97	0.26*	0
	I	5.65	3.16	0.28	0	2.52	3.78	0.20	0
	J	4.01	1.83	0.37	1	5.70	3.63	0.22	0
Group with ICP < 20 mmHg	K	13.68	8.38	0.24	1	7.22	3.04	0.41	0
	L	7.98	4.60	0.27	1	9.12	11.78	0.13	0
	M	17.47	10.64	0.24	0	-	-	-	2
	N	5.20	3.62	0.18	0	1.52	5.69	0.58	1
	O	15.94	16.83	0.03*	1	8.15	3.96	0.35	0
	P	4.90	5.61	0.07*	0	5.52	10.32	0.30	1

Table 7.3. Results from analysis where datasets with out-of-plane motion (grade 2) were excluded

Transverse pulsatile displacements d_{Left} and d_{Right} were measured in percentage of a pixel.

* Values that are wrongly classified using a cut-off value of 0.121.

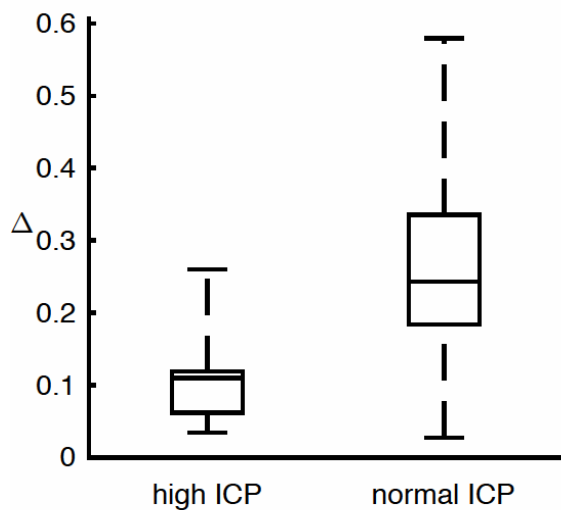


Figure 7.6. Box and whisker plot: DI in ICP ≥ 20 mmHg (high ICP) and < 20 mmHg (normal ICP).

Choosing a cut-off value of $\Delta = 0.121$ demonstrated a sensitivity of 90% and a specificity of 87%. AUROC was 0.85 (95% CI: 0.61- 0.97). Three out of twenty five (12%) datasets would be wrongly classified using this cut-off value.(Figure 7.7)

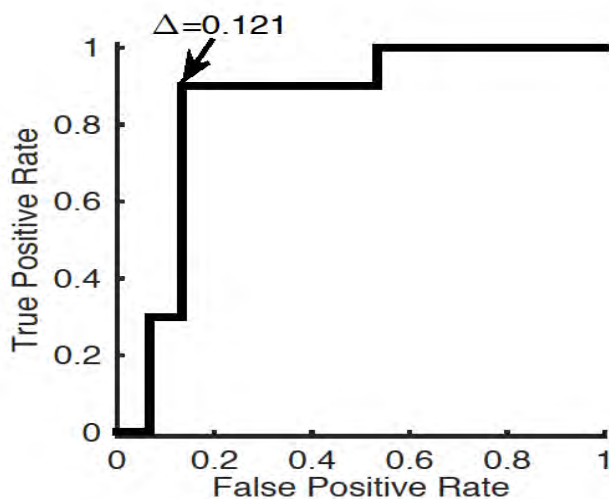


Figure 7.7. Receiver operator curve for a cut-off value of $\Delta = 0.121$. Demonstrated a sensitivity of 90%, a specificity of 87% and an AUC of 0.85.

7.2.4. Discussion

The hypothesis of this study was that increased ICP leads to increased stiffness (i.e. reduced deformability) of the ONS. The aim of this study was therefore to develop a method for analyzing the pulsatile dynamic properties of the ONS as a marker of sheath stiffness, using transorbital ultrasound imaging, and to further investigate a possible relationship with ICP. The DI was formulated as an index to quantify the measurable displacement of the ONS during the captured pulsatile dynamic imaging of the ONS. The arterial architecture and its variability within the ONS, described in chapter 2, played an important role in the decision to perform measurements on both the left and the right side of the ONS, and calculate the relative motion, resulting in formulation of the DI.

The most important finding of this study was the difference between the deformability of the ONS in the group with $ICP \geq 20$ mmHg compared to the group with $ICP < 20$ mmHg, thus clearly supporting the hypothesis. ROC analysis demonstrated an AUC of 0.85, and suggested a cut-off value of $\Delta = 0.121$, with lower values indicating ICP mmHg and higher values indicating ICP < 20 mmHg in this study.

The main limitations of this study were the relatively small number of patients, and the fact that the analysis was performed retrospectively and not in a blinded fashion. The paediatric cohort examined may warrant further validation of the technique in an adult study population. Further, although an exploratory research design was suitable for providing insight into the unknown relation between ONS motion and ICP, this may limit the ability to draw definite conclusions. Notwithstanding these limitations, the difference between the two groups in this study appears convincing. These are however preliminary data and care should be taken not to overestimate the value for patient-specific diagnosis.

It has been shown previously that the retrobulbar segment of the ONS is distensible and therefore dilates when ICP is increased.^{28,46,50,56} The technique of ONSD measurement has gained steady support as a non-invasive surrogate marker of raised ICP.¹⁶⁻³⁴ However, measurement of the ONSD alone has not yet provided a completely accurate assessment of ICP, largely because the described optimal cut-off value for ONSD measurement in patients has varied considerably.^{23,28-33,157,261} Data from SECTION C of this study supported the use of ONSD as a marker of raised ICP in children, but the described

variability in diagnostic accuracy underscores the need to explore the dynamic nature of the ONS. The noted variation in ONSD between studies is likely due to a more complex relationship between the ONS and ICP.^{154,252} The magnitude of ONS distension caused by the increase in pressure within the subarachnoid space may depend on a variety of factors, including the degree to which ICP is increased, the rapidity of the increase in ICP and the elastic characteristics of the ONS, all of which influence the capability for distension and retraction of the ONS.²⁵² The relationship between ICP and nerve sheath distension is therefore integrally related to the stiffness of the sheath itself.

This study investigated how pulsatile forces deform the ONS dynamically during the cardiac cycle, rather than the absolute distention related to the increased pressure within the ONS. This approach may contribute to an overall improvement in assessing the ONS in cases of suspected increased ICP, either as an individual marker or by augmenting the interpretation of ONSD measurements. The concept of pulsatile dynamics of the ONS could also improve specificity when compared to ONSD measurement alone, by differentiating between pathological distension of the ONS due to raised ICP and a widened ONS not related to raised ICP.

Since the data were retrospectively analyzed, image acquisition was not optimized with respect to avoiding out-of-plane motion, which may deteriorate correlation-based tracking. To investigate the effect of the out-of-plane motion, we also processed the excluded datasets. We found that if all datasets were included (Table 7.2) the median of the group with ICP \geq 20 mmHg and the group with ICP $<$ 20 mmHg would still be significantly different ($p = 0.03$). However, the AUC would be reduced to 0.69 (95% CI: 0.46-0.87), and 7 out of 32 datasets (22%) would have been wrongly classified. The example in Fig 7.8, shows the influence of out-of-plane motion for the (excluded) right eye dataset of patient A. In this dataset, a clear out-of-plane motion occurs at approximately 3 seconds into the sequence. An option for this dataset might therefore be to constrain the analysis to the period from 4 to 10 seconds. Instead, we chose to let one blinded operator grade the datasets, and exclude those interpreted to have extensive out-of-plane motion (grade 2). Although improving the quality of the study, the grading is to some extent subjective, with no definite cut-off. Indeed, some out-of-plane motion could still be seen in some of the remaining images (grade 1), and might therefore still be an

explanation to why the approach failed for some of the remaining datasets (12%). The possibility of minimizing out-of-plane motion by further stabilisation of the image acquisition technique should be taken into account in protocols for future studies.

Also, the calculated displacements were small, and extracted by extensive spatial (region of interest window) and temporal (Fourier) averaging. Accuracy, reproducibility and possible technical refinements of this novel ultrasound processing method should be further studied. Finally, it could be of interest to consider additional information, e.g. longitudinal motion, phase content of the Fourier transform (i.e. delay between motion at left and right side of the nerve) and perhaps other motion components than the fundamental heart rate frequency.

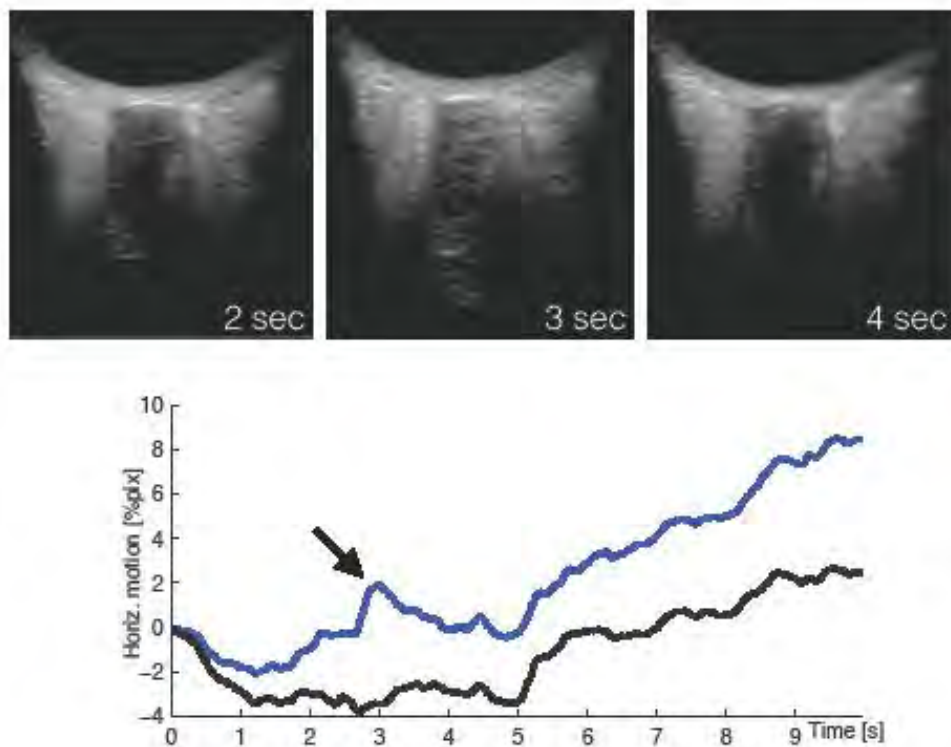


Figure 7.8. Illustrating the effect of out-of-plane motion (patient A, right eye)

The upper row in Figure 7.8. shows the ultrasound image sequence at 2, 3 and 4 seconds into the sequence. The appearance of the ONS at 3 seconds is clearly different compared with the appearance at 2 and 4 seconds, thus scoring an out-of-plane motion grade 2 (and hence excluded from the analysis). Lower: transverse motion on left (blue line) and right side (black) of the ONS (before extraction of the heart rate frequency component). At approximately 3 seconds, the processing method interpreted the out-of-plane motion as if the left side had a large pulsatile motion, with duration approximately the same as the heart cycle (78 bpm, i.e. 0.77 second period). The analysis therefore failed for this dataset.

7.2.5. Conclusion

This study illustrates the feasibility of non-invasive transorbital ultrasound for assessing optic nerve sheath pulsatile dynamics. The preliminary results demonstrate a significant difference between patient groups with $ICP \geq 20$ mmHg versus those with $ICP < 20$ mmHg, and thus support the suggested hypothesis of a relationship between deformability of the ONS and ICP. The suggested measure may therefore be relevant as a non-invasive marker of raised ICP and contribute to our understanding of the ONS response to changes in ICP. Further validation of this technique in prospective, blinded studies would be helpful.

SECTION D

Chapter 8. Perspective and future direction

The use of transorbital ultrasound measurement of the ONSD as a surrogate marker of ICP is certainly an elegant technique. The major shortcoming in children is the lack of consensus regarding age appropriate cut-off values, mostly due to the lack of studies comparing ONSD to directly measured ICP. This work has specifically addressed this shortfall in the literature by comparing these two parameters. The finding that age at 1 year is a more appropriate age at which to define different ONSD cut-off values, is important as it demonstrates that there are a different set of values best suited to patients before and after a certain threshold. The previously described age categories of >1 to ≤ 4 years and above 4 years of age, were found to be of less clinical value in this study. This finding may serve to clarify this discordance in the literature. This study also described the best diagnostic accuracy for a range of appropriate ICP thresholds which, in children may be of specific benefit.

Compliance of the skull differs significantly in patients with an open AF compared to those where the AF has closed. This physiological concept, well described by the Monroe-Kellie doctrine served as the basis for evaluating use of the AF as a more reliable clinical marker for defining different ONSD cut-off values in children. Using patency of the AF for describing ONSD cut-off values in children was a further recommendation of this study.

All current published work assessing the ONS as a marker of ICP, have been based on static measurements of the ONSD. These measurements have generally demonstrated a strong relationship with ICP and change in ICP, though the diagnostic accuracy for detecting raised ICP has varied considerably. The reasons for this variability have been described and some of these issues in children have been addressed in this study. The limited specificity of this technique has been suggested as a factor preventing its widespread use.

Analysis of the pulsatile dynamic response of the ONS as a marker of its stiffness in states of normal and raised ICP has not been described before. The dynamic analysis in the final part of this work uses relative motion on both sides of the ONS, referred to as the DI, to describe the pulsatile motion of the ONS. This index has potential to improve our overall understanding of the ONS as a marker of ICP, and possibly improve the accuracy of this technique by differentiating a widened ONSD that is a normal variant from one that is due to raised ICP, based on the stiffness of the ONS.

Future work will involve testing the validity of the DI in a larger prospective, blinded study. This study should ideally include adult and paediatric patients and should allow analysis over a spectrum of normal and raised ICP values. The value of a laboratory-based study, using cadaver models to evaluate the ONS response and test the dynamic parameters described in this study would be an ideal scientific environment.

Use of a combination of appropriate non-invasive techniques is an appealing option to potentially improve their diagnostic accuracy. In this light, future planned work involves combining the measurement of the ONSD, with other features detectable on transorbital ultrasound, especially bulge of the optic nerve head (described in raised ICP)^{238,255} and measurement of the optic nerve diameter (OND) to try and better define the physiological and morphological changes in the ONS during increases in ICP. Combining the dynamic assessment technique described in this work with standard ONSD and possibly with Doppler flow assessment of the ocular vessels^{285,286} may improve the accuracy of this promising diagnostic technique. The use of three dimensional imaging of the ONS is an interesting option which may in time help to better delineate the ONS.^{290,291} The option of measuring the IOP and interpreting this together with data from the ONS may also serve to provide a more holistic picture of the effect that raised ICP has on the ONS complex. The value of repeat ONSD measurement in individual patients, before and after treatment may also serve to provide reference ranges for individual patients which would make it more applicable in monitoring certain groups of patients, especially those with V/P shunts.²³⁴

The eye and its ONS complex, apart from its primary role as an organ of vision, can also provide valuable information about ICP, and the search to better understand and interpret

the changes that occur in this anatomical structure during changes in ICP remains a fascinating avenue of research.

Appendices

Appendix I

Strobe checklist

STROBE Statement—checklist of items that should be included in reports of observational studies

	Item No	Recommendation
Title and abstract	1	<p>(a) Indicate the study's design with a commonly used term in the title or the abstract</p> <p>(b) Provide in the abstract an informative and balanced summary of what was done and what was found</p>
Introduction		
Background/rationale	2	Explain the scientific background and rationale for the investigation being reported
Objectives	3	State specific objectives, including any prespecified hypotheses
Methods		
Study design	4	Present key elements of study design early in the paper
Setting	5	Describe the setting, locations, and relevant dates, including periods of recruitment, exposure, follow-up, and data collection
Participants	6	<p>(a) <i>Cohort study</i>—Give the eligibility criteria, and the sources and methods of selection of participants. Describe methods of follow-up</p> <p><i>Case-control study</i>—Give the eligibility criteria, and the sources and methods of case ascertainment and control selection. Give the rationale for the choice of cases and controls</p> <p><i>Cross-sectional study</i>—Give the eligibility criteria, and the sources and methods of selection of participants</p> <p>(b) <i>Cohort study</i>—For matched studies, give matching criteria and number of exposed and unexposed</p> <p><i>Case-control study</i>—For matched studies, give matching criteria and the number of controls per case</p>
Variables	7	Clearly define all outcomes, exposures, predictors, potential confounders, and effect modifiers. Give diagnostic criteria, if applicable
Data sources/ measurement	8*	For each variable of interest, give sources of data and details of methods of assessment (measurement). Describe comparability of assessment methods if there is more than one group
Bias	9	Describe any efforts to address potential sources of bias
Study size	10	Explain how the study size was arrived at
Quantitative variables	11	Explain how quantitative variables were handled in the analyses. If applicable, describe which groupings were chosen and why
Statistical methods	12	<p>(a) Describe all statistical methods, including those used to control for confounding</p> <p>(b) Describe any methods used to examine subgroups and interactions</p> <p>(c) Explain how missing data were addressed</p> <p>(d) <i>Cohort study</i>—If applicable, explain how loss to follow-up was addressed</p> <p><i>Case-control study</i>—If applicable, explain how matching of cases and controls was addressed</p> <p><i>Cross-sectional study</i>—If applicable, describe analytical methods taking account of sampling strategy</p>

Results		
Participants	13*	<p>(a) Report numbers of individuals at each stage of study—eg numbers potentially eligible, examined for eligibility, confirmed eligible, included in the study, completing follow-up, and analysed</p> <hr/> <p>(b) Give reasons for non-participation at each stage</p> <hr/> <p>(c) Consider use of a flow diagram</p>
Descriptive data	14*	<p>(a) Give characteristics of study participants (eg demographic, clinical, social) and information on exposures and potential confounders</p> <hr/> <p>(b) Indicate number of participants with missing data for each variable of interest</p> <hr/> <p>(c) <i>Cohort study</i>—Summarise follow-up time (eg, average and total amount)</p>
Outcome data	15*	<p><i>Cohort study</i>—Report numbers of outcome events or summary measures over time</p> <hr/> <p><i>Case-control study</i>—Report numbers in each exposure category, or summary measures of exposure</p> <hr/> <p><i>Cross-sectional study</i>—Report numbers of outcome events or summary measures</p>
Main results	16	<p>(a) Give unadjusted estimates and, if applicable, confounder-adjusted estimates and their precision (eg, 95% confidence interval). Make clear which confounders were adjusted for and why they were included</p> <hr/> <p>(b) Report category boundaries when continuous variables were categorized</p> <hr/> <p>(c) If relevant, consider translating estimates of relative risk into absolute risk for a meaningful time period</p>
Other analyses	17	Report other analyses done—eg analyses of subgroups and interactions, and sensitivity analyses
Discussion		
Key results	18	Summarise key results with reference to study objectives
Limitations	19	Discuss limitations of the study, taking into account sources of potential bias or imprecision. Discuss both direction and magnitude of any potential bias

Interpretation	20	Give a cautious overall interpretation of results considering objectives, limitations, multiplicity of analyses, results from similar studies, and other relevant evidence
----------------	----	--

Generalisability	21	Discuss the generalisability (external validity) of the study results
------------------	----	---

Other information

Funding	22	Give the source of funding and the role of the funders for the present study and, if applicable, for the original study on which the present article is based
---------	----	---

Appendix II

Details of analysis in age categories 1 to 4 years old and above 4 year old

i. Children aged 1 to 4 years old (> 1 and ≤ 4 years old)

i) ONSD for ICP dichotomised at 20 mmHg

Thirty nine children were > 1 and ≤ 4 years old, the median age in this group was 23 months (IQR 17 - 35). Sixteen patients had an ICP < 20 mmHg, with a mean ICP reading of 13.75 mmHg (SD 4.34), and twenty three patients had an ICP ≥ 20 mmHg, with a mean reading of 22.91 mmHg (SD 3.77) (Table IIa). The correlation between ONSD and ICP in this age group was good ($r = 0.65$, $p < 0.001$, PCC) (Figure IIa).

ICP in mmHg	N (%)	Median age in months (IQR)	Mean ICP in mmHg (SD)	Mean ONSD in mm (SD)
Overall	39	23 (17 – 35)	19.15 (6.04)	5.94 (0.6)
< 20 mmHg	16 (41%)	22.5 (16.5 – 34.5)	13.75 (4.3)	5.43 (0.6)
≥ 20 mmHg	23 (59%)	23 (18 – 35)	22.91 (3.8)	6.29 (0.4)
p – value		$p = 0.95$	$p < 0.001$	$p < 0.001$

Table IIa. Age, ICP and ONSD values for ICP dichotomised at 20 mmHg in patients aged > 1 and ≤ 4 years old

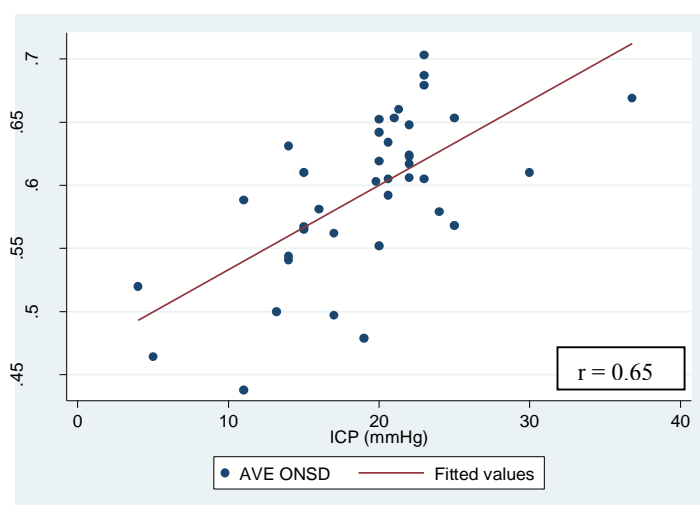


Figure IIa. Scatterplot for ONSD against ICP in patients aged > 1 and ≤ 4 years old.

The mean ONSD in the group with ICP < 20 mmHg was 5.43 mm (SD 0.6), and in the group with ICP \geq 20 mmHg, was 6.29 mm (SD 0.4) ($p < 0.001$) (Figure IIb).

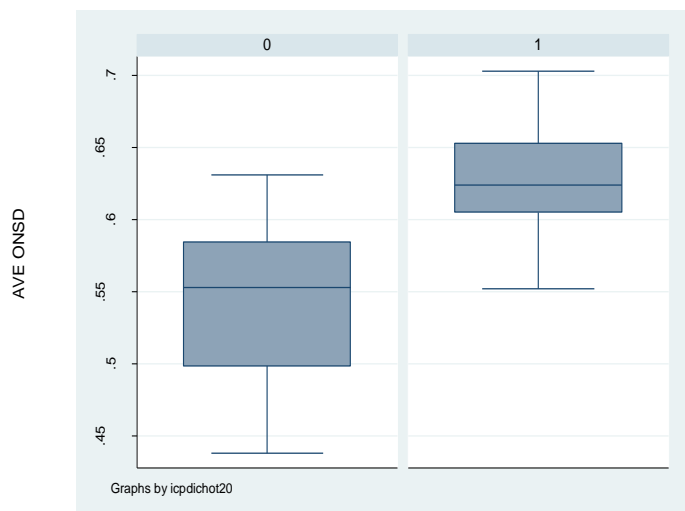


Figure IIb. Box and whisker plot of ONSD for ICP < 20 mmHg (0) and ICP \geq 20 mmHg (1) in patients aged > 1 and \leq 4 years old

In this age group, the optimal ONSD for predicting an ICP \geq 20 mmHg was 5.92 mm, with a sensitivity of 82.6%, specificity of 81.3%, PPV of 86.4%, NPV of 76.5%. The AUROC was 0.82 (Figure IIc), with an OR of 20.6 (Table 6.23)

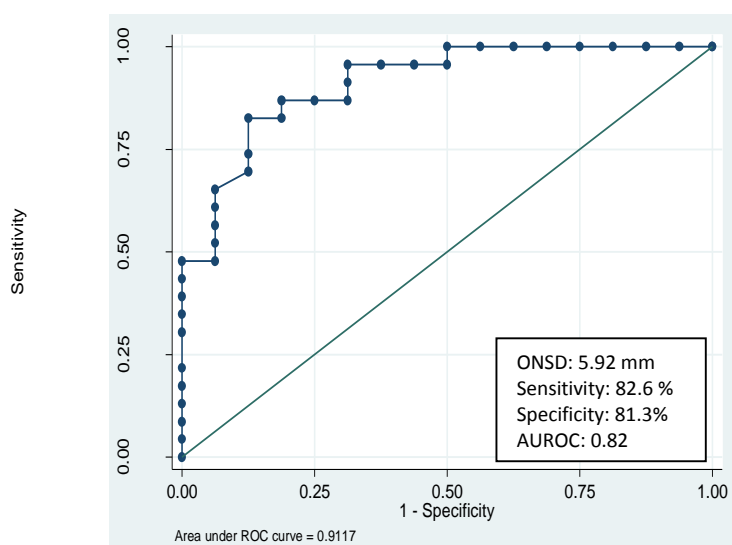


Figure IIc. AUROC for ONSD to detect ICP \geq 20 mmHg in patients aged > 1 and \leq 4 years old

ii) ONSD for ICP dichotomised at 15 mmHg

There were thirty nine children in this group, eight had an ICP < 15 mmHg and thirty one had an ICP \geq 15 mmHg. The data and comparative p –values are summarised in table IIb.

ICP in mmHg	N (%)	Median age in months (IQR)	Mean ICP in mmHg (SD)	Mean ONSD in mm (SD)
Overall	39	23 (17 – 35)	19.15 (6.04)	5.94 (0.6)
< 15 mmHg	8 (20.5)	25.5 (16.5 – 43)	10.78 (4.1)	5.28 (0.6)
\geq 15 mmHg	31 (79.5)	23 (18 – 34)	21.31 (4.3)	6.11 (0.5)
p – value		p = 0.47	p < 0.001	p = 0.006

Table IIb. Age, ICP and ONSD values for ICP dichotomised at 15 mmHg in patients aged > 1 and \leq 4 years old

The optimal ONSD cut-off value for detecting ICP \geq 15 mmHg in this age group was 5.52 mm, with a sensitivity of 90.3%, specificity of 75% and an OR of 28 (Table II).

iii) ONSD for ICP dichotomised at 10 mmHg

Of the thirty nine children in this group, two had an ICP < 10 mmHg and thirty seven had an ICP \geq 10 mmHg. The data and comparative p – values are summarised in table IIc.

ICP in mmHg	N (%)	Median age in months (IQR)	Mean ICP in mmHg (SD)	Mean ONSD in mm (SD)
Overall	39	23 (17 – 35)	19.15 (6.04)	5.94 (0.6)
< 10 mmHg	2 (5)	43 (42 – 44)	4.5 (0.7)	4.92 (0.4)
\geq 10 mmHg	37 (95)	23 (17 – 34)	19.94 (5.1)	6 (0.6)
p – value		p = 0.03	p = 0.002	p = 0.017

Table IIc. Age, ICP and ONSD values for ICP dichotomised at 10 mmHg in patients aged > 1 and ≤ 4 years old

The optimal ONSD cut-off value for predicting an ICP \geq 10 mmHg in this age group was 5.41 mm, with a sensitivity of 86.5% and a specificity of 100%. The OR was not defined (Table 6.23).

iv) ONSD for ICP dichotomised at 5 mmHg

One patient in this age group had an ICP < 5 mmHg, with a reading of 4 mmHg. Thirty eight patients had an ICP \geq 5 mmHg, with a mean ICP reading of 19.55 mmHg (SD 5.6) (Table IIId).

ICP in mmHg	N (%)	Median age in months (IQR)	Mean ICP in mmHg (SD)	Mean ONSD in mm (SD)
Overall	39	23 (17 – 35)	19.15 (6.04)	5.94 (0.6)
< 5 mmHg	1 (2.5)	42	4	5.2
\geq 5 mmHg	38	23 (17 – 34)	19.55 (5.6)	5.96 (0.6)

Table IIId. Age, ICP and ONSD values for ICP dichotomised at 5 mmHg in patients aged > 1 and ≤ 4 years old

The ONSD measurement for the patient with ICP < 5 mmHg was 5.2 mm. The mean reading in the group with ICP \geq 5 mmHg was 5.96 mm (SD 0.6). The optimal ONSD

cut-off value for predicting an ICP ≥ 5 mmHg was 5.2 mm, with a sensitivity of 86.8% and specificity of 100% (Table IIe).

ICP (mmHg)	ONSD cut-off (mm)	Sensitivity% (95%CI)	Specificity % (95%CI)	PPV % (95%CI)	NPV % (95%CI)	AUROC (95%CI)	OR (95%CI)
≥ 20	5.94	82.6 (61.2-95)	81.3 (54.4-96)	86.4 (65.1-97.1)	76.5 (50.1-93.2)	0.82 (0.69-0.95)	20.6 (4.1-102)
≥ 15	5.5	90.3 (74.2-98)	75 (34.9-96.8)	93.3 (77.9-99.2)	66.7 (29.9-92.5)	0.83 (0.66-0.99)	28 (4.19-185)
≥ 10	5.4	86.5 (71.2-95.5)	100 (15.8-100)	100 (89.1-100)	28.6 (3.7-71)	0.93 (0.88-0.99)	Nil
≥ 5	5.2	86.8 (71.9-95.6)	100 (2.5-100)	100 (89.4-100)	16.7 (0.42 – 64.1)	0.93 (. - 1)	Nil

Table IIe. Relationship between various ICP thresholds and ONSD in patients aged > 1 and ≤ 4 years

c) Relationship between ONSD and ICP in children aged over 4 years (> 4 years old)

i) ONSD for ICP dichotomised at 20 mmHg

Seventy nine patients were aged over 4 years old, with a median age of 82 months (65 – 108). Thirty eight of these patients had an ICP < 20 mmHg with a mean ICP reading of 10.15 mmHg (SD 4.95) and 41 patients had an ICP \geq 20 mmHg, with a mean ICP reading of 24.74 mmHg (SD 4.6). (Table IIf) There was good correlation between ONSD and ICP in this group ($r = 0.71$, $p < 0.001$, PCC) (Figure IId).

ICP in mmHg	N (%)	Median age in months (IQR)	Mean ICP in mmHg (SD)	Mean ONSD in mm (SD)
Overall	79	82 (65 – 108)	17.72 (8.7)	5.9 (0.8)
< 20 mmHg	38 (48.1)	81.5 (63 – 107)	10.15 (5)	5.33 (0.6)
\geq 20 mmHg	41 (51.9)	87 (69 – 125)	24.74 (4.6)	6.43 (0.6)
p – value		p = 0.45	p < 0.001	p < 0.001

Table IIf. Age, ICP and ONSD values for ICP dichotomised at 20 mmHg in patients aged > 4 years

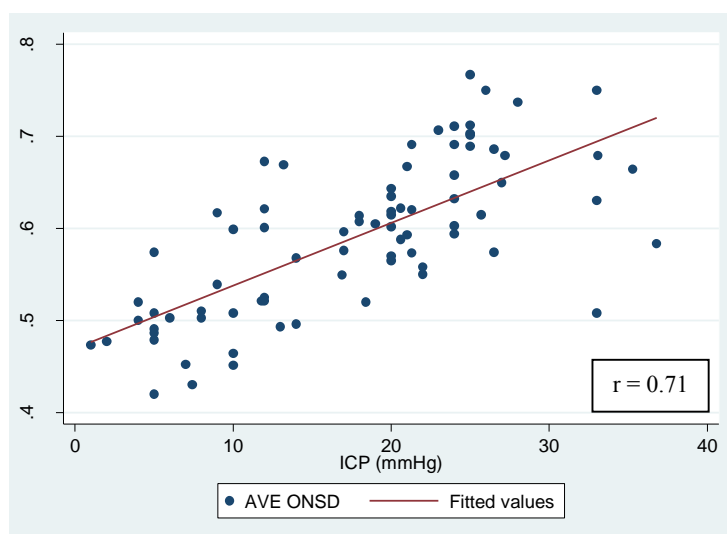


Figure IId. Scatterplot for ONSD against ICP in patients aged > 4 years.

The mean ONSD in the group with ICP < 20 mmHg was 5.33 mm (SD 0.6), and 6.43 mm (SD 0.6) in the group with ICP \geq 20 mmHg (Figure IIe).

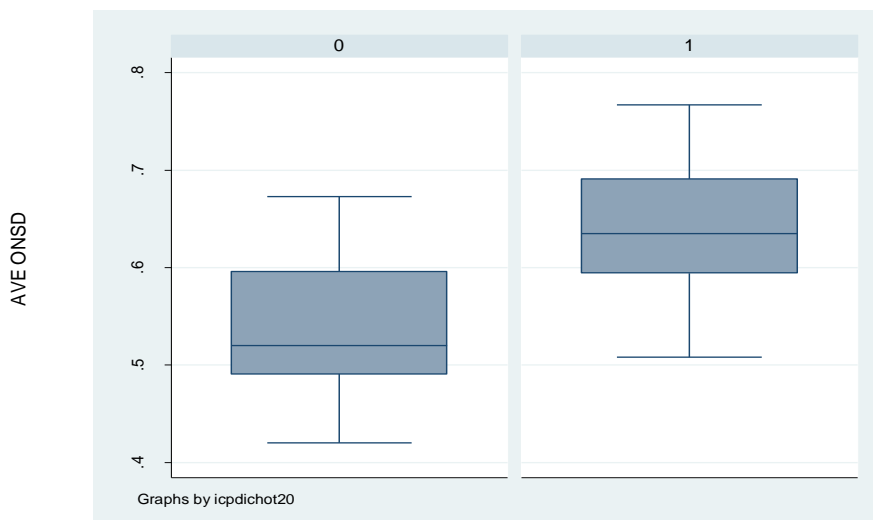


Figure IIe. Box and whisker plot of ONSD for ICP < 20 mmHg (0) and ICP \geq 20 mmHg (1) in patients aged > 4 years.

The optimal ONSD cut-off value for detecting ICP \geq 20 mmHg was 5.7 mm, with a sensitivity of 87.8%, specificity of 68.4%, PPV of 75%, NPV 83.9%. The AUROC was 0.78 (Figure IIj), with a diagnostic OR of 15.6 (Table IIj).

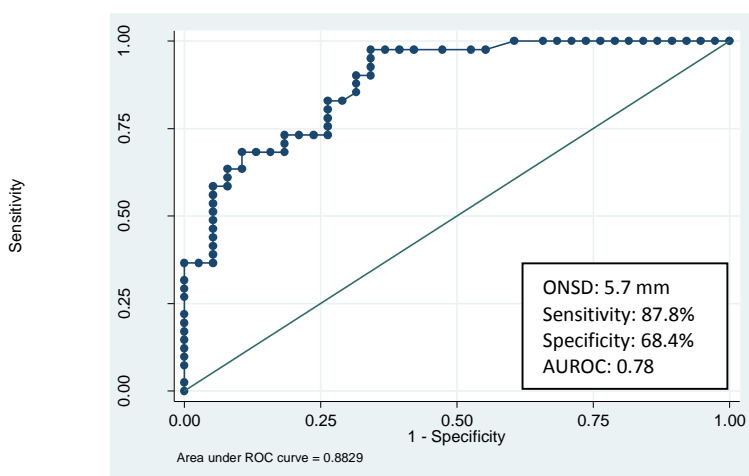


Figure IIj. AUROC for ONSD to detect ICP \geq 20 mmHg in patients aged > 4 years.

ii) ONSD for ICP dichotomised at 15 mmHg

Thirty one children had an ICP < 15 mmHg and forty eight children had an ICP \geq 15 mmHg, the results are summarised in table IIg.

ICP in mmHg	N (%)	Median age in months (IQR)	Mean ICP in mmHg (SD)	Mean ONSD in mm (SD)
Overall	79	82 (65 – 108)	17.72 (8.7)	5.9 (0.8)
< 15 mmHg	31 (39.2)	86 (63 -114)	8.43 (3.7)	5.22 (0.6)
\geq 15 mmHg	48 (60.8)	82 (68 – 107)	23.72 (4.9)	6.34 (0.6)
p – value		p = 0.96	p < 0.001	p < 0.001

Table IIg. Age, ICP and ONSD values for ICP dichotomised at 15 mmHg in patients aged > 4 years old

The optimal ONSD cut-off value for detecting ICP ≥ 15 mmHg in this group was 5.49 mm, with a sensitivity of 93.8%, specificity of 74.2% and a diagnostic OR of 43.1 (Table IIj).

iii) ONSD for ICP dichotomised at 10 mmHg

Seventeen children in this group had an ICP < 10 mmHg and sixty two children had an ICP ≥ 10 mmHg. The results are summarised in table IIIh.

ICP in mmHg	N (%)	Median age in months (IQR)	Mean ICP in mmHg (SD)	Mean ONSD in mm (SD)
Overall	79	82 (65 – 108)	17.72 (8.7)	5.9 (0.8)
< 10 mmHg	17 (21.5)	76 (57 – 116)	5.61 (2.3)	4.99 (0.5)
≥ 10 mmHg	62 (78.5)	89 (69 – 107)	21.04 (6.6)	6.15 (0.7)
p – value		p = 0.82	p < 0.001	p < 0.001

Table IIIh. Age, ICP and ONSD values for ICP dichotomised at 10 mmHg in patients aged > 4 years old

The optimal ONSD cut-off value for detecting ICP ≥ 10 mmHg was 5.2 mm, with a sensitivity of 88.7%, specificity of 82.4% and a diagnostic OR of 36.7 (Table IIj).

iv) ONSD for ICP dichotomised at 5 mmHg

Four children in this group had an ICP < 5 mmHg and seventy five children had an ICP ≥ 5 mmHg. The results are summarised in table II i

ICP in mmHg	N (%)	Median age in months (IQR)	Mean ICP in mmHg (SD)	Mean ONSD in mm (SD)
Overall	79	82 (65 – 108)	17.72 (8.7)	5.9 (0.8)
< 5 mmHg	4 (5.1)	109.5 (75.5 – 148.5)	2.75 (1.5)	4.93 (0.2)
≥ 5 mmHg	75 (94.9)	82 (65 – 107)	18.52 (8.2)	5.96 (0.8)
p - value		p = 0.19	p = 0.003	p = 0.01

Table Iii. Age, ICP and ONSD values for ICP dichotomised at 5 mmHg in patients aged > 4 years old

The optimal ONSD cut-off value for detecting ICP \geq 5 mmHg in this age group was 5 mm, with a sensitivity of 80%, specificity of 75%, PPV of 98.4%, NPV of 16.7%. The AUROC was 0.78 with a diagnostic OR of 12 (Table IIj).

ICP (mmHg)	ONSD cut-off (mm)	Sensitivity% (95%CI)	Specificity % (95%CI)	PPV % (95%CI)	NPV % (95%CI)	AUROC (95%CI)	OR (95%CI)
\geq 20	5.7	87.8 (73.8 – 95.9)	68.4 (51.3 – 82.5)	75 (60.4 – 86.4)	83.9 (66.3 – 94.5)	0.78 (0.69 – 0.87)	15.6 (5 – 48.2)
\geq 15	5.49	93.8 (82.8 – 98.7)	74.2 (55.4 – 88.1)	84.9 (72.4 – 93.3)	88.5 (69.8 – 97.6)	0.84 (0.75 – 0.93)	43.1 (10.9 – 167)
\geq 10	5.2	88.7 (78.1 – 95.3)	82.4 (56.6 – 96.2)	94.8 (85.6 – 98.9)	66.7 (43 – 85.4)	0.86 (0.75 – 0.96)	36.7 (8.8 – 150)
\geq 5	5	80 (69.2 – 88.4)	75 (19.4 – 99.4)	98.4 (91.2 – 100)	16.7 (3.6 – 41.1)	0.78 (0.53 – 1)	12 (1.6 – .)

Table IIj. ONSD cut-off values for various ICP thresholds in patients aged > 4 years

The ONSD cut-off values with the best diagnostic accuracy for detecting ICP at the selected thresholds, within each of the described age categories are summarised in below in Table IIIk.

ICP in mmHg	Age threshold (in years)	ONSD cut-off values (in mm)
≥ 20	Overall	5.5
	≤ 1	5.16
	$> 1 - \leq 4$	5.94
	> 4	5.7
≥ 15	Overall	5.3
	≤ 1	4.97
	$> 1 - \leq 4$	5.5
	> 4	5.49
≥ 10	Overall	5.04
	≤ 1	4.3
	$> 1 - \leq 4$	5.4
	> 4	5.2
≥ 5	Overall	5
	≤ 1	Nil
	$> 1 - \leq 4$	0.52
	> 4	0.5

Table 6.IIk. ONSD cut-off values for different ICP thresholds within the various age categories

Appendix III

Dynamic study: additional data

Individual measurements for motion D_{left} and D_{right} for the left eye:

		Left eye									
		Left side of ONS (d_{Left})					Right side of ONS (d_{Right})				
A		7.85	7.53	8.36	8.46	8.41	8.94	9.12	8.78	8.93	9.17
B		7.51	7.51	7.55	8.50	7.74	8.90	8.80	8.56	8.50	8.98
C		3.16	2.79	3.56	2.94	2.97	6.26	6.14	6.31	6.28	6.28
D		5.28	4.21	5.91	5.36	5.08	4.25	3.83	4.37	4.18	4.22
E		15.53	15.25	15.53	15.28	15.28	13.62	12.67	13.83	13.80	14.00
F		20.37	20.96	20.92	19.98	20.24	26.01	26.38	26.09	26.02	26.10
G		4.45	4.22	4.56	5.6	5.06	11.4	11.28	11.18	11.28	11.01
H		6.8	6.96	6.68	6.29	7.09	5.41	5.50	5.27	5.09	5.58
I		5.78	4.84	5.64	4.46	7.53	3.25	2.81	3.28	3.24	3.22
J		3.85	4.14	4.01	3.84	4.21	1.94	1.70	1.56	1.99	1.94
K		13.61	14.30	14.33	12.57	13.61	8.13	8.80	8.63	8.29	8.03
L		7.68	7.25	8.49	7.68	8.78	4.50	4.32	4.97	5.07	4.12
M		18.06	17.59	17.73	16.75	17.21	10.30	11.03	11.05	11.39	9.42
N		5.02	5.18	5.16	5.17	5.48	3.81	3.62	3.58	3.64	3.47
O		18.25	15.69	16.61	13.95	15.18	17.07	16.59	16.5	16.81	17.16
P		5.68	4.23	4.75	5.47	4.38	5.56	5.12	5.37	6.01	6.01

Individual measurements for motion D_{left} and D_{right} for the right eye:

		Right eye									
		Left side of ONS (d_{Left})					Right side of ONS (d_{Right})				
A		7.35	7.38	7.57	6.97	7.45	1.34	1.59	1.86	1.59	1.36
B		9.46	10.30	9.29	10.03	10.32	9.48	8.96	9.59	8.97	9.17
C		3.00	2.87	2.74	2.32	2.74	3.24	3.34	3.49	3.35	3.69
D		8.90	8.66	9.76	8.84	9.5	11.08	10.12	13.71	12.59	9.62
E		13.60	14.25	13.91	13.52	13.40	17.67	16.85	17.19	17.80	17.67
F		12.82	12.86	12.75	12.86	12.77	10.78	10.77	10.96	10.96	10.86
G		11.35	11.53	10.66	11.11	11.44	9.05	9.44	9.43	10.27	10.78
H		3.46	3.52	3.54	3.51	3.51	5.98	6.09	5.79	5.99	5.99
I		2.36	2.55	3.07	2.55	2.09	3.84	3.98	3.64	3.77	3.66
J		5.75	4.93	5.89	5.54	6.40	3.42	3.79	3.30	4.34	3.28
K		6.40	6.92	8.18	8.77	5.83	1.95	2.57	3.56	2.67	4.47
L		9.33	8.76	9.51	9.35	8.65	11.80	11.21	12.24	11.70	11.96
M		13.46	13.41	14.90	13.58	13.85	11.00	12.07	13.10	12.67	12.30
N		1.16	1.21	1.65	1.52	2.04	6.2	5.8	5.39	5.46	5.62
O		8.78	8.71	8.95	5.92	8.39	3.75	3.74	3.91	4.22	4.16
P		5.53	5.46	5.53	5.63	5.46	10.37	10.12	10.46	10.17	10.46

Reference list

- 1 Luerssen, TG. Intracranial pressure: Current status in monitoring and management. *Seminars in Pediatric Neurology*. 1997; 4(3): 146-155.
- 2 Wiegand C, Richards P. Measurement of intracranial pressure in children: a critical review of current methods. *Developmental Medicine and Child Neurology*. 2007; 49(12): 935-941.
- 3 Anderson RC, Kan P, Klimo P, Brockmeyer DL, Walker ML, Kestle JR. Complications of intracranial pressure monitoring in children with head trauma. *Journal of Neurosurgery: Pediatrics*. 2004; 101(2): 53-58.
- 4 Rosenberg JB, Shiloh AL, Savel RH, Eisen LA. Non-invasive methods of estimating intracranial pressure. *Neurocritical Care*. 2011; 15(3): 599-608.
- 5 Harvey CJ, Pilcher JM, Eckersley RJ, Blomley MJ, Cosgrove DO. Advances in ultrasound. *Clinical Radiology*. 2002; 57(3): 157-177.
- 6 Newman PG, Rozycki GS. The history of ultrasound. *Surgical clinics of North America*. 1998; 78(2): 179-195.
- 7 Chandler WF, Knake JE, McGillicuddy JE, Lillehei KO, Silver TM. Intraoperative use of real-time ultrasonography in neurosurgery. *Journal of Neurosurgery*. 1982; 57(2): 157-163.

- 8 Comeau RM, Sadikot AF, Fenster A, Peters TM. Intraoperative ultrasound for guidance and tissue shift correction in image-guided neurosurgery. *Medical Physics*. 2000; 27(4): 787-800.
- 9 Sosna J, Barth MM, Kruskal JB, Kane RA. Intraoperative sonography for neurosurgery. *Journal of Ultrasound in Medicine*. 2005; 24(12): 1671-1682.
- 10 Sutcliffe JC. The value of intraoperative ultrasound in neurosurgery. *British Journal of Neurosurgery*. 1991; 5(2): 169-178.
- 11 Ivanov M, Wilkins S, Poata I, Brodbelt A. Intraoperative ultrasound in neurosurgery—a practical guide. *British Journal of Neurosurgery*. 2010; 24(5): 510-517.
- 12 Slovis TL, Kuhns LR. Real-time sonography of the brain through the anterior fontanelle. *American Journal of Roentgenology*. 1981; 136(2): 277-286.
- 13 Leijser LM, de Vries LS, Cowan F.M. Using cerebral ultrasound effectively in the newborn infant. *Early human development*. 2006; 82(12): 827-835.
- 14 Foster P, Khaw KT. The eye: window to the soul or a mirror of systemic health? *Heart*. 2009; 95(5): 348-349.
- 15 London A, Benhar I, Schwartz M. The retina as a window to the brain—from eye research to CNS disorders. *Nature Reviews Neurology*. 2013; 9(1): 44-53

- 16 Geeraerts T, Launey Y, Martin L, et al. Ultrasonography of the optic nerve sheath may be useful for detecting raised intracranial pressure after severe brain injury. *Intensive Care Medicine*. 2007; 33(10): 1704-1711.
- 17 Geeraerts T, Duranteau J, Benhamou D. Ocular sonography in patients with raised intracranial pressure: the papilloedema revisited. *Critical Care*. 2008; 12(3): 150.
- 18 Rajajee V, Vanaman M, Fletcher JJ, Jacobs TL. Optic nerve ultrasound for the detection of raised intracranial pressure. *Neurocritical Care*. 2011; 15(3): 506-515.
- 19 Soldatos T, Karakitsos D, Chatzimichail K, Papathanasiou M, Gouliamos A, Karabinis A. Optic nerve sonography in the diagnostic evaluation of adult brain injury. *Critical Care*. 2008; 12(3): R67.
- 20 Moretti R, Pizzi B, Cassini F, Vivaldi N. Reliability of optic nerve ultrasound for the evaluation of patients with spontaneous intracranial hemorrhage. *Neurocritical Care*. 2009; 11(3): 406-410.
- 21 Blaivas M, Theodoro D, Sierzenski PR. A study of bedside ocular ultrasonography in the emergency department. *Academic Emergency Medicine*. 2002; 9(8): 791-799.
- 22 Girisgin AS, Kalkan E, Kocak S, Cander B, Gul M, Semiz M. The role of optic nerve ultrasonography in the diagnosis of elevated intracranial pressure. *Emergency Medicine Journal*. 2007; 24(4): 251-254.

- 23 Tayal VS, Neulander M, Norton HJ, Foster T, Saunders T, Blaivas M. Emergency department sonographic measurement of optic nerve sheath diameter to detect findings of increased intracranial pressure in adult head injury patients. *Annals of Emergency Medicine*. 2007; 49(4): 508-514.
- 24 Goel RS, Goyal NK, Dharap SB, Kumar M, Gore MA. Utility of optic nerve ultrasonography in head injury. *Injury*. 2008; 39(5): 519-524.
- 25 Major R, Girling S, Boyle A. Ultrasound measurement of optic nerve sheath diameter in patients with a clinical suspicion of raised intracranial pressure. *Emergency Medicine Journal*. 2011; 28(8): 679-81.
- 26 Školoudík D, Herzig R, Fadrná T, et al. Distal enlargement of the optic nerve sheath in the hyperacute stage of intracerebral haemorrhage. *British Journal of Ophthalmology*. 2010; 95(2) pp.217.
- 27 Bäuerle J, Lochner P, Kaps M, Nedelmann M. Intra- and inter-observer reliability of sonographic assessment of the optic nerve sheath diameter in healthy adults. *Journal of Neuroimaging*. 2012; 22(1): 42-45.
- 28 Helmke K, Hansen HC. Fundamentals of transorbital sonographic evaluation of optic nerve sheath expansion under intracranial hypertension. *Pediatric Radiology*. 1996; 26(10): 701-705.
- 29 Ballantyne J, Hollman A, Hamilton R, et al. Transorbital optic nerve sheath ultrasonography in normal children. *Clinical Radiology*. 1999; 54(11): 740-742.

- 30 Newman WD, Hollman AS, Dutton GN, Carachi R. Measurement of optic nerve sheath diameter by ultrasound: a means of detecting acute raised intracranial pressure in hydrocephalus. *British Journal of Ophthalmology*. 2002; 86(10): 1109-1113.
- 31 Moretti R, Pizzi B. Ultrasonography of the optic nerve in neurocritically ill patients. *Acta Anaesthesiologica Scandinavica*. 2011; 55(6): 644-652.
- 32 Malayeri AA, Bavarian S, Mehdizadeh M. Sonographic evaluation of optic nerve diameter in children with raised intracranial pressure. *Journal of Ultrasound in Medicine*. 2005; 24(2): 143-147.
- 33 Beare NA, Kampondeni S, Glover SJ, et al. Detection of raised intracranial pressure by ultrasound measurement of optic nerve sheath diameter in African children. *Tropical Medicine International Health*. 2008; 13(11): 1400-1404.
- 34 Steinborn M, Friedmann M, Hahn H, et al. Normal values for transbulbar sonography and magnetic resonance imaging of the optic nerve sheath diameter (ONSD) in children and adolescents. *Ultraschall in der Medizin*. 2015; 36(1): 54-58.
- 35 Bradley MM, Miccoli L, Escrig MA, Lang PJ. The pupil as a measure of emotional arousal and autonomic activation. *Psychophysiology*. 2008; 45(4): 602-607.
- 36 Partala T, Surakka V. Pupil size variation as an indication of affective processing. *International Journal of Human-Computer Studies*. 2003; 59(1): 185-198.

- 37 Hess EH, Polt JM. Pupil size in relation to mental activity during simple problem-solving. *Science*. 1964; 143(3611): 1190-1192.
- 38 Beatty J, Kahneman D. Pupillary changes in two memory tasks. *Psychonomic Science*. 1966; 5(10): 371-372.
- 39 Kahneman D, Tursky B, Shapiro D, Crider A. Pupillary, heart rate, and skin resistance changes during a mental task. *Journal of Experimental Psychology*. 1969; 79(1p1): 164.
- 40 Kahneman D, Peavler WS. Incentive effects and pupillary changes in association learning. *Journal of Experimental Psychology*. 1969; 79(2p1): 312.
- 41 Beatty J. Task-evoked pupillary responses, processing load, and the structure of processing resources. *Psychological Bulletin*. 1982; 91(2): 276.
- 42 Beatty J, Lucero-Wagoner B. The pupillary system. *Handbook of Psychophysiology*. 2000; 2: 142-162.
- 43 Laeng B, Sirois S, Gredebäck G. Pupillometry a window to the preconscious? *Perspectives on Psychological Science*. 2012; 7(1): 18-27.
- 44 Kaye LD, Rothner AD, Beauchamp GR, Meyers SM, Estes ML. Ocular findings associated with neurofibromatosis type II. *Ophthalmology*. 1992; 99(9): 1424-1429.

- 45 Von Graefe A. Complications of optic neuritis with cerebral disease. *Archives of Ophthalmology*. 1860; 7: 58.
- 46 Hayreh SS. Pathogenesis of oedema of the optic disc (papilloedema): a preliminary report. *The British Journal of Ophthalmology*. 1964; 48(10): 522.
- 47 Ossoinig KC, Cennamo G, Frazier-Byrne S. Echographic differential diagnosis of optic-nerve lesions. *Ultrasonography in Ophthalmology*. 1981; 29: 327-332.
- 48 Galetta S, Frazier BS, Smith JL. Echographic correlation of optic nerve sheath size and cerebrospinal fluid pressure. *Journal of Neuro-Ophthalmology*. 1989; 9(2): 79-82.
- 49 Liu D, Kahn M. Measurement and relationship of subarachnoid pressure of the optic nerve to intracranial pressures in fresh cadavers. *American Journal of Ophthalmology*. 1993; 116 (5): 548-556.
- 50 Hansen HC, Helmke K. The subarachnoid space surrounding the optic nerves. An ultrasound study of the optic nerve sheath. *Surgical and Radiologic Anatomy*. 1996; 18(4): 323-328.
- 51 Rajajee V, Fletcher JJ, Rochlen LR, Jacobs TL. Comparison of accuracy of optic nerve ultrasound for the detection of intracranial hypertension in the setting of acutely fluctuating vs stable intracranial pressure: post-hoc analysis of data from a prospective, blinded single center study. *Critical Care*. 2012; 16(3): R79.

- 52 Killer HE, Jaggi GP, Flammer J, Miller NR, Huber AR, Mironov A. Cerebrospinal fluid dynamics between the intracranial and the subarachnoid space of the optic nerve. Is it always bidirectional? *Brain*. 2007; 130(2): 514-520.
- 53 Killer HE, Laeng HR, Flammer J, Groscurth P. Architecture of arachnoid trabeculae, pillars, and septa in the subarachnoid space of the human optic nerve: anatomy and clinical considerations. *British Journal of Ophthalmology*. 2003; 87(6): 777-781.
- 54 Hayreh SS. *Ischemic Optic Neuropathies* (Springer Science and Business Media). Chapter 2: Structure of the optic nerve. 2011; XII: 7-34.
- 55 Rothman MI, Zoarski GH, Sutton D. The orbit. *Textbook of Radiology and Imaging*. 2003; 2: 1573-1595.
- 56 Hayreh SS. The sheath of the optic nerve. *Ophthalmologica*. 1984; 189(1-2): 54-63.
- 57 Francois P, Lescanne E, Velut S. The dural sheath of the optic nerve: descriptive anatomy and surgical applications. *Advances and Technical Standards in Neurosurgery*. 2011; 36: 187-198.
- 58 Seoane E, Rhoton Jr AL, de Oliveira E. Microsurgical anatomy of the dural collar (carotid collar) and rings around the clinoid segment of the internal carotid artery. *Neurosurgery*. 1998; 42(4): 869-884.
- 59 Snell RS, Lemp MA. *Clinical anatomy of the eye*. Second edition. Wiley-Blackwell. 1997; 278-285.

- 60 Saul TG, Ducker TB. Effect of intracranial pressure monitoring and aggressive treatment on mortality in severe head injury. *Journal of Neurosurgery*. 1982; 56(4): 498-503.
- 61 McAllister AS. A review of the vascular anatomy of the optic nerve head and its clinical implications. *Cureus*. 2013; 5(2): e98.
- 62 Biousse V, Newman NJ. Ischemic optic neuropathies. *New England Journal of Medicine*. 2015; 372: 2428-2436.
- 63 Mundt GH, William FH. Ultrasonics in ocular diagnosis. *American journal of Ophthalmology*. 1956; 41(3): 488-498.
- 64 Baum G, Greenwood I. The application of ultrasonics locating techniques to ophthalmology: Theoretic considerations and acoustic properties of ocular media: Part I, reflective properties. *American Journal of Ophthalmology*. 1958; 46(5): 319-329.
- 65 Bronson NR, Turner FT. A simple B-scan ultrasonoscope. *Archives of Ophthalmology*. 1973; 90(3): 237-238.
- 66 Ossoinig KC. Standardized echography: basic principles, clinical applications, and results. *International Ophthalmology Clinics*. 1979; 19(4): 127-210.
- 67 Cennamo G, Gangemi M, Stella L. The correlation between endocranial pressure and optic nerve diameter: an ultrasonographic study. *Ophthalmic Echography*. 1987; 603-606.

- 68 Hansen HC, Helmke K, Kunze K. Optic nerve sheath enlargement in acute intracranial hypertension. *Neuro-ophthalmology*. 1994; 14(6): 345-354.
- 69 Hayreh SS. Blood supply of the optic nerve head and its role in optic atrophy, glaucoma, and oedema of the optic disc. *The British Journal of Ophthalmology*. 1969; 53(11): 721-748.
- 70 Fledelius HC. Ultrasound in ophthalmology. *Ultrasound in Medicine Biology*. 1997; 23(3): 365-375.
- 71 Brunell KS. Ophthalmic ultrasonography. *Journal of Diagnostic Medical Sonography*. 2014; 30(3): 136-142.
- 72 Hall MK, Spiro DM, Sabbaj A, Moore CL, Hopkins KL, Meckler GD. Bedside optic nerve sheath diameter ultrasound for the evaluation of suspected pediatric ventriculoperitoneal shunt failure in the emergency department. *Child's Nervous System*. 2013; 29(12): 2275-2280.
- 73 Kimberly HH, Shah S, Marill K, Noble V. Correlation of optic nerve sheath diameter with direct measurement of intracranial pressure. *Academic Emergency Medicine*. 2008; 15(2): 201-204.
- 74 Silva CT, Brockley CR, Crum A, Mandelstam SA. Pediatric ocular sonography. *Seminars in Ultrasound, CT and MRI*. 2011; 32(1): 14-27.

- 75 Kilker BA, Holst JM, Hoffmann B. Bedside ocular ultrasound in the emergency department. *European Journal of Emergency Medicine*. 2014; 21(4): 246-253.
- 76 Ramji FG, Slovis TL, Baker JD. Orbital sonography in children. *Pediatric Radiology*. 1996; 26(4): 245-258.
- 77 Lizzi FL, Mortimer AJ. Bioeffects considerations for the safety of diagnostic ultrasound—preface. *Journal of Ultrasound in Medicine*. 1988; 7(9): S1-S38.
- 78 Fielding JA. Ocular ultrasound. *Clinical Radiology*. 1996; 51(8): 533-544.
- 79 Silverman RH, Lizzi FL, Ursea BG, et al. Safety levels for exposure of cornea and lens to very high-frequency ultrasound. *Journal of Ultrasound in Medicine*. 2001; 20(9): 979-986.
- 80 Fowlkes JB, Holland CK. Mechanical bioeffects from diagnostic ultrasound: AIUM consensus statements. *Journal of Ultrasound in Medicine*. 2000; 19(2): 69-72.
- 81 United States Department of Health and Human Services, Food and Drug Administration, Center for Devices and Radiological Health. Information for Manufacturers Seeking Marketing Clearance of Diagnostic Ultrasound Systems and Transducers. Washington, DC. 2008. <http://www.fda.gov/cdrh/ode/guidance/560.pdf>.
- 82 Nelson TR, Fowlkes JB, Abramowicz JS, Church CC. Ultrasound Biosafety Considerations for the Practising Sonographer and Sonologist. *Journal of Ultrasound in Medicine*. 2009; 28: 139-150.

- 83 European Federation for Societies of Ultrasound in Medicine and Biology (EFSUMB) Clinical safety statement for diagnostic ultrasound safety. Tours, France. 1998. *European Journal of Ultrasound*. 1998; 8: 67-68.
- 84 Toms DA. The mechanical index, ultrasound practices, and the ALARA principle. *Journal of Ultrasound in Medicine*. 2006; 25(4): 560-561.
- 85 Bioeffects Committee of the American Institute of Ultrasound in Medicine. American Institute of Ultrasound in Medicine consensus report on potential bioeffects of diagnostic ultrasound: executive summary. *Journal of Diagnostic Medical Sonography*. 2011; 27(1): 3-13.
- 86 Kendall CJ, Prager TS, Cheng H, Gombos D, Tang RA, Schiffman JS. Diagnostic Ophthalmic Ultrasound for Radiologists. *Neuroimaging Clinics of North America*. 2015; 25(3): 327-365.
- 87 Guillaume J, Janny P. Continuous intracranial manometry; importance of the method and first results. *Revue Neurologique*. 1951; 84(2): 131.
- 88 Lundberg, N. Continuous Recording and Control of Ventricular Fluid Pressure in Neurosurgical Practice. *Acta Psychiatrica Et Neurologica Scandanavica (Suppl 149)*. 1960; (36): 1-193.
- 89 Miller JD, Becker DP, Ward JD, Sullivan HG, Adams WE, Rosner MJ. Significance of intracranial hypertension in severe head injury. *Journal of Neurosurgery*. 1977; 47(4): 503-516.

- 90 Becker DP, Miller JD, Ward JD, Greenberg RP, Young HF, Sakalas R. The outcome from severe head injury with early diagnosis and intensive management. *Journal of Neurosurgery*. 1977; 47(4): 491-502.
- 91 Narayan RK, Greenberg RP, Miller JD, et al. Improved confidence of outcome prediction in severe head injury: a comparative analysis of the clinical examination, multimodality evoked potentials, CT scanning, and intracranial pressure. *Journal of Neurosurgery*. 1981; 54(6): 751-762.
- 92 Czosnyka M, Pickard JD. Monitoring and interpretation of intracranial pressure. *Journal of Neurology, Neurosurgery and Psychiatry*. 2004; 75(6): 813-821.
- 93 Marmarou A, Maset AL, Ward JD, et al. Contribution of CSF and vascular factors to elevation of ICP in severely head-injured patients. *Journal of Neurosurgery*. 1987; 66(6): 883-890.
- 94 Michaud LJ, Rivara FP, Grady MS, Reay DT. Predictors of survival and severity of disability after severe brain injury in children. *Neurosurgery*. 1992; 31(2): 254-26.
- 95 Chambers IR, Siddique MS, Banister K, Mendelow AD. Clinical comparison of the Spiegelberg parenchymal transducer and ventricular fluid pressure. *Journal of Neurology, Neurosurgery and Psychiatry*. 2001; 71(3): 383-385.
- 96 Davson H, Hollingsworth G, Segal MB. The mechanism of drainage of the cerebrospinal fluid. *Brain*. 1970; 93: 665-678.

- 97 Juul N, Morris GF, Marshall SB, Marshall LF. Intracranial hypertension and cerebral perfusion pressure: influence on neurological deterioration and outcome in severe head injury. *Journal of Neurosurgery*. 2000; 92(1): 1-6.
- 98 Avezaat CJ, Van Eijndhoven JH, Wyper DJ. Cerebrospinal fluid pulse pressure and intracranial volume-pressure relationships. *Journal of Neurology, Neurosurgery and Psychiatry*. 1979; 42(8): 687-700.
- 99 Padayachy LC, Figaji AA, Bullock MR. Intracranial pressure monitoring for traumatic brain injury in the modern era. *Child's Nervous System*. 2010; 26(4): 441-452.
- 100 Marshall LF, Smith RW, Shapiro HM. The outcome with aggressive treatment in severe head injuries: Part I: the significance of intracranial pressure monitoring. *Journal of Neurosurgery*. 1979; 50(1): 20-25.
- 101 Smith M. Monitoring intracranial pressure in traumatic brain injury. *Anesthesia & Analgesia*. 2008; 106(1): 240-248.
- 102 Chesnut RM, Marshall LF, Marshall SB. Medical management of intracranial pressure. *Head Injury*. 1993; 4: 229-263.
- 103 Salim A, Hannon M, Brown C, et al. Intracranial pressure monitoring in severe isolated pediatric blunt head trauma. *The American Surgeon*. 2008; 74(11): 1088-1093.

- 104 Shafi S, Diaz-Arrastia R, Madden C, Gentilello L. Intracranial pressure monitoring in brain-injured patients is associated with worsening of survival. *Journal of Trauma and Acute Care Surgery*. 2008; 64(2): 335-340.
- 105 Saul TG, Ducker TB. Effect of intracranial pressure monitoring and aggressive treatment on mortality in severe head injury. *Journal of Neurosurgery*. 1982; 56(4): 498-503.
- 106 Citerio G, Andrews PJ. Intracranial pressure. *Intensive Care Medicine*. 2004; 30(10): 1882-1885.
- 107 Czosnyka M, Smielewski P, Kirkpatrick P, Laing RJ, Menon D, Pickard JD. Continuous assessment of the cerebral vasomotor reactivity in head injury. *Neurosurgery*. 1997; 41: 11-17.
- 108 Treggiari MM, Schutz N, Yanez ND, Romand JA. Role of intracranial pressure values and patterns in predicting outcome in traumatic brain injury: a systematic review. *Neurocritical Care*. 2007; 6(2): 104-112.
- 109 Kristiansson H, Nissborg E, Bartek Jr J, Andresen M, Reinstrup P, Romner B. Measuring elevated intracranial pressure through noninvasive methods: a review of the literature. *Journal of Neurosurgical Anesthesiology*. 2013; 25(4): 372-385.
- 110 Adelson PD, Bratton, SL, Carney NA, et al. Guidelines for the acute medical management of severe traumatic brain injury in infants, children, and adolescents. Chapter 5. Indications for intracranial pressure monitoring in

- pediatric patients with severe traumatic brain injury. *Pediatric Critical Care Medicine*. 2003; 4(3 Suppl): S19-24.
- 111 Morris KP, Forsyth RJ, Parslow RC, et al. UK Paediatric Traumatic Brain Injury Study Group. Intracranial pressure complicating severe traumatic brain injury in children: monitoring and management. *Intensive Care Medicine*. 2006; 32(10): 1606-1612.
- 112 Rickert K, Sinson G. Intracranial pressure monitoring. *Operative Techniques in General Surgery*. 2003; 5(3): 170-175.
- 113 Lozier AP, Sciacca RR, Romagnoli MF, Connolly Jr ES. Ventriculostomy-related infections: a critical review of the literature. *Neurosurgery*. 2002; 51(1): 170-182.
- 114 Ghajar J. Intracranial pressure monitoring techniques. *New Horizons*. 1995; 3(3): 395-399.
- 115 Paramore CG, Turner DA. Relative risks of ventriculostomy infection and morbidity. *Acta Neurochirurgica*. 1994; 127(1-2): 79-84.
- 116 Raboel PH, Bartek J, Andresen M, Bellander BM, Romner B. Intracranial pressure monitoring: invasive versus non-invasive methods—a review. *Critical care Research and Practice*. 2012; 2012(12): 1-14.
- 117 Koskinen LOD, Olivecrona M. Clinical experience with the intraparenchymal intracranial pressure monitoring Codman MicroSensor system. *Neurosurgery*. 2005; 56(4): 693-698.

- 118 Poca MA, Sahuquillo J, Arribas M, Báguena M, Amorós S, Rubio E. Fiberoptic intraparenchymal brain pressure monitoring with the Camino V420 monitor: reflections on our experience in 163 severely head-injured patients. *Journal of Neurotrauma*. 2002; 19(4): 439-448.
- 119 Kass MA, Heuer DK, Higginbotham EJ, et al. The Ocular Hypertension Treatment Study: a randomized trial determines that topical ocular hypotensive medication delays or prevents the onset of primary open-angle glaucoma. *Archives of Ophthalmology*. 2002; 120(6): 701-713.
- 120 Eddy VA, Vitsky JL, Rutherford EJ, Morris Jr JA. Aggressive use of ICP monitoring is safe and alters patient care. *The American Surgeon*. 1995; 61(1): 24-29.
- 121 Münch E, Weigel R, Schmiedek P, Schürer L. The Camino intracranial pressure device in clinical practice: reliability, handling characteristics and complications. *Acta Neurochirurgica*. 1998; 140(11): 1113-1120.
- 122 Marmarou A, Anderson RL, Ward JD, et al. Impact of ICP instability and hypotension on outcome in patients with severe head trauma. *Special Supplements*. 1991; 75(1): 59-66.
- 123 Crutchfield JS, Narayan RK, Robertson CS, Michael LH. Evaluation of a fiberoptic intracranial pressure monitor. *Journal of Neurosurgery*. 1990; 72(3): 482-487.

- 124 Piper I, Barnes A, Smith D, Dunn L. The Camino intracranial pressure sensor: is it optimal technology? An internal audit with a review of current intracranial pressure monitoring technologies. *Neurosurgery*. 2001; 49(5): 1158-1165.
- 125 Schickner DJ, Young RF. Intracranial pressure monitoring: fiberoptic monitor compared with the ventricular catheter. *Surgical Neurology*. 1992; 37(4): 251-254.
- 126 Chambers IR, Mendelow AD, Sinar EJ, Modha P. A clinical evaluation of the Camino subdural screw and ventricular monitoring kits. *Neurosurgery*. 1990; 26(3): 421-423.
- 127 Zhong J, Dujovny M, Park HK, Perez E, Perlin A, Diaz F. Advances in ICP monitoring techniques. *Neurological Research*. 2003; 25: 339-350.
- 128 Lilja A, Andresen M, Hadi A, Christoffersen D, Juhler M. Clinical experience with telemetric intracranial pressure monitoring in a Danish neurosurgical center. *Clinical Neurology and Neurosurgery*. 2014; 120: 36-40.
- 129 Cartwright C, Igbaseimokumo U. Lumbar Puncture Opening Pressure Is Not a Reliable Measure of Intracranial Pressure in Children. *Journal of Child Neurology*. 2015; 30(2): 170-173.
- 130 Bratton SL, Chestnut RM, Ghajar J, et al. Guidelines for the management of severe traumatic brain injury. VI. Indications for intracranial pressure monitoring. *Journal of Neurotrauma*. 2006; 24(S1): S37-44.

- 131 Hanlo PW, Gooskens RH, Faber JA, et al. Relationship between anterior fontanelle pressure measurements and clinical signs in infantile hydrocephalus. *Child's Nervous System*. 1996. 12(4): 200-209.
- 132 Wealthall SR, Smallwood R. Methods of measuring intracranial pressure via the fontanelle without puncture. *Journal of Neurology, Neurosurgery and Psychiatry*. 1974; 37(1): 88-96.
- 133 Tuite GF, Chong WK, Evanson J, et al. The effectiveness of papilledema as an indicator of raised intracranial pressure in children with craniosynostosis. *Neurosurgery*. 1996; 38(2): 272-278.
- 134 Sajjadi SA, Harirchian MH, Sheikhabaehi N, Mohebbi MR, Malekmadani MH, Saberi H. The relation between intracranial and intraocular pressures: study of 50 patients. *Annals of Neurology*. 2006; 59(5): 867-870.
- 135 Hedges TR, Zaren HA. The relationship of optic nerve tissue pressure to intracranial and systemic arterial pressure. *American Journal of Ophthalmology*. 1973; 75(1): 90-98.
- 136 Hedges TR. Papilledema: its recognition and relation to increased intracranial pressure. *Survey of Ophthalmology*. 1974; 19(4): 201-223.
- 137 Lashutka MK, Chandra A, Murray HN, Phillips GS, Hiestand BC. The relationship of intraocular pressure to intracranial pressure. *Annals of Emergency Medicine*. 2004; 43(5): 585-591.

- 138 Salman MS. Can intracranial pressure be measured non-invasively? *The Lancet*. 1997; 350(9088): 1367.
- 139 Czarnik T, Gawda R, Kolodziej W, Latka D, Sznajd-Weron K, Weron R. Associations between intracranial pressure, intraocular pressure and mean arterial pressure in patients with traumatic and non-traumatic brain injuries. *Injury*. 2009; 40(1): 33-39.
- 140 Han Y, McCulley TJ, Horton JC. No correlation between intraocular pressure and intracranial pressure. *Annals of Neurology*. 2008; 64(2): 221-224.
- 141 Kirk T, Jones K, Miller S, Corbett J. Measurement of intraocular and intracranial pressure: is there a relationship? *Annals of Neurology*. 2011; 70(2): 323-326.
- 142 Muchnok T, Deitch K, Giraldo P. Can intraocular pressure measurements be used to screen for elevated intracranial pressure in emergency department patients? *The Journal of Emergency Medicine*. 2012; 43(3): 532-537.
- 143 Spentzas T, Henricksen J, Patters AB, Chaum E. Correlation of intraocular pressure with intracranial pressure in children with severe head injuries. *Pediatric Critical Care Medicine*. 2010; 11(5): 593-598.
- 144 Lehman RA, Krupin T, Podos SM. Experimental effect of intracranial hypertension upon intraocular pressure. *Journal of Neurosurgery*. 1972; 36(1): 60-66.

- 145 Yavin D, Luu J, James MT, et al. Diagnostic accuracy of intraocular pressure measurement for the detection of raised intracranial pressure: meta-analysis: a systematic review. *Journal of Neurosurgery*. 2014; 121(3): 680-687.
- 146 Li Z, Yang Y, Lu Y, et al. Intraocular pressure vs intracranial pressure in disease conditions: a prospective cohort study (Beijing iCOP study). *BMC Neurology*. 2012; 12(1): 66.
- 147 Larson MD, Muhiudeen I. Pupillometric analysis of the absent light reflex. *Archives of neurology*. 1995; 52(4): 369-372.
- 148 Du R, Meeker M, Bacchetti P, Larson MD, Holland MC, Manley GT. Evaluation of the portable infrared pupillometer. *Neurosurgery*. 2005; 57(1): 198-203.
- 149 Taylor WR, Chen JW, Meltzer H, et al. Quantitative pupillometry, a new technology: normative data and preliminary observations in patients with acute head injury: technical note. *Journal of Neurosurgery*. 2003; 98(1): 205-213.
- 150 Boev AN, Fountas KN, Karamelas I, et al. Quantitative pupillometry: normative data in healthy pediatric volunteers. *Journal of Neurosurgery: Pediatrics*. 2005; 103(6 Suppl): 496-500.
- 151 Geeraerts T, Newcombe VF, Coles JP, et al. Use of T2-weighted magnetic resonance imaging of the optic nerve sheath to detect raised intracranial pressure. *Critical Care*. 2008; 12(5): R114.

- 152 Gibby WA, Cohen MS, Goldberg HI, Sergott RC. Pseudotumor cerebri: CT findings and correlation with vision loss. *American Journal of Roentgenology*. 1993; 160(1): 143-146.
- 153 Sekhon MS, Griesdale DE, Robba C, et al. Optic nerve sheath diameter on computed tomography is correlated with simultaneously measured intracranial pressure in patients with severe traumatic brain injury. *Intensive Care Medicine*. 2014; 40(9): 1267-1274.
- 154 Hansen HC, Helmke K. Validation of the optic nerve sheath response to changing cerebrospinal fluid pressure: ultrasound findings during intrathecal infusion tests. *Journal of Neurosurgery*. 1997; 87(1): 34-40.
- 155 Wang L, Feng L, Yao Y, et al. Optimal optic nerve sheath diameter threshold for the identification of elevated opening pressure on lumbar puncture in a Chinese population. *PloS one*. 2015; 10(2): e0117939.
- 156 Bäuerle J, Nedelmann M. Sonographic assessment of the optic nerve sheath in idiopathic intracranial hypertension. *Journal of Neurology*. 2011; 258(11): 2014-2019.
- 157 Dubourg J, Javouhey E, Geeraerts T, Messerer M, Kassai B. Ultrasonography of optic nerve sheath diameter for detection of raised intracranial pressure: a systematic review and meta-analysis. *Intensive Care Medicine*. 2011; 37(7): 1059-1068.
- 158 Soldatos T, Chatzimichail K, Papathanasiou M, Gouliamos A. Optic nerve sonography: a new window for the non-invasive evaluation of intracranial pressure in brain injury. *Emergency Medicine Journal*. 2009; 26(9): 630-634.

- 159 Hee MR, Izatt JA, Swanson EA, et al. Optical coherence tomography of the human retina. *Archives of Ophthalmology*. 1995; 113(3): 325-332.
- 160 Scott CJ, Kardon RH, Lee AG, Frisen L, Wall M. Diagnosis and grading of papilledema in patients with raised intracranial pressure using optical coherence tomography vs clinical expert assessment using a clinical staging scale. *Archives of Ophthalmology*. 2010; 128(6): 705-711.
- 161 Driessen C, Eveleens J, Bleyen I, Van Veelen ML, Joosten K, Mathijssen I. Optical coherence tomography: a quantitative tool to screen for papilledema in craniosynostosis. *Childs Nerv Syst*. 2014; 30: 1067-1073.
- 162 Kruse FE, Burk RO, Völcker HE, Zinser G, Harbarth U. Reproducibility of topographic measurements of the optic nerve head with laser tomographic scanning. *Ophthalmology*. 1989; 96(9): 1320-1324.
- 163 Rohrschneider K, Burk RO, Kruse FE, Völcker HE. Reproducibility of the optic nerve head topography with a new laser tomographic scanning device. *Ophthalmology*. 1998; 101(6): 1044-1049.
- 164 Trick GL, Vesti E, Tawansy K, Skarf B, Gartner J. Quantitative evaluation of papilledema in pseudotumor cerebri. *Investigative Ophthalmology Visual Science*. 1998; 39(10): 1964-1971.
- 165 Heckmann JG, Weber M, Jünemann AG, Neundörfer B, Mardin CY. Laser scanning tomography of the optic nerve vs CSF opening pressure in idiopathic intracranial hypertension. *Neurology*. 2004; 62(7): 1221-1223.

- 166 Jacks AS, Miller NR. Spontaneous retinal venous pulsation: aetiology and significance. *Journal of Neurology, Neurosurgery and Psychiatry*. 2003; 74(1): 7-9.
- 167 Levin BE. The clinical significance of spontaneous pulsations of the retinal vein. *Archives of Neurology*. 1978; 35(1): 37-40.
- 168 Wong SH, White RP. The clinical validity of the spontaneous retinal venous pulsation. *Journal of Neuro-Ophthalmology*. 2013; 33(1): 17-20.
- 169 Baurmann M. On the origin and clinical significance of retinal venous pulse. *Zusammenkunft Deutschen Ophthalmologie*. 1925; 45: 53-59.
- 170 Firsching R, Schütze M, Motschmann M, Behrens-Baumann W. Venous ophthalmodynamometry: a noninvasive method for assessment of intracranial pressure. *Journal of Neurosurgery*. 2000; 93(1): 33-36.
- 171 Samuel M, Burge DM, Marchbanks RJ. Quantitative assessment of intracranial pressure by the tympanic membrane displacement audiometric technique in children with shunted hydrocephalus. *European Journal of Pediatric Surgery*. 1998; 8(4): 200-207.
- 172 Jerin C, Berman A, Krause E, Ertl-Wagner B, Gürkov R. Ocular vestibular evoked myogenic potential frequency tuning in certain Meniere's disease. *Hearing Research*. 2014; 310: 54-59.

- 173 Shimbles S, Dodd C, Banister K, Mendelow AD, Chambers IR. Clinical comparison of tympanic membrane displacement with invasive intracranial pressure measurements. *Physiological Measurement*. 2005; 26(6): 1085.
- 174 Silverman CA, Linstrom CJ. How to measure cerebrospinal fluid pressure invasively and noninvasively. *Journal of Glaucoma*. 2013; 22: S26-S28.
- 175 Voss SE, Horton NJ, Tabucchi TH, Folowosele FO, Shera CA. Posture-induced changes in distortion-product otoacoustic emissions and the potential for noninvasive monitoring of changes in intracranial pressure. *Neurocritical Care*. 2006; 4(3): 251-257.
- 176 Büki B, Avan P, Lemaire JJ, Dordain M, Chazal J, Ribari O. Otoacoustic emissions: a new tool for monitoring intracranial pressure changes through stapes displacements. *Hearing Research*. 1996; 94(1): 125-139.
- 177 Frank AM, Alexiou C, Hulin P, Janssen T, Arnold W, Trappe AE. Non-invasive measurement of intracranial pressure changes by otoacoustic emissions (OAEs) - a report of preliminary data. *Zentralblatt für Neurochirurgie*. 1999; 61(4): 177-180.
- 178 Kiesler J, Ricer R. The abnormal fontanel. *American Family Physician*. 2003; 67(12): 2547-2552.

- 179 Purin VR. Measurement of the cerebrospinal fluid pressure in the infant without puncture. A new method. *Pediatrics*. 1964; 43: 82-85.
- 180 Vidyasagar D, Raju TNK. A simple noninvasive technique of measuring intracranial pressure in the newborn. *Pediatrics*. 1977; 59(6): 957-961.
- 181 Peters RJA, Hanlo PW, Gooskens RHJ, Braun KPJ, Tulleken CAF, Willemsse J. Non-invasive ICP monitoring in infants: the Rotterdam Teletransducer revisited. *Child's Nervous System*. 2005; 11(4): 207-213.
- 182 Lupetin AR, Davis DA, Beckham I, Dash N. Transcranial Doppler Sonography. Part 1. Principles, technique, and normal appearances. *Radiographics*. 1995; 15(1): 179-191.
- 183 Aaslid R, Markwalder TM, Nornes H. Noninvasive intracranial doppler ultrasound recording of flow velocity in basal cerebral arteries. *Journal of Neurosurgery*. 1982; 57: 769-774.
- 184 Bellner J, Romner B, Reinstrup P, Kristiansson KA, Ryding E, Brandt L. Transcranial Doppler sonography pulsatility index (PI) reflects intracranial pressure (ICP). *Surgical Neurology*. 2004; 62(1): 45-51.
- 185 Adams RJ. TCD in sickle cell disease: an important and useful test. *Pediatric Radiology*. 2005; 35(3): 229-234.

- 186 Radolovich DK, Aries MJH, Castellani G, et al. Pulsatile intracranial pressure and cerebral autoregulation after traumatic brain injury. *Neurocritical Care*. 2011; 15(3): 379-386.
- 187 Leliefeld PH, Gooskens RH, Peters RJ, et al. New transcranial Doppler index in infants with hydrocephalus: transsystolic time in clinical practice. *Ultrasound in Medicine Biology*. 2009; 35(10): 1601-1606.
- 188 Krejza J, Mariak Z, Babikian V. Importance of Angle Correction in the Measurement of Blood Flow Velocity with Transcranial Doppler Sonography. *American Journal of Neuroradiology*. 2001; 22: 1743-1747.
- 189 Voulgaris SG, Partheni M, Kaliora H, Haftouras N, Pessach IS, Polyzoidis KS. Early cerebral monitoring using the transcranial Doppler pulsatility index in patients with severe brain trauma. *Annals of Transplantation*. 2005; 11(2): CR49-CR52.
- 190 Figaji AA, Zwane E, Fieggen AG, Siesjo P, Peter JC. Transcranial Doppler pulsatility index is not a reliable indicator of intracranial pressure in children with severe traumatic brain injury. *Surgical Neurology*. 2009; 72(4): 389-394.
- 191 Melo JRT, Di Rocco F, Blanot S, et al. Transcranial Doppler can predict intracranial hypertension in children with severe traumatic brain injuries. *Child's Nervous System*. 2011; 27(6): 979-984.
- 192 Ragauskas A, Matijosaitis V, Zakelis R, et al. Clinical assessment of noninvasive intracranial pressure absolute value measurement method. *Neurology*. 2012; 78(21): 1684-1691.

- 193 Ragauskas A, Bartusis L, Piper I, et al. Improved diagnostic value of a TCD-based non-invasive ICP measurement method compared with the sonographic ONSD method for detecting elevated intracranial pressure. *Neurological Research*. 2014; 36(7): 607-614.
- 194 Alperin NJ, Lee SH, Loth F, Raksin PB, Lichtor T. MR-intracranial pressure (ICP): a method to measure intracranial elastance and pressure noninvasively by means of MR imaging: baboon and human study 1. *Radiology*. 2000; 217(3): 877-885.
- 195 Muehlmann M, Koerte IK, Laubender RP, et al. Magnetic resonance-based estimation of intracranial pressure correlates with ventriculoperitoneal shunt valve opening pressure setting in children with hydrocephalus. *Investigative Radiology*. 2013; 48(7): 543-547.
- 196 Glick RP, Niebruegge J, Lee SH, Egibor O, Lichtor T, Alperin N. Early experience from the application of a noninvasive magnetic resonance imaging-based measurement of intracranial pressure in hydrocephalus. *Neurosurgery*. 2006; 59(5): 1052-1061.
- 197 Ghosh A, Elwell C, Smith M. Cerebral near-infrared spectroscopy in adults: a work in progress. *Anesthesia and Analgesia*. 2012; 115(6): 1373-1383.
- 198 Kampfl A, Pfausler B, Denchev D, Jaring P, Schmutzhard E. Near Infrared Spectroscopy (NIRS) in Patients with Severe Brain Injury and Elevated Intracranial Pressure. *Acta Neurochirurgica Supplements*. 1997; 70: 112-114.

- 199 Weerakkody RA, Czosnyka M, Zweifel C, et al. Near infrared spectroscopy as possible non-invasive monitor of slow vasogenic ICP waves. *Acta Neurosurgical Supplement*. 2012; 114: 181-185.
- 200 Zweifel C, Castellani G, Czosnyka M, et al. Continuous assessment of cerebral autoregulation with near-infrared spectroscopy in adults after subarachnoid hemorrhage. *Stroke*. 2010; 41(9): 1963-1968.
- 201 Chen H, Wang J, Mao S, Dong W, Yang H. A new method of intracranial pressure monitoring by EEG power spectrum analysis. *Canadian Journal of Neurological Sciences*. 2012; 39(4): 483-487.
- 202 Liasis A, Thompson DA, Hayward R, Nischal KK. Sustained raised intracranial pressure implicated only by pattern reversal visual evoked potentials after cranial vault expansion surgery. *Pediatric neurosurgery*. 2003; 39(2): 75-80.
- 203 Rosenfeld JP, Owen RL. Instrumental conditioning of photic evoked potentials: mechanisms and properties of late component modification. *Physiology and Behavior*. 1972; 9(5): 851-858.
- 204 Wu X, Ji Z. Non-invasive detection for intracranial high pressure with FVEP picked-up by independent component analysis. *Journal of Biomedical Engineering*. 2007; 24(5): 1015-1018.
- 205 York DH, Pulliam MW, Rosenfeld JG, Watts C. Relationship between visual evoked potentials and intracranial pressure. *Journal of Neurosurgery*. 1981; 55(6): 909-916.

- 206 York D, Legan M, Benner S, Watts C. Further studies with a noninvasive method of intracranial pressure estimation. *Neurosurgery*. 1984; 14(4): 456-461.
- 207 Desch LW. Longitudinal stability of visual evoked potentials in children and adolescents with hydrocephalus. *Developmental Medicine Child Neurology*. 2001; 43(02): 113-117.
- 208 Zhao YL, Zhou JY, Zhu GH. Clinical experience with the noninvasive ICP monitoring system. *Intracranial Pressure and Brain Monitoring XII*. 2005; 151-155.
- 209 Andersson L, Sjölund J, Nilsson J. Flash visual evoked potentials are unreliable as markers of ICP due to high variability in normal subjects. *Acta Neurochirurgica*. 2012; 154(1): 121-127.
- 210 Hiler M, Czosnyka M, Hutchinson P, et al. Predictive value of initial computerized tomography scan, intracranial pressure, and state of autoregulation in patients with traumatic brain injury. *Journal of Neurosurgery*. 2006; 104(5): 731-737.
- 211 Tuite GF, Evanson J, Chong WK, Thompson DN, Harkness WF, Jones BM, et al. The beaten copper cranium: a correlation between intracranial pressure, cranial radiographs, and computed tomographic scans in children with craniosynostosis. *Neurosurgery*. 1996; 39(4): 691-699.
- 212 Thompson P, Toga AW. A surface-based technique for warping three-dimensional images of the brain. *Medical Imaging*. 1996; 15(4): 402-417.

- 213 Reed MJ, Browning JG, Wilkinson AG, Beattie T. Can we abolish skull x-rays for head injury? *Archives of Disease in Childhood*. 2005; 90(8): 859-864.
- 214 Sadhu VK, Sampson J, Haar FL, Pinto RS, Handel SF. Correlation between computed tomography and intracranial pressure monitoring in acute head trauma patients 1. *Radiology*. 1979; 133(2): 507-509.
- 215 Eisenberg HM, Gary Jr HE, Aldrich EF, et al. Initial CT findings in 753 patients with severe head injury: a report from the NIH Traumatic Coma Data Bank. *Journal of Neurosurgery*. 1990; 73(5): 688-698.
- 216 Eide PK. The relationship between intracranial pressure and size of cerebral ventricles assessed by computed tomography. *Acta Neurochirurgica*. 2003; 145(3): 171-179.
- 217 Miller MT, Pasquale M, Kurek S, et al. Initial head computed tomographic scan characteristics have a linear relationship with initial intracranial pressure after trauma. *Journal of Trauma and Acute Care Surgery*. 2004; 56(5): 967-973.
- 218 Kouvarellis AJ, Rohlwink UK, Sood V, Van Breda D, Gowen MJ, Figaji AA. The relationship between basal cisterns on CT and time-linked intracranial pressure in paediatric head injury. *Child's Nervous System*. 2011; 27(7): 1139-1144.

- 219 Mizutani T, Manaka S, Tsutsumi H. Estimation of intracranial pressure using computed tomography scan findings in patients with severe head injury. *Surgical Neurology*. 1990; 33(3): 178-184.
- 220 Toutant SM, Klauber MR, Marshall LF. Absent or compressed basal cisterns on first CT scan: ominous predictors of outcome in severe head injury. *Journal of neurosurgery*. 1984; 61(4): 691-694.
- 221 Pauwels EK, Bourguignon MH. Radiation dose features and solid cancer induction in pediatric computed tomography. *Medical Principles and Practice*. 2012; 21(6): 508-515.
- 222 Krille L, Zeeb H, Jahnen A. Computed tomographies and cancer risk in children: a literature overview of CT practices, risk estimations and an epidemiologic cohort study proposal. *Radiation and Environmental Biophysics*. 2012; 51(2): 103-111.
- 223 Smyth MD, Narayan P, Tubbs RS, et al. Cumulative diagnostic radiation exposure in children with ventriculoperitoneal shunts: a review. *Child's Nervous System*. 2008; 24(4): 493-497.
- 224 Pearce MS, Salotti JA, Little MP, et al. Radiation exposure from CT scans in childhood and subsequent risk of leukaemia and brain tumours: a retrospective cohort study. *The Lancet*. 2012; 380(9840): 499-505.
- 225 Brenner DJ, Hall EJ. Computed tomography: an increasing source of radiation exposure. *New England Journal of Medicine*. 2007; 357(22): 2277-2284.

- 226 Zhang X, Burstein R, Levy D. Local action of the proinflammatory cytokines IL-1 β and IL-6 on intracranial meningeal nociceptors. *Cephalalgia*. 2012; 32(1): 66-72.
- 227 Marshall I, MacCormick I, Sellar R, Whittle I. Assessment of factors affecting MRI measurement of intracranial volume changes and elastance index. *British Journal of Neurosurgery*. 2008; 22(3): 389-397.
- 228 Gass A, Barker GJ, Riordan-Eva P, et al (1996). MRI of the optic nerve in benign intracranial hypertension. *Neuroradiology*. 1996; 38(8): 769-773.
- 229 Raskin PB, Alperin N, Sivaramakrishnan A, Surapaneni S, Lichtor T. Noninvasive intracranial compliance and pressure based on dynamic magnetic resonance imaging of blood flow and cerebrospinal fluid flow: review of principles, implementation, and other noninvasive approaches. *Neurosurgical Focus*. 2003; 14(4): 1-8.
- 230 Alperin N, Hushek SG, Lee SH, Sivaramakrishnan A, Lichtor T (2005). MRI study of cerebral blood flow and CSF flow dynamics in an upright posture: the effect of posture on the intracranial compliance and pressure. *Intracranial Pressure and Brain Monitoring XII*. 2005; 177-181.
- 231 Lagreze WA, Lazzaro A, Weigel M, Hansen H, Hennig J, Bley TA. Morphometry of the retrobulbar human optic nerve: comparison between conventional sonography and ultrafast magnetic resonance sequences. *Investigative Ophthalmology and Visual Science*. 2007; 48(5): 1913.
- 232 Greitz D. Radiological assessment of hydrocephalus: new theories and implications for therapy. *Neurosurgical Review*. 2004; 27(3): 145-165.

- 233 Dinçer A, Özek MM. Radiologic evaluation of pediatric hydrocephalus. *Child's Nervous System*. 2011; 27(10): 1543-1562.
- 234 McAuley D, Paterson A, Sweeney L. Optic nerve sheath ultrasound in the assessment of paediatric hydrocephalus. *Child's Nervous System*. 2009; 25(1): 87-90.
- 235 Tsung JW, Blaivas M, Cooper A, Levick NR. A rapid noninvasive method of detecting elevated intracranial pressure using bedside ocular ultrasound: application to 3 cases of head trauma in the pediatric emergency department. *Pediatric Emergency Care*. 2005; 21(2): 94-98.
- 236 Agrawal S, Brierley J. Optic nerve sheath measurement and raised intracranial pressure in paediatric traumatic brain injury. *European Journal of Trauma and Emergency Surgery*. 2012; 38(1): 75-77.
- 237 Steinborn M, Fiegler J, Kraus V, et al. High resolution ultrasound and magnetic resonance imaging of the optic nerve and the optic nerve sheath: anatomic correlation and clinical importance. *Ultraschall in der Medizin*. 2011; 32(6): 608-613.
- 238 Singhal A, Yang MM, Sargent MA, Cochrane DD. Does optic nerve sheath diameter on MRI decrease with clinically improved pediatric hydrocephalus? *Child's Nervous System*. 2013; 29(2): 269-274.
- 239 Padayachy LC, Kilborn T, Carrara H, Figaji AA, Fieggen GA. Change in optic nerve sheath diameter as a radiological marker of outcome from endoscopic

- third ventriculostomy in children. *Child's Nervous System*. 2015; 31(5): 721-728.
- 240 Shofty B, Ben-Sira L, Constantini S, Freedman S, Kesler A. Optic nerve sheath diameter on MR imaging: establishment of norms and comparison of pediatric patients with idiopathic intracranial hypertension with healthy controls. *American Journal of Neuroradiology*. 2012; 33(2): 366-369.
- 241 Driessen C, Van Veelen ML, Lequin M, Joosten KM, Mathijssen I. Nocturnal ultrasound measurements of optic nerve sheath diameter correlate with intracranial pressure in children with craniosynostosis. *Plastic and Reconstructive Surgery*. 2012; 130(3): 448-451.
- 242 Le A, Hoehn ME, Smith ME, Spentzas T, Schlappy D, Pershad J. Bedside sonographic measurement of optic nerve sheath diameter as a predictor of increased intracranial pressure in children. *Annals of Emergency Medicine*. 2009; 53(6): 785-791.
- 243 Blaiwas M, Theodoro D, Sierzenski PR. Elevated Intracranial Pressure Detected by Bedside Emergency Ultrasonography of the Optic Nerve Sheath. *Academic Emergency Medicine*. 2003; 10(4): 376-381.
- 244 Shirodkar CG, Rao SM, Mutkule DP, Harde YR, Venkategowda PM, Mahesh MU. Optic nerve sheath diameter as a marker for evaluation and prognostication of intracranial pressure in Indian patients: An observational study. *Indian Journal of Critical Care Medicine*. 2014; 18(11): 728-734.

- 245 Cammarata G, Ristagno G, Cammarata A, Mannanici G, Denaro C, Gullo A. Ocular ultrasound to detect intracranial hypertension in trauma patients. *Journal of Trauma and Acute Care Surgery*. 2011; 71(3): 779-781.
- 246 Frumin E, Schlang J, Wiechmann W, et al. Prospective analysis of single operator sonographic optic nerve sheath diameter measurement for diagnosis of elevated intracranial pressure. *Western Journal of Emergency Medicine*. 2014; 15(2): 217.
- 247 Amini A, Kariman H, Dolatabadi AA, et al. Use of the sonographic diameter of optic nerve sheath to estimate intracranial pressure. *The American Journal of Emergency Medicine*. 2013; 31(1): 236-239.
- 248 Guthoff R, Thijssen JM. *Ultrasound in ophthalmologic diagnosis: a practical guide*. Georg Thieme Verlag. 1991.
- 249 Ossoinig KC. Standardized echography of the optic nerve. *Ophthalmic Echography*. 1993; 13: 3-99.
- 250 Lochner P, Mader C, Nardone R, et al. Sonography of the optic nerve sheath beyond the hyperacute stage of intracerebral hemorrhage. *Journal of Ultrasound*. 2014; 17(3): 225-228.
- 251 Qayyum H, Ramlakhan S. Can ocular ultrasound predict intracranial hypertension? A pilot diagnostic accuracy evaluation in a UK emergency department. *European Journal of Emergency Medicine*. 2013; 20(2): 91-97.

- 252 Hansen HC, Lagreze W, Krueger O, Helmke K. Dependence of the optic nerve sheath diameter on acutely applied subarachnoidal pressure—an experimental ultrasound study. *Acta Ophthalmologica*. 2011; 89(6): e528-e532.
- 253 Watanabe A, Kinouchi H, Horikoshi T, Uchida M, Ishigame K. Effect of intracranial pressure on the diameter of the optic nerve sheath. *Journal of Neurosurgery*. 2008; 109(2): 255-258.
- 254 Xie X, Zhang X, Fu J, Wang H, et al. Noninvasive intracranial pressure estimation by orbital subarachnoid space measurement: the Beijing Intracranial and Intraocular Pressure (iCOP) study. *Critical Care*. 2013; 17(4): 162.
- 255 Kramer LA, Sargsyan AE, Hasan KM, Polk JD, Hamilton DR. Orbital and intracranial effects of microgravity: findings at 3-T MR imaging. *Radiology*. 2012; 263(3): 819-827.
- 256 Legrand A, Jeanjean P, Delanghe F, Peltier J, Lecat B, Dupont H. Estimation of optic nerve sheath diameter on an initial brain computed tomography scan can contribute prognostic information in traumatic brain injury patients. *Critical Care*. 2013; 17(2): R61.
- 257 Vaiman M, Gottlieb P, Bekerman I. Quantitative relations between the eyeball, the optic nerve, and the optic canal important for intracranial pressure monitoring. *Head Face Medicine*. 2014; 10(1): 32.
- 258 Hwan Kim Y, Ho Lee J, Kun Hong C, et al. Feasibility of Optic Nerve Sheath Diameter Measured on Initial Brain Computed Tomography as an Early

Neurologic Outcome Predictor After Cardiac Arrest. *Academic Emergency Medicine*. 2014; 21(10): 1121-1128.

- 259 Sekhon MS, McBeth P, Zou J, et al. Association between optic nerve sheath diameter and mortality in patients with severe traumatic brain injury. *Neurocritical care*. 2014; 21(2): 245-252.
- 260 Blehar DJ, Gaspari RJ, Montoya A, Calderon R. Correlation of visual axis and coronal axis measurements of the optic nerve sheath diameter. *Journal of Ultrasound in Medicine*. 2008; 27(3): 407-411.
- 261 Strumwasser A, Kwan RO, Yeung L, et al. Sonographic optic nerve sheath diameter as an estimate of intracranial pressure in adult trauma. *Journal of Surgical Research*. 2011; 170(2): 265-271.
- 262 Keyes LE, Paterson R, Boatright D, Browne V, Leadbetter G, Hackett P. Optic nerve sheath diameter and acute mountain sickness. *Wilderness environmental medicine*. 2013; 24(2): 105-111.
- 263 Caffery TS, Perret JN, Musso MW, Jones GN. Optic nerve sheath diameter and lumbar puncture opening pressure in nontrauma patients suspected of elevated intracranial pressure. *The American Journal of Emergency Medicine*. 2014; 32(12): 1513-1515.
- 264 Dubourg J, Messerer M, Karakitsos D, et al. Individual patient data systematic review and meta-analysis of optic nerve sheath diameter ultrasonography for detecting raised intracranial pressure: protocol of the ONSD research group. *Systematic Reviews*. 2013; 2(1): 1-6.

- 265 Von Elm E, Altman DG, Egger M, Pocock SJ, Gøtzsche PC, Vandenbroucke JP. Strengthening of Reporting of Observational Studies in Epidemiology (STROBE) statement: guidelines for reporting observational studies. *Preventive Medicine*. 2007; 45(4): 247-251.
- 266 Vandenbroucke JP, Von Elm E, et al. Strengthening the Reporting of Observational Studies in Epidemiology (STROBE): explanation and elaboration. *Annals of Internal Medicine*. 2007; 147(8): W-163.
- 267 Schoeman JF, Van Zyl LE, Laubscher JA, Donald PR. Serial CT scanning in childhood tuberculous meningitis: prognostic features in 198 cases. *Journal of Child Neurology*. 1995; 10 (4): 320-329.
- 268 Bruwer GE, Van der Westhuizen S, Lombard CJ, Schoeman JF. Can CT predict the level of CSF block in tuberculous hydrocephalus? *Child's Nervous System*. 2004; 20 (3): 183-187.
- 269 Drummond JC, Todd MM, Scheller MS, Shapiro HM. A comparison of the direct cerebral vasodilating potencies of halothane and isoflurane in the New Zealand white rabbit. *Anesthesiology*. 1986; (5): 462-467.
- 270 Matta BF, Heath KJ, Tipping K, Summors AC. Direct cerebral vasodilatory effects of sevoflurane and isoflurane. *Anesthesiology*. 1999; 91(3): 677-680.
- 271 Pulitanò S, Mancino A, Pietrini D, et al. Effects of positive end expiratory pressure (PEEP) on intracranial and cerebral perfusion pressure in pediatric

- neurosurgical patients. *Journal of neurosurgical anesthesiology*. 2013; 25(3): 330-334.
- 272 Potgieter DW, Kippin A, Ngu F, McKean C. Can accurate ultrasonographic measurement of the optic nerve sheath diameter (a non-invasive measure of intracranial pressure) be taught to novice operators in a single training session? *Anaesthesia and Intensive Care*. 2011; 39: 95-100.
- 273 Bäuerle J, Schuchardt F, Schroeder L, Egger K, Weigel M, Harloff A. Reproducibility and accuracy of optic nerve sheath diameter assessment using ultrasound compared to magnetic resonance imaging. *BMC Neurology*. 2013; 13(1): 187.
- 274 Shah S, Kimberly H, Marill K, Noble VE. Ultrasound techniques to measure the optic nerve sheath: is a specialized probe necessary? *Medical Science Monitor*. 2009; 15(5): MT63-MT68.
- 275 Geeraerts T, Bergès O, Merceron S, et al. Reply to Copetti and Cattarossi. *Intensive Care Medicine*. 2009; 35(8): 1490-1491.
- 276 Adelson PD, Bratton SL, Carney NA, et al. Guidelines for the acute medical management of severe traumatic brain injury in infants, children, and adolescents. Chapter 6. Threshold for treatment of intracranial hypertension *Pediatric Critical Care Medicine*. 2003; 4(3 Suppl): S25-27.

- 277 Kim JY, Min HG, Ha SI, Jeong HW, Seo H, Kim JU. Dynamic optic nerve sheath diameter responses to short-term hyperventilation measured with sonography in patients under general anesthesia. *Korean Journal of Anesthesiology*. 2014; 67(4): 240-245.
- 278 Launey Y, Nessler N, Le Maguet P, Mallédant Y, Seguin P. Effect of osmotherapy on optic nerve sheath diameter in patients with increased intracranial pressure. *Journal of Neurotrauma*. 2014; 31(10): 984-988.
- 279 Whiteley JR, Taylor J, Henry M, Epperson TI, Hand WR. Detection of elevated intracranial pressure in robot-assisted laparoscopic radical prostatectomy using ultrasonography of optic nerve sheath diameter. *Journal of Neurosurgical Anesthesiology*. 2015; 27(2): 155-159.
- 280 Kim MS, Bai SJ, Lee JR, Choi YD, Kim YJ, Choi SH. Increase in intracranial pressure during carbon dioxide pneumoperitoneum with steep trendelenburg positioning proven by ultrasonographic measurement of optic nerve sheath diameter. *Journal of Endourology*, 2014; 28(7): 801-806.
- 281 Maissan IM, Dirven PJ, Haitzma IK, Hoeks SE, Gommers D, Stolker RJ. Ultrasonographic measured optic nerve sheath diameter as an accurate and quick monitor for changes in intracranial pressure. *Journal of Neurosurgery*. 2015; 1-5.
- 282 Karakitsos D, Soldatos T, Gouliamos A, et al. Transorbital sonographic monitoring of optic nerve diameter in patients with severe brain injury. *Transplantation Proceedings*. 2006; 38(10): 3700-3706.

- 283 Singleton J, Dagan A, Edlow JA, Hoffmann B. Real-time optic nerve sheath diameter reduction measured with bedside ultrasound after therapeutic lumbar puncture in a patient with idiopathic intracranial hypertension. *The American Journal of Emergency Medicine*. 2015; 33(6): 860.e5-860.e7.
- 284 Querfurth HW, Arms SW, Lichy CM, Irwin WT, Steiner T. Prediction of intracranial pressure from noninvasive transocular venous and arterial hemodynamic measurements. *Neurocritical Care*. 2004; 1(2): 183-194.
- 285 Querfurth HW, Lagrèze WD, Hedges TR, Heggerick PA. Flow velocity and pulsatility of the ocular circulation in chronic intracranial hypertension. *Acta Neurologica Scandinavica*. 2002; 105(6): 431-440.
- 286 Querfurth HW, Lieberman P, Arms S, Mundell S, Bennett M, Van Horne C. Ophthalmodynamometry for ICP prediction and pilot test on Mt. Everest. *BMC Neurology*. 2010; 10(1): 106.
- 287 Miller MM, Chang T, Keating R, Crouch E, Sable C. Blood flow velocities are reduced in the optic nerve of children with elevated intracranial pressure. *Journal of Child Neurology*. 2009; 24(1): 30-35.
- 288 Goebel W, Lieb WE, Ho A, Sergott RC, Farhoumand R, Grehn F. Color Doppler imaging: a new technique to assess orbital blood flow in patients with diabetic retinopathy. *Investigative Ophthalmology & Visual science*. 1995; 36(5): 864-870.

- 289 Baxter GM, Williamson TH, McKillop G, Dufton GN. Color Doppler Ultrasound of Orbital and Optic Nerve Blood Flow: Effects of Posture and Timolol 0.5%. *Investigative Ophthalmology and Visual science*. 1992; 33(3): 604-610.
- 290 Garcia JP, Garcia PT, Rosen RB, Finger PT. A 3-dimensional ultrasound C-scan imaging technique for optic nerve measurements. *Ophthalmology*. 2004; 111(6): 1238-1243.
- 291 Zhang Y, Karl WC, Van Der Wilden G, et al. Automated 3-D intraocular ultrasound detection of elevated intracranial pressure. In *Biomedical Imaging (ISBI)*. 9th IEEE International Symposium. 2012; 1571-1574.
- 292 Willekens K, Pinto LA, Vandewalle E, Marques-Neves C, Stalmans I. Higher optic nerve sheath diameters are associated with lower ocular blood flow velocities in glaucoma patients. *Graefes Archive for Clinical and Experimental Ophthalmology*. 2014; 252: 477-483.
- 293 Lewis JP. Fast template matching. In *Vision interface*. 1995; 95(120123): 15-19.
- 294 Tappert FD. The parabolic approximation method. In *Wave propagation and underwater acoustics (Springer Berlin Heidelberg)*. 1977; 224-287.
- 295 Stein EM, Weiss GL. *Introduction to Fourier analysis on Euclidean spaces*. Princeton university press (Vol. 1). 1971.

- 296 Pinsky MA. Introduction to Fourier analysis and wavelets. (Pacific Grove: Brooks/Cole). 2002; 181-194.
- 297 Lee SS, Kim NJ, Sun K, et al. Association between arterial stiffness and the deformability of red blood cells (RBCs). *Clinical Hemorheology and Microcirculation*. 2006; 34(4): 475-482.
- 298 Tsai CHD, Sakuma S, Arai F, Kaneko M. A new dimensionless index for evaluating cell stiffness-based deformability in microchannel. *Biomedical Engineering (IEEE Transactions)*. 2014; 61(4): 1187-1195.

